RADC-TDR-64-368
Final Report

FRESNEL ZONE ANALYSIS

TECHNICAL DOCUMENTARY REPORT NO. RADC-TDR-64-368

October 1964

Vulnerability Reduction Branch
Rome Air Development Center
Research and Technology Division
Air Force Systems Command
Griffiss Air Force Base, New York

Project No. 4540, Task No. 454002

(Prepared under Contract AF 30(602)-3020 by Melpar, Inc., 3000 Arlington Boulevard, Falls Church, Virginia.)

BLANK PAGE

FOREWORD

The work on this project was performed under Contract AF 30(602)-3020 for the Electromagnetic Vulnerability Laboratory, Rome Air Development Center. Project direction from RADC was given by Mr. Hollis J. Hewitt, EMCVR. Project direction at Melpar was obtained from Mr. L. L. Bonham, Mr. P. E. Taylor, and Mr. C. W. Morrow. Other people contributing to the project include Dr. Glenn Camp, Consultant from Case Institute of Technology, Dr. Chen To Tai , Consultant from Ohio State University, and Dr. R. Wayne Masters of Melpar. The guidance and aid supplied are gratefully acknowledged by the authors.

ABSTRACT

This report presents the objectives and results of an investigation of the interference effects of Fresnel region phenomena. Analytical techniques are described that will enable calculation of Fresnel region radiation patterns for monopulse antennas, elliptically or irregularly shaped apertures, and phased arrays. The results from investigations of defocusing techniques, radial E-field in the Fresnel region, effects of reflections in the Fresnel region, antenna to antenna coupling in the Fresnel region, and spurious frequency response are also presented. A unique measurement technique, called Fresnel ring focusing, is described, and gives testimony for a feasible means for obtaining the far-field pattern of a large aperture antenna with measurements taken well within the far-field-Fresnel region boundary. In comparison with other means using the Sommerfield expansion to produce such results, the Fresnel ring focusing technique appears to have many advantages, which are outlined.

Recommendations for future investigation including a study of parameter errors and their effect upon the latter technique are also contained in this report.

PUBLICATION REVIEW

This report has been reviewed and is approved. For further technical information on this project, contact

Approved:

JOHN H. EDWARDS
Contract Engineer
Interference Research Section

Approved:

T. B. SWANSON
Colonel, USAF
Chief, Communications Division

FOR THE COMMANDER:

for IRVING J. GABELMAN
Chief, Advanced Studies Group

TABLE OF CONTENTS

LIST OF ILLUSTRATIONS

LIST OF ILLUSTRATIONS (Cont.)

LIST OF ILLUSTRATIONS (Cont.)

LIST OF ILLUSTRATIONS (Cont.)

LIST OF ILLUSTRATIONS (Cont.)

EVALUATION

This final report of the Fresnel Zone Analysis contract by Melpar, Inc. completes the objectives and results of an investigation of the interference effects of fresnel region phenomena. This contract has provided the information necessary to predict the field intensities and antenna patterns for an interference analysis of a co-site problem when large and irregular shaped antennas are located in the fresnel zone of each other. Also presented in the final report is a unique technique for the determination of the far-field pattern of a large aperture from measurements taken well within the far-field fresnel boundary. This technique appears to be feasible and will provide a means to determine the far-field pattern of antennas with great far-field distances (over five miles). The information contained in this report will be used in an interference prediction and analysis program and will provide the Air Force community with the capability to provide greater system effectiveness and compatibility in radar and communication complexes.

Charles R Miller

CHARLES R. MILLER, Chief
Interference Research Section
Vulnerability Reduction Branch

INTRODUCTION

The purpose of this final report is to present the results of an investigation of Fresnel Region phenomena that may produce variable interference parameters. This study was conducted under Contract AF 30(602)-3020 for the Rome Air Development Center. The basic objectives of the study were the examination of various aperture types, development of analytical techniques for solution of Fresnel region problems, and examination of other parameters that would result in the description of the antenna radiation characteristics at arbitrary positions within the Fresnel region boundaries.

The investigation of methods to extract the far-field data of an antenna from measurements within the Fresnel region includes a theoretical analysis of a technique that had been suggested by Hougardy[1] as a promising way (Time/Frequency Method) to accomplish such ends. Section 1.1 discusses various aspects of the analysis of this technique indicating parameters that result in this technique being unfeasible theoretically and also impractical from an instrumentation aspect. Another technique was formulated that suggests a unique approach to this problem. Section 1.2 describes the Fresnel Ring Harmonic Focusing technique that will enable the measurement of the Fraunhofer pattern at ranges from the antenna aperture which are well within the Fresnel region of the antenna. The development procedure presented consists of an analysis in Section 1.2.1 of the limitations to the Fresnel approximation for a large antenna with an arbitrary vector source distribution and the resulting implications for producing an array design that will produce a far-field measurement characteristic. The array element design problem is solved by making a transformation to the complex plane as shown in Section 1.2.3. The characteristics

1. H. H., Hougardy, "Study and Design of a Time/Frequency Near Zone Pattern Range," ASI Technical Report No. 61-ESD-1, April 1961

Manuscript released by author for publication on 15 July 1964.

of a physically realizable array are considered with respect to obtaining the characteristics which are obtained with a theoretical point source array. An example is presented for an array of eight elements which will produce the far-field pattern of an aperture with a radius of 100λ, and the array weighting factor is shown in figure 6. Section 1.2.4 is a discussion of various tolerance considerations for array alignment and element gain when using physical array elements. It was found that the error magnification relative to the focusing function, shown plotted in figure 7., does not prohibit application of the Fresnel ring harmonic focusing technique as it has been found to do in other approaches to the problem.

Another portion of the contract includes a theoretical analysis of various types of apertures. Section 2.1 is a survey of various methods for calculating Fresnel region patterns; a technique for calculation of the primary and secondary monopulse patterns for both sum and difference modes of operation is included in Section 2.2. The method of analytically determining the Fresnel Zone radiation characteristics of the difference mode is illustrated with a detailed example calculation in Section 2.2.5. A four-step procedure is given which consists of (1) determining a polynomial approximation for the aperture illumination due to a single primary antenna, (2) calculating an analytical expression for the monopulse aperture distribution, (3) modification of the aperture distribution by expressing it in a Fourier-Zernike Series and, (4) calculation of the Fresnel Zone Pattern. Table 1 in the Appendix of this report is the result of an IBM 7090 computer program to enable calculation of monopulse Fresnel zone patterns on a desk calculator and is utilized in the example problem described. Section 2.2.6 illustrates the comparison of

the analytical and experimental results for the monopulse antenna.

Other apertures, for which a theoretical analysis was conducted, include elliptical apertures and phased arrays. The elliptical apertures are defined as irregular shaped apertures other than circular or rectangular shapes for the purposes of this treatment. A general technique was formulated utilizing a strip approximation technique as described in Section 3.1. Experimental patterns obtained by RADC personnel of an AN/TPS-1D antenna were used for comparison (see Section 3.2) with the calculated examples. Another comparison, using a circular aperture, was also used to indicate the adequacy of the technique. The theoretical analysis performed for phased arrays is contained in Section 4. and discusses the development of a Fresnel zone array factor and summation techniques developed by Ishimaru[2] for unequally spaced arrays at arbitrary field points.

Section 5.1 reports on the results of an investigation of the spurious frequency response of a simple probe fed electromagnetic horn, and compares the calculated patterns of a pyramidal horn with its measured patterns. Section 5.2. describes the results of an investigation that was performed to aid in defining the far field-Fresnel region boundary for spurious frequencies.

The effects of Fresnel zone ground reflections and their influence upon the far field-Fresnel region boundary are presented in Section 6.

A theoretical investigation was performed to determine the antenna to antenna coupling characteristics in the Fresnel zone, and results of the study, utilizing various size circular and rectangular apertures illuminated with uniform and tapered distributions, are presented in Section 9. Other

2. A. Ishimaru, "Theory of Unequally-Spaced Arrays;" IRE Transactions on Antennas and Propogation (AP-10), November 1962, pp. 691-702

areas of investigation during this contract included the Fresnel region radial E-field description and defocusing techniques which may be used with paraboloidal reflectors for obtaining a small angle far-field pattern in the Fresnel zone. Descriptions of the effort in these areas are included in Sections 7 and 10. Experimental verification of theoretical radiation patterns both on and off axis in the Fresnel zone is shown for the case of a circular aperture (Section 8). Other experimental verification was performed also for the monopulse and AN/TPS-1D antennas.

The conclusions drawn from the investigation conducted during the tenure of this contract are contained in Section 11 and recommendations for future effort based upon the results are outlined in Section 12.

1. ANALYSIS OF TECHNIQUES FOR OBTAINING FAR FIELD DATA FROM FRESNEL ZONE MEASUREMENTS

One objective of this contract was to evaluate techniques for obtaining Far Field radiation patterns of an antenna from measurements taken in the Fresnel region. One method which has been proposed to accomplish this is described in a report prepared for the Jet Propulsion Laboratory, has been the subject of a detailed study during the first part of this study with a view toward determining its feasibility. The method described consists essentially of an analog technique for detecting the component of the radiated field of an antenna associated with the Fraunhofer field term as contained in a Sommerfeld expansion. This is accomplished by multiplying the field, detected by a number of rapidly scanned stationary probes, by a voltage of the same form as that produced by the variation of the probe position from the test antenna. The harmonic frequency corresponding to the Far Field term is then filtered out from the resulting signal.

The following describes in detail the results of the analysis of this system, performed with the assistance of Melpar Consultant, Dr. Glenn Camp of Case Institute of Technology, who outlined the mathematical critique of this method and indicated some of the problem areas associated with its practical implementation.

1.1 Discussion of Problem Areas in the Time/Frequency Technique

There are three major problem areas of the proposed measurement method which are principally theoretical in nature. Perhaps the most obvious of these is the fact that no consideration is made of the effect of the theoretical errors "off axis" in the error graphs on pages 18 and 19 of the report.[1]

It should be noted that these graphs are made on axis where one would expect that the effect of the other, somewhat smaller, terms due to coefficients $B_{N+1}(\theta, \phi)$, $B_{N+2}(\theta, \phi)$, ... have a minimum effect on $B_0(\theta, \phi)$ which has its maximum on axis. An evaluation of the coefficients at a point off axis shows that this is a very serious limitation.

The coefficients may be evaluated off axis in the same manner as for the on axis case. Using the generalization of Hougardy's equation (13) (See page 8) for the off axis case (See also Section 2.1).

$$U_{P_{fresnel}}(R, \Theta) = jka^2 \left(\frac{e^{-jkR}}{R}\right) \int_0^1 F(\zeta)\, J_0(u\rho)\, e^{-j\frac{\gamma}{2}\zeta^2}\, \zeta d\zeta \qquad (1)$$

where $F(\rho) = 1 - \zeta^2$ and we expand the exponential in a power series

$$e^{-j\frac{\gamma}{2}\zeta^2} = \sum_{n=0}^{\infty} \frac{(-j)^n}{n!}\left(\frac{\gamma\zeta^2}{2}\right)^n, \quad \left(\gamma = \frac{ka^2}{R}\right)$$

eq. (1) becomes

$$E(R,\Theta) = j\gamma e^{-jkR} \int_0^1 \left(\sum_{n=0}^{\infty} \frac{(-j)^n}{n!}\left(\frac{\gamma}{2}\right)^n \left(\zeta^{2n+1} - \zeta^{2n+3}\right) J_0(u\zeta) \right) d\zeta$$

$$E(R,\Theta) = j\gamma e^{-jkR} \left\{ \sum_{n=0}^{\infty} \frac{(-j)^n}{n!}\left(\frac{\gamma}{2}\right)^n \int_0^1 J_0(u\zeta) \left(\zeta^{2n+1} - \zeta^{2n+3}\right) d\zeta \right\} \qquad (2)$$

Let us make use of the identity[3]

$$\int_0^1 J_0(u\zeta)\zeta^m d\zeta = \frac{1}{u^{m+1}} \int_0^u J_0(t)\, t^m dt = \frac{1}{m+1} \sum_{k=0}^{\infty} \frac{\left(\frac{m+1}{2}\right)!\, u^k\, J_k(u)}{\left(\frac{m+1}{2} + k\right)!\, 2^k}$$

3. Y. L. Luke, "Integrals of Bessel Functions," McGraw Hill, 1962, p. 52.

then (2) becomes

$$U_{\text{fresnel}}(R,\theta) = jve^{-jkR}\left\{\sum_{n=o}^{\infty} \frac{(-j)^n}{n!}\left(\frac{\gamma}{2}\right)^n \left[\sum_{k=o}^{\infty}\left(\frac{u^k n!\, J_k(u)}{2^{k+1}\,(n+k+1)!} - \frac{u^k (n+1)!\, J_k(u)}{2^{k+1}\,(n+k+2)!}\right)\right]\right\}$$

or

$$= jv/2\; e^{-jkR}\left\{\sum_{n=o}^{\infty}(-j)^n\left(\frac{\gamma}{2}\right)^n \sum_{k=o}^{\infty}\frac{u^k\, J_k(u)(k+1)}{2^k(n+k+2)!}\right\}$$

Note for u=0 this expression reduces to that given by Hougardy for the on axis case. The Sommerfeld coefficients are given by

$$B_n = -(-j)^{n+1}\left(\frac{ka^2}{2}\right)^{n+1}\sum_{k=o}^{\infty}\frac{u^k\, J_k(u)\;(k+1)}{2^k\;(n+k+2)!}$$

Now if we calculate the coefficients at u=5 ($\theta = 0.44^o$ in the example considered by Hougardy) $U_p(u=5) = \frac{e^{-jkR}}{R}\left\{0.0191\, j + \ldots - \frac{0.09816\, j}{R^4} - \frac{0.01723}{R^5}\right.$

$$+ \frac{.006753\, j}{R^6} + \frac{.001916}{R^7} - \frac{.0004744\, j}{R^8} - \frac{.0001138}{R^9}$$

$$\left. + \frac{.00002428\, j}{R^{11}} + \frac{.00000479}{R^{12}} + \ldots\right\}$$

Thus if we calculate the theoretical error term in Hougardy's equation (33) of the report we find

$$-\sum_{n\geq 4}\frac{(n-1)!\; B_n(u=5)}{(n-4)!\;3!} = .0982\, j + .0689$$

$$-.0675\, j - .0383$$

$$+.0166\, j + .0064$$

$$-.0020\, j - .0006 = 0.0364 + j\,0.0453$$

thus the error term is much larger than the theoretical Fraunhofer coefficient $B_o(u=5) = .0191\ j$ and the system would theoretically give a -27.1 db result instead of the desired -36.7 db down from the on axis reading. This indicates that no nulls or sidelobe structure below about 15 db can be predicted accurately due to the large magnitude of the error terms on the third harmonic.

A second difficulty found is that a calculation of the points on the graph on page 19 of the report fails to give agreement with the point number 4, which is the theoretical error due to these error terms in equation (33). This is a very important point since it is an error in the far field pattern on axis for the proposed system. If the error terms are written out in detail we have:

$$\sum_{n=4}^{\infty} \frac{(-1)\ (n-1)!\ B_n(0)}{(n-4)!\ 3!} = \begin{aligned} & 0.1311 - j\ 0.1961 \\ & -0.1609 + j\ 0.0938 \\ & +0.0430 - j\ 0.0215 \\ & -.0071 + j\ .0020 + \ldots \\ = \quad & +.0061 - j\ .1218 \end{aligned}$$

which gives an error of approximately 12.2% for the measurement distance $0.3D^2/\lambda$ modulated with N = 3, a far greater error than is shown in figure 5. Actually this error is nearly as large as that in method 6, the field measurement taken in the usual manner, which has an error of 17.5% compared to the true far field measurement.

Another effect which is not considered is the possibility of a third harmonic distortion of the fundamental frequency. Even a small amount of third harmonic distortion may destroy the desired signal since the fundamental

is 107 db above the desired 3rd harmonic signal. A major source of third harmonic distortion is the amplitude adjustment of the probes to simulate the voltage multiplication $\left[1 + \mu F(t)\right]^{N+1}$. Each probe p must be adjusted by a factor $\left[1 + \mu\beta_p\right]^{N+1}$ as shown in figure 1.

The measurement method suggested, in the report, for adjusting the probes has a resolution accuracy of 0.002 db = 1.00025 and if an error of this magnitude is made in adjusting the voltage of one of the probes, for example, the first probe, then by superposition the effect of this error may be considered separately. (See figure 2.) A harmonic analysis of this signal shows the amplitude of the third harmonic is $C_3 = A(0.1718) = 0.000043$ or -87.3 db below the fundamental frequency. However, since the fundamental is 107 db above the desired third harmonic signal we are attempting to detect, the third harmonic distortion caused by this error in adjusting the probe is 19.7 db above this signal, making detection impossible. This implies a rather severe problem in adjusting the probes to simulate the voltage multiplication.

Another problem in implementing such a system arises from the relatively high level of near (10 kc) neighbors of the signal which must be detected with great accuracy if the system is to give good results. This matter is not mentioned in the report although the author seems aware of it because he specifies a crystal filter with 60 db of rejection 10 kc away from its center. A relatively simple calculation can be performed to compute the neighboring (N-1) line. If we assume that equation (31) is rigorously correct and neglect contributions from $n \geq N + 1$ whereupon all contributions come from $n = 0$ and $n = 1$, we have

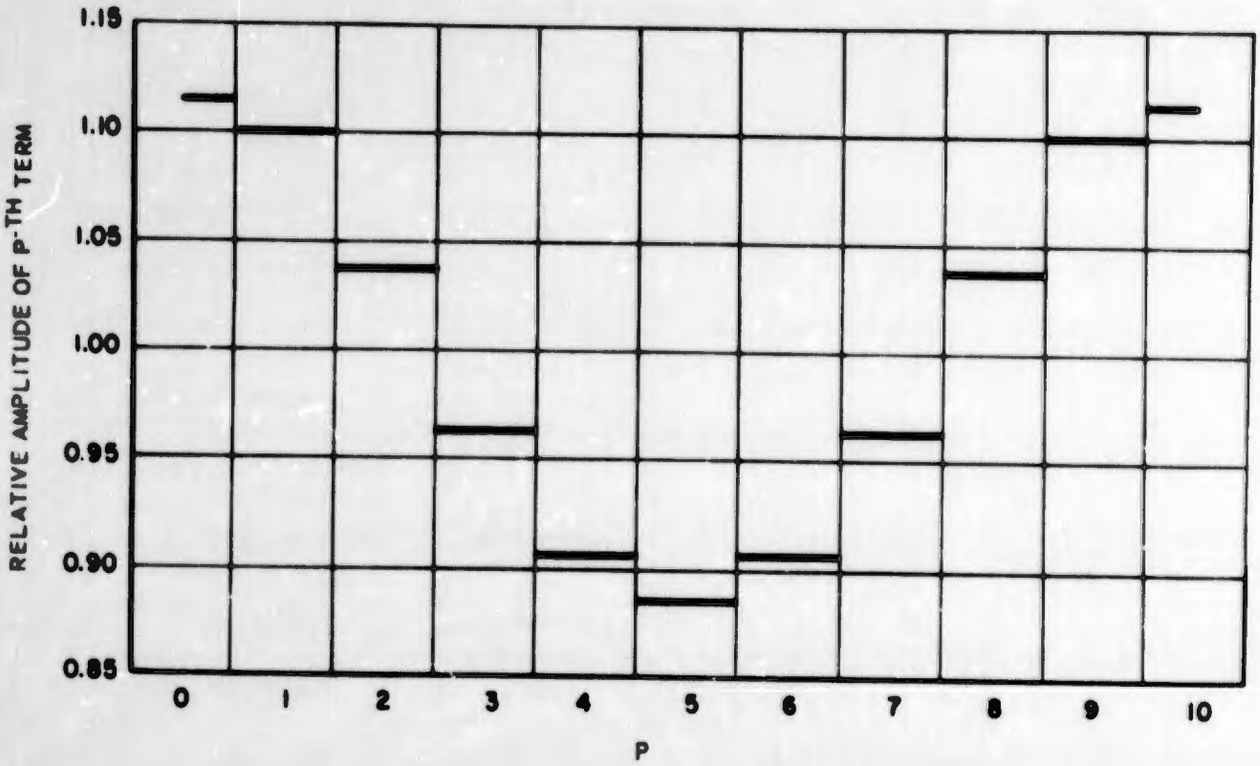

Figure 1. Amplitude Adjustment of Probes

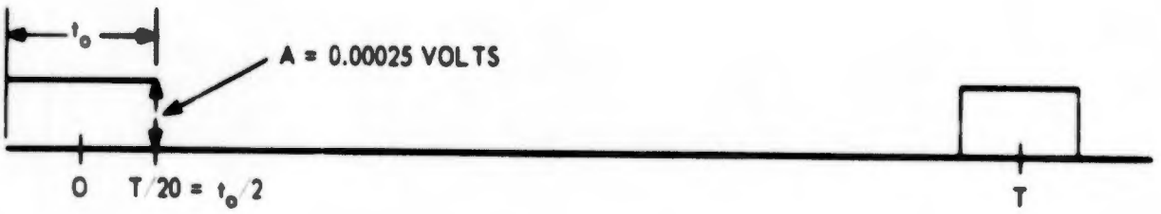

Figure 2. Error in Amplitude Adjustment of the First Probe

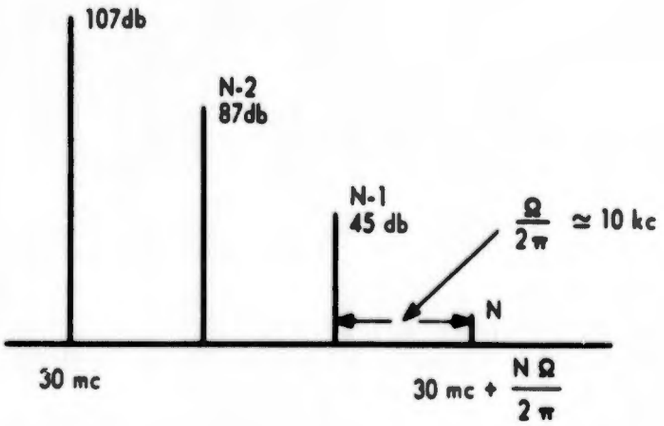

Figure 3. Amplitude of NΩ Line and its Neighbors

$$V_{if}\ V_m = V_o\left\{\frac{B_o}{R_o}\ (1 + \mu\cos\theta)^N + \frac{B_1}{R_o^2}\ (1 + \mu\cos\theta)^{N-1} + \ldots\right\},\ \theta = \Omega t$$

$$= V_o\left\{\frac{B_o}{R_o}\left[(\mu\cos\theta)^N + N\ (\mu\cos\theta)^{N-1}\right] + \frac{B_1}{R_o^2}\ (\mu\cos\theta)^{N-1} + \ldots\right\}$$

Since

$$(\cos\theta)^p = \left[\frac{1}{2}\ (e^{i\theta} + e^{-i\theta})\right]^p$$

$$= \frac{1}{2^{p-1}}\left[\cos p\theta + p\cos(p-2)\theta + \ldots\right]$$

From this analysis we see that to achieve a 40 db dynamic range on the pattern recorder a filter with better than 147 db rejection, at 30 kc away from the third harmonic is required.

Another problem area, which is briefly discussed by the author, is that of the frequency stability of the transmitter. Some degree of long-term stability is required because of the necessity of adjusting the phase of the individual probes. Due to the large separation of the probes, a rather small change in frequency causes an error in the phase adjustment. Each probe is adjusted by a phase ϕ where

$$e^{j\phi} = e^{jkR_o\mu\beta_p} = e^{j\ 2418.7\beta_p}$$

Suppose the frequency f varies from the calibration frequency f_o:

$$f = f_o + \Delta f$$

then

$$\mu k\ R_o = 2418.7 + 1.0078\ (10^{-6})\ \Delta f$$

If a degree of accuracy of 0.1 radian is required in the phase adjustment then Δf (the deviation of the frequency from the fixed calibration frequency) must be less than 0.1 mc or 4 parts in 10^4. At least this degree of long term

frequency stability is required even if a closed loop system is used to obtain the local oscillator frequency.

Another major equipment problem is the third harmonic distortion in the mixer and pre-amplifier since this distorts the desired third harmonic signal. Here again this is a critical problem since the fundamental frequency of the receiver signal is of much greater magnitude than the third harmonic. Thus

$$V_{if}\, V_m = V_o \frac{B_o}{R_o} \frac{\mu^N}{2^{N-1}} \cos N\theta + \left(\frac{NB_o}{R_o} + \frac{B_1}{R_o^2}\right)\left(\frac{\mu^{N-1}}{2^{N-2}}\right) \cos (N-1)\theta + \ldots$$

$$= V_o \frac{B_o}{R_o} \frac{\mu^N}{2^{N-1}} \cos N\theta + \frac{2N}{\mu}\left(1 + \frac{B_1}{NB_o R_o}\right) \cos (N-1)\theta + \ldots \quad (3)$$

Equation (3) discloses two serious concerns, only the first of which is mentioned by the author. First, the amplitude of the $N\Omega$ - line is afflicted by a factor $\mu^N/2^{N-1} = (.03)^3/4 = 7 \times 10^{-6}$ (for N=3 and $\mu = .03$). This leads to a "coefficient loss" of 107 db. Second, the amplitude of the $(N-1)\Omega$ - line is $\frac{2N}{\mu}\left[1 + \frac{B_1}{NB_o R}\right] = 200$ (for N=3 and $\mu = .03$) relative to the $N\Omega$ line; that is, the nearest neighbor to the $N\Omega$ -line is about 45 db above it. The next nearest neighbor has been calculated similarly and is 87 db above it and hence we see a picture as shown in figure 3.

Due to the limitations of the Time/Frequency technique for measuring the far-field pattern in the Fresnel zone it was felt that no further investigation of this technique was warranted. Indeed it was shown by Galindo[4] that the Sommerfeld expansion which was used by Hougardy to develop this technique has no practical value for extrapolation of near-field data to obtain a

4. V.Galindo, "Extrapolation of Near-Field Data to Obtain Far-Field Data," University of Calif., Report No. 63-1, March 4, 1963.

far-field pattern. This is due to practical limitations of such a system, particularly because of the magnification of extrapolation errors.

For this reason an alternate technique, which is discussed in Section 1.2, was developed. This technique is basically different from that investigated by Hougardy and Galindo in that it does not attempt to eliminate higher order coefficients from the Sommerfeld expansion.

1.2 An Array Model For Fresnel Zone Measurement of Far Field

The region of validity of the Fresnel approximation to the scalar Green's function for an arbitrary source distribution and field point correspondence determines the electromagnetic field region known as the Fresnel zone. In the reciprocal concept, the Fresnel retardation function of a point source radiating to the receptor distribution consists of a paraboloidal phase front approximation to the spherical one of the scalar Green's function. This results in phase structures on the projected apertures of the distribution that are called Fresnel rings. The Fresnel approximation is useful in a very large geometric region between the Fraunhofer zone and the near field zone for apertures that are large with respect to wavelength. The objective here is to utilize the field structure in this geometric region by a Fresnel ring harmonic focusing technique that will permit measuring the source or receptor distribution's Fraunhofer pattern at antenna ranges deep in the Fresnel zone. By properly sampling the antenna field, or by arraying a number of point sources with proper weight (phase and amplitude adjustments) on a radial line through the receptor distribution and spaced in harmonic increments of some R^{-1} from any point near the center of the distribution, a plane wave can be synthesized on the line through the distribution by virtue of the proper harmonic combination of Fresnel rings. This is a complex analogy similar to the manner in which the properly weighted harmonic sine terms of the Fourier series can be made to synthesize a unit step function.

1.2.1 The Fresnel Approximation

The vector potential for an arbitrary time harmonic source can be written as follows. The coordinate system origin as shown in figure 4 is near the center of the source distribution.

$$\vec{A}_{x,y,z}(R,\theta,\phi) = \frac{(\hat{x},\hat{y},\hat{z})\,\mu_o}{4\pi}\int_V J_{x,y,z}(R',\theta',\phi')\,\frac{e^{ikR''}}{R''}\,dV \qquad (4)$$

$$R'' = (R^2 + R'^2 - 2RR'\cos\gamma)^{1/2},\quad \cos\gamma = \hat{R}\cdot\hat{R}'$$

$$kR'' = kr\left[1-\frac{R'}{R}\cos\gamma + \frac{1}{2}\left(\frac{R'}{R}\right)^2\sin^2\gamma + \frac{1}{2}\left(\frac{R'}{R}\right)^3\sin^2\gamma\cos\gamma - \frac{1}{8}\left(\frac{R'}{R}\right)^4(\sin^4\gamma - \sin^2\gamma) + \cdots\right]$$

$$\frac{1}{R''} = \frac{1}{R}\left[1 + \frac{R'}{R}\cos\gamma + \frac{1}{2}\left(\frac{R'}{R}\right)^2(\cos^2\gamma + \cos 2\gamma) + \cdots\right]$$

The Fresnel approximation to the scalar Green's function is the following:

$$\frac{e^{ikR''}}{R''} \sim \frac{e^{i(kR - kR'\cos\gamma + \frac{kR'^2}{2R}\sin^2\gamma)}}{R}$$

Consequently two inequalities must be satisfied.

$$\frac{R'\cos\gamma}{R} \ll 1,\quad \frac{kR'^3}{2R^2}\sin^2\gamma\cos\gamma < \frac{\pi}{8}\ (\text{max. } \sin^2\gamma\cos\gamma \approx .384) \qquad (5)$$

The phase tolerance of $\frac{\pi}{8}$ radians is the traditional number for maximum phase error in quadratic deviation from an assumed linear distribution on an aperture. The tolerance for equivalent field error due to linear phase deviations is about $\frac{\pi}{16}$. This is shown in Section 6 on reflections in the

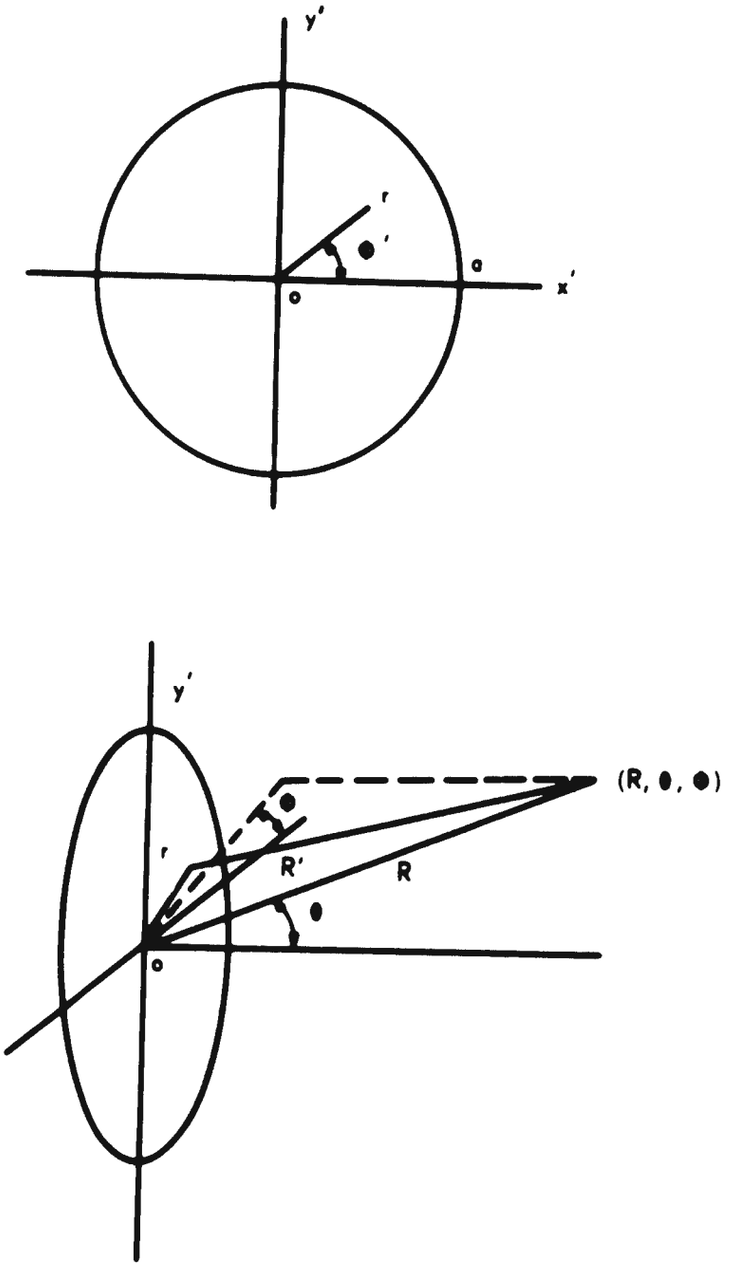

Figure 4. Coordinate System

Fresnel zone. The antisymmetric cubic curve with a maximum amplitude of $\frac{\pi}{8}$ has an average linear deviation in amplitude of $\frac{\pi}{16}$. A two dimensional aperture, or an aperture with tapered illumination, has a smaller linear average. Consequently, $\frac{\pi}{8}$ is considered to be an equally reasonable number for cubic phase tolerance. Higher order symmetric antisymmetric phase deviations on an aperture have less stringent tolerance for field conformity to that of the assumed quadratic and linear distributions. The series expansions indicated for the factors of the scalar Green's function converge rapidly, and consequently inequalities (5) define the boundaries of the Fresnel zone, with maximum field error comparable to that of the $\frac{2D^2}{\lambda}$ - criterion for far field. Thus with maximum error for the equality sign, the following inequalities apply at all angles.

Fraunhofer pattern: $R > 2D^2/\lambda$, $(D = 2R'_{o\infty})$

Fresnel pattern: $R > \sqrt{\pi D^3/8\lambda}$ (6)

For the Fresnel zone field, smaller ranges can be used (provided $\frac{R'\cos\psi}{R} \ll 1$) with the same error incurred if angular restrictions of the field point relative to the aperture are taken into account.

The vector field components in the Fresnel zone are obtained by performing the following operations on the rectangular components of the vector potential.

$$\vec{E} = i\omega\left[\vec{A} + \frac{1}{k^2}\ \nabla\nabla\cdot\vec{A}\right]$$

$$\vec{B} = \nabla \times \vec{A} = \mu\vec{H}$$

$$\omega = 2\pi f,\ k = 2\pi/\lambda$$

The spherical vector components are obtained from the rectangular ones as follows.

$$A_R\hat{R} = \sin\theta\cos\phi\, A_x\hat{x} + \sin\theta\sin\phi\, A_y\hat{y} + \cos\theta\, A_z\hat{z}$$

$$A_\theta\hat{\theta} = \cos\theta\cos\phi\, A_x\hat{x} + \cos\theta\sin\phi\, A_y\hat{y} - \sin\theta\, A_z\hat{z}$$

$$A_\phi\hat{\phi} = -\sin\phi\, A_x\hat{x} + \cos\phi\, A_y\hat{y}$$

$$\nabla\nabla\cdot\vec{A} = \begin{vmatrix} R\dfrac{\partial}{\partial R} & & \\ \dfrac{\theta}{R}\dfrac{\partial}{\partial\theta} & & \\ \dfrac{\hat{\phi}}{R\sin\theta} & \dfrac{\partial}{\partial\phi} & \end{vmatrix} \left[\frac{1}{R^2}\frac{\partial}{\partial R}(R^2A_R) + \frac{1}{R\sin\theta}\frac{\partial}{\partial\theta}(\sin\theta A_\theta) + \frac{1}{R\sin\theta}\frac{\partial A}{\partial\phi}\phi\right] \quad (7)$$

$$\nabla\cdot\vec{A} = \frac{2A_R}{R} + \frac{\partial A_R}{\partial R} + \frac{1}{R}\frac{\partial A_\theta}{\partial\theta} + \frac{\cos\theta A_\theta}{R\sin\theta} + \frac{1}{R\sin\theta}\frac{\partial A_\phi}{\partial\phi}$$

$$= (\sin\theta\cos\phi\frac{\partial A_x}{\partial R} + \sin\theta\sin\phi\frac{\partial A_y}{\partial R} + \cos\theta\frac{\partial A_z}{\partial R})$$

$$+ \frac{1}{R}(\cos\theta\cos\phi\frac{\partial A_x}{\partial\theta} + \cos\theta\sin\phi\frac{\partial A_y}{\partial\theta} - \sin\theta\frac{\partial A_z}{\partial\theta})$$

$$+ \frac{1}{R\sin\theta}(-\sin\phi\frac{\partial A_x}{\partial\phi} + \cos\phi\frac{\partial A_y}{\partial\phi})$$

$$\frac{\partial}{\partial\alpha}\left(\frac{e^{ikR''}}{R''}\right) = \frac{e^{ikR''}}{R''}(ik-\frac{1}{R''})\frac{\partial R''}{\partial\alpha} = \frac{e^{ikR''}}{R''}(ik-1/R'')\frac{1}{2R''}\frac{\partial}{\partial\alpha}(R^2-2RR'\cos\Psi)$$

$$\frac{\partial R''}{\partial R} = \frac{R}{R''}(1-\frac{R'}{R}\cos\Psi),\ \frac{R}{R''} \simeq (1+\frac{R'}{R}\cos\Psi)$$

$$\cos\Psi = \cos\theta\cos\theta' + \sin\theta\sin\theta'\cos(\phi-\phi')$$

$$\frac{\partial \cos \Psi}{\partial \phi} = -\sin\theta \sin\theta' \sin(\phi-\phi')$$

$$\frac{\partial \cos \Psi}{\partial \theta} = \sin\theta \cos\theta' + \cos\theta \sin\theta' \cos(\phi-\phi')$$

$$\frac{1}{R}\frac{\partial R''}{\partial \theta, \phi} = \frac{R'}{R''}\frac{\partial \cos\Psi}{\partial \theta, \phi}$$

All of the angular derivatives involve higher order powers in $\frac{1}{R}$ and are of the same order or less than the term $\frac{R'}{R}\cos\Psi$, which is assumed to be negligible compared to unity by the Fresnel inequalities indicated in equation (5). Thus the only remaining term of the operation (7) is the R term.

$$\nabla\nabla\cdot\vec{A} \simeq -k^2 A_R \hat{R}\,, \quad kR''>>1.$$

$$E \simeq i\omega(A_\theta\hat{\theta} - A_\phi\hat{\phi})$$

The same considerations follow for the magnetic intensity.

$$\nabla \times \vec{A} = \frac{\hat{R}}{R\sin\theta}\left[\frac{\partial}{\partial\theta}(\sin\theta A_\phi) - \frac{\partial A_\theta}{\partial\phi}\right]$$

$$-\frac{\hat{\theta}}{R}\left[\frac{1}{\sin\theta}\frac{\partial A_R}{\partial\phi} - \frac{\partial}{\partial R}(RA_\phi)\right]$$

$$+\frac{\hat{\theta}}{R}\left[\frac{\partial}{\partial R}(RA_\theta) - \frac{\partial A_R}{\partial\theta}\right],$$

$$B_R = \frac{1}{R}\frac{\partial A_\phi}{\partial\theta} - \frac{1}{R\sin\theta}\left(\cos\theta\cos\phi\frac{\partial A_x}{\partial\phi} + \cos\theta\sin\phi\frac{\partial A_y}{\partial\phi} - \sin\theta\frac{\partial A_z}{\partial\phi}\right)$$

$$B_\theta = \frac{\cos\phi}{R}\frac{\partial A_x}{\partial\phi} + \frac{\sin\phi}{R}\frac{\partial A_y}{\partial\phi} + \frac{\cos\theta}{R\sin\theta}\frac{\partial A_z}{\partial\phi} - \frac{\partial A_\phi}{\partial R}$$

$$\simeq -\frac{\partial A_\phi}{\partial R} \simeq -ikA_\phi$$

$$B_\phi = \frac{A_\theta}{R} + \frac{\partial A_\theta}{\partial R} - \frac{1}{R}\frac{\partial A_R}{\partial \theta} \simeq ikA_\theta$$

$$\vec{E} \simeq -ik\left(A_\phi \hat{\theta} - A_\theta \hat{\phi}\right)$$

$$\left|E_{t_1}\right| \simeq \eta \left|H_{t_2}\right| \quad , \hat{t}_1 \cdot \hat{t}_2 = 0, \; n = \sqrt{\frac{\mu}{\epsilon}}$$

The field is specified by either the electric or magnetic components. All the terms in higher order powers of 1/R, which includes the radial field components, are negligible as the factor $\frac{R' \cos \gamma}{R}$ compared to unity in the integrands of the vector potential. Numerical calculations of the radial field components in the forward area of the antenna at near ranges for a specific case indicates these components are quite small compared to the transverse components. (This subject is discussed in Section 7 of this report). Consequently a safe range for true Fresnel patterns is from $R \simeq 10\,R'$.(provided the inequality for the phase variations is satisfied) out to the Fraunhofer boundary. For antennas large with respect to wavelength, the Fresnel zone is large. A useful measure of the size of the Fresnel zone for a particular antenna is indicated by the number of Fresnel rings available. A Fresnel ring is the annular region over which the phase changes by π radians in projection from an axial field point to the aperture. The number of Fresnel rings (N) for an axial field point is obtained from the quadratic phase variable in the Fresnel approximation.

$$N = \frac{1}{\pi} \left(\frac{kR_o'^2}{2R}\right)$$

Thus, for an aperture with $R_o' = 100\lambda$, at $R = 10\ R_o'$, 10 Fresnel rings are available. The Fraunhofer boundary is the range at which 1/8 the central ring (disk) covers the aperture.

For an antenna with a completely general source function, the Fresnel zone field is essentially an optical field. Its vector characteristic is a matter of transverse polarization. Consequently there is no loss in generality in basing on array design for Fresnel ring focusing on the scalar theory, and the notation is thereby simplified. The essential restriction arising from this basis is that the array elements must be confined to the true Fresnel zone, as defined by the inequalities (5). A diagram of the Fresnel zone boundary for a plane circular aperture with $R_o' = 100\lambda$ is shown in figure 5.

1.2.2 Fresnel Ring Harmonic Focusing

For linear polarization, or for one polarization component, the Fresnel zone field intensity can be written as a scalar integral for arbitrary source distribution.

$$E(\vec{R}) = \int_V f(\vec{R}') \frac{e^{ikR''}}{R''} \, dV$$

The difference between the Fraunhofer and the Fresnel approximations consists of the quadratic phase variable.

$$\frac{e^{ikR''}}{R''} \simeq \frac{e^{ik(R-R' \cos \Psi)}}{R} \, e^{i \frac{kR'^2}{2R} \sin^2 \Psi}$$

Consequently, a signal sampling or processing which reduces the quadratic phase factor in the integrand of the potential to a factor of unity reduces

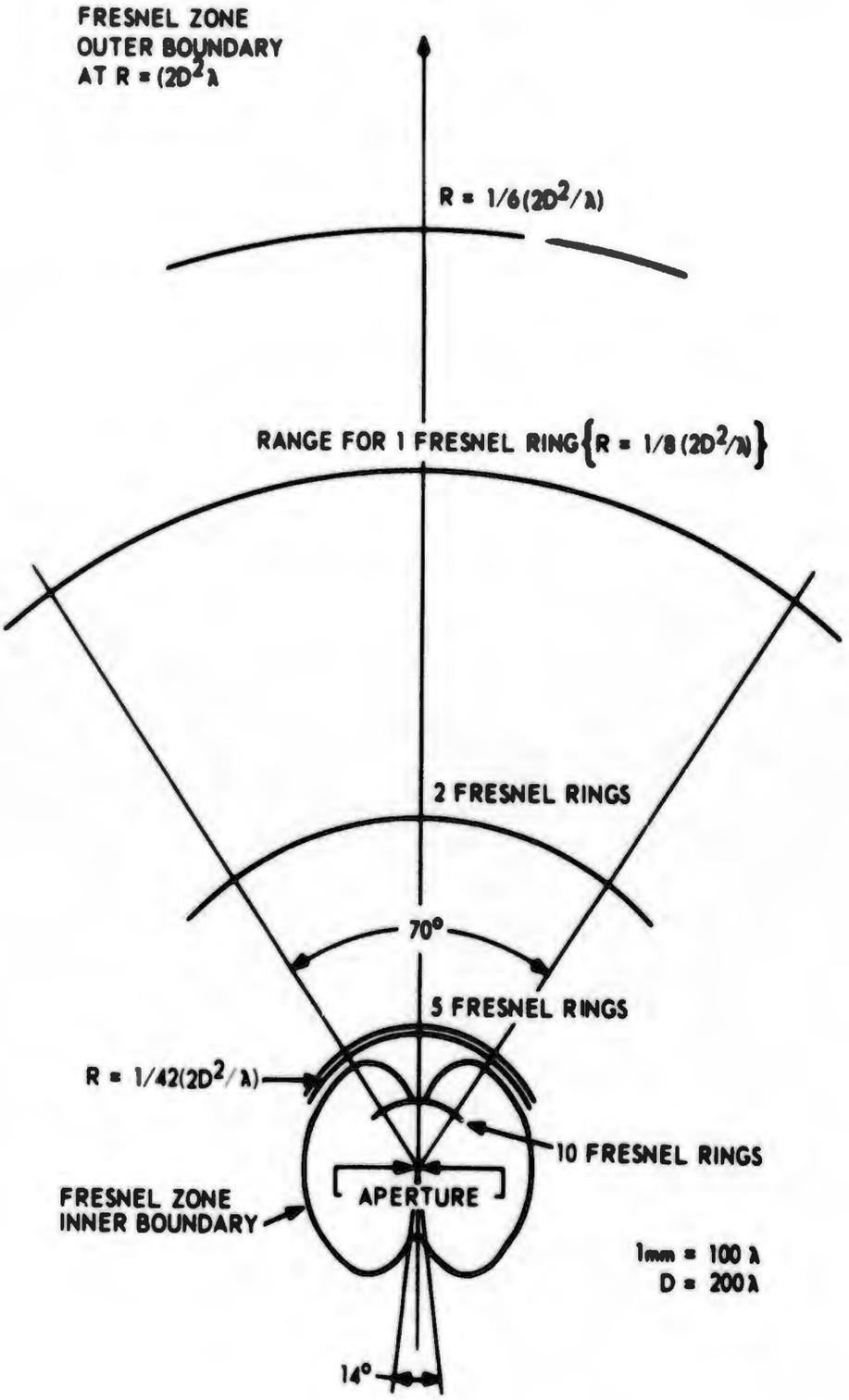

Figure 5. Fresnel Zone Diagram for Aperture Diameter = 200 λ

the scalar Fresnel integral to the Fraunhofer integral. An array of field points (R_n) on a radius through the origin have the same factor $\sin^2\Psi$ in the phase variable. The field intensity at these points may be designated as follows:

$$E_n = \frac{e^{ikR_n}}{R_n} \int_V F(R') \, e^{\frac{ikR'^2}{2R_n}} \sin^2\Psi \; dV$$

These values may be summed at harmonic intervals of R_1^{-1}. If each sampling point is phase adjusted by the factor $e^{ik(R_o-R_n)}$ for end-fire condition, the series may be given the following representation:

$$E_A = \sum_{n=1}^{N} C_n E_n \, e^{ik(R_o-R_n)} \frac{e^{ikR_o}}{R_1} \sum_n nC_n \int_V F(R') \, e^{in\beta_1 \left(\frac{R' \sin\Psi}{R'_o}\right)^2} dV \quad (8)$$

$$\frac{e^{ikR_o}}{R_1} \int_V F(R') \left[\sum_n nC_n \, e^{in\beta_1 (R' \sin\Psi/R'_o)^2} \right] dV = \frac{e^{ikR_o}}{R_1} \int_V F(\vec{R}') g(\rho \sin\Psi) dV$$

kR_o=arbitrary phase reference, $\beta_1 = \frac{kR'^2_o}{2R_1}$, C_n=array element weighting.

$$g(\rho \sin\Psi) = \sum_n nC_n \, e^{in\beta_1(\rho \sin\Psi)^2} = 1, \; 0 \le \rho = R'/R'_o \le 1. \quad (9)$$

($\rho \sin\Psi$=normalized source position radius projection for array angle). In this manner an analytic function, $g(\rho^2 \sin^2\Psi)$, as factor of the far-field integrand can be synthesized. For a source distribution function in a plane, in the above integral, $|R' \sin\Psi|$ describes the projected aperture for the

array angle. Since the function to be synthesized, $g(\rho^2 \sin^2 \Psi)$, is unity in the interval of ρ, $|\sin \Psi|$ is arbitrary if all the array points are in the true Fresnel zone. Consequently the source function may occupy any volume in the focal domain of $g(\rho)$. By rotating the antenna in the focal domain, the far-field transfer pattern may be obtained. Translation of the antenna within the focal domain has negligible effect on the transfer characteristic. The convergence of the focal domain is determined by the number of terms in the series expansion of $g(\rho)$. In principle an arbitrary number of terms are available, but the nearest array point, corresponding to $nc_n e^{i N \beta_1 (\rho \sin \Psi)^2}$ in the series, is limited by the Fresnel approximation. Consequently the more terms that are used, the more distant the farthest term. The technique has most appeal for the case of antennas large with respect to wavelength, for which many Fresnel rings are available. The theoretical design problem consists of determining the array weighting for the desired focal domain with the nearest possible array for focusing convergence corresponding to the traditional far field criterion. Good convergence characteristics with the far field pattern range reduced by nearly an order of magnitude, are possible for an antenna with 10 Fresnel rings available.

1.2.3. Array Weighting Problem

It is desired to obtain a complex power series with a sum of unity. Consider the following transformations:

$$e^{i\beta_1(\rho \sin \Psi)^2} = re^{i\beta} = z, \; r_o e^{i\beta_o} = z_o.$$

The Taylor series has the representation:

$$f(z) = f(z_o) + f'(z_o)(z-z_o) + f''(z_o)(z-z_o)^2/2 + \cdots + f^{(n)}(z_o)(z-z_o)^n/n!$$

$$f(z) = z^{-1}, \; f'(z) = -z^{-2}, \; f^{(n)}(z) = (-1)^n \, n \, ! \, z^{-(n+1)}$$

$$z^{-1} = z_o^{-1} - z_o^{-2}(z-z_o) + z_o^{-3}(z-z_o)^2 + \cdots + (-1)^n z_o^{-(n+1)}(z-z_o)^n$$

$$1 = \frac{r}{r_o} e^{i(\beta-\beta_o)} \sum_{n=o}^{\infty} \left[1 - \frac{r}{r_o} e^{i(\beta-\beta_o)} \right]^n, \; |z-z_o| < r^* \qquad (10)$$

Thus the inverse power of z is one complex power series with desirable properties. In this transformation r is an amplitude factor of the quadratic phase variable, which is the constant unity, and consequently z describes a unit circular arc in the complex plane for the scalar Fresnel integration. It is desired to select a z_o for optimum focusing properties. The Taylor series region of convergence is a circular disk centered at z_o. The radius of the convergence r^* is determined as follows:

$$c_n = (-1)^n z^{-(n+1)}, \; (f(z) = z^{-1})$$

$$r^* = \lim_{n \to \infty} \left| \frac{c_n}{c_{n+1}} \right| = |z_o| = r_o$$

By referring to figure 6, it can be seen that half a complete unit circle of z can never be covered by this series. Other maps of z are available,

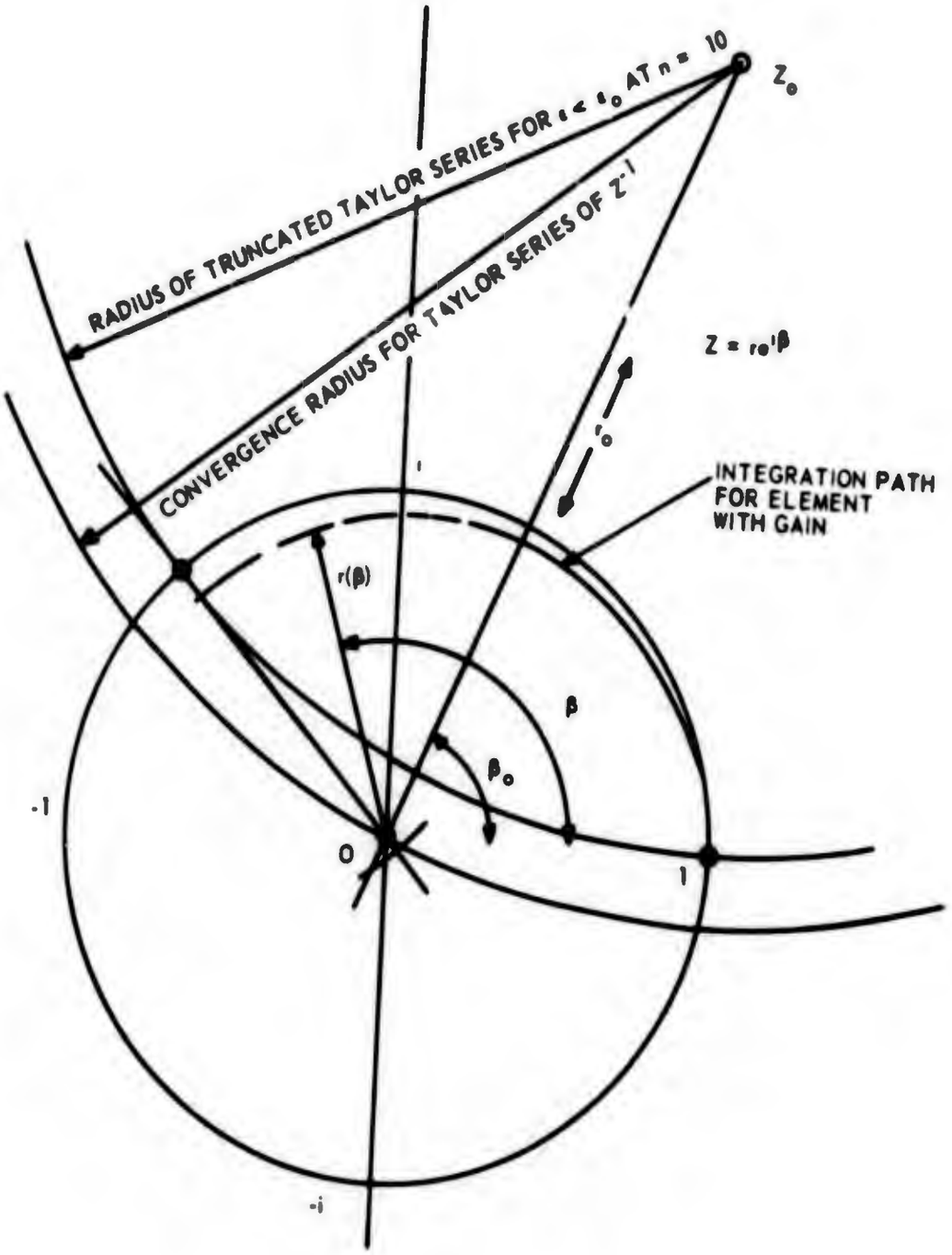

Figure 6. Complex Plane of the Focusing Function

however, such as z^n. The derivities of z^{-1} have the same radius of convergence. The available coverage of (7) is defined by $\beta \leq 2\beta_o$. Maximum coverage of the arc of z is obtained when $\cos \beta_o = r_o^{-1}$. The series (7) can be summed as a geometric series and the error estimated for finite terms as follows:

$$\sum_{n=o}^{N} \xi^n \frac{1-\xi^{N+1}}{1-\xi}, \quad \xi = (1-\frac{z}{z_o})$$

$$\varepsilon_N = 1-\frac{z}{z_o}\sum_{o}^{N}\xi^n = (1-\frac{z}{z_o})^{N+1} = |\varepsilon|e^{i\gamma}$$

$$\varepsilon\varepsilon^* = (\frac{1}{r_o^2})^{N+1}\left[r_o^2-2r_o\cos(\beta-\beta_o)+1\right]^{N+1}, \quad |\varepsilon_N| = (\frac{r_1}{r_o})^{N+1}, \quad r_1 = |z_o-z|$$

$$|\varepsilon|(\text{min.}) = \left(\frac{r_o-1}{r_o}\right)^{N+1}, \quad |\varepsilon|(\text{max.}) = \frac{r_o^2-1}{r_o^2}^{\frac{N+1}{2}}$$

$$\gamma = (N+1)\tan^{-1}\left(\frac{-\sin(\beta-\beta_o)}{r_o-\cos(\beta-\beta_o)}\right)$$

$$\gamma(\text{min.}) = o, \quad \gamma(\text{max.}) = (N+1)\tan^{-1}(\cot\beta_o) = (N+1)(\tfrac{\pi}{2}-\beta_o).$$

The usual acceptable "focusing" error for Fraunhofer pattern is given by:

$$\varepsilon = 1-e^{i\frac{\pi}{8}\rho^2}, \quad o \leq \rho \leq 1; \quad \varepsilon_o = .076-i\ .383, \quad |\varepsilon_o| = .391$$

A design error smaller than ε_o may be used. By expanding the finite series (10) in powers of $\frac{e^{i(\beta-\beta_o)}}{r_o}$, the array coefficients are obtained in general form.

$$\sum_{n=o}^{N}(1-x)^n = \sum_{n=o}^{N}\sum_{k=o}^{n}\frac{(-1)^k\, n!\, x^k}{(n-k)!\,k!} = \sum_{k=o}^{N}\sum_{n=k}^{N}\frac{(-1)^k x^k}{k!}\,\frac{n!}{(n-k)!}$$

$$= \sum_{k=o}^{N}\frac{(-1)^k x^k}{k!}\,\frac{(N+1)!}{(k+1)(N-k)!} = \sum_{n=o}^{N}\frac{(-1)^k(N+1)!}{(N-k)!(k+1)!}x^k, \quad x = \frac{e^{i(\beta-\beta_o)}}{r_o}$$

$$1 \propto \sum_{n=o}^{N}\frac{(-1)^n(N+1)!}{(N-n)!(n+1)!}\,\frac{e^{i(n+1)(\beta-\beta_o)}}{r_o(n+1)} = \sum_{n=1}^{N+1}\frac{(-1)^{n+1}(N+1)!}{(N+1-n)!\,n!}\,\frac{e^{in(\beta-\beta_o)}}{r_o^n}, \quad o \leq \beta \leq 2\beta_o \qquad (11)$$

Thus the array coefficients of (9) are given by:

$$n\,c_n = \frac{(-1)^{n+1}\,N!}{(N-n)!\,n!}\,\frac{e^{-in\beta_o}}{r_o^{\,n}},\quad n = 1 \to N,\quad r_o > 1$$

$$\beta_o = \cos^{-1}(r_o^{-1}),\quad r_o = (1-\varepsilon_o^{\,2/N})^{-1/2},\quad |\varepsilon| \le |\varepsilon_o|$$

In general, the last few terms of (11) will be negligible compared to the assumed error, and consequently a larger N can be used than the number of array points.

The same procedure may be followed for synthesizing the function z^{-2}, with the following result:

$$1 = \left(\frac{z}{z_o}\right)^2 \sum_{n=o}^{\infty} (n+1)\left(1-\frac{z}{z_o}\right)^n,\quad o \le \beta \le 2\,\beta_o$$

For a finite series summed to N:

$$\varepsilon_n = \left(1+N\,\frac{z}{z_o}\right)\left(1-\frac{z}{z_o}\right)^N$$

$$\sum_{n=o}^{N} (n+1)(1-x)^n = \sum_{n=o}^{N}\sum_{k=o}^{n} \frac{(-1)^k\,x^k\,(n+1)n!}{(n-k)!\,k!} = \sum_{k=o}^{N}\sum_{n=k}^{N} \frac{(-1)^k\,x^k}{k!}\,\frac{(n+1)!}{(n-k)!}$$

$$= \sum_{k=o}^{N} \frac{(-1)^k\,x^k}{k!}\,\frac{(N+2)!}{(k+2)(N-k)!} = \sum_{k=o}^{N} \frac{(-1)^k(k+1)(N+2)!}{(k+2)!(N-k)!}\,x^k$$

$$1 \simeq \sum_{n=1}^{N+1} \frac{(-1)^{n+1}(N+2)!\,n}{(n+1)!\,(N+1-n)!}\,\frac{e^{i(n+1)(\beta-\beta_o)}}{r_o^{\,(n+1)}}$$

$$nc_n = \frac{n(N+1)!}{(N-n)!(n+1)!}\,\frac{e^{i(n+1)(\pi-\beta_o)}}{r_o^{\,n+1}},\quad n = 1 \to N,\quad r_o > 1$$

The advantage of this series is that the phase interval of the 1st term is $4\beta_o$, and assuming the availability of an arbitrary number of terms, a 2π phase cycle in the 1st term can be covered. Series based on the expansion

of z^{-n} have phase intervals of $2n\beta_o$, and the larger the value of n, the more terms that are required for the same degree of convergence. It is possible to derive several array weighting distributions that will work for the same array element positions.

As a simple example of the method, the array coefficients for the series based on the expansion of z^{-1} were worked out for an aperture radius of 100λ. An array of only eight elements was considered, which puts the most distant element at about $\frac{1}{6}\left(\frac{2D^2}{\lambda}\right)$. (The 8th element could be discarded with no significant change in the result.) This is the pattern range that has been considered for other approaches to the problem. A brief consideration of the series, based on the expansion of z^{-2} for this problem, indicates that with 10 elements the pattern range can be contracted further. A rigorous analysis of an optimum series would involve consideration of the effect of the array weighting on error signals.

The aperture coverage with specific error ($\varepsilon<\varepsilon_o$) for the example considered is defined by $2\beta_o \cong 133^\circ$. For a given aperture radius (k_o') and frequency, the range R_1 to the distant element is specified by $2\beta_o = \frac{kR_o'^2}{2R_1}$. The array elements are calibrated for end-fire phase and equal amplitude by the factors n^{-1} and e^{-ikR_n}. This might be accomplished by using the far field of a standard gain horn at the focal center. Then the array weighting factor $nc_n = -n|c_n|e^{in(\pi-\beta_o)}$ is superposed. The amplitude weighting factors are shown in table 1. The resultant amplitude weight $|c_n/c_1|$, is shown with the array layout of figure 7. The maximum value of $|c_n|$ has a significance analogous to magnification or "amplitude

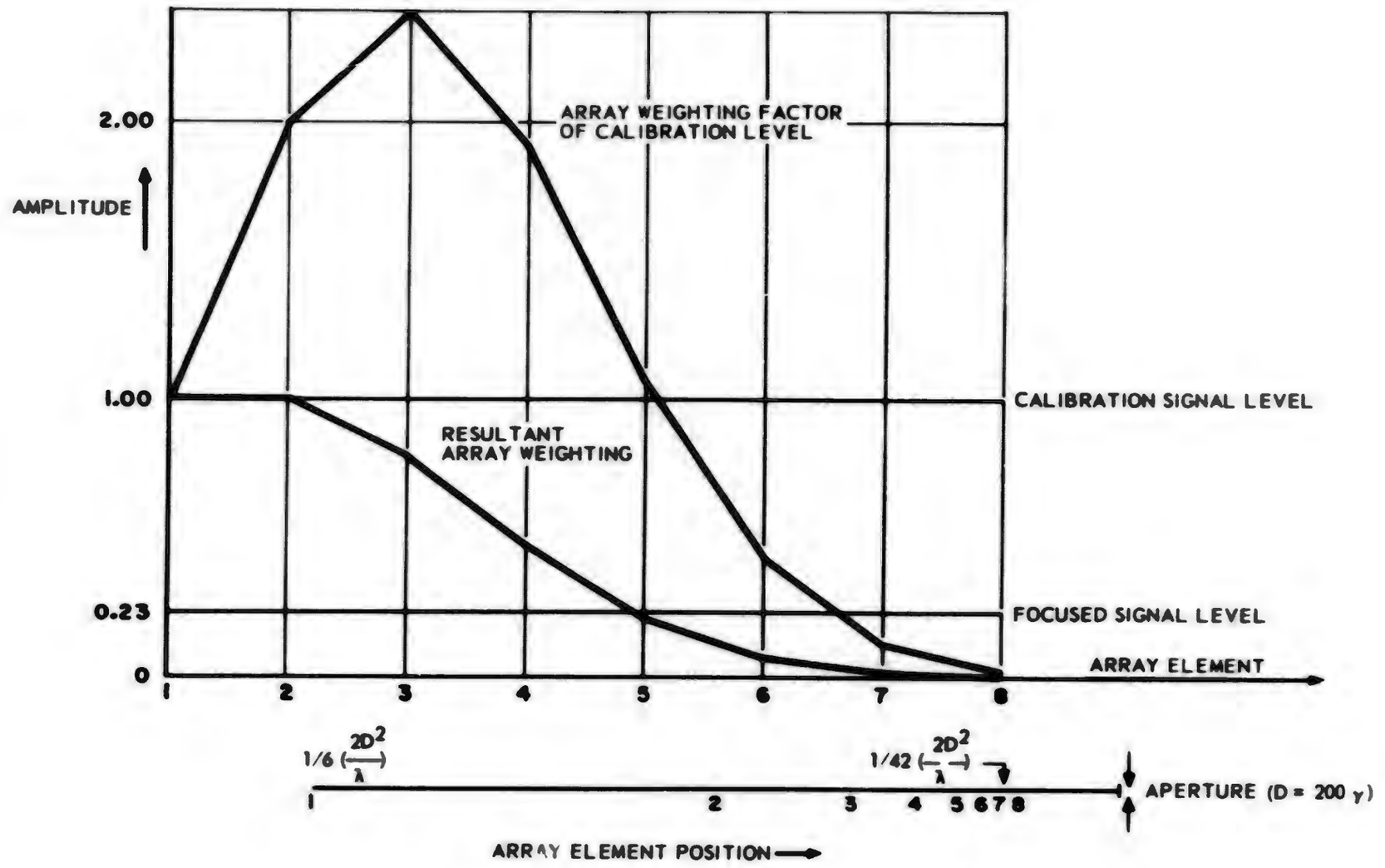

Figure 7. Array Weighting Factors

Table 1

ARRAY WEIGHTING FACTOR

n	$\lvert n\, C_n \rvert$	$\lvert n\, C_n/C_1 \rvert$	$\lvert C_n/C_1 \rvert$	$\epsilon < \frac{\pi}{16}$ $\pm$ ($\delta R/\lambda$ X ℓ_n/λ)
1	4.40	1.0000	1.0000	1144 X 4.23
2	8.80	2.0000	1.0000	286 X 2.12
3	10.560	2.4000	0.8000	127 X 1.41
4	8.4480	1.9200	0.4800	71.6 X 1.06
5	4.73088	1.0752	0.2150	45.8 X .85
6	1.89235	0.4301	0.0717	31.8 X .71
7	0.54067	0.1229	0.0176	23.4 X .60
8	0.10813	0.0246	0.0031	17.9 X .53
9	0.01442	0.0033	0.0004	
10	0.00115	0.0003		
11	0.00004			

extrapolation" relative to what the "far" field strength would be if the aperture were physically focused at the range R_1. The phase adjustment $e^{in(\pi-\beta_o)}$ scans the optimum focal radius points about the unit circle of figure 6. This is analogous to conical beam scanning of an end-fire array, but it is not ordinary scanning, since the elements are unequally spaced. The phase conditions for array focusing occurs at 2π multiples of β, and consequently the focusing will occur in rings about the central disk, so long as the Fresnel inequalities are satisfied. The effect of amplitude taper on the aperture for an array element with gain is represented in figure 6. The focusing function $g(\rho)$ (equation 9) for the problem cited is shown plotted in figure 8. An array design for the upper frequency in a desired band will work better with a fixed aperture size at the lower frequencies, provided there is a separate phase calibration for each frequency.

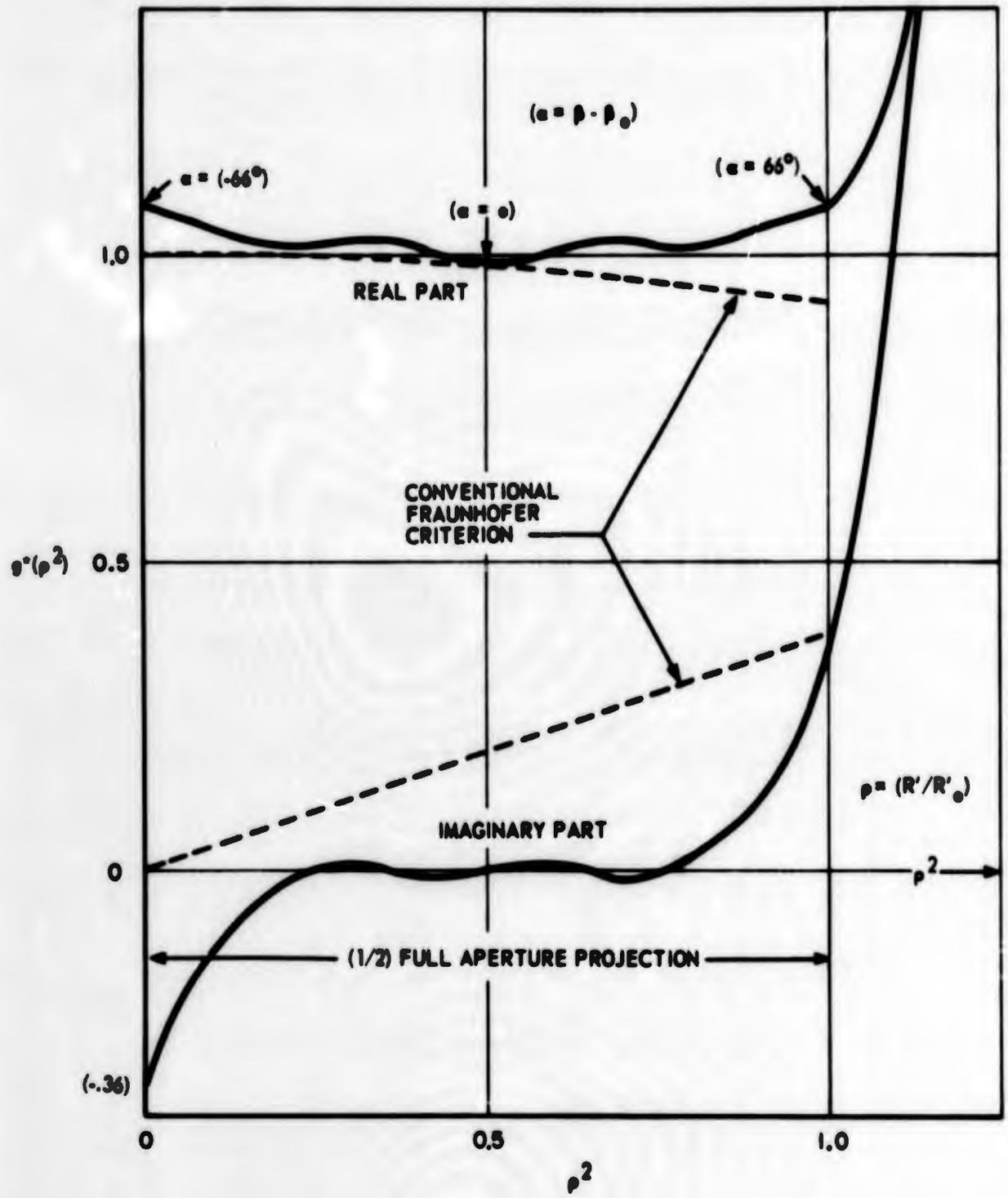

Figure 8. Full Aperture Projection of the Focal Domain

1.2.4 Error Considerations for Physical Array Elements

An indication of the feasibility of Fresnel ring harmonic focusing must include considerations on the tolerances for array alignment and element gain. These tolerances are estimated for individual elements by using the traditional criterion for Fraunhofer correspondence between two antennas. The statistical problem of integrated errors for large array summation is not considered. Consider the scalar case of radiation from a uniformly weighted circular aperture in the Fresnel zone.

$$E(\hat{R}) = \frac{ik\,(1+\cos\theta)}{4\pi}\int_0^{R_o'}\int_0^{2\pi} E_o\,\frac{e^{ikR''}}{R'}\,R'dR'd\varphi'$$

$$R''^{-1} \simeq R^{-1},\ \cos\theta \simeq 1,\ \frac{1}{2}\left[\left(\frac{R'}{R}\right)^2 - \frac{2R'\cos\psi}{R}\right]^2 \ll \frac{1}{2}\left(\frac{R'}{R}\right)^2$$

$$\cos\psi \approx \hat{R}\cdot\hat{R}' = \sin\theta\cos(\varphi-\varphi')$$

In this case the field strength is given by the Lommel functions.[5]

$$E(\hat{R}) = ie^{ikR}\,e^{-ikR_o'^2/2R}\left\langle U_1(w,z) - iU_2(w,z)\right\rangle$$

$$w = kR_o'^2/R,\ z = kR_o'\sin\theta,\ E_o = 1,\ \left|E(\hat{R})\right| \le 1 \qquad (13)$$

$$U_k(w,z) = \sum_0^{\infty}(-1)^n\left(\frac{w}{z}\right)^{n+k} J_{n+k}(z)$$

---

5. G. N. Watson, "Theory of Bessel Functions," Cambridge Univ. Press, 1952, pg. 537

At the asymptotic range:

$$E(\vec{R}) = \frac{w}{\pi}\frac{J_1(z)}{z/2} - i\left(\frac{w}{2}\right)^2\frac{J_2(z)}{(z/2)^2}$$

$$= \frac{\pi}{8}\left\{\Lambda_1(z) - i\left(\frac{\pi}{16}\right)\Lambda_2(z)\right\}, \quad \frac{w}{2} = \frac{\pi}{8}, \quad R = \frac{2D^2}{\lambda}$$

$$\frac{J_n(z)}{(z/2)^n} = \frac{\Lambda_n(z)}{n!}, \quad |\Lambda_n(z)| \leq 1$$

The asymptotic field pattern is $\Lambda_1(z)$, and the "error" pattern is $-i\frac{\pi}{16}\Lambda_2(z)$, for probe to aperture transmission. On the lobe peaks of Λ_1, $|\Lambda_2| \leq |\Lambda_1|$. In this sense the commonly acceptable pattern error criterion has a maximum value of $i\frac{\pi}{16}$. For the reciprocal concept, the normalized field from the probe on axis illuminating the aperture is given as follows:

$$E_p = \cos\frac{\pi}{8}\left(\frac{R'}{R_o'}\right)^2 + i\sin\frac{\pi}{8}\left(\frac{R'}{R_o'}\right)^2, \quad \frac{kR_o'^2}{2R} = \frac{\pi}{8}$$

The maximum phase derivation $\frac{\pi}{8}$ is a measure of the acceptable spherical phase front curvature from the assumed plane phase front. The phase front curvature criterion for probes within the Fresnel zone should be within this value. The required probe position accuracy may be estimated from the Lommel functions as follows:

$$E(\vec{R}) = e^{-i\frac{w}{2}}F(w,z), \quad F = U_1(w,z) - iU_2(w,z)$$

$$\frac{\partial U_1}{\partial w} = \frac{1}{2}\left[U_o + \left(\frac{z}{w}\right)^2 U_2\right], \quad U_o = J_o(z) - U_2$$

$$\frac{\partial U_2}{\partial w} = \frac{1}{2}\left[U_1 + \left(\frac{z}{w}\right)^2 U_3\right], \quad U_3 = \left(\frac{w}{z}\right) J_1(z) - U_1$$

$$\frac{\partial F}{\partial w} = \frac{1}{2}\left\langle J_o - i\left(\frac{z}{w}\right) J_1 - i\left[1 - \left(\frac{z}{w}\right)^2\right] F\right\rangle$$

$$\delta_R E = -\left\langle \left(J_o - i\,\frac{z}{w}\,J_1\right) - i\left[2 - \left(\frac{z}{w}\right)^2\right] e^{-i\,\frac{kR_o'^2}{2R}\left(\frac{kR_o'^2}{2R}\right)} \left(\frac{\delta R}{R}\right)\right.$$

$$|J_o(z)| \leq 1, \; |J_1(z)| < .5819, \; |F(w,z)| < 1.$$

$$z \ll w: \; \delta_R E \simeq -(J_o - 1 2F)\, e^{-i\,\frac{kR_o'^2}{2R}\left(\frac{kR_o'^2}{2R}\right)} \frac{\delta R}{R}$$

$$z \simeq w; \; \delta_R E \simeq iF\, e^{-i\,\frac{kR_o'^2}{2R}\left(\frac{kR_o'^2}{2R}\right)} \left(\frac{\delta R}{R}\right)$$

The radial position error sensitivity is greater for larger values of w and smaller values of z. For large axial angles (z >> w) the Lommel functions are invalid, but increased axial angle decreases tolerance, since

$$\frac{kR_o'^2}{2R} \to \frac{kR_o'^2}{2R} \sin^2 \Psi.$$

For axial positions (z = 0) equation (13) reduces to the following expression.

$$E(R) = -2ie^{ikR}\, e^{i\,\frac{kR_o'^2}{4R}} \sin \frac{kR_o'^2}{4R}$$

$$\delta_R E = -2i\, e^{i\,\frac{kR_o'^2}{4R}} \left(-\frac{kR_o'^2}{4R}\,\frac{dR}{R}\right)\left(i \sin \frac{kR_o'^2}{4R} + \cos \frac{kR_o'^2}{4R}\right)$$

$$= i\, e^{i\,\frac{kR_o'^2}{2R}} \left(\frac{kR_o'^2}{2R}\right) \frac{\delta_R}{R}$$

Consequently, the criterion assumed for radial position tolerance is the following:

$$\left|\left(\frac{kR_o'^2}{2R}\right)\frac{\delta_R}{R}\right| \leq \frac{\pi}{16}$$

This assures that the relative phase front curvatures of the array points are within the $\frac{\pi}{8}$ criterion for their assumed relative values at the aperture. The angular position tolerance may be similarly estimated.

$$\frac{\partial U_1}{\partial z} = -\frac{z}{w}U_2$$

$$\frac{\partial U_2}{\partial w} = -\frac{z}{w}U_3 = \frac{z}{w}U_1 - J_1(z)$$

$$\frac{\partial F}{\partial z} = i\frac{z}{w}\left[F - \frac{w}{z}J_1(z)\right]$$

$$\delta_z F = i\,\delta z\left[\frac{z}{w}F - J_1(z)\right]$$

$z \ll w$: $\delta F \cong -i\delta z J_1(z)$, $\delta z = kR_o' \cos\theta\,\delta\theta$

$z \simeq w$: $\delta F \simeq iF\delta z$, $\delta\theta = \Delta/R$

Thus the criterion for angular alignment is the following:

$$|kR_o' \ell_{\Delta/R})| \leq \pi/16.$$

As an example, for the case of $R_o' = 100\,\lambda$, at $R = 10R_o'$:

$$\pm\,\delta R_{10} < \frac{\pi}{16}\cdot\frac{2R^2}{kR_o'^2} = 6.25\lambda\,, \quad \frac{kR_o'^2}{2R} = 10\pi \tag{14}$$

$$\pm\,\ell_{\Delta_{10}} < \frac{\pi}{16}\cdot\frac{R}{kR_o'} = .32\lambda\,,$$

At the range for one Fresnel ring ($\frac{kR_n^2}{2R} = \pi$):

$$\delta R_1 = 100\ \delta R_{10},\ \ell_{A_1} = 10\ \ell_{A_{10}}$$

With uniform position tolerance, the error signal due to array misalignment for the distant element is one to ten percent the error for the near element. The actual position tolerance depends upon the array weighting and integrated errors. For the example cited, the array weight of the distant element is about 4 relative to the unit focusing function, (see figure 7) and the theoretical weights for the elements beyond the eighth element result in a relatively negligible signal. Consequently, error magnification relative to the focused function does not prohibit application of the technique, as it has been found to do in other approaches to the problem. Since the incident signal level is approximately equal to the array weight relative to the focused signal level, the error criterion for the distant element is about an order of magnitude smaller than the traditionally acceptable value for a single element. (The focusing design error for Fraunhofer approximation is not an array signal error.) A statistical consideration of the integrated random errors over N elements will result in a probable factor of less than $\sqrt{N}$ for the focusing function error. This aspect of the problem requires study.

The array point position is assumed to be confined to a prolate spheroidal domain with axes defined by the inequalities of (14). For a physical array element with gain, the element's point source distribution must be contained in this spheroid. In the example cited, the end-fire gain

available is about 17 db. This is the gain figure for which the element's far field range is within the range error for the phase front curvature tolerance at the aperture antenna.

The amplitude taper at the aperture may be described as $r'(\beta)$ in figure 6. By referring to this figure it is clear that $r'(\beta)$ need not equal one to be contained in the disk of convergence about a_o. If $r'(\beta)$ has the taper shown; however, the nth element must have the taper $r^n(\beta)$, for the array summation to be unity. For the gain figure cited, the taper is negligible.

For small θ the element pattern has the form:

$$\cos\theta \simeq 1 - \frac{1}{2}\theta^2, \quad \cos^m\theta \simeq 1 - \frac{m}{2}\theta^2.$$

Let the aperture amplitude decrement be 10% for the near element.
For the aperture of the array example previously indicated:

$$R_{10} = 10\,R_o', \quad \theta_{10} = 0.1$$

$$\cos^M\theta_{10} = 0.9 = 1 - \frac{M}{2}\theta_{10}^2, \quad M = 20$$

The element pattern has the form:

$$E(\theta) = \cos^{20}\theta, \quad P(\theta) = \cos^{40}(\theta).$$

This pattern has a directive gain of 19 db., and the amplitude taper effect on the focusing is negligible. Allowing for efficiency, an element gain of up to 15 db is indicated for the example. With this gain the available power level with practical transmitters is adequate for pattern measurement.

The array points are too far apart for element interaction. If 10 elements were used with an aperture of $R_o' = 100\lambda$, the closest elements would be separated by over 100λ. Second order interaction with the aperture can also be shown to be negligible.

Dish radiation: $E_{T_2} = iE_o e^{ikR} e^{-kR_o'^2/2R} F(kR_o'^2/R, z)$

Dipole radiation: $E_{T_1} = -\frac{i\eta I_o kh}{4\pi R} e^{ikR}$

Dish aperture field: $E_D \simeq -\frac{i\eta I_c kh}{4\pi R} e^{ikR} e^{ikR'^2/2R} e^{-ikR'\cos\Psi}$

Dipole reception: $I_d \simeq iE_{T_2} \frac{3\lambda/2}{\eta kh}$

$$E_o < E_D = -E_{T_1} e^{ikR'^2/2R} e^{-ikR'\cos\Psi}$$

$$E_{T_2} < -i E_{T_1} \left(\tfrac{1}{2}\right) e^{ikR} e^{-ikR_o'^2/R} F(kR_o'^2/R, 2z)$$

$$I_d < \frac{\frac{3}{2}\lambda I_o}{8\pi R} F\left(\frac{kR_o'^2}{R/2}, 2z\right), |F| \leq 1$$

$$I_d/I_o < \frac{3\lambda}{16\pi R}$$

For the case of $R = 10 R_c' = 1000\lambda$, the interaction is negligible with an element gain factor of 100.

One of the more stringent requirements of this technique consists of the necessary phase stability and end-fire phase calibration over a very

long array. For the example considered, the desired frequency stability is within the state-of-the-art for an array length of about $10^{4}\lambda$. The requisite phase stability, and the fact that the focused signal amplitude level is about 1/4 the signal level on the largest weighted array elements, constitute the most serious problems inherent in the system. Assuming the random error signal problem can be controlled, it has been shown that the entire Fraunhofer pattern can in principle be measured with normal error at a pattern range reduced to 1/6 (or less) the normal range ($R = 2D^2/\lambda$) with an array of 7 or 8 elements for a general antenna contained in a sphere with a diameter of 200λ. To the same degree of accuracy, an absolute gain measurement can be made with the array by using a standard gain horn in the calibration, and the appropriate array factor.

2. MONOPULSE ANTENNAS

2.1 Survey of Methods for Calculating Fresnel Patterns of Circular Apertures with Circularly Symmetric Distributions

This survey is included in this report as a discussion of the relative accuracy, the limitations, and the ease of computation of Fresnel patterns of circular apertures with each of several available methods. In addition, the possibilities of generalizing each of these methods to calculate the patterns of circular aperture monopulse antennas was considered.

There are two basically different points of departure for calculating the Fresnel patterns of an antenna. Perhaps the starting point used most often is a scalar diffraction type integral [6,7] which, omits all terms of order higher than 1/r and ignores edge effects due to the discontinuity at the edge of the aperture. This integral takes the form

$$E(R, \theta, \phi) = \frac{j\,k}{4\pi} \int_A F(\rho,\beta) \frac{e^{-jkr}}{r} \left(1 + \frac{Z}{r} \right) dA \qquad (15)$$

where $E(R,\theta, \phi)$ is the complex magnitude of the electric field intensity, r is the distance from the aperture point to the field point, and $F(\rho,\beta)$ is the aperture distribution (see figure 9). The usual assumption for circular apertures is that the phase is uniform across the aperture. However, for a nonuniform phase illumination $F(\rho,\beta)$ is complex and can be separated into a real and imaginary part

6. M. K. Hu, "Study of Near-Zone Fields of Large Aperture Antennas," Syracuse Univ., Research Inst., Syracuse, N.Y., Final Report, Pt. 2 (April 1957)
7. R. A. Gerlock, "Study of Interference Aspects of Fresnel Region Phenomena," Final Report Contract No. AF 30(602)-2507.

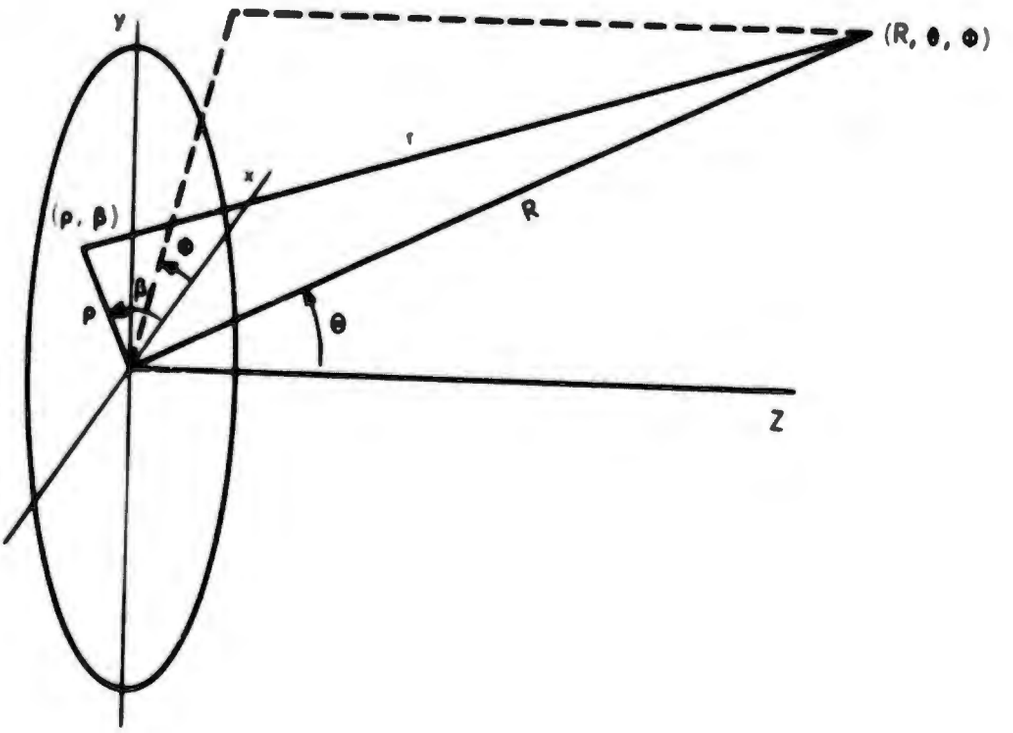

Figure 9. Coordinate System for the Circular Aperture

$$F(\rho,\beta) = \mathrm{Re}\left\{F(\rho,\beta)\right\} + i\,\mathrm{Im}\left\{F(\rho,\beta)\right\}$$

and the integral given in equation (15) may be applied to the real and imaginary part separately.

A second method, which is more exact, is based on the integrated vector wave equation[8]

$$E(R,\theta,\phi) = \frac{j\eta}{4\pi}\iint_A \left\{(\vec{J}\cdot\nabla)\nabla\psi + k^2\vec{J}\psi + \frac{1}{j\eta}\vec{K}\times\nabla\psi\right\} dA \quad (16)$$

where $\vec{J}_s = \hat{n}\times\vec{H}$ and $\vec{K} = \hat{n}\times\vec{E}$ are the electric and magnetic surface currents on the aperture and $\psi = \frac{e^{-jkr}}{kr}$. This method is mathematically rigorous and the scalar equation may be derived from it by neglecting certain terms in this expression; however, computation of Fresnel fields from this expression is quite difficult.

2.1.1 Hansen and Balin's Vector Method

Hansen and Balin[9] have performed an analysis of the Fresnel field based upon the integrated vector wave equation. This is a desirable starting point for computing the Fresnel field of an antenna since the fields calculated by this method satisfy Maxwell's equations subject to the boundary conditions at the source. This method takes into account induction field terms i.e., terms $(1/r)^2$ and higher, and includes the line integrals which express the effects caused by discontinuities at the edge of the antenna. These terms are necessary to produce a field which is mathematically rigorous, however they are neglected by the scalar theory. The edge integral becomes significant only for wide angles near the aperture and has little effect on the field near axis.

8. S.S. Silver, "Microwaves Antenna Theory and Design," Lab. Series, McGraw-Hill Hill, p 160. Vol 12 Rad.
9. R.C. Hansen and L.L. Balin, "A New Method of Near Field Analysis," IRE Trans. on Antennas & Propagation, December, 1959, p 458-467.

The terms associated with higher powers of 1/r also become significant near the antenna; however, the effect of these terms becomes negligible at radial distances greater than several antenna diameters.

By expanding the vector operators in the above integral an expression is obtained which is reduced to an infinite series with coefficients which are integrals of Bessel functions and integrals of Gegenbauer polynominals. Some sample computations were performed by Hansen and Balin using an IBM 704 computer for a 10λ aperture. This method has the computational disadvantage that a large number of integrals must be evaluated; in addition, if one desires to retain rigor and accuracy, a new computation must be performed for each antenna size. These features make it a rather undesirable method for tabulating a set of tables which enhance Fresnel pattern calculations.

2.1.2 Method of Lommel and Hu

This method starts with the scalar diffraction integral and using approximations to simplify the analysis reduces the integral to Lommel functions. This was done by Lommel for the case of a uniform aperture distribution and was generalized by Hu for aperture distributions of the form

$$(1 - (\rho/a)^2)^n.$$

Newton's recursion formula is used to obtain the Fresnel approximation for r in the exponential function and it is assumed that $\frac{2}{R} \approx \frac{1}{r}\left(1 + \frac{Z}{r}\right)$ outside the exponential. Since the aperture illumination $F(\rho,\beta)$ is assumed to have circular symmetry, i.e., $F(\rho,\beta) = F(\rho)$, $E(R, \theta, \phi)$ is independent of ϕ. Hence the scalar integral is reduced to

$$E(r,\theta) = jk \frac{e^{-jkR}}{R} \int_0^a F(\rho)\, J_0(k\rho \sin\theta)\, e^{-jk\frac{\rho^2}{2R}}\, \rho\, d\rho$$

which by a change of variable

$$\rho = \rho/a,\ u = k\,a \sin\theta, \nu = \frac{k\,a^2}{R}$$

the equation becomes

$$E(R,\theta) = \nu e^{-jkR}\, e^{-j\left(\frac{\pi}{2} + \frac{\nu}{2}\right)} \int_0^1 F(\rho)\, J_0(u\rho)\, e^{-j\frac{\nu}{2}(1-\rho^2)}\, \rho\, d\rho$$

For $F(\rho) = (1-\rho^2)^n$

$$E(r,\theta) = \nu\, e^{-jkR}\, e^{-j\left(\frac{\pi}{2} + \frac{\nu}{2}\right)}\, W_o^n\,(\nu,u)$$

where

$$W_o^n(\nu,u) = \left(\frac{2}{j}\right)^n \left\{ -\frac{\partial^n}{\partial \nu^n} \frac{U_1(\nu,u)}{\nu} + j \frac{\partial^n}{\partial \nu^n} \frac{U_2(\nu,u)}{\nu} \right\}$$

and

$$U_k(\nu,u) = \sum_{n=0}^{\infty} (-1)^n \left(\frac{\nu}{u}\right)^{2n+k} J_{2n+k}(u)$$

$U_k(\nu,u)$ is a Lommel function of two variables. Thus the near field patterns may be calculated by evaluating these series for $U_k(\nu,u)$ and their derivatives. It should be noted that due to the nature of the Fresnel approximation this method is limited to an area at least a few antenna diameters away from the aperture and to an angular region including the main beam and the first few sidelobes.

Hansen and Balin have computed patterns for a 10λ aperture by this method and compared the results to those computed from the vector method and found that the Lommel function method gave good results even at distances only 10λ away from the aperture. This method should have an even closer correlation to computations made with Gerlock's computer program [7] since both start with the scalar diffraction integral and differ only in the approximations which are used. Several patterns were computed by both methods in section 8 and identical results were obtained.

2.1.3 Computer Program of the Scalar Diffraction Integral

Gerlock[7] has performed a computer program for the scalar integral using the relationship

$$1 + \frac{z}{r} \doteq 2$$

and expanding $\frac{e^{-jkr}}{r}$ in terms of a series of products of Bessel functions and Legendre polynominals. Although the above approximation is the only one used in performing the computer program for the scalar integral, a different computer program must be performed for each aperture size. This difficulty was eliminated by modifying the range variable to be a function of the aperture size and thus generalizing the patterns of a 40λ aperture so as to be able to compute the patterns for an arbitrary sized aperture. This approximation also shows up in the small angle Fresnel approximation of Lommel and Hu. Thus the Fresnel fields for unequal sized apertures calculated by this method are the same for corresponding values of $R\lambda/D^2$.

2.2 Amplitude Monopulse Antennas

2.2.1 Aperture Illumination from an Offset Feed

The monopulse antenna to which this study was devoted consisted of a paraboloidal reflector fed by four horns whose phase centers are placed symmetrically about the focal point of the reflector as shown in figure 10. However, the results which were obtained may be applied immediately to circular aperture lens monopulse antennas or monopulse antennas having Cassegrain subreflectors and to monopulse antennas having only two-horn feed systems. The only additional complication is that in the case of Cassegrain reflectors the radiation blocking of the subreflector must be subtracted from the radiation pattern produced by the main reflector. The following analysis assumes that the radiation pattern of each of the monopulse horns are known and are identical and that the antenna dimensions are known. It will be assumed that the displacement, δ, of the phase center of each feed horn from the focal point be sufficiently smaller than the antenna radius such that the amplitude distribution across the aperture is approximately the same as for an on-center feed. For the monopulse antenna which was considered, each feed antenna had approximately a circularly symmetric radiation pattern. However, in the following analysis we shall assume that the amplitude of the aperture distribution of a single horn is given by

$$F(\rho,\theta) = F_{\xi}(\rho)\cos^2\theta + F_{\eta}(\rho)\sin^2\theta \qquad (17)$$

where $F_{\xi}(\rho)$ and $F_{\eta}(\rho)$ are the radiation patterns in the ξ and η planes respectively. This is a good approximation to the radiation properties of a rectangular aperture where $F(\xi,\eta) = F(\xi)F(\eta)$. In the case $F_{\xi}(\rho) = F_{\eta}(\rho)$ equation (17) reduces to a circularly symmetric distribution.

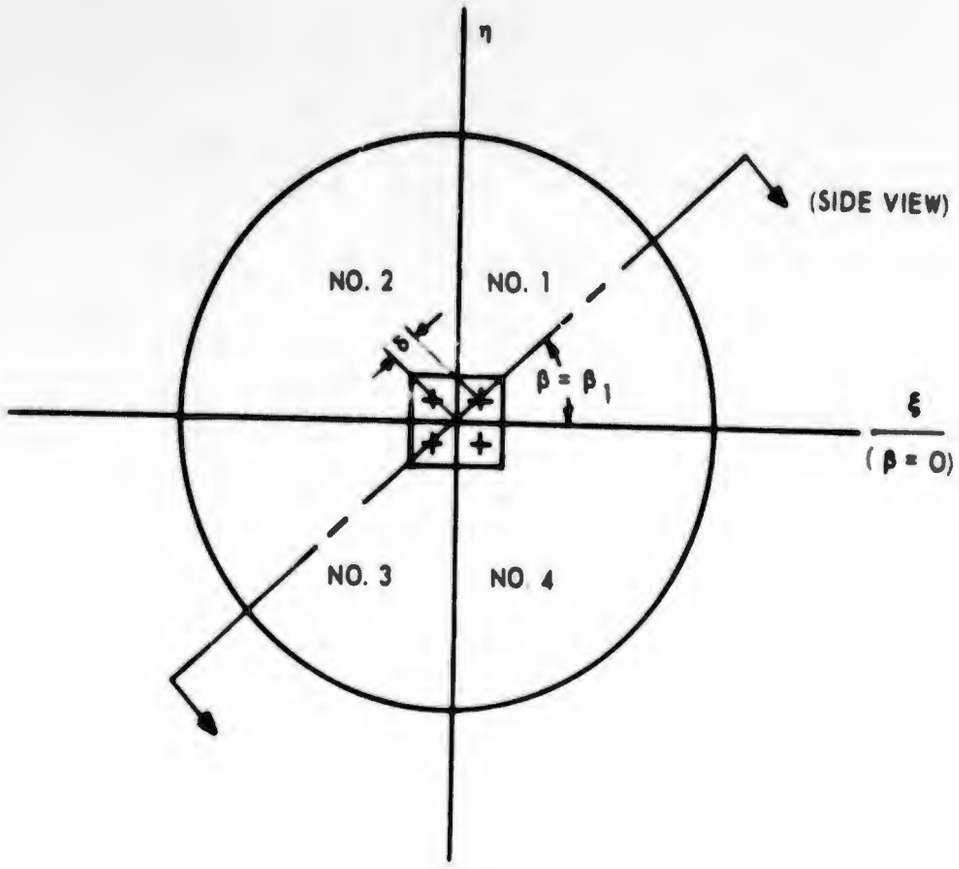

Figure 10. Front View of Monopulse Feed and Aperture

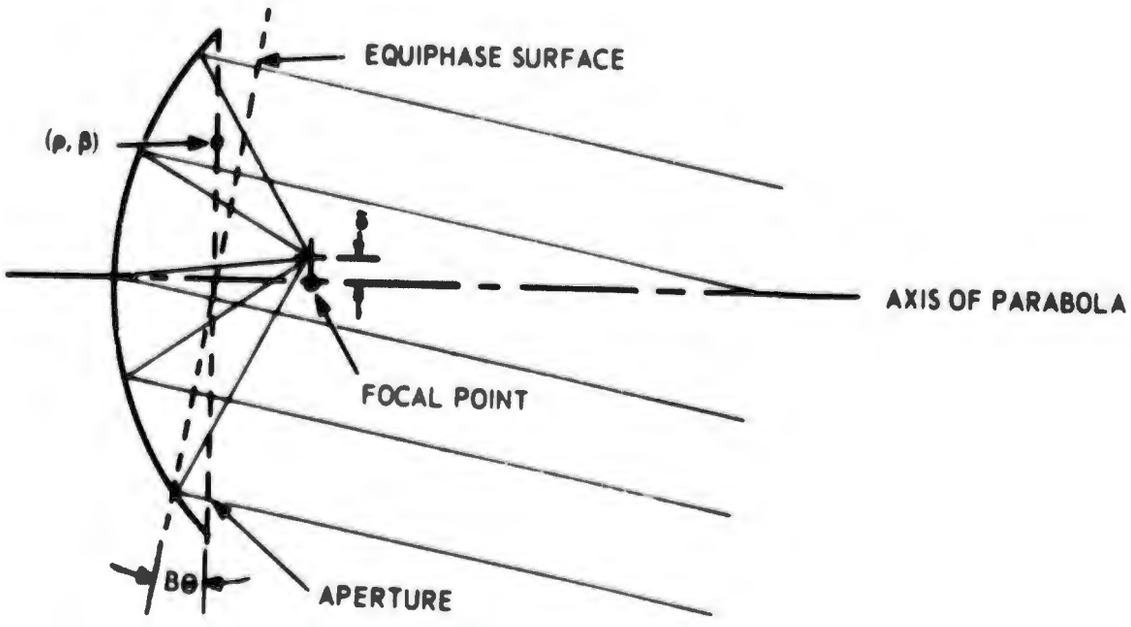

Figure 11. Side View of Offset Feed

If the feed is moved laterally a small distance δ in the direction $\theta = \theta_o$ from the focal point as shown in figure 10 this creates a non-uniform phase front across the aperture. However if δ is sufficiently small the phase variation $\phi(\rho)$ in the plane $\theta = \theta_o$ of the feed and the antenna axis is approximately linear and is given by

$$\phi(\zeta,\theta_o) = B\rho \tan^{-1}\frac{\delta}{f} \simeq B\rho\,\theta - (\theta = \tan^{-1}\frac{\delta}{f}) \qquad (18)$$

where f is the focal length and B is the beam deviation factor.[10]

$B = \frac{\text{Beam offset angle}}{\text{Feed offset angle}}$. Thus in general the aperture distribution from a single offset feed will be given by $F'(\zeta,\theta) = F(\zeta,\theta)e^{jkBa\theta\,\zeta\cos(\theta-\theta_o)}$ where $\zeta = \rho/a$ is the normalized radial coordinate and "a" is the antenna radius.

2.2.2 Illumination from Four Horn Monopulse Difference Feed

Let us consider the azimuth difference mode of a four feed monopulse in detail. Since the sum and the other difference mode radiation characteristics may be calculated in the same manner only a few of the more important steps will be shown for the sum mode in section 2.2.4. For the azimuth difference mode let $F_i(\zeta,\theta), i = 1,2,3,4$ denote the amplitude of the aperture illumination of the i-th primary feed antenna, then due to the opposing phase condition in the monopulse circuitry with primary antennas 1 and 4 fed out of phase with 2 and 3 (see figure 11)

$$F_1(\zeta,\theta) = F_4(\zeta,\theta) = -F_2(\zeta,\theta) = -F_3(\zeta,\theta) \qquad (19)$$

---

10. Y. T. Lo, "On the Beam Deviation Factor of A Parabolic Reflector", Trans. IRE, Vol. AP-8, May 1960, pp. 347-349

(Note that this assumption requires that any mutual coupling effect on the horn patterns be negligible.) It is assumed that the primary feeds are symmetrically placed such that $\beta_1 = \pi - \beta_2 = -\beta_4 = \beta_3 - \pi$, then due to the difference in coordinates of the feeds, the phase of the horns at the aperture is

$$\begin{aligned} \phi_1(\zeta,\beta) &= -\phi_3(\zeta,\beta) = Ba\,\theta\,\zeta\cos(\beta-\beta_1) \\ \phi_4(\zeta,\beta) &= -\phi_2(\zeta,\beta) = Ba\,\theta\,\zeta\cos(\beta+\beta_1) \end{aligned} \tag{20}$$

So the total aperture illumination is given by (where $\theta' = kBa\theta$)

$$F'(\zeta,\beta) = \sum_1^4 F_i(\zeta,\beta) = F_1(\zeta,\beta)\left\{ e^{j\theta'\zeta\cos(\beta-\beta_1)} - e^{-j\theta'\zeta\cos(\beta-\beta)} + e^{j\theta'\zeta\cos(\beta+\beta_1)} - e^{-j\theta'\zeta\cos(\beta+\beta_1)} \right\}$$

$$= 2i\,F_1(\zeta,\beta)\left\{ \sin\left[\zeta\theta'\cos(\beta-\beta_1)\right] + \sin\left[\zeta\theta'\cos(\beta+\beta_1)\right] \right\} \tag{21}$$

Now since $\theta' = kBa\theta$ is rather small ($\theta' < 3$ for a well designed monopulse antenna) the sine terms in (21) may be approximated by the first few terms of the power series

$$\sin\left[\zeta\theta'\cos(\beta\pm\beta_1)\right] = \left[\zeta\theta'\cos(\beta\pm\beta_1)\right] - \frac{\zeta^3\theta'^3}{3!}\cos^3(\beta\pm\beta_1) + \cdots$$

(In the numerical example considered in 2.2.6 the first 5 terms were significant.) Then eq.(21) may be reduced to the desired form by the following trigonometric identities. First by use of the multiple angle formulas and the above power series

$$\cos^3 \xi = \tfrac{1}{4}\left[3 \cos \xi + \cos 3\xi\right]$$

$$\cos^5 \xi = 1/16\left[10 \cos \xi + 5 \cos 3\xi + 1 \cos 5\xi\right]$$

$$\cos^7 \xi = 1/64\left[35 \cos \xi + 21 \cos 3\xi + 7 \cos 5\xi + 1 \cos 7\xi\right]$$

$$\cos^9 \xi = 1/256\left[126 \cos \xi + 84 \cos 3\xi + 36 \cos 5\xi + 9 \cos 7\xi + 1 \cos 9\xi\right]$$

and by use of the formula

$$\cos m(\theta \pm \theta_1) = \cos m\theta \cos m\theta_1 \mp \sin m\theta \sin m\theta_1$$

We may reduce (21) to the following form

$$F'(\zeta,\theta) = 2iF_1(\zeta,\theta) \sum_{m \text{ odd}} \left\{ P_m(\zeta) \cos m\theta + R_m(\zeta) \sin m\theta \right\} \tag{23}$$

where P_m and R_m are polynomials in odd powers of ζ which are determined by the above substitutions. Since the assumed aperture amplitude distribution (17) may be rewritten

$$F_1(\zeta,\theta) = \tfrac{1}{2}\left[F_\xi(\zeta) + F_\eta(\zeta)\right] + \tfrac{1}{2}\left[F_\xi(\zeta) - F_\eta(\zeta)\right] \cos 2\theta \tag{24}$$

then by use of the identities

$$\begin{aligned} \cos 2\theta \cos m\theta &= \tfrac{1}{2}\left[\cos (m+2)\theta + \cos (m-2)\theta\right] \\ \cos 2\theta \sin m\theta &= \tfrac{1}{2}\left[\sin (m+2)\theta + \sin (m-2)\theta\right] \end{aligned} \tag{25}$$

The aperture distribution may be written as a series

$$F'(\zeta,\theta) = \sum_{m \text{ odd}} \left\{ P'_m(\zeta) \cos m\theta + R'_m(\zeta) \sin m\theta \right\} \tag{26}$$

However only 4 or 5 terms of the series are necessary to give an accurate description of the monopulse aperture distribution.

For the special case of $\theta_1 = 45^\circ$ we may write the second part of (21) as

$$\sin\left[\zeta\theta' \cos\left(\theta-\tfrac{\pi}{4}\right)\right] + \sin\left[\zeta\theta'\left(\theta+\tfrac{\pi}{4}\right)\right] = \sum_{m \text{ odd}} \left[P_m(\zeta)\cos m\theta + R_m(\zeta)\sin m\theta\right]$$

$$= \sqrt{2}\left\{\cos\theta\left[\theta'\zeta - \frac{3(\theta'\zeta)^3}{4(3!)} + \frac{10(\theta'\zeta)^5}{16(5!)} - \frac{35(\theta'\zeta)^7}{64(7!)} + \frac{126(\theta'\zeta)^9}{256(9!)} - \cdots\right]\right.$$

$$+ \cos 3\theta\left[\frac{(\theta'\zeta)^3}{4(3!)} - \frac{5(\theta'\zeta)^5}{16(5!)} + \frac{21(\theta'\zeta)^7}{64(7!)} - \frac{84(\theta'\zeta)^9}{256(9!)} + \cdots\right] \qquad (27)$$

$$+ \cos 5\theta\left[-\frac{(\theta'\zeta)^5}{16(5!)} + \frac{7(\theta'\zeta)^7}{64(7!)} - \frac{36(\theta'\zeta)^9}{256(9!)} + \cdots\right]$$

$$\left. + \cos 7\theta\left[-\frac{(\theta'\zeta)^7}{64(7!)} + \frac{9(\theta'\zeta)^9}{256(9!)} - \cdots\right] + \cdots\right\}$$

Since the method of calculating the pattern from this expression for the aperture distribution is the same for both the sum and difference mode we shall first derive the corresponding expression for the sum mode.

2.2.3 Illumination from Four Horn Monopulse Sum Feed

For the sum mode each of the four primary antennas are fed in phase, thus each has the same amplitude illumination function

$$F_1(\zeta,\theta) = F_2(\zeta,\theta) = F_3(\zeta,\theta) = F_4(\zeta,\theta)$$

Thus the sum of the four primary feed aperture illuminations is given by

$$F'(\zeta,\theta) = 2F_1(\zeta,\theta)\left\{\cos\left[\zeta\theta' \cos(\theta-\theta_1)\right] + \cos\left[\zeta\theta' \cos(\theta+\theta_1)\right]\right\} \qquad (28)$$

Then by expanding the cosine terms in power series

$$\cos\left[\zeta\theta' \cos(\theta\pm\theta_1)\right] = 1 - \frac{\left[\zeta\theta' \cos(\theta\pm\theta_1)\right]^2}{2!} + \frac{\left[\zeta\theta' \cos(\theta\pm\theta_1)\right]^4}{4!} - \cdots$$

and expanding the $\cos^n(\theta \pm \beta_1)$ in their finite Fourier series

$$\cos^2 \xi = \frac{1}{2}(1 + \cos 2\xi)$$

$$\cos^4 \xi = \frac{1}{8}(3 + 4\cos 2\xi + 1\cos 4\xi) \tag{29}$$

$$\cos^6 \xi = \frac{1}{32}(10 + 15\cos 2\xi + 6\cos 4\xi + 1\cos 6\xi)$$

$$\cos^8 \xi = \frac{1}{128}(35 + 56\cos 2\xi + 28\cos 4\xi + 8\cos 6\xi + 1\cos 8\xi)$$

$$\cos^{10} \xi = \frac{1}{512}(126 + 210\cos 2\xi + 120\cos 4\xi + 45\cos 6\xi + 10\cos 8\xi + \cos 10\xi)$$

and using the relationship

$$\cos m(\theta \pm \beta_1) = \cos m\theta \cos m\beta_1 \pm \sin m\theta \sin m\beta_1$$

We may reduce (28) to the form

$$F'(\zeta,\theta) = 2F_1(\zeta,\theta) \sum_{m \text{ even}} \left[Q_m(\zeta)\cos m\theta + T_m(\zeta)\sin m\theta\right] \tag{30}$$

where $Q_m(\zeta)$ and $T_m(\zeta)$ are polynomials in even powers of ζ which are determined by the above substitutions.

For the special case $\beta_1 = \frac{\pi}{4}$, (30) is somewhat simpler than in the general case and may be written

$$F'(\zeta,\theta) = 2F_1(\zeta,\theta)\left\{\left[1 - \frac{\zeta^2\theta,^2}{2!(2)} + \frac{3\zeta^4\theta,^4}{4!(8)} - \frac{10\zeta^6\theta,^6}{6!(32)} + \frac{35\zeta^8\theta,^8}{8!(128)} - \frac{126\zeta^{10}\theta,^{10}}{10!(512)} + \cdots\right]\right.$$

$$- \cos 4\theta\left[\frac{\zeta^4\theta,^4}{4!(8)} - \frac{6\zeta^6\theta,^6}{6!(32)} + \frac{28\zeta^8\theta,^8}{8!(128)} - \frac{120\zeta^{10}\theta,^{10}}{(10)!(512)} + \cdots\right] \tag{31}$$

$$\left. + \cos 8\theta\left[\frac{\zeta^8\theta,^8}{8!(128)} - \frac{10\zeta^{10}\theta,^{10}}{10!(512)} + \cdots\right] + \cdots\right\}$$

It may be noted that in this case not only have all the sine terms cancelled, but also the cos 2θ, cos 6θ, cos 10θ,... terms have also cancelled. However, if $F_1(\zeta,\theta)$ is not independent of θ, i.e. if the primary feed pattern is not circularly symmetric, all even cosine terms will appear in the expression for $F'(\zeta,\theta)$.

2.2.4 **Fresnel Zone Radiation in Terms of the Aperture Distribution**

Hu[1] has shown that a particularly convenient form of writing the aperture distribution is in terms of what he calls a Fourier-Zernike series

$$F'(\zeta,\beta) = \sum_{\substack{n\geq m\geq 0 \\ (n-m)\text{even}}}\sum (a_{nm}\cos m\beta + b_{nm}\sin m\beta)\, R_n^m(\zeta) \qquad (32)$$

where $R_n^m(\zeta)$ are the Zernike Polynomials which are defined in table II, where a brief tabulation is given. However, it should be noted that his claim that any function may be written as a Fourier-Zernike series on the unit disk is not true, since the restriction that (n-m) be even, requires that even functions of ζ be associated with only even trigonometric terms. Likewise the odd functions of ζ must be associated with only the odd trigonometric terms. However, this does not prevent writing (26) and (30) in the form of (32) if the principal plane aperture illuminations $F_\xi(\zeta)$ & $F_\eta(\zeta)$ are written as even functions of ζ; e.g. of the form $F_\xi(\zeta) = a_0 + a_2\zeta^2 + a_4\zeta^4 + \ldots$. In this case the functions $P_m'(\zeta)$ and $R_m'(\zeta)$ in (26) contain only odd powers of ζ and only odd trigonometric terms are present. Likewise in (30) $Q_m'(\zeta)$ and $R_m'(\zeta)$ are even polynomials associated with even Fourier terms.

The desirable feature of Zernike polynomials is that they may be conveniently rewritten in terms of the correct powers of ζ and $(1-\zeta^2)$ such that the scalar diffraction integral

$$\mathbf{E}(R,\Theta,\Phi) = \frac{jk}{4\pi}(1+\cos\theta)\iint_A F'(\rho,\beta)\,\frac{e^{-jkr}}{r}\,\rho\,d\rho\,d\beta \qquad (33)$$

(where the variables are those shown in figure 9) may be evaluated in terms of a series expansion. More precisely we may write

$$R_n^m(\zeta) = \zeta^m \sum_{\nu=0}^{(n-m)/2} C_{mn}^{\nu}(1-\zeta^2)^{\nu} = \zeta^m\, z_n^m(1-\zeta^2) \qquad (34)$$

where

$$C_{mn}^{\nu} = \frac{(-1)^{\nu}\left(\frac{n-m}{2}\right)!\left(\frac{n+m}{2}+\nu\right)!}{\left(\frac{n-m}{2}-\nu\right)!\left(\frac{n+m}{2}\right)!(\nu!)^2}$$

Using the Fresnel approximation for r in (33)

$$r \doteq R + \frac{\rho^2}{2R} - \rho \sin\theta \cos(\gamma-\beta)$$

the Fresnel region field expression can be written as

$$E(R,\theta,\phi) = je^{\frac{-jkR-j\gamma/2}{2\pi}} \int_0^1 \int_0^{2\pi} F'(\zeta,\beta)\, e^{iu\zeta\cos(\phi-\beta)}\, d\phi\, e^{i\frac{\gamma}{2}(1-\zeta^2)}\, \zeta\, d\zeta \qquad (35)$$

where

$$u = ka\sin\theta$$

$$\gamma = \frac{ka^2}{R}$$

Then by substitution of the Fourier-Zernike series for $F'(\zeta,\beta)$ into (35) and by use of the identities

$$\int_0^{2\pi} e^{iu\zeta\cos(\phi-\beta)} \begin{Bmatrix}\cos m\beta \\ \sin m\beta\end{Bmatrix} d\beta = 2\pi i^m \begin{Bmatrix}\cos m\phi \\ \sin m\phi\end{Bmatrix} J_m(u\zeta)$$

and

$$W_n^m(\gamma,u) = \int_0^1 (1-\zeta^2)^n J_m(u\zeta)\, e^{j\frac{\gamma}{2}(1-\zeta^2)}\, \zeta^{m+1}\, d\zeta \qquad (36)$$

We may write (35) in terms of Zernike Polynomials of the $W_n^m(\gamma,u)$ functions

$$E(\cdot,\theta,\phi) = i\gamma e^{-jkR-j\frac{\gamma}{2}} \sum_{\substack{m \geq n \geq 0 \\ m,\ n\ \text{odd}}} \sum j^m \left(a_{mn}\cos m\phi + b_{mn}\sin m\phi\right) Z_n^m(W_m) \qquad (37)$$

where

$$Z_n^m(W_m) = \sum_{\nu=0}^{(n-m)/2} C_{mn}^{\nu}\, W_m^{\nu}(\gamma,u) \qquad (38)$$

$W_m^n(v,u)$ are generalized Lommel functions of two variables. Their relationship to the Lommel functions $U_m(v,u)$ given by Watson[5] is indicated by the following equation

$$W_m^\nu(v,u) = \left|\frac{2}{j}\right|^\nu u^m \frac{\partial^\nu}{\partial v^\nu}\left\{\frac{U_{m+1}(v,u)}{v^{m+1}} + i\,\frac{U_{m+2}(v,u)}{v^{m+1}}\right\} \tag{39}$$

A table of these functions $W_m^\nu(v,u)$ was computed on a IBM 7010 computer and is given in table 1,Appendix II of this report. In order to use these tables it is most convenient to transform (37) to the form:

$$E(R,\theta,\varphi) = jve^{-j(kR-v/2)} \sum_{m\ \text{odd}} \sum_{\nu=o}^{\infty} (j)^m \left(c_{m\nu}\cos m\varphi + d_{m\nu}\sin m\varphi\right) W_m^\nu(v,u) \tag{40}$$

where

$$c_{m\nu} = \sum_{n=2\nu+m}^{\infty} C_{mn}^\nu\, a_{mn} \qquad d_{m\nu} = \sum_{n=2\nu+m}^{\infty} C_{mn}^\nu\, b_{mn}$$

A partial table of these coefficient C_{mn}^ν may be found in table 2, Volume II, where they are in the form of coefficients for Zernike polynomials $Z_n^m(\zeta)$. Approximately three hours of calculations are necessary on a desk calculator to complete one Fresnel zone or Fraunhofer pattern once the coefficients $c_{m\nu}$ and $d_{m\nu}$ are known. For the monopulse antenna considered in Section 2.2.5, fifteen terms of the series (40) were required to obtain results with three place accuracy. However, about nine terms of the corresponding series for the sum radiation characteristics gave three place accuracy in the sum patterns.

A special case, which is of particular interest, is the far-field radiation pattern ($v = 0$ in (40)). In this case the Lommel functions reduce

---

5. G. N. Watson, "Theory of Bessel Functions," Cambridge, 1952, pp. 536-550

to finite sums of Bessel Functions. Although the equivalent $\frac{2D^2}{\lambda}$ calculation may be made from table 1, Appendix, it is somewhat simpler to evaluate the field from the following analytic expression which has been given by Hu[11]

$$E(R,\theta,\varphi) = jVe^{-jkR} \sum_m \sum_n j^n (a_{mn}\cos m\varphi + b_{mn}\sin m\varphi) \frac{J_{n+1}(u)}{u} \qquad (41)$$

where a_{mn} are the coefficients in (37). Note that (41) may be written

$$E(R,\theta,\varphi) = jVe^{-jkR} \sum_n j^n k_n(\varphi) \frac{J_{n+1}(u)}{u} \qquad (42)$$

where

$$k_n(\varphi) = \sum_m (a_{mn}\cos m\varphi + b_{mn}\sin m\varphi)$$

Thus, if only the far-field pattern is desired, the equation (37) need not be reduced to the form of (40).

2.2.5 Sample Calculation of Monopulse Difference Pattern

This section shows in detail how to calculate the Fresnel zone radiation characteristics of the monopulse antenna described in the preceding sections. A specific example will be considered, the difference pattern of the experimental X-band monopulse antenna described in Section 2.2.6. To make these calculations, the following parameters must be determined.

δ - lateral diagonal displacement of the primary antenna from the focal point

$F_\xi(\zeta), F_\eta(\zeta)$ - radiation patterns of the primary antennas in two orthogonal planes

β_1 - angular displacement of antenna #1 from ξ axis (see figure 20)

B - beam deviation factor (See Lo 9 for graphs of this function.)

---

11. M. K. Hu, Modified Zernike Polynomials and Their Application to the Analysis of Fresnel Region Fields, June Opt. Soc. of Am., Vol. 53, No. 6 Feb. 1963

f - focal length of antenna

a - radius of aperture

For the example considered

$\delta = 0.675$

$\beta_1 = \pi/4$

$\beta = .90$

$f = 21.8$ (inches)

$a = 24$ (inches)

$k = \frac{2\pi}{\lambda}$

then $\theta' = kBa\,\theta \simeq kBa\,\frac{\delta}{f} = \frac{2\pi}{\lambda}(.90)(20\lambda)\left|\frac{.675}{21.8}\right| = 3.50$

Step 1. Polynomial approximation to $F_\xi(\zeta)$ and $F_\eta(\zeta)$

As explained in section 2.2.3, $F_\xi(\zeta)$ and $F_\eta(\zeta)$ must be written in the form $F_\xi(\zeta) = a_0 + a_2\zeta^2 + a_4\zeta^4 + a_6\zeta^6$

$F_\eta(\zeta) = b_0 + b_2\zeta^2 + b_4\zeta^4 + b_6\zeta^6$

The patterns of the individual primary antennas are shown in figure 12 superimposed with the approximation $F_\xi(\zeta) = F_\eta(\zeta) = F_1(\zeta) = 1 - \zeta^2 + .4\zeta^4$ (43). This equation may be found by a curve fitting procedure. Since the odd powers of ζ are not permissible in this expansion no rigorous means (such as a Legendre polynomial expansion) can be given for finding such an expression, however, for most physically realizable aperture distributions, it is a simple matter to obtain a reasonable approximation. It may be noted by examining figure 12 that a better approximation could have been obtained if a linear term were permissible in equation (43).

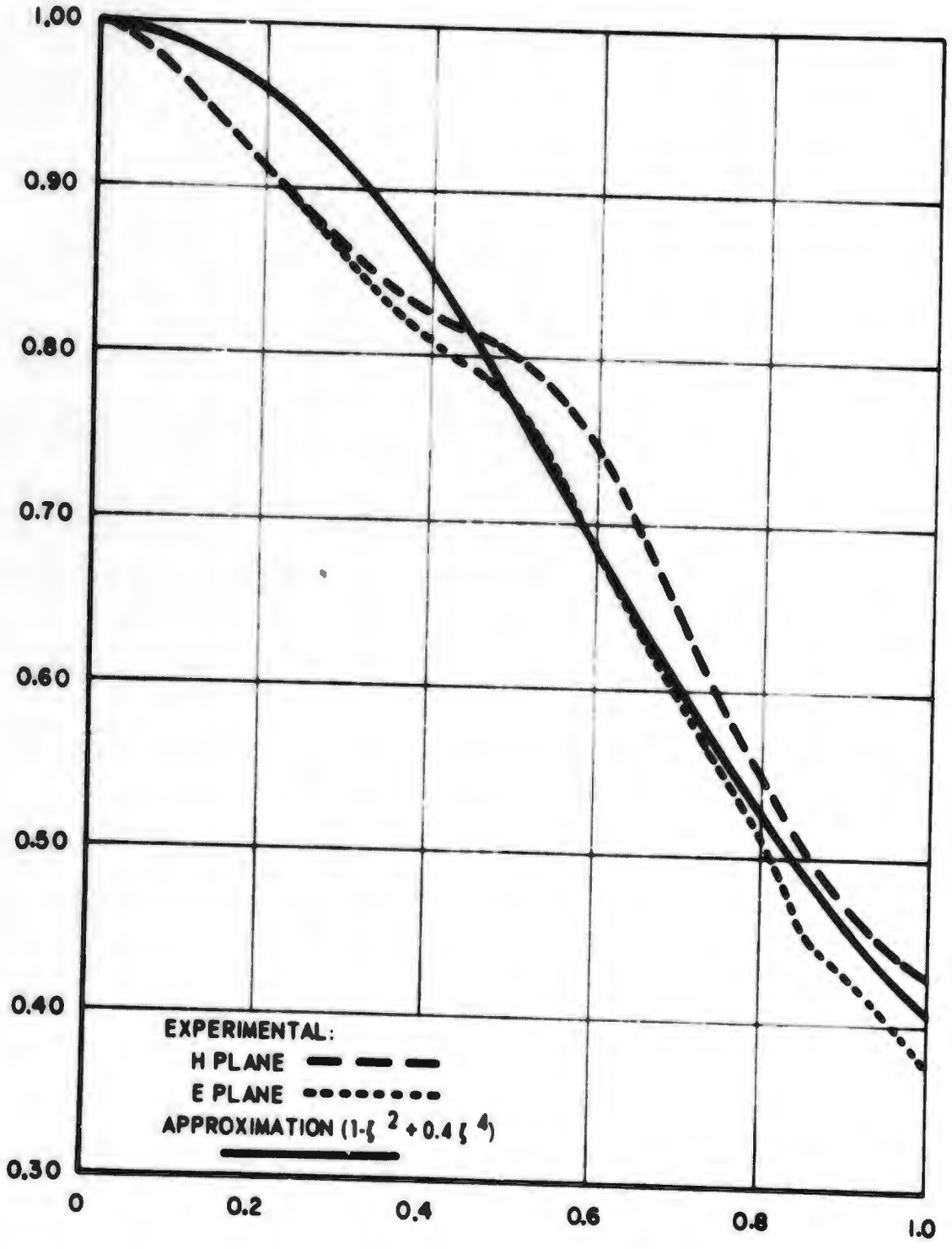

Figure 12. Pattern of a Single Horn used in the Monopulse Antenna

Step 2. The Total Monopulse Aperture Illumination

By letting $\zeta = 3.5$ in equation 27 we find that

$$\sin\left[\zeta\theta' \cos(\beta - \tfrac{\pi}{4})\right] + \sin\left[\zeta\theta' \cos(\beta + \tfrac{\pi}{4})\right] \simeq$$

$$\sqrt{2}\Big\{\cos\beta\,\left[+3.5000\zeta - 5.3592\zeta^3 + 2.7355\zeta^5 - .6981\zeta^7 + .1069\zeta^9\right]$$
$$\cos 3\beta\,\left[+1.7860\zeta^3 - 1.3678\zeta^5 + .4189\zeta^7 - .0713\zeta^9\right]$$
$$\cos 5\beta\,\left[- .2736\zeta^5 + .1396\zeta^7 - .0305\zeta^9\right]$$
$$\cos 7\beta\,\left[- .0199\zeta^7 + .00764\zeta^9\right]$$
$$\cos 9\beta\,\left[+ .0008\zeta^9\right]\Big\} \qquad (44)$$

Multiplying this expression by $2j\,F_1(\zeta)$ we get (eq. 26)

$$F'(\zeta) \simeq 2\sqrt{2}\,j\Big\{\cos\beta\,\left[3.5000\zeta - 8.8592\zeta^3 + 9.4947\zeta^5 - 5.5773\zeta^7 + 1.8992\zeta^9 - .3861\zeta^{11} + .0427\zeta^{13}\right]$$
$$+ \cos 3\beta\,\left[1.7864\zeta^3 - 3.1542\zeta^5 + 2.5013\zeta^7 - 1.0373\zeta^9 + .2388\zeta^{11} - .2851\zeta^{13}\right]$$
$$+ \cos 5\beta\,\left[-.2736\zeta^5 + .4132\zeta^7 - .2796\zeta^9 + .0864\zeta^{11} - .0122\zeta^{13}\right]$$
$$+ \cos 7\beta\,\left[-.0199\zeta^7 + .0376\zeta^9 - .0156\zeta^{11} + .0031\zeta^{13}\right]$$
$$+ \cos 9\beta\,\left[.00085\zeta^9 - .00085\zeta^{11} + .00034\zeta^{13}\right]\Big\} \qquad (45)$$

This analytical approximation to the difference aperture distribution is plotted in figure 13 along with the experimental primary feed difference pattern. The corresponding results for the sum mode are shown in figure 14. It should be noted that the above expression should differ from the experimental result by the effect of the beam deviation factor B on θ'.

Step 3. Reduction of the Aperture Distribution to a Fourier Zernike Series

In order to write the Fresnel radiation terms of generalized Lommel functions, we must rewrite the above polynomials $P'_{4}(\rho)$ (see equation 26.) in a Zernike series

$$P'_m(\zeta) = \sum_n a_{nm} R^m_n(\zeta)$$

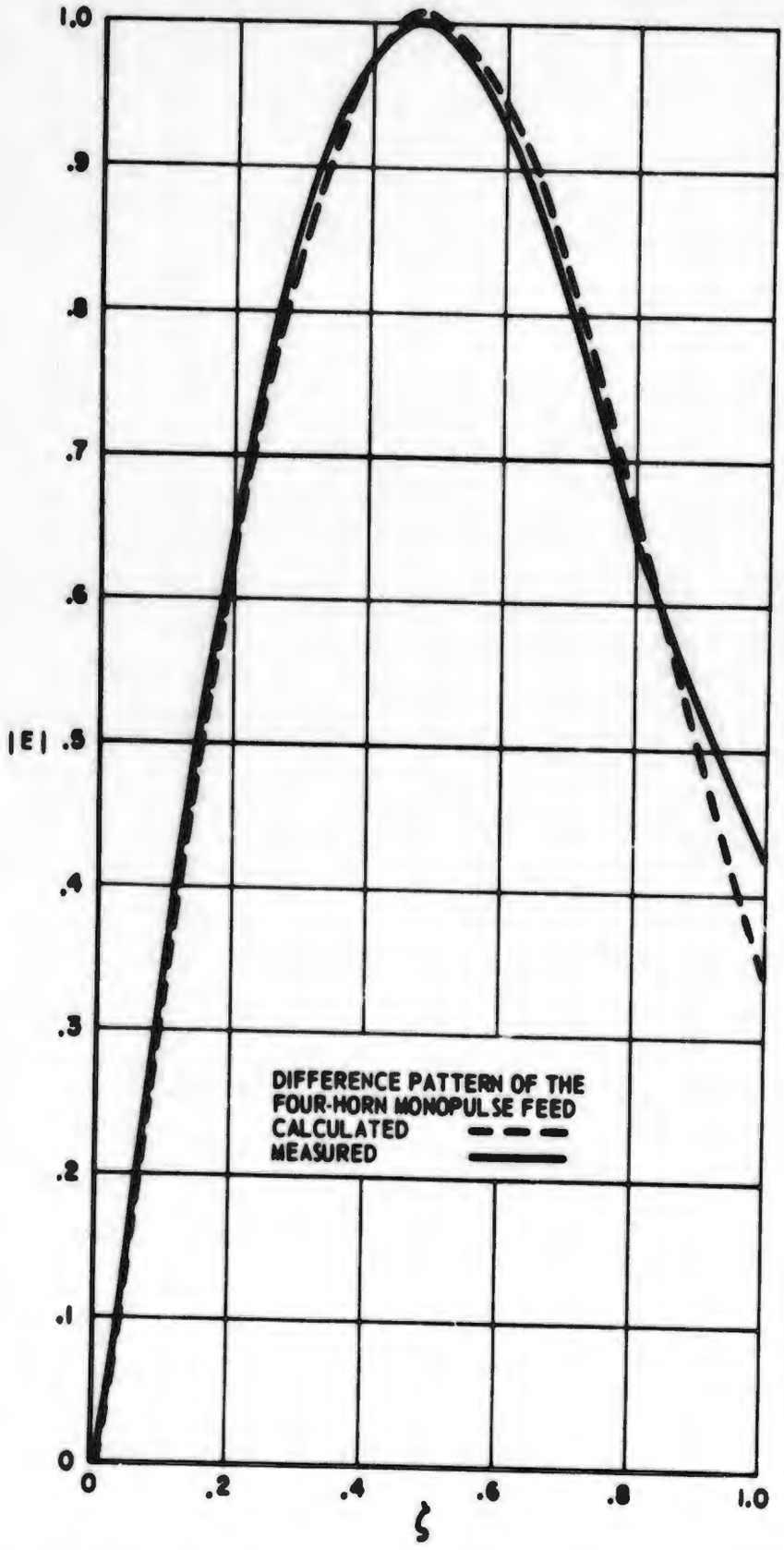

Figure 13. Calculated and Measured Difference Patterns of Four-Horn Monopulse Feed

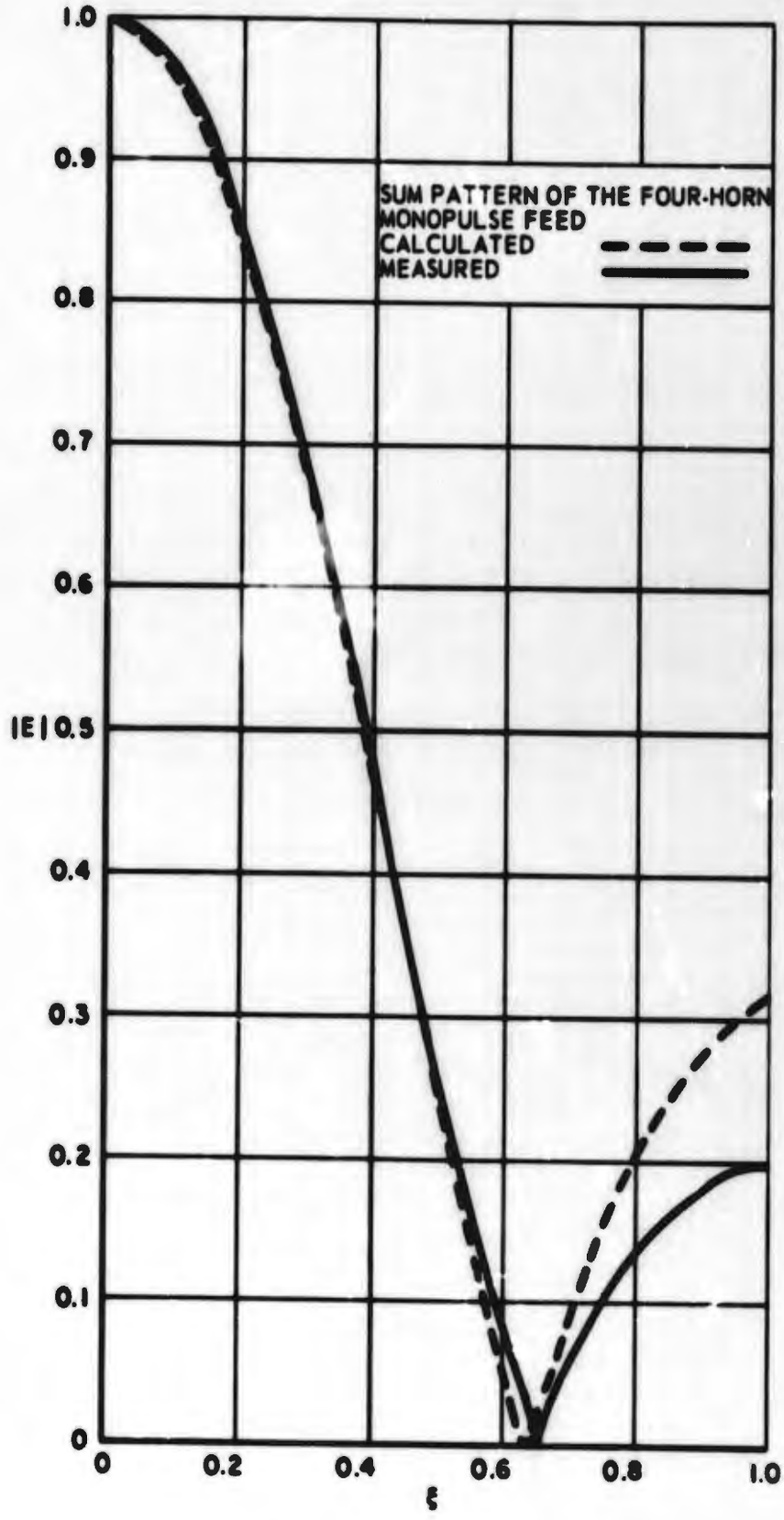

Figure 14. Calculated and Measured Sum Pattern of Four-Horn Monopulse Feed

The polynomials $R_n^m(\zeta)$ are a complete orthogonal series on the linear space of polynomials of the type $P_m'(\zeta)$ and the above Fourier coefficients a_{rm} are given by

$$a_{rm} = (n + 1)\ (2 - \delta_{om}) \int_0^1 P_m'(\zeta)\ R_n^m(\zeta)\zeta d\zeta \qquad (46)$$

where

δ_{om} is the Kroneker delta ($\delta_{oo} = 1$, $\delta_{om} = 0$, $m \neq 0$)

However, since the above expression becomes quite lengthy for large n, a simpler method of calculating the coefficients is to equate the coefficients of equal powers of ζ. The following example for the cos 5β polynomial in equation (45) illustrates the method:

$$P_5'(\zeta) = \sum_{n \geq 5} a_{n5} R_n^5(\zeta)$$

From equation (45) and table 2, the Appendix, of Zernike polynomials $R_n^m(\zeta)$ we may write

$$-.2736\zeta^5 + .4132\zeta^7 - .2796\zeta^9 + .0864\zeta^{11} - .0122\zeta^{13}$$
$$= a_{5,5}\ (\zeta^5) + a_{7,5}\ (-6\zeta^5 + 7\zeta^7) + a_{9,7}(21\zeta^5 - 56\zeta^7 + 36\zeta^9)$$
$$a_{11,5}(-56\zeta^5 + 252\zeta^7 - 360\zeta^9 + 165\zeta^{11}) + a_{13,5}(126\zeta^5 - 840\zeta^7 + 1980\zeta^9$$
$$-1980\zeta^{11} + 715\zeta^{13}).$$

Equating the ζ^{13} coefficients gives

$$-.0211 = a_{13,5}\ (712), \qquad a_{13,5} = -1.71\ \ (10^{-5})$$

Equating the ζ^{11} coefficients

$$.0864 = a_{11,5}(165) + a_{13,5}(-1980)$$

$$a_{11,5} = \frac{.0864 - .0338}{165} = \frac{.0526}{165} = 3.18\ (10^{-4})$$

Equating the ζ^9 coefficients

$$-.2796 = a_{9,5}(36) + a_{11,5}(-360) + a_{13,5}(1980)$$

$$a_{9,5} = \frac{-.2796 + .1147 + .0338}{36} = \frac{-.1311}{36} = -3.64(10^{-3})$$

Equating the ζ^7 coefficients

$$-.4132 = a_{7,5}(7) + a_{9,5}(-56) + a_{11,5}(252) + a_{13,5}(-840)$$

$$a_{7,5} = \frac{.4132 - .2039 - .0803 - .0144}{7} = \frac{.1147}{7} = 1.638\ (10^{-2})$$

Equating the ζ^5 coefficients

$$-.2736 = a_{55}(1) + a_{75}(-6) + a_{95}(21) + a_{11,5}(-56) + a_{13,5}(126)$$

$$a_{5,5} = -.2736 + .0983 + .0765 + .0178 + .0021 + -.0788$$

Now we may use (46) to calculate $a_{5,5}$ as a convenient check for all the above calculations since a significant error in any of the above calculations will show up in $a_{5,5}$

$$a_{5,5} = 12 \int_0^1 (-.2736\zeta^5 + .4132\zeta^7 - .2796\zeta^9 + .0864\zeta^{11} - .0122\zeta^{13})\zeta^6\, d\zeta$$

$$a_{5,5} = 12\left(\frac{-.2736}{12} + \frac{.4132}{14} - \frac{.2796}{16} + \frac{.0864}{18} - \frac{.0122}{20}\right)$$

$$a_{5,5} = 12\left(-.0228 + .0295 - .0175 + .0048 - .0006\right)$$

$$a_{5,5} = -.0788$$

Which agrees with the above result.

By this method the following table of significant coefficients, a_{nm}, may be calculated

	m = 1	3	5	7	9
n = 1	.6439				
3	-.7862	.4446			
5	.3191	-.1795	-.07883		
7	-.07036	.04755	.01638	-.00570	
9	.008335	-.00655	-.00364	.00092	.00036

Table 2 Coefficients a_{nm} in Equation (38) for the Experimental Monopulse Antenna

Step 4. Calculation of a Fresnel Zone Pattern

The field of the monopulse antenna is given by equation (37) in terms of the above coefficients as

$$E(R,\theta,\varphi) = -\gamma e^{-jkR-j\frac{\gamma}{2}} \sum_{m,n \text{ odd}} (-1)^{\frac{m-1}{2}} a_{mn} \cos m\varphi \, Z_n^m(W_m)$$

However, to use the available table of Lommel functions we must first calculate the coefficients c_{mn} in equation (40)

$$c_{m\nu} = \sum_{\substack{n=\nu+m \\ \text{odd}}}^{\infty} C_{mn}^{\nu} A_{mn}$$

Note that for each m the summation should be truncated at the same value of n since although $Z_n^m(W_m)$ is small, ($|Z_n^m(W_m)| < 1$), its component parts $C_{mn}^{\nu} W_n^m(\gamma,u)$ may not be small and use of several but not all of these terms will cause significant errors. By truncating this series at n=9, the above table 2 may be used along with table 2, Appendix , of modified Zernike Polynomials to find

$c_{m\nu}$, e.g.:

$$c_{1,1} = \sum_{\substack{n=3 \\ \text{odd}}}^{9} C^{1}_{1n}\, a_{1n}$$

$$= C^{1}_{13}\, a_{13} + C^{1}_{15}\, a_{15} + C^{1}_{1,7}\, a_{1,7} + C^{1}_{1,9}\, a_{1,9}$$

$$= -3(-.7862) - 8(.3191) - 15(-.07036) - 24(.008335)$$

$$c_{1,1} = .6692$$

In this manner the following table of coefficients $c_{m\nu}$ may be calculated

	m = 1	3	5	7	9
ν = 0	.1148	.3061	.0661	.0048	.0004
1	.6692	.4645	.0564	.0083	
2	1.0750	.4482	.1311		
3	.5956	.5504			
4	1.0502				

Table 3. Coefficients $c_{m\nu}$ of the Lommel Functions in Equation (40) for the Experimental Monopulse Antenna

Thus from table 3 we may calculate the complete small angle Fresnel zone field of the antenna from the following equation

$$E(R,\theta,\phi) = -\gamma e^{-jkR-j\frac{\gamma}{2}} \sum_{m,\nu \text{ odd}} (-1)^{\frac{m-1}{2}}\, c_{m\nu} \cos m\phi\, W^{\nu}_{m}(\gamma,u)$$

assuming the Lommel functions have been tabulated at the desired range $\gamma = \frac{ka^2}{R}$ and angle $u = ka\sin\theta$.

In table 1, the Appendix, a list of Lommel functions has been tabulated for $\gamma = \pi/4, \pi/2, \pi, \frac{3\pi}{2}, 2\pi, 3\pi, 4\pi$. This enables calculations to be made at the ranges $R = \frac{2D^2}{\lambda}, \frac{D^2}{\lambda}, \frac{D^2}{2\lambda}, \frac{D^2}{3\lambda}, \frac{D^2}{4\lambda}, \frac{D^2}{6\lambda}, \frac{D^2}{8\lambda}$ and the variable u is stepped in interger values u = 1, 2, 3..., 20 which enables calculations for the main

beam and approximately the first four side-lobes. These functions are tabulated with all the functions necessary for calculation of the field at a given point on one page. For example

$$E(\gamma = \pi, u = 10, \varphi = 0) = -\pi e^{-jkR - j\frac{\gamma}{2}} X$$

$$\Big\{.1148\ (+.02759 + j.00262) -.3061\ (-.02153 - j.00794) -.0661\ (-.00439 + j.00594)$$
$$+.6692\ (+.00273 - j.00262) -.4645\ (-.00570 - j.00090) - .0564\ (+.00272 + j.00350)$$
$$+1.0750(-.00136 - j.00216) - .4482\ (-.00139 + j.00097) - .1311\ (+.00163 + j.00191)$$
$$+.5956(-.00172 - j.00087) - .5504\ (-.00015 + j.00135) + .0048\ (+.00298 + j.00880)$$
$$+1.0502\ (-.00137 + j.00026)$$
$$+ .0083\ (+.00514 + j.00245)$$
$$+ .0004\ (+.02013 + j.00378)\Big\}$$

$$E(\pi, 10, 0) = -\pi e^{-jkR - j\frac{\gamma}{2}} \left\{-.00317 + j.01111\right\}$$

The Fresnel zone difference patterns at the distances $\gamma = \frac{\pi}{4}$, π, 2π and 4π are plotted along with the experimental patterns in section 2.2.6.

2.2.6 Comparison with Experimental Results

A monopulse antenna was constructed to indicate the amount of deviation from experimental results which may be expected for the calculations. The primary feed for this antenna is a four horn cluster, the aperture of each horn is approximately one inch and the horns are arranged to form a square two horns on a side. Each horn has approximately a circularly symmetric pattern as is shown in figure 12 with approximately a seven db aperture taper. The feed system consists of a magic tee hybrid and two waveguide H plane tees. Although all three monopulse modes cannot be obtained simultaneously without four hybrids, the H plane difference mode and the sum mode could be obtained with this arrangement and with a circularly symmetric distribution for each horn the two difference mode patterns should be identical. Therefore it was

felt that this partial model satisfactorily indicated the desired characteristics. The reflector is a four foot diameter parabolic dish with a 21.8 inch focal length.

Although the desirable operating band of this monopulse antenna is in the lower x-band region, a frequency of 9835 mc was chosen to achieve a 40λ aperture. At this frequency the sum pattern has a slight null caused by the larger electrical separation of the primary feeds at this wavelength. However, the calculations illustrate the method for a general case and the large value of $\theta' = 3.50$ is somewhat larger than in the design band. This assures that the series expansions in sections 2.2.4 will be even more rapidly convergent in the design band of any monopulse antenna than for this example.

The Fraunhoffer and Fresnel zone H-plane sum and difference patterns for this antenna are shown in figures 15 through 22 at the distances $\frac{2D^2}{\lambda}$, $\frac{D^2}{2\lambda}$, $\frac{D^2}{4\lambda}$ and $\frac{D^2}{8\lambda}$. The calculated patterns may be calculated from the table of Lommel functions in table 1, Volume II, as described in the preceding sections. It may be seen that for both the sum and difference patterns the main beam and location of side lobes can be predicted with a fair degree of accuracy as can the lobe fill-in in the Fresnel zone. However in the amplitude of the side-lobes there is a significant difference in the calculated and measured patterns.

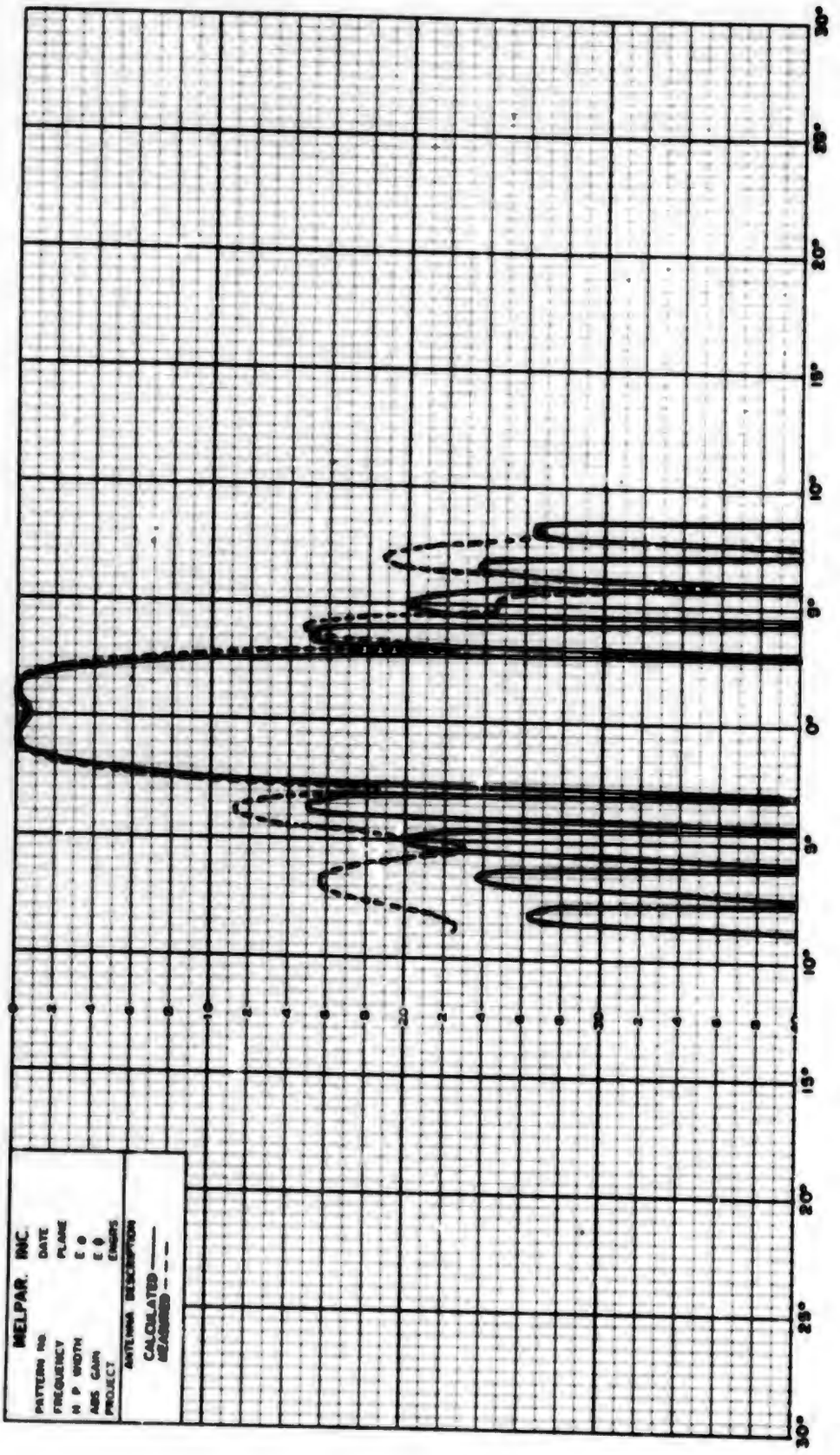

Figure 15. Far Field, Monopulse Sum Pattern

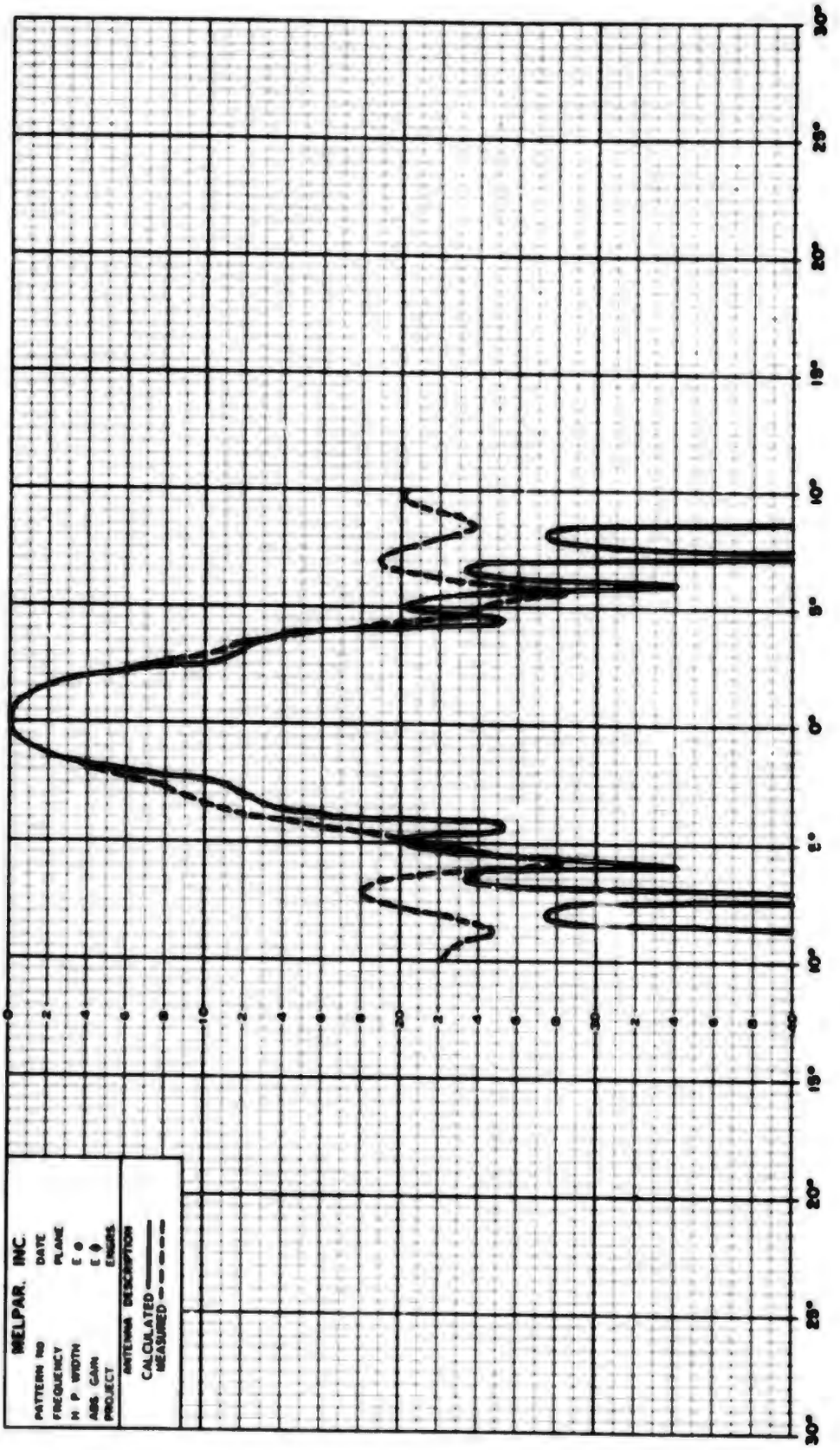

Figure 16. $D^2/2\lambda(80')$ Fresnel Zone, Monopulse Sum Pattern

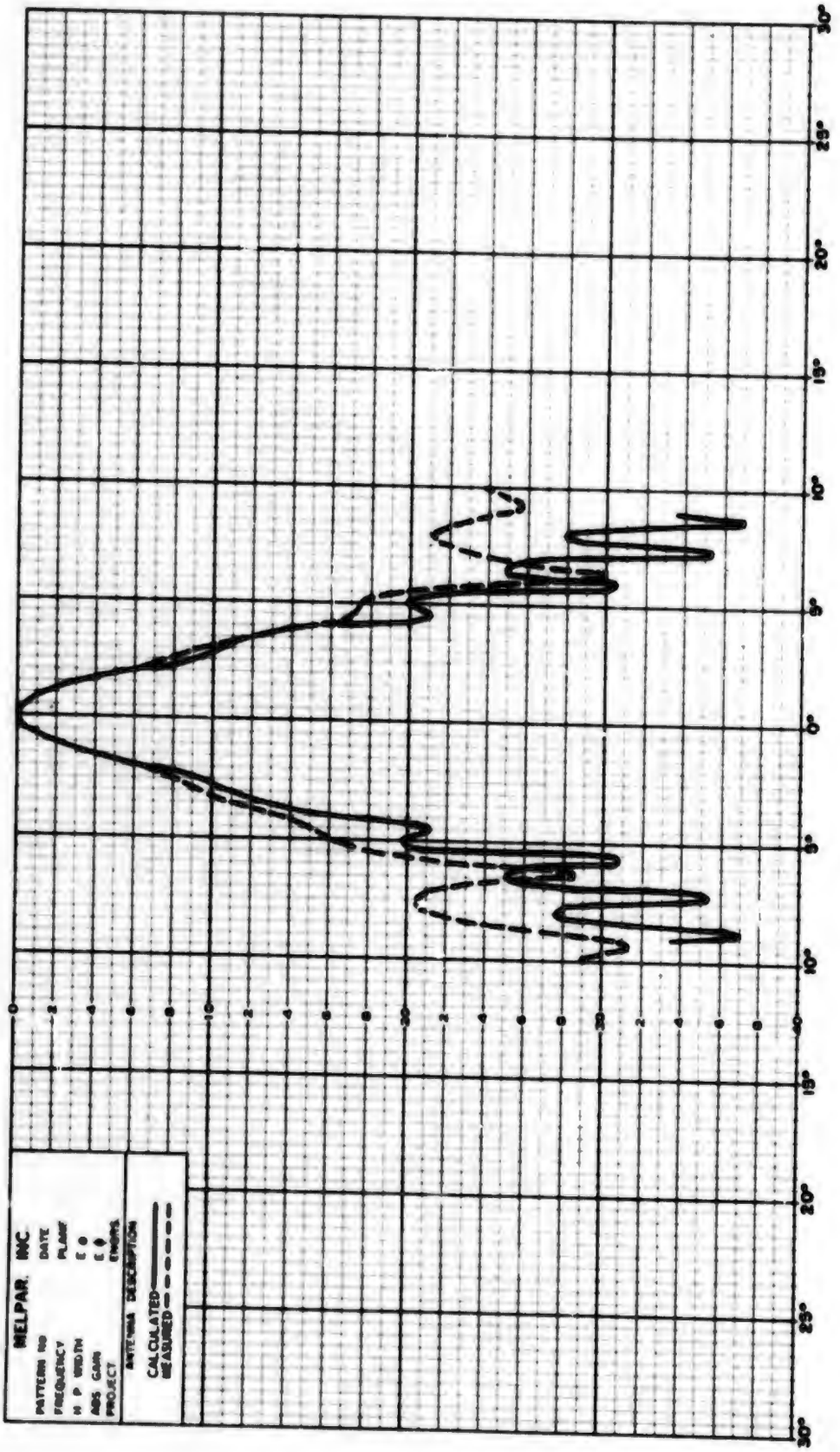

Figure 17. D2/4 λ(40') Fresnel Zone, Monopulse Sum Pattern

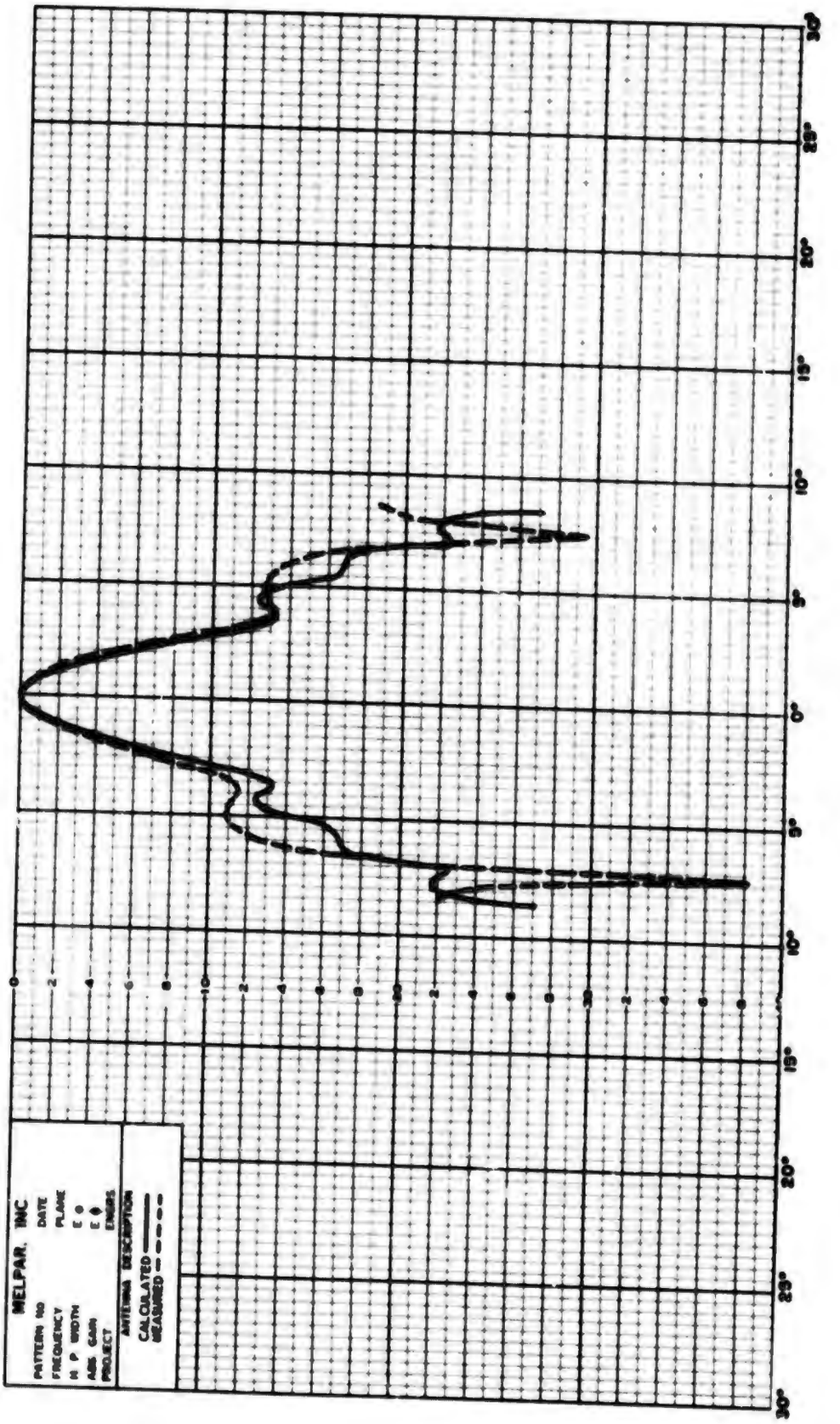

Figure 18. $D^2/8\lambda(20')$ Fresnel Zone, Monopulse Sum Pattern

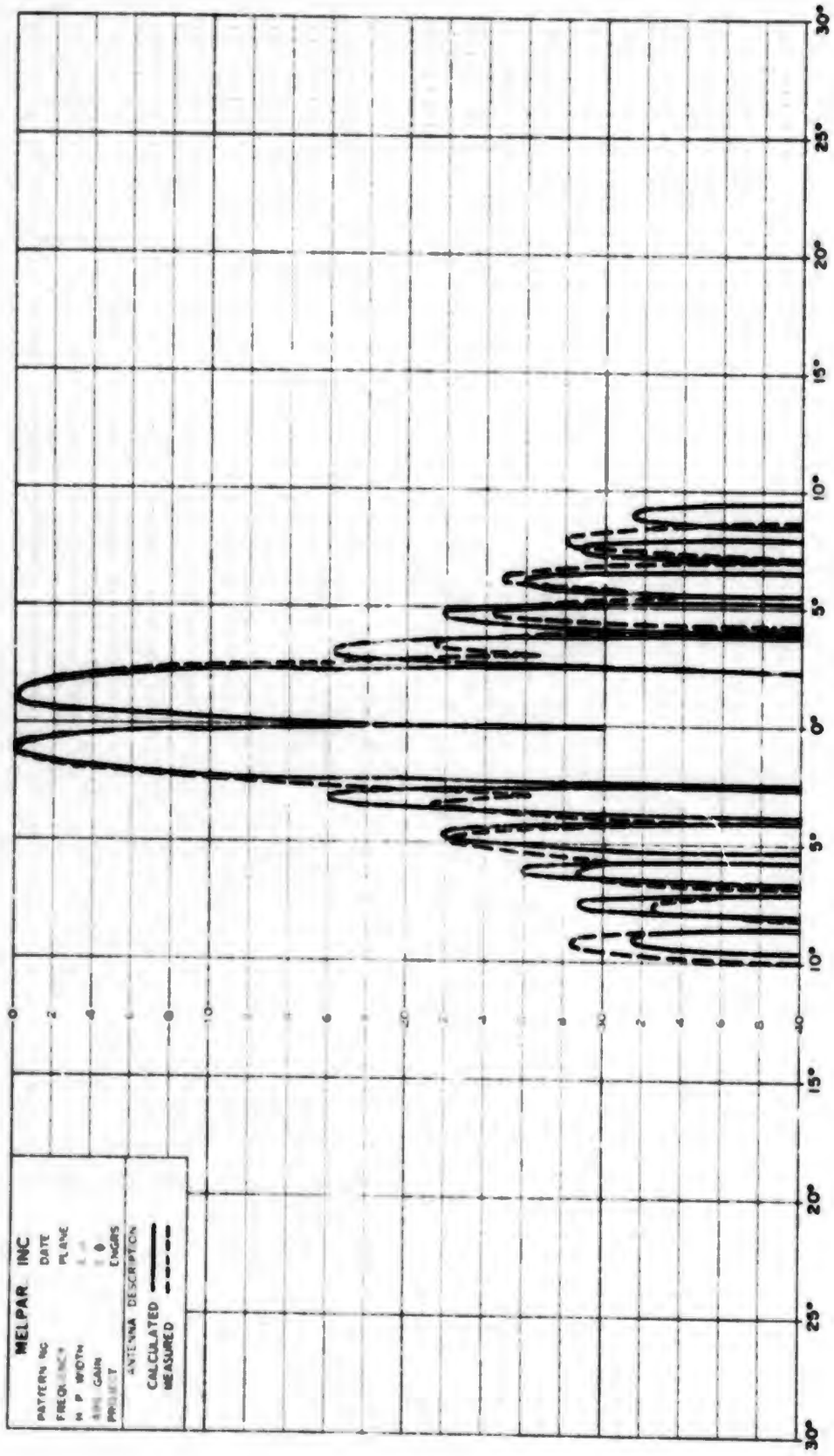

Figure 19. Far Field, Monopulse Difference Pattern

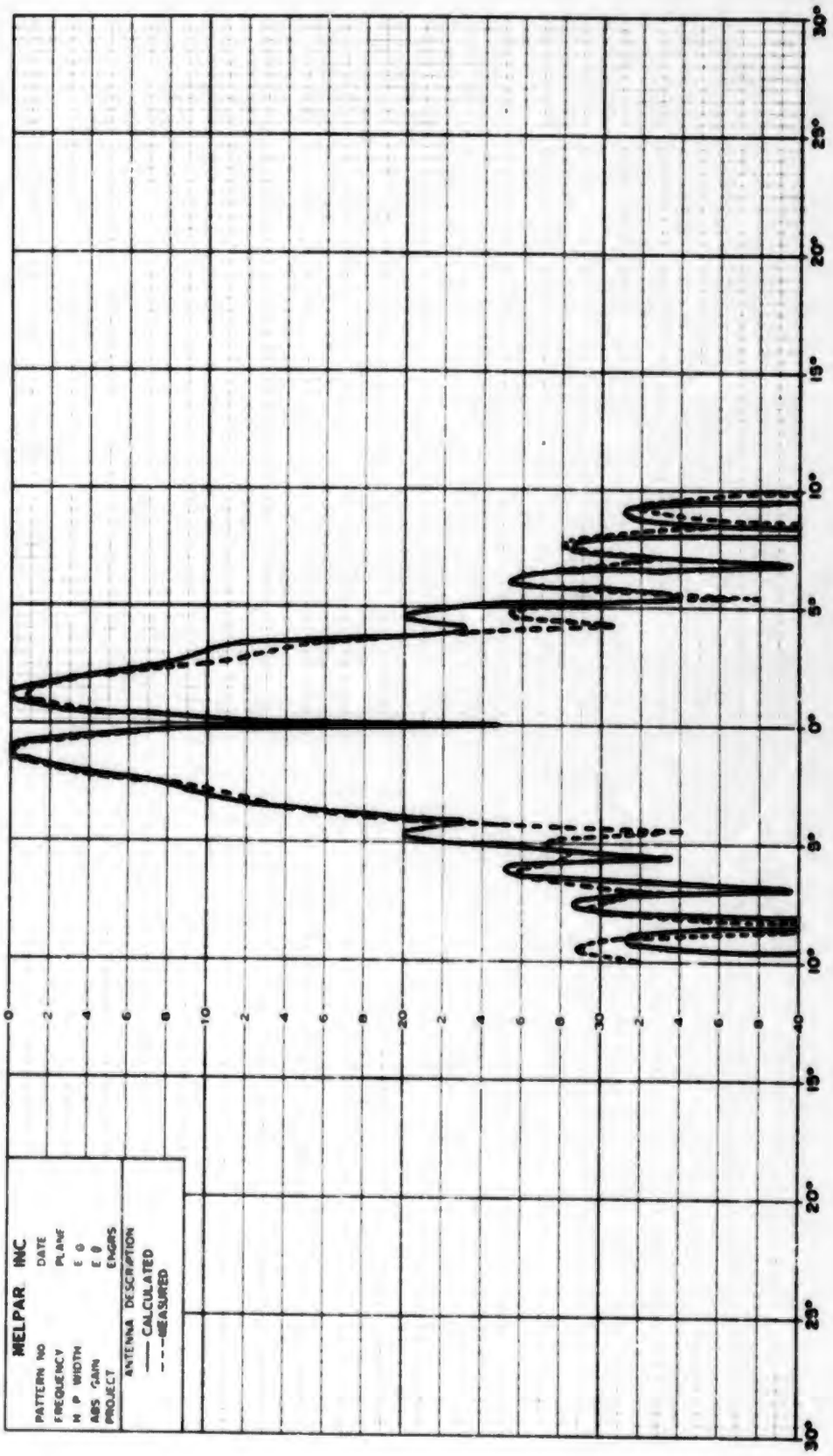

Figure 20. $D^2/2\lambda$ (80') Fresnel Zone, Monopulse Difference Pattern

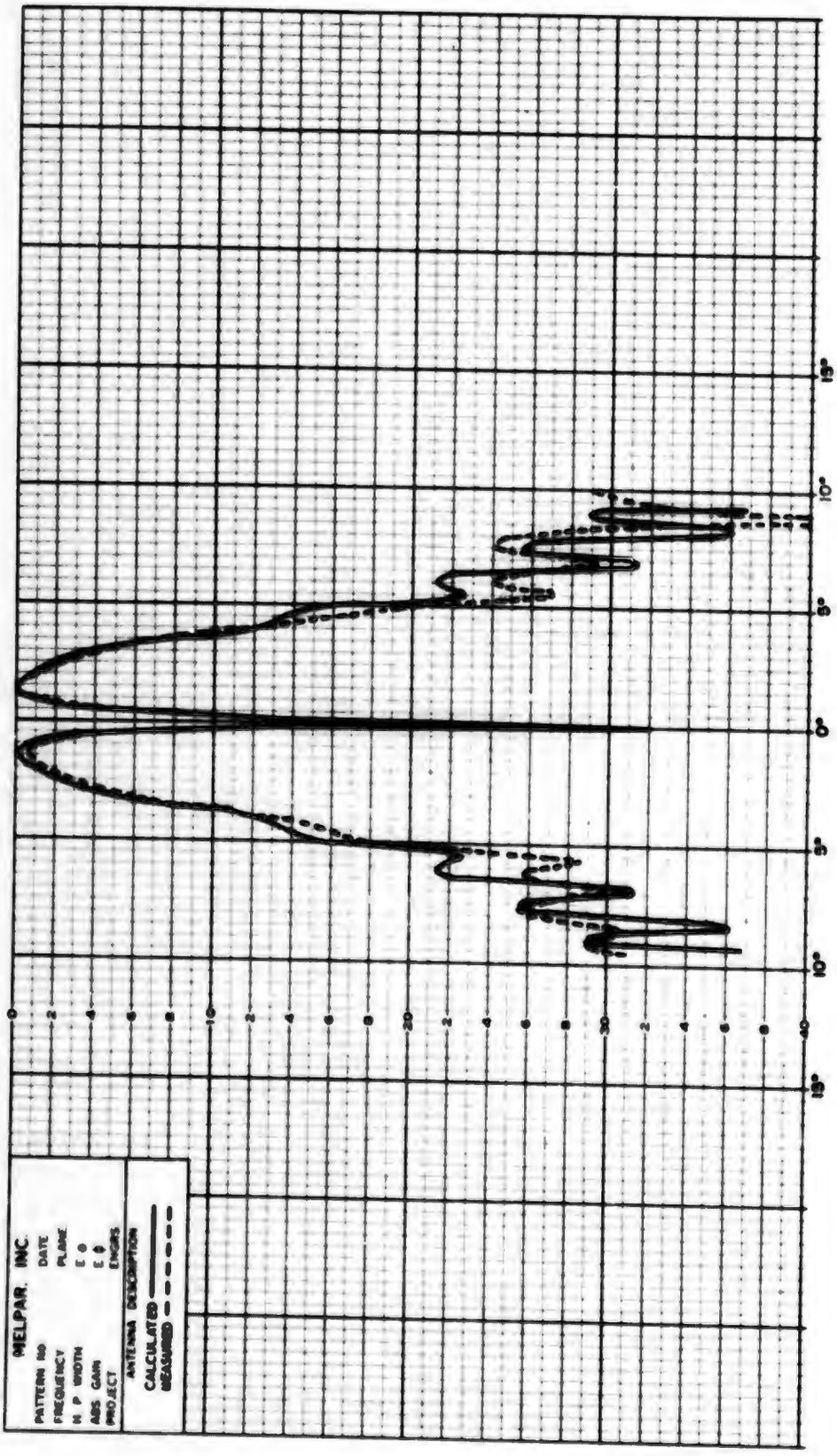

Figure 21. $D^2/4\lambda(40')$ Fresnel Zone, Monopulse Difference Pattern

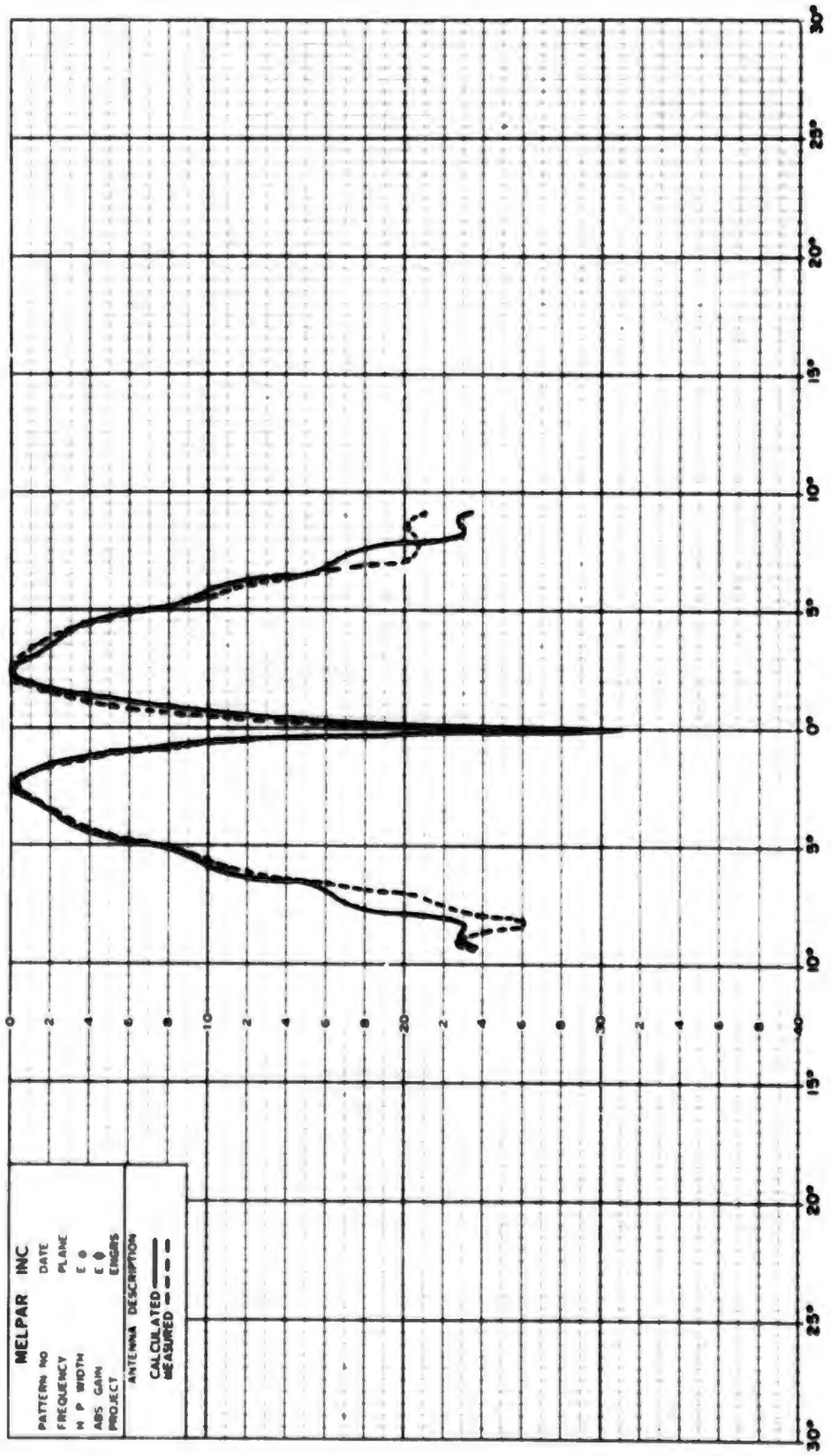

Figure 22. $D^2/8\lambda(20')$ Fresnel Zone, Monopulse Difference Pattern

3. ELLIPTICAL APERTURES AND APERTURES OF OTHER SHAPES

The methods previously considered for Fresnel Region antenna pattern calculation were limited to the two simplest aperture shapes, rectangular and circular, and required a uniform phase front across the aperture. Because of the large variety of shapes of microwave antennas, it is desirable to have a more general method of Fresnel zone pattern calculation. Ideally, this method should be flexible enough to give a good approximation of the field intensity for an arbitrarily shaped aperture and, in addition, should be capable of predicting the field produced by a shaped-beam antenna in the Fresnel region. The effort in this area was directed toward finding such a general method of pattern computation that is simple enough to be carried out on a desk calculator in a relatively short time.

3.1 Strip Approximation Method

The method of calculation which was considered uses a strip approximation of the aperture. This is a powerful technique since it can be used for apertures with irregularly shaped outlines and a great variety of aperture illuminations. With the correct modification for the phase term this method may also be generalised to include beam shaping antennas.

In order to reduce the calculation time required for this method, it is most convenient to take the strips perpendicular to the plane in which the pattern is being computed while making the width (w) of the strips small enough that

$$R_{min} \geq \frac{2w^2}{\lambda} \quad \text{or} \quad w \leq \sqrt{\frac{\lambda R_{min}}{2}} \tag{47}$$

where R_{min} is the shortest range at which the field is desired. (For example for the AN/TPS-1D, w, should be chosen less than 4.5, since the closest pattern is taken at $30\lambda = R_{min}$ which is twice the greatest aperture dimension). This assures that the pattern at R in the plane of the narrow dimension has far field characteristics. It is most convenient to assume a uniform amplitude across the width of each strip since in this case, each strip has the familar $\frac{\sin u}{u}$ pattern. Therefore the strips should be narrow enough such that the resulting step function approximates the actual aperture distribution across the complete aperture.

The use of the scalar diffraction integral to express the Fresnel field results in an expression for the field of the form

$$E(R,\theta) = \frac{j}{\lambda R} \iint_A F(x_s,y_s)\, e^{-jkr}\, dx_s\, dy_s$$

If the aperture is divided into 2N strips of width $w = \frac{a}{2N}$ along the x-axis where, a, is the aperture width in the X dimension, and (x_s, y_s) denotes the aperture coordinates as shown in figure 23. Then the total field from the aperture is the sum of the fields from each of the strips

$$E(R,\theta) = \sum_{n=-N}^{N} E_n(R,\theta)$$

where E_n is given by

$$E_n(R,\theta) = \frac{j}{\lambda R} \iint_{An} F_n(x_s,y_s)\, e^{-jkr}\, dx_s\, dy_s \qquad (48)$$

But since we assumed uniform illumination across each of the strips, $F_n(x_s,y_s) = F_n(y_s)$. If the usual small angle Fresnel approximation for, r, is used (see figure 24). Then in the X -Z plane

$$r = \sqrt{(x-x_s)^2 + y_s^2 + s^2} \qquad (y = 0)$$

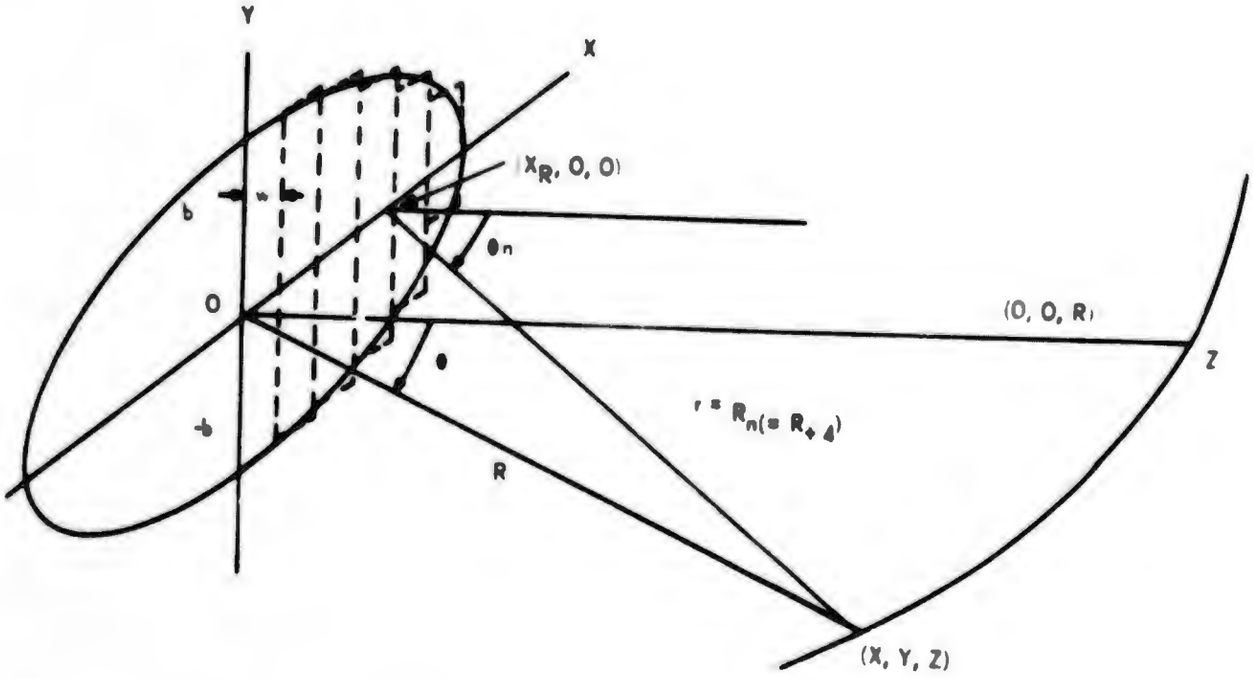

Figure 23. Strip Approximation of an Elliptical Aperture

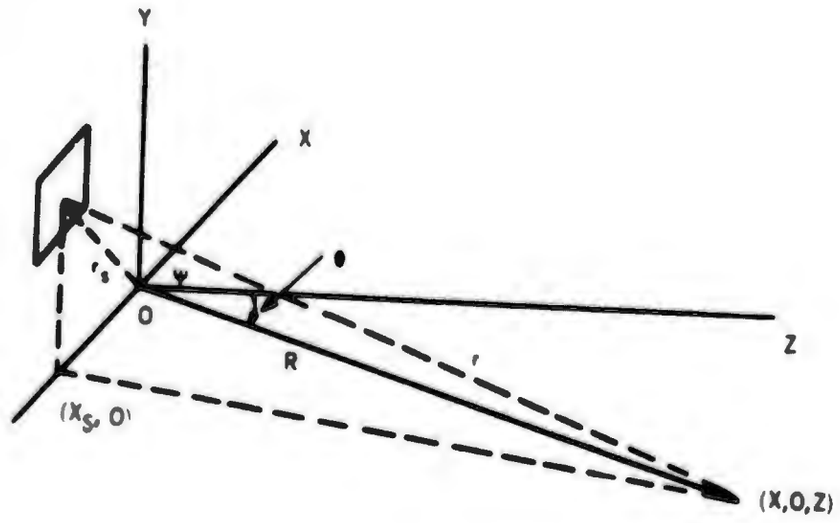

Figure 24. Aperture and Field Coordinate System

$$r = \sqrt{R^2 + x_s^2 + y_s^2 - 2x_s x}, \quad (R = x^2 + z^2)$$

$$r \simeq R + \frac{r_s^2}{2R} - \frac{x_s x}{R}, \qquad r_s = x_s^2 + y_s^2$$

$$r \simeq R + \frac{r_s^2}{2R} - x_s \sin\theta \quad \text{since } x = R\sin\theta$$

and the integral in equation 48 may be separated as follows:

$$E_n(R,\theta) = \frac{jc^{-jkR}}{R}\left\{\int_{b_n}^{b_n} F_n(y_s)e^{-j\frac{ky_s^2}{2R}}\,dy_s\right\}\left\{\int_{x_n - w/2}^{x_n + w/2} e^{j(kx_s \sin\theta - \frac{kx_s^2}{2R})}\,dx_s\right\} \tag{49}$$

where x_n is the center of the nth strip now let $x_s = x_n + \delta$ (δ variable).

Then

$$kx_s \sin\theta - \frac{kx_s^2}{2R} = kx_n \sin\theta + k\delta \sin\theta - \frac{kx_n^2}{2R} - \frac{k\delta x_n}{R} - \frac{k\delta^2}{2R} \tag{50}$$

Since in the region of integration $\frac{k\delta^2}{2R} < \frac{k(\frac{w}{2})^2}{2R}$ and our hypothesis

(eq. 47) $R \geq \frac{2w^2}{\lambda}$ implies $kw^2 < \pi R$ thus

$$\frac{k\delta^2}{2R} < \frac{kw^2}{R} \leq \frac{\pi}{8}$$

thus to a good approximation $\frac{k\delta^2}{2R} = 0$ and we have

$$\int_{x_n - w/2}^{x_n + w/2} e^{j(k x_s \sin\theta - \frac{kx_s^2}{2R})}\,dx_s \simeq e^{j(kx_n \sin\theta - \frac{kx_n^2}{2R})}\int_{-w/2}^{w/2} e^{jk\delta(\sin\theta - \frac{x_n}{R})}\,d\delta$$

(Since $\sin\theta_n \simeq \sin\theta - \frac{x_n}{R}$)

$$\simeq e^{j(kx_n \sin\theta - \frac{kx_n^2}{2R})} \int_{-w/2}^{w/2} e^{jk\delta \sin\theta_n}\, d\delta \qquad (51)$$

$$= e^{j(kx_n \sin\theta - \frac{kx_n^2}{2R})} \quad w\left(\frac{\sin(k\frac{w}{2}\sin\theta_n)}{(k\frac{w}{2}\sin\theta_n)}\right)$$

(let $\xi_n = k\frac{w}{2}\sin\theta_n$)

$$\int_{x_n - w/2}^{x_n + w/2} e^{j(kx_s \sin\theta - \frac{kx_s^2}{2R})}\, dx_s = e^{j(kx_n \sin\theta - \frac{kx_n^2}{2R})} \quad w\left(\frac{\sin\xi_n}{\xi_n}\right) \qquad (52)$$

Thus, if we let $I_n(\gamma)$ denote

$$I_n(\gamma) = \int_{-b_n}^{b_n} F_n(y_s)\, e^{-jk\frac{y_s^2}{2R}}\, dy_s \qquad (53)$$

where γ is the normalized radial variable $\gamma = \frac{ka^2}{4R}$ then (49) becomes

$$E_n(R,\theta) = \frac{jwe^{-jkR}}{R}\left(\frac{\sin\xi_n}{\xi_n}\right) I(\gamma)\, e^{j(kx_n \sin\theta - \frac{kx_n}{2R})} \qquad (54)$$

and we may find the total Fresnel field of the aperture from the following expression

$$E(R,\theta) = \frac{jwe^{-jkR}}{R} \sum_{\substack{n=-N \\ n\neq 0}}^{N} I_n(\gamma)\left(\frac{\sin\xi_n}{\xi_n}\right) e^{j(kx_n \sin\theta - \frac{kx_n}{2R})} \qquad (55)$$

The last two terms in the summand present no major difficulty unless N is so large that the computation is too lengthy for desk calculations. The remaining intergral, $I_n(\gamma)$, is merely the field intensity on the axis of the nth line source which has an illumination $F_n(y_s)$.

at which the field intensity is desired, is in the far field of the y dimension of the aperture then the integral reduces to

$$I_n(\psi) = \int_{-b_n/2}^{b_n/2} F_n(y_s)\, dy_s \tag{56}$$

However, if we consider points in the Fresnel zone of the y dimension of the strips, then the integral may be reduced to a sum of Fresnel integrals for which tables are available. For example if $F_n(y_s) = C_n$, a constant uniform illumination, then

$$I_n(\psi) = c_n \int_{-b_n/2}^{b_n/2} e^{-jk \frac{y_s^2}{2R}}\, dy_s = 2 c_n \int_0^{b_n/2} e^{-jk \frac{y_s^2}{2R}}\, dy_s$$

$$= 2 c_n \sqrt{\frac{\pi R}{k}} \left[C\left(b_n \sqrt{\frac{k}{\pi R}}\right) - iS\left(b_n \sqrt{\frac{k}{\pi R}}\right) \right] \tag{57}$$

where C(x) and S(x) are the cosine and sine Fresnel integrals. A more general approximation will have the form

$$F_n(y_s) = c_{0_n} + c_{1_n} y_s + c_{2_n} y_s^2 + c_{3_n} y_s^3 + c_{4_n} y_s^4$$

Such an expression will give a good approximation of the aperture field across most focused antennas. For an aperture which is not focused in the y dimension $F_n(y_s)$ is complex and the real and imaginary parts may be treated separately. For an expression of the above form, $I_n(\psi)$ may also be reduced to a sum of Fresnel integrals; however, the expression is somewhat more complicated. If the illumination of the nth strip may be approximated by an expression of the less general form, $F_n(y_s) = C_{0_n} + C_{2_n} y_s^2 + C_{4_n} y_s^4$ then the data computed by Gerlock[7] may be used since it represents the field of a rectangular aperture

on axis. In this case

$$I_n(\gamma) \cong \sum_{n=0}^{2} \left[W_2(2_n)\, R_2(2n, M, 0) + j\, W_2(2n)\, I_2(2n, M, 0) \right] \qquad (58)$$

This method of calculating the integral has the disadvantage that the increments of M in Gerlock's tables may not be small enough to permit calculation at the desired ranges and, in addition, the permissible form of the aperture illumination is not sufficiently general.

The method described above requires more time to make the calculations than for the case of a simple aperture shape with a symmetric aperture illumination such as rectangular or circular apertures. However, this method may be used for most antennas which are encountered in practice if the phase and the intensity of the aperture illumination are known functions of the aperture coordinates. Since the computation of the field by this method is quite lengthy, it was felt that it would be convenient to calculate a normalised table of functions

$$F_n(\gamma, u) = \left(\frac{\sin \xi_n}{\xi_n} \right) e^{-jk \frac{x_n^2}{2R} + j k x_n \sin \theta}$$

However, an additional simplification may be obtained for apertures with symmetry in the plane of the desired field calculation, since for this case $I_n(\gamma) = I_{-n}(\gamma)$.

A Fresnel approximation must be used for ξ_n in order to normalise that variable in terms of u and γ

$$\xi_n = k \frac{w}{2} \sin \theta_n = k \frac{w}{2} \left(\frac{x_n - R \sin \theta}{R_n} \right)$$

$$\simeq \left(\frac{(2n-1)}{2N^2} \right) \gamma - \frac{u}{2R} \qquad (59)$$

It was found by comparison with the exact expression for ξ_n for a 40λ aperture that this approximation gave a maximum error for the calculation of $\frac{\sin \xi_n}{\xi_n}$ of less than .025 for $\nu = 4\pi$, $(R = \frac{D^2}{8\lambda})$ and $u < 16$.

For a symmetric aperture, the expression for $S_n(\nu,u)$ may be reduced to

$$F_n(\nu,u) = e^{-j\frac{(2n-1)^2}{8N^2}} \left\{ e^{j\left(\frac{2n-1}{2N}\right)u} \left(\frac{\sin \xi_n}{\xi_n}\right) + e^{-j\left(\frac{2n-1}{2N}\right)u} \left(\frac{\sin \xi_{-n}}{\xi_{-n}}\right) \right\} \quad (60)$$

A program of these functions was performed on an IBM 7090 digital computer to calculate these functions for $N = 4$ and a tabulation is given in table 3 of the Appendix. These tables facilitate the calculation of the Fresnel field for any symmetric aperture which may be approximated with eight strips. These tables reduce the calculations to evaluating the following expression

$$E(\nu,u) = \sum_{n=1}^{4} I_n(\nu)\, F_n(\nu, u) \quad (61)$$

which, if I_n is complex, consists of 16 multiplications for each ν and u. Thus, about two hours are required to calculate a complete small angle Fresnel pattern for 20 values of u.

In order to indicate the degree of accuracy which is obtained in an idealized case these tables have been used to calculate two patterns, one at $2D^2/\lambda$ and another at $D^2/8\lambda$, for a hypothetical uniformly illuminated, circular aperture. A comparison of the strip approximation method with the scalar small-angle Fresnel method discussed in the section 2.1. has been made in figures 25 and 26. It is obviously impossible to get a good geometrical approximation of a circular aperture with eight strips of equal width; however, the results agree fairly well, with the largest deviation being in the region of the infinite null on axis for the $D^2/8\lambda$ pattern.

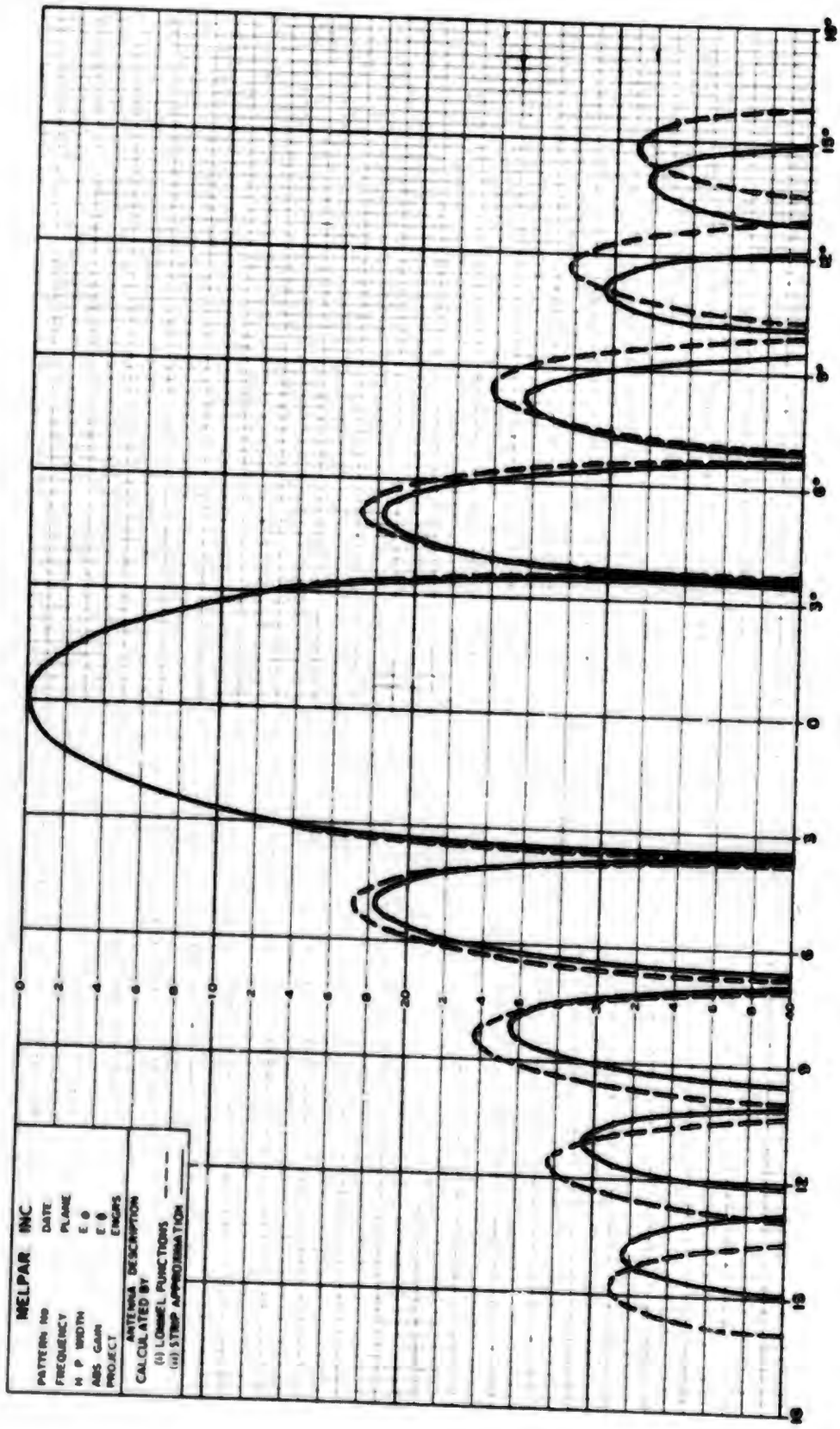

Figure 25. Far Field Strip Approximation for Uniformly Illuminated Aperture

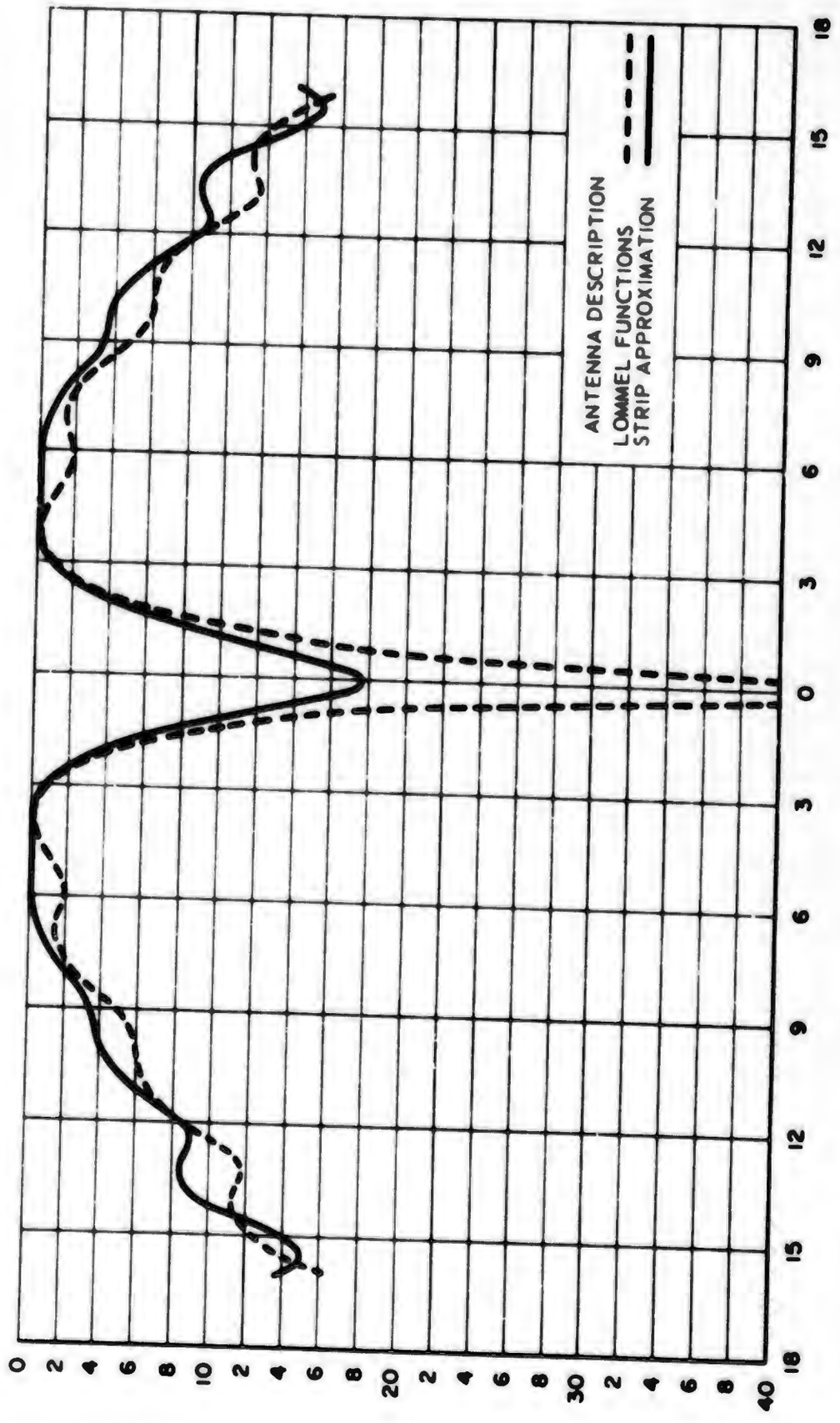

Figure 26. $D^2/8\lambda$ Fresnel Zone Pattern of Uniformly Illuminated Aperture

From the above discussion it may be seen that the strip approximation method achieves the desired result of being able to calculate the Fresnel zone radiation from an aperture with an arbitrary outline and arbitrary phase front in the aperture. For apertures which have even symmetry in the plane of interest table 3 the Appendix may be used to make desk calculations of the pattern in this plane.

3.2 Calculations of the AN/TPS-1D Patterns

The method described in Section 3.1 was used for calculating the Fresnel patterns of an AN/TPS-1D. This antenna consists of a sector of a paraboloidal reflector fed by a hog horn. The aperture of the reflector is approximately rectangular, however, the aperture illumination lacks vertical symmetry since the horn is not at the center of the aperture but rather is placed beneath the reflector and directed upward as shown in figure 27. The resulting aperture illumination may be approximately calculated for the two experimental principal plane patterns. The assumption is made that the field produced by the horn is the product of the fields in the two principal planes, and then the total field at various angles, subtended by the reflector, may be determined.

The aperture field has been calculated in this manner and the resultant illumination is illustrated in figure 27. An alternate method of calculating the aperture distribution was also used. This method consisted of actually calculating the pattern from the hog horn aperture assuming a uniform phase TE_{10} mode in the aperture and projecting this pattern on the aperture. The aperture distribution obtained by this method was in close agreement with that obtained from the measured primary patterns. It should be noted that the fact

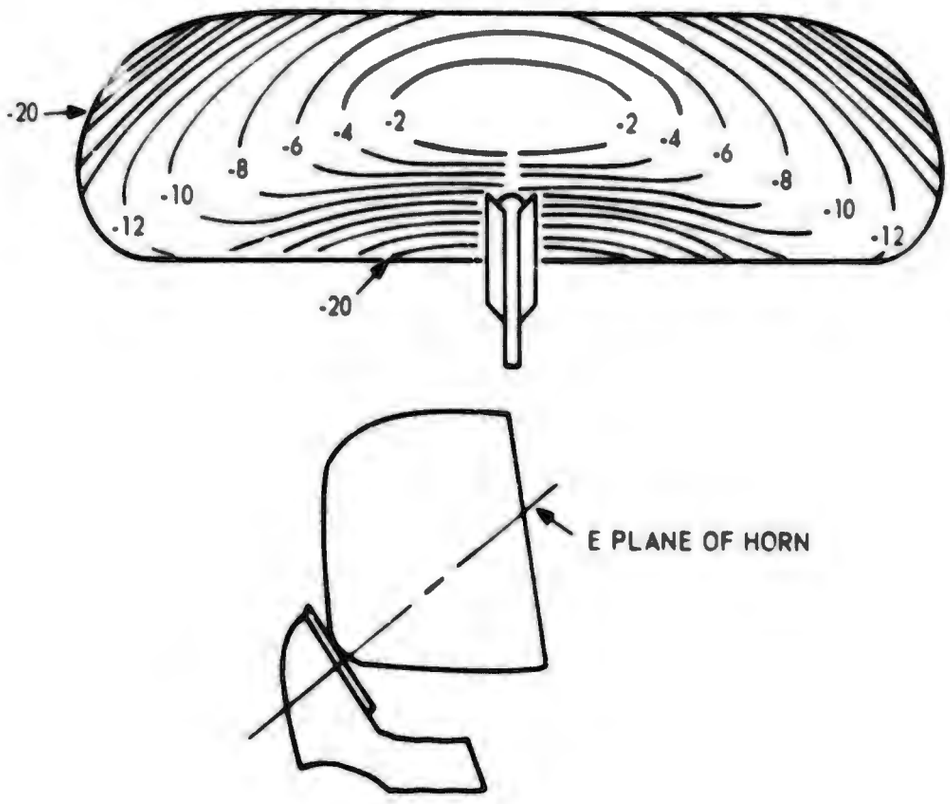

Figure 27. Front View and Profile of AN TPS-1D Reflector and Feed Horn Showing Approximate Aperture Illumination

that the aperture is in the Fresnel zone of the primary feed has a negligible effect on the aperture distribution.

For the calculation of the E-plane patterns, the aperture was divided into eight equal strips. Since $\frac{2H^2}{\lambda} = 43'$ (where H = height of each strip) and the closest measured pattern was at 30', it was assumed that the measurements were essentially in the far-field of each strip, thus, I_n may be found by integrating the illumination over each of the strips. The I_n calculated in this manner were used to calculate the E-plane patterns of the AN/TPS-1D which are shown in figures 28 through 31.

The H-plane patterns were found by breaking the aperture into five vertical strips and approximating the distribution across each strip by a polynominal of the form

$$P_n(\rho) = a_0 + a_2 \rho^2 + a_4 \rho^4 + a_6 \rho^6$$

Since the ranges at which the pattern measurements were taken correspond to the values of M given by Gerlock,[7] $I_n(v)$ may be calculated by equation (58) as suggested in section 3.1. This method was used to calculate the farfield and the $D^2/8\lambda$ H-plane pattern and it was found that there was only a slight difference in the two calculated patterns. Although the intermediate patterns were not computed it was assumed that there was little deviation in the theoretical H-plane patterns throughout this range. The resulting H-plane pattern is shown in figure 32 plotted with the measured H-plane patterns of the AN/TPS-1D. It may be noted that there is a significant difference between the calculated and the measured patterns. This may be due to several factors. First the effect of reflector tolerances and feed defocus could cause the higher side-

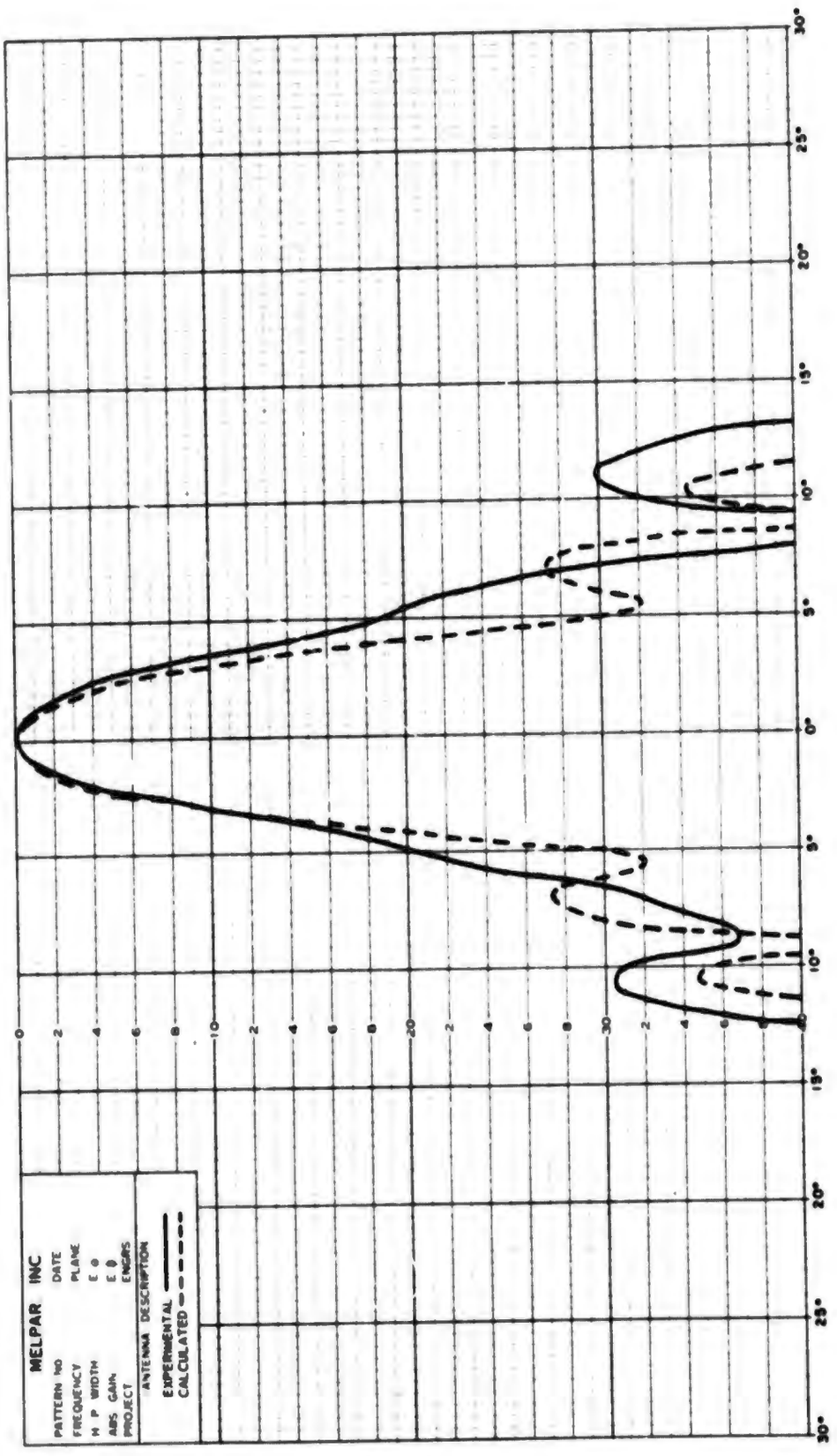

Figure 28. Far Field AN/TPS-1D E-Plane Pattern

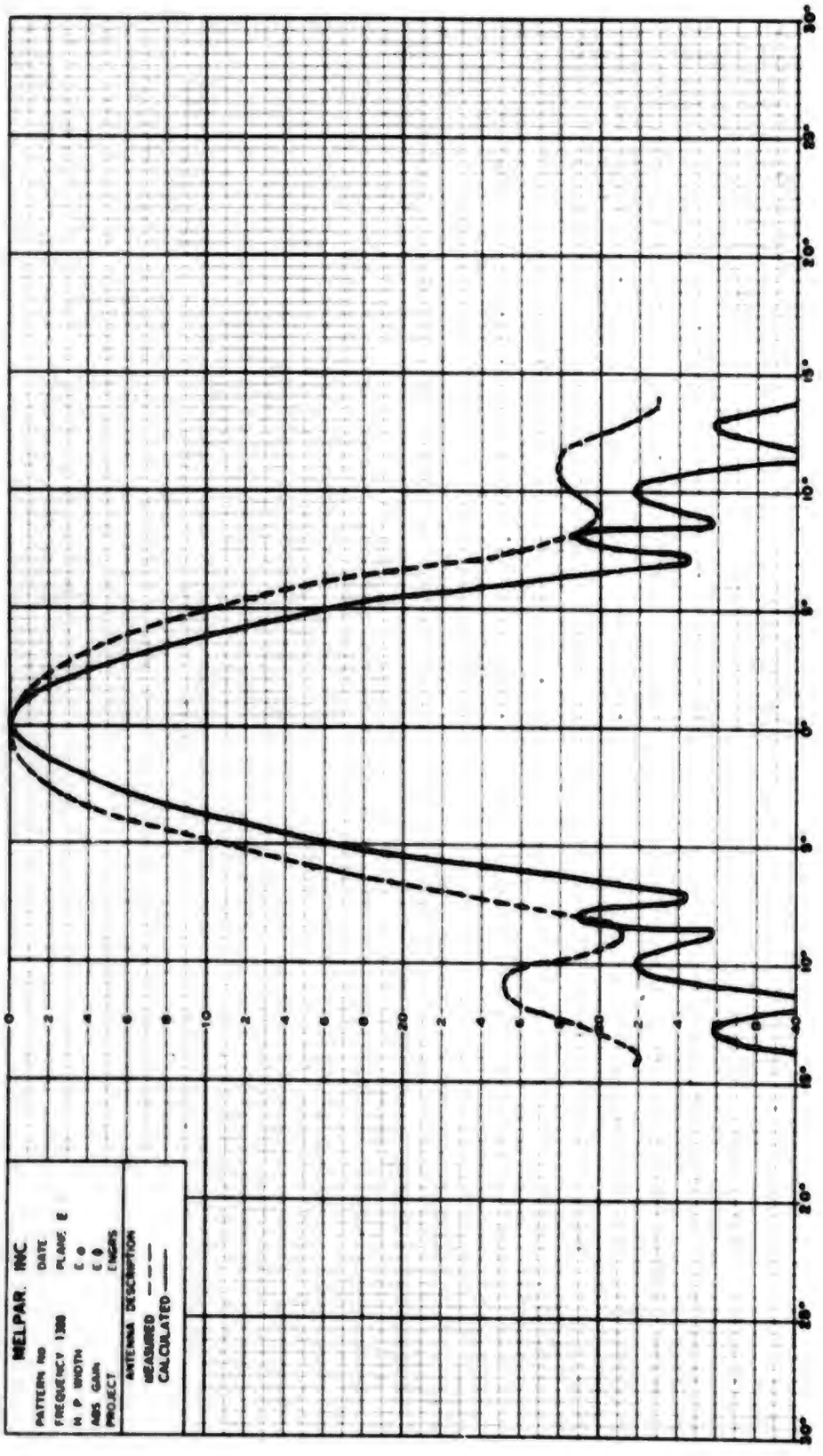

Figure 29. AN/TPS-1D, $D^2/2\lambda$ (135') Fresnel E-Plane Pattern

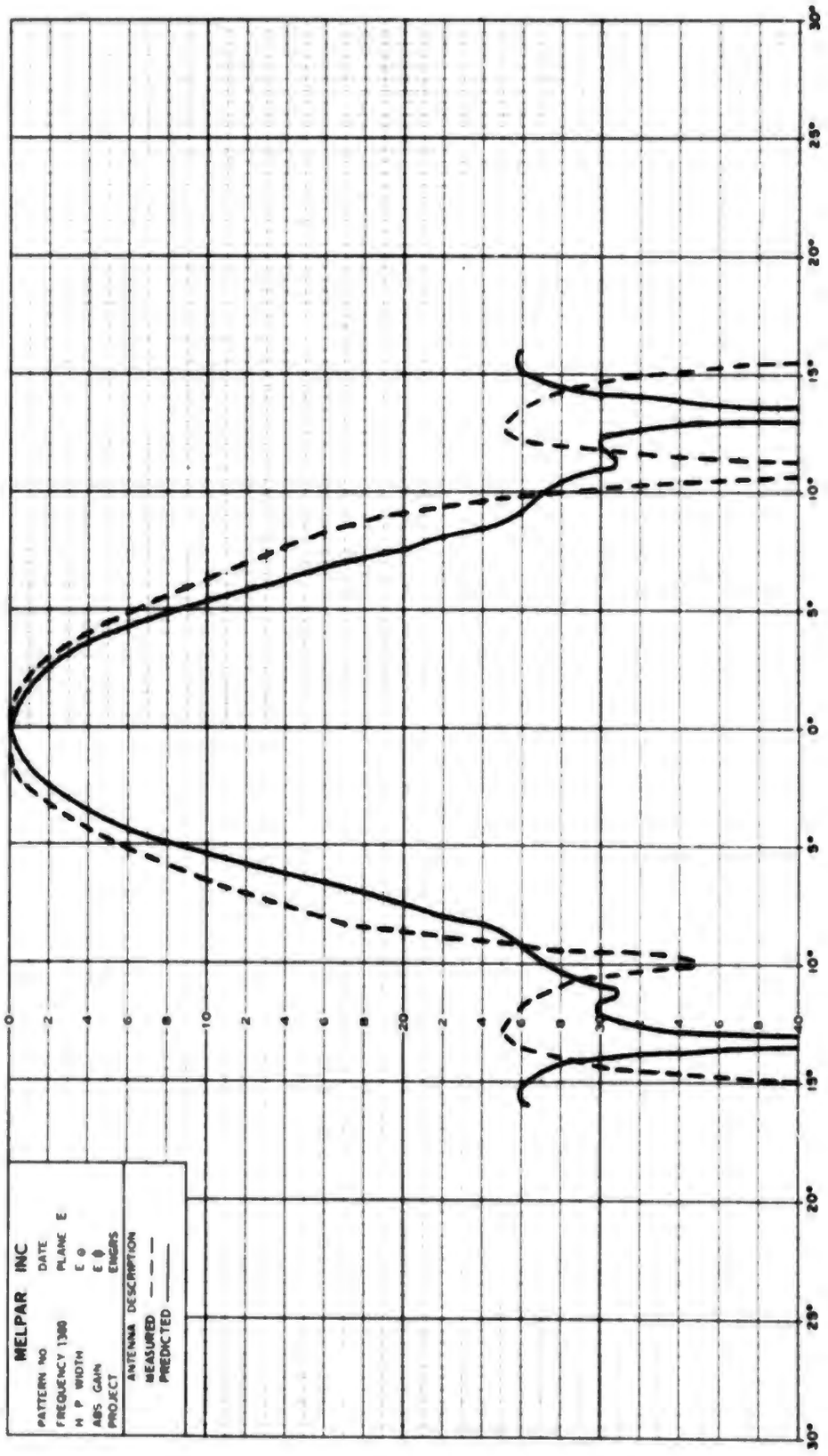

Figure 30. AN/TPS-1D, $D^2/4\ \lambda$ (67′) Fresnel E-Plane Pattern

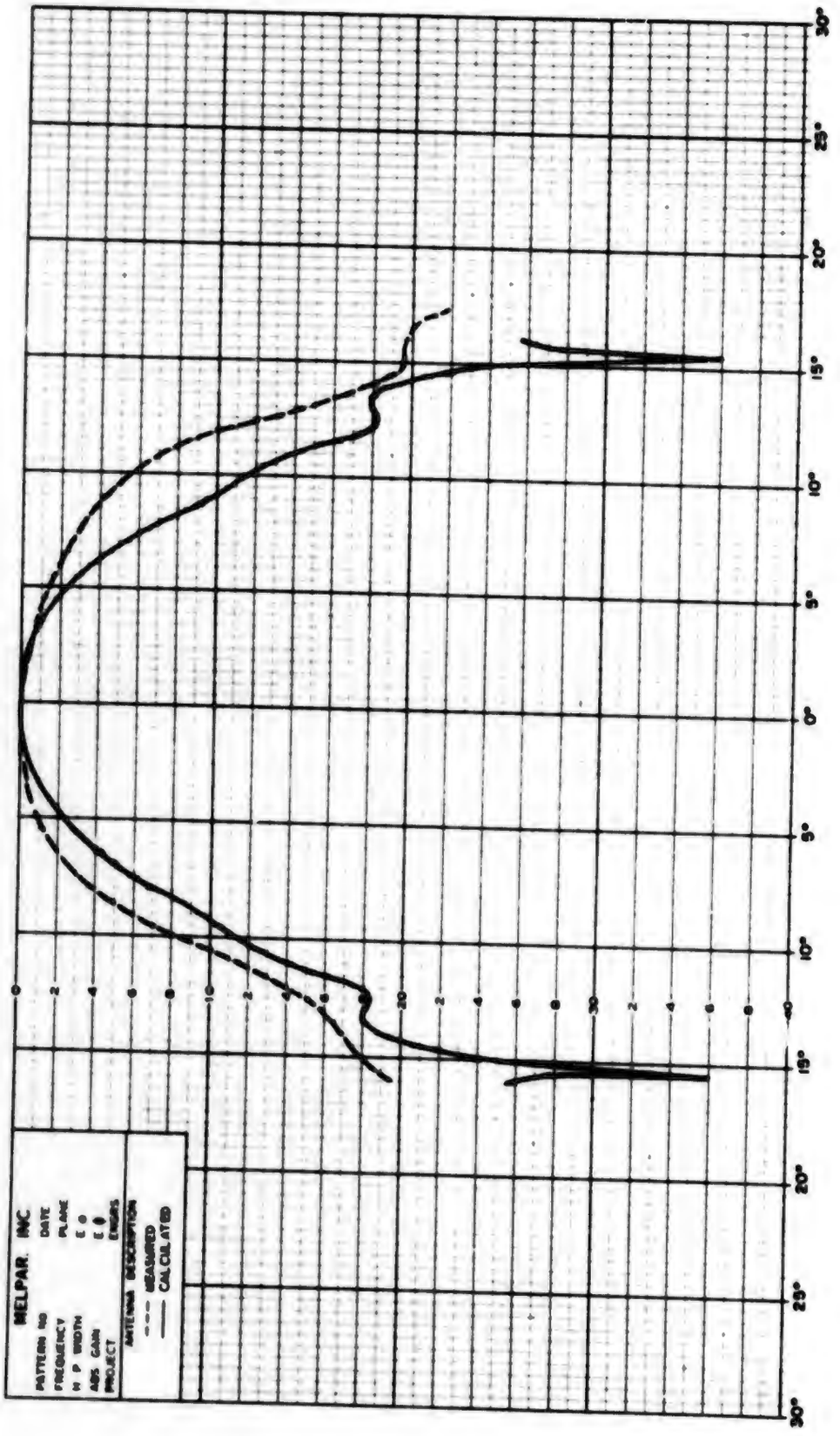

Figure 31. AN/TPS-1D, $D^2/8\lambda$ (30') Fresnel E-Plane Pattern

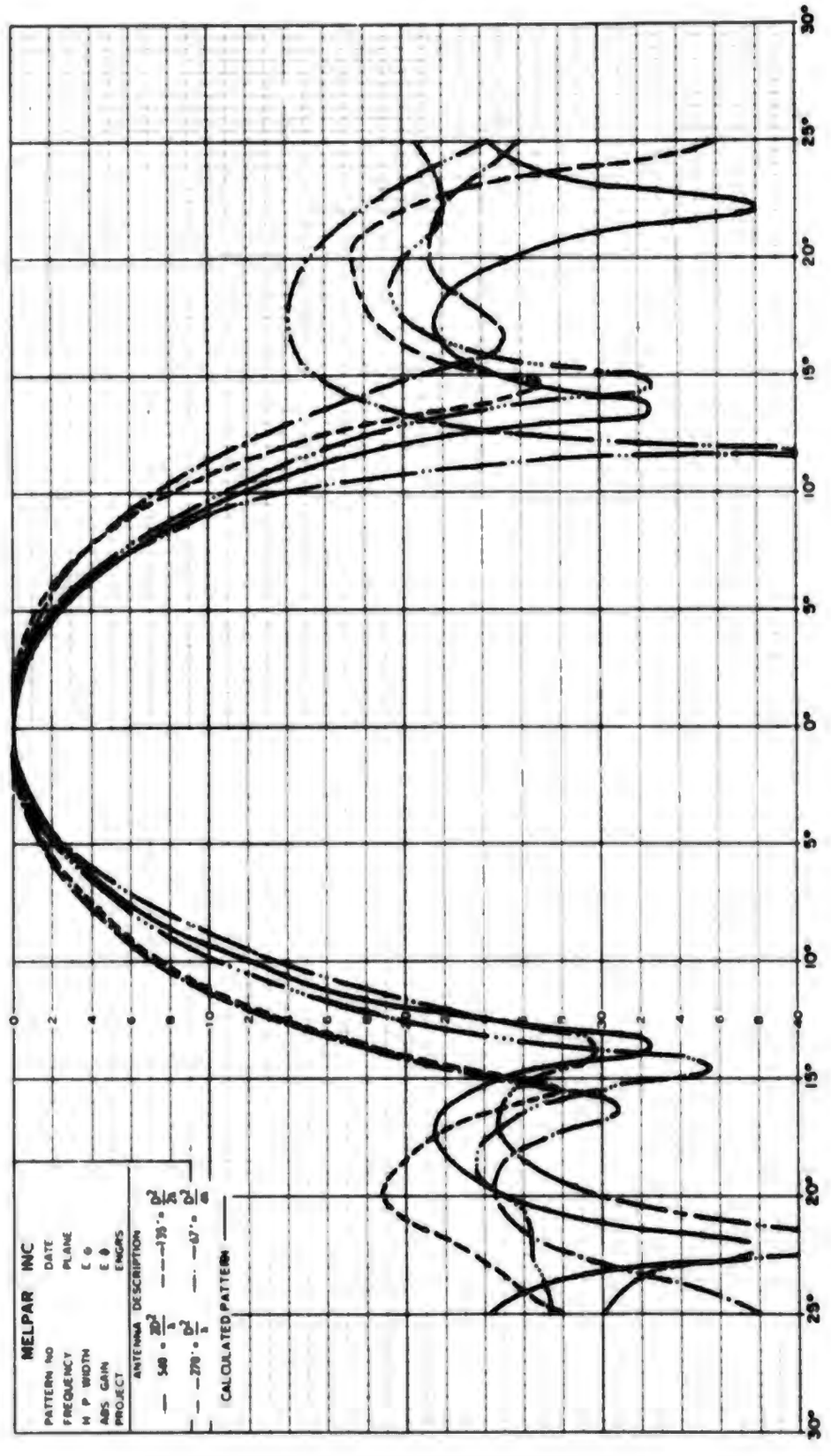

Figure 32. AN/TPS-1D H-Plane Patterns

lobes and broader main beam which is evident in the measured patterns. The calculated aperture illumination may also be slightly in error due to the lack of precise antenna dimensions for calculating the illumination. In addition the effect of ground reflections may be present in the measured H-plane patterns and possibly to a lesser degree in the measured E-plane patterns.

In Appendix III the details of the calculation of a Fresnel Zone E-plane pattern of the AN/TPS-1D are shown. A sample calculation of the strip illumination function $F_n(y_s)$ is given and the evaluation of the expression (61) at $v = 4\pi$ is shown in detail.

4. PHASED ARRAYS

The determination of the field vectors of an arbitrary array at an arbitrary field point requires a complicated computer summation of the field vectors over all the elements for each field point. The assumption of a single rectangular vector potential for a large planar array of identical elements at ranges restricted to the areas of validity of the scalar Fresnel approximation simplifies such a summation to the determination of a single scalar field component. For unequally spaced arrays, the summation will assume its simplest form when the element positions are defined by a single spacing function. In general, however, double summation indices or at least two spacing functions will be involved. For the case of a single spacing function, if the Green's function associated with the element position description is not excessively complicated, the simplest summation is available via Ishmaru's theory of unequally spaced arrays[12]. For the simple case of a straight line array with uniform spacing, or unequal spacing with linear element density taper, a computer summation is not needed. The Fresnel zone field can be described with tabulations of trigonometric functions and Fresnel integrals. Other tabulations are available which are applicable to particular classes of element ordering laws. The theory can be extended to two dimensional problems for particular array designs and excitation representation. The main point emphasized by these illustrations is that a "Fresnel zone array factor" is available for describing the field. The problem of more general array designs may be simplified by using the approach in a row-by-row summation, or by summing in array strips.

The problem may be explicitly stated in spherical coordinates, where the primed coordinates represent the element distribution. The origin is at the array center. The vector potential is written as follows:

$$\vec{A}(R, \theta, \phi) = \sum_n \vec{A}_n(R,\theta,\phi; R'_n, \theta'_n, \phi'_n) = \hat{y} \sum_n A_n(\vec{R};\vec{R}'_n)$$

The field components are:

$$\vec{B}(\vec{R}) = \nabla(\vec{R}) \times \vec{A}(\vec{R}) \ , \quad \vec{E}(\vec{R}) = i\omega \left[\vec{A}(\vec{R}) - \frac{1}{k^2} \nabla(\vec{R}) \nabla(\vec{k}) \cdot \vec{A}(\vec{R}) \right]$$

where: $\vec{B} = \mu \vec{H}$, $\omega = 2\pi f$, $k = 2\pi/\lambda$, $\eta = \sqrt{\mu/\epsilon}$

The problem is greatly simplified by the following restrictions.

$$k|\vec{R}-\vec{R}'| \gg 1 \ , \quad \vec{R}-\vec{R}' \simeq \vec{R} \ .$$

In this case:

$$\nabla\nabla\cdot\vec{A} \simeq -k^2 A_R \hat{R} \ , \quad \vec{E}(\vec{R}) \simeq i\omega \left[A_\theta \hat{\theta} + A_\phi \hat{\phi} \right]$$

Orthogonal components of the transverse field have the relation:

$$E_{t_1} \simeq \eta H_{t_2} \ , \quad \hat{t}_1 \cdot \hat{t}_2 = 0.$$

Consequently, at a range of a few array diameters, the field can be described by a single scalar component. In the convenient coordinate system orientation.

$$E(\vec{R}) = \sum_n E_n(\vec{R};\vec{R}'_n)$$

Since the angle between the ray from a field point to an array element and the array normal is essentially constant over the array, and by virtue of the identity of the elements and essential constancy of the space attenuation

from the field point to the array elements, the field expression may be written as follows:

$$E(\vec{R}) = E_o(\hat{R})\, e^{-ikR} \sum_n C_n e^{ikR_n} \qquad (62)$$

$$R_n = \left(R^2 + R'^2_n - 2\,\vec{R}\cdot\vec{R}'_n \right)^{1/2} \simeq R - R'_n \cos\Psi_n + \frac{R'^2_n}{2R} \sin^2\Psi_n$$

where $E_o(\hat{R})$ = element pattern

and C_n = n^{th} element amplitude and phase.

The array factor of the plane array is analogous to the usual focused aperture integral problem where the integral is an array factor to the cardioid pattern of the Huygens' wavelet.

As an example, for a plane array of electric (or magnetic) Hertz dipoles the field would take the following form.

$$\vec{A} = \sum_n \vec{p}_n \frac{e^{ikR_n}}{R_n} \simeq \frac{\hat{z}}{R} \sum_n p_n\, e^{ikR_n}$$

$$\cos\Psi_n = \cos\theta \cos\theta'_n + \sin\theta \sin\theta'_n \cos(\phi-\phi'_n)$$

$$E_\theta = \frac{-i\omega \sin\theta}{R} \sum_n p_n\, e^{ikR_n}$$

Or for an alternate coordinate orientation:

$$\vec{A} \simeq \frac{\hat{y}}{R} \sum_n p_n e^{ikR_n}, \quad \cos\Psi_n = \sin\theta \cos(\phi-\phi'_n)$$

$$E_\theta = \frac{i\omega \cos\theta \sin\phi}{R} \sum_n p_n\, e^{ikR_n}$$

$$E_\phi = \frac{i\omega \cos\phi}{R} \sum_n p_n e^{ikR_n}$$

Plane arrays of more complicated elements may be represented by the vector sum of the rectangular component vector potentials. Consequently, the array factor form of equation (1) is of primary interest. The only different thing about the ordinary far field array factor of an equally spaced array is that the array factor can be represented as a polynominal and simply summed. A summation technique for unequally spaced arrays at arbitrary field points has been developed by Ishimaru. The summation may be represented on a curve expressed as follows.

$$\vec{E}(\vec{R}) = \sum_{n=1}^{N} f(n) \quad , \quad f(n) = C(\vec{R}_n') \quad G(\vec{R}; \vec{R}_n') \tag{63}$$

$G(\vec{R};\vec{R}_n')$ = appropriate Green's function.

$$\sum_{n=1}^{N} f(n) = \sum_{n=1}^{N} \int_{0<\varepsilon<1}^{\varepsilon+N} f(v)\, \delta(v-n) \, dv = \sum_{m=-\infty}^{\infty} \int_{\varepsilon}^{\varepsilon+N} f(v)\, e^{-i2\pi mv} \, dv$$

$\delta(v-n)$ = delta function in range from ε to $\varepsilon+N$.

The function $f(v)$ contains the continuous extension of $C(\vec{R}')$ and $G(\vec{R};\vec{R}')$ as envelopes of $C(\vec{R}_n')$ and $G(\vec{R};\vec{R}_n')$. With a change of variable, the sum is written as follows.

$$\vec{E}(\vec{R}) = \sum_{m=-n}^{n} \int_{s(o)}^{s(N)} f\left[v(s)\right] \, e^{-i2\pi m v(s)} \, \frac{dv(s)}{ds} \, ds$$

$ds = |d\vec{R}'|$, $\frac{dv}{ds}$ = element density.

The m-series is rapidly convergent. This approach may be extended to two summation indices for particular array designs. For an array problem that can be properly given a product representation, equation (4) may be re-written as follows:

$$E(\vec{R}) = \sum_{m=1}^{M} \sum_{n=1}^{N} f(m)\, f(n) = \sum_{m=-\infty}^{\infty} \sum_{n=-\infty}^{\infty} \int_{\varepsilon}^{\varepsilon+M} \int_{\varepsilon}^{\varepsilon+N} f(u)\, f(v)\, e^{-i2\pi(mu+nv)}\, du\,dv$$

For elements arrayed at the intersections of a rectangular grid, the following relation applies in the small angle Fresnel zone.

$$G(\vec{R};\, x')\, G(\vec{R};\, y')_R\, e^{-ikR} = G(\vec{R};\vec{R}')\ ,\ \vec{R}' = \vec{x}' + \vec{y}.$$

The quantity R is independent of the integration variables. Unequally spaced arrays are generally equally fed. Consequently, the following is a useful expression for the grid array within the applicable region for the small angle scalar Fresnel approximation.

$$E(\vec{R}) = E_o(\vec{R}) \sum_{m=-\infty}^{\infty} \sum_{n=-\infty}^{\infty} \int_{x'(\varepsilon)}^{x'(\varepsilon+M)} \int_{y'(\varepsilon)}^{y'(\varepsilon+N)} e^{ik\left(\frac{x'^2}{2R} - \frac{xx'}{R} + \frac{y'^2}{2R} - \frac{yy'}{R}\right)} e^{-i2\pi(mu+nv)} \frac{dv}{dx'} \frac{du}{dy'}\, dx'\,dy'$$

The continuous extension of the phasing for beam steering in the direction defined by the direction cosines $\frac{x_o}{R}$, $\frac{y_o}{R}$, has the following representation.

$$C(x',\, y') = e^{ik\left(\frac{x_o}{R} x' + \frac{y_o}{R} y'\right)}$$

If the array summation is performed row-by-row on rows of x', each row must be adjusted in phase by the quantity: $e^{ik\left(\frac{y_m'^2}{2R} - \frac{yy'_m}{R}\right)}$. Thus the summation

has the following representation.

$$E(\vec{R}) = \sum_{m} \sum_{n} f_m(n) \; e^{ik\left(\frac{y_n^2}{2R} - \frac{yy'_n}{R} \right)}$$

If the summation is performed in strips with each strip given its average phase weight, the strip widths must satisfy the following inequalities.

$$k \frac{y}{R} \Delta y' < \frac{\pi}{10} \quad \text{or} \quad \frac{k(\Delta y')^2}{2R} < \frac{\pi}{8} .$$

As one example of the method, Ishimaru gives the following representation for a uniform line array in the far field in normalized variables.

$$E(u) = \sum_{m=-\infty}^{\infty} (-1)^{m(N-1)} E_m(u) \quad , \; u = ka \sin\theta \; , \; 2a = s(N) - s(o).$$

$$E_m(u) = \frac{1}{2} \int_{-1}^{1} A(x) \; e^{i\Psi(x)} \; e^{-i(u + m\pi N)x} \, dx \tag{64}$$

$$A(x) \, e^{i\Psi(x)} = C(s) \left\{ = C(\vec{R}') \right\}_{1}$$

x = normalized "source position function" s(v).

$$E_o(u) = \frac{1}{2} \int_{-1}^{1} A(x) \, e^{i(\Psi(x) - ux)} \, dx$$

$$E_m(u) = E_o(u + m\pi N)$$

$(-1)^{m(N-1)} = (-1)^m$, (N even); $(-1)^{m(N-1)} = 1$, (N odd).

For the case of C(s) = 1:

$$E(u) = \sum_{m=-\infty}^{\infty} (-1)^{m(N-1)} \frac{\sin(u+m\pi N)}{(u+m\pi N)} \tag{65}$$

The well known result by geometric summation is:

$$E(u) = \frac{\sin\left(\frac{1}{2} Nkd \sin\theta\right)}{N \sin\left(\frac{1}{2} kd \sin\theta\right)} = \frac{\sin u}{N \sin\left(\frac{u}{N}\right)}, \quad Nd = 2a$$

The series representation of this expression in equation (64) requires about three terms for adequate convergence. The advantage of (65) is that it can be modified to determine the Fresnel zone field in terms of tabulated Fresnel integrals, instead of tabulating the array summation for each field point. This may be illustrated by considering the small angle Fresnel approximation to the Green's function. The integral desired for the zero order term is of the following form.

$$I = \int_{-x_1}^{x_1} e^{ikR''} dx' \tag{66}$$

$$R'' = \left\{(x'-x)^2 + y^2 + z^2\right\}^{1/2} \simeq R - \frac{xx'}{R} + \frac{x'^2}{2R}$$

$$= R - b^2 + \left(\sqrt{\frac{x'}{2R}} - b\right)^2$$

$$b = \sqrt{\frac{x}{2R}}$$

$$I = e^{ik\left(R - \frac{x^2}{2R}\right)} \int_{x_1}^{x_1} e^{i\frac{k}{2R}(x'-x)^2} dx', \quad \frac{kx'^2}{2R} \left(\frac{x}{R}\right)^2 < \frac{\pi}{8}$$

$$\int_{-x_1}^{x_1} e^{i\frac{k}{2R}(x'-x)^2}\,dx' = \int_{\xi(-x_1)}^{\xi(x_1)} e^{i\phi\xi^2}\,d\xi$$

$$\xi^2 = (x'-x)^2 \quad , \quad d\xi = dx' \quad , \quad \phi = \frac{k}{2R}$$

In conformity with the traditional parameters for Fresnel integral tabulations, the following notation is introduced.

$$F(w) = \int_0^w e^{i\frac{\pi}{2}\tau^2}\,d\tau = C(w) + i\,S(w) \ ,$$

$$C(w) = \int_0^w \cos\left(\frac{\pi}{2}\tau^2\right)d\tau, \quad S(w) = \int_0^w \sin\left(\frac{\pi}{2}\tau^2\right)d\tau.$$

$$\int_{\xi(-x_1)}^{\xi(x_1)} e^{i\phi\xi^2}\,d\xi = \sqrt{\frac{\pi}{2\phi}}\left[F(w_2) - F(w_1)\right]$$

$$w_2 = \sqrt{\frac{2\phi}{\pi}}\,(x_1 - x) \ , \quad w_1 = \sqrt{\frac{2\phi}{\pi}}\,(-x_1 - x)$$

Fresnel integral tabulations are given in Jahnke and Emde[13] for values of w up to w = 50.0. The integrals for larger values are accurately given by the asymptotic expansion of the error function.[13]

---

13. E. Jahnke and F. Emde, "Tables of Functions," Dover Publ, 1945, pg. 34 and 36.

$$F*(w) = \sqrt{\frac{1}{2i}}\ \mathrm{erf}\ \left(\sqrt{iz}\right),\ i\tfrac{\pi}{2}w^2 = iz$$

$$\sqrt{\frac{1}{2i}}\ \mathrm{erf}\left(w\sqrt{i\tfrac{\pi}{2}}\right) - \sqrt{\frac{1}{2i}} - \frac{e^{-i\frac{\pi}{2}w^2}}{i\pi w}\left\{1 - \frac{1}{(i\pi w^2)} + \frac{1\cdot 3}{(i\pi w^2)^2} - \frac{1\cdot 3\cdot 5}{(i\pi w^2)^3} + \cdots\right\}$$

$$F(w) \approx \sqrt{\frac{1}{-2i}} - \frac{i\, e^{i\frac{\pi}{2}w^2}}{w}\ ,\ |\pi w^2| \gg 1$$

$$\int_{\xi_-}^{\xi_+} e^{i\phi\xi^2}\, d\xi \propto \frac{1}{\pi}\sqrt{\frac{\pi}{2\phi}}\left[\frac{e^{i\frac{\pi}{2}(w_2^2 - 1)}}{w_2} - \frac{e^{i\frac{\pi}{2}(w_1^2 - 1)}}{w_1}\right]\ ,\ w^2 \gg 1 \qquad (67)$$

By virtue of this expression, the convergence of the array factor series is evident for large arguments.[14] Few more terms are required in the Fresnel zone then in the far field. In the far field (66) reduces to:

$$I = 2x_1\, e^{ikR}\, \frac{\sin\left(k\frac{x}{R}x_1\right)}{\left(k\frac{x}{R}x_1\right)}$$

The normalizing factor is $\frac{e^{-ikR}}{2x_1}$. The quantity $\Psi(x)$ in (64) may be interpreted as the quadratic Fresnel zone phase variable. Thus the zero order term:

$$E_o(u) = e^{-i\frac{kx^2}{2R}}\sqrt{\frac{\pi R}{4kx_1^2}}\left[F(w_2) - F(w_1)\right]\ ,\ u = \frac{kxx_1}{R}$$

14. F. Peirce and R. Foster, "A Short Table of Integrals," Ginn and Co., 1956, pg. 97.

$$w_2 = \sqrt{\frac{kR}{\pi}}\left(\frac{x_1 - x}{R}\right), \quad w_1 = \sqrt{\frac{kR}{\pi}}\left(\frac{-x_1 - x}{R}\right)$$

For the m^{th} order term, the phase variables in (64) are given by:

$$kR'' = kR - \frac{kxx'}{R} - m\pi N\frac{x'}{x_2} + \frac{kx'^2}{2R} = kR - kb^2 + k\left(\frac{x'}{\sqrt{2R}} - b\right)^2$$

$$b = \frac{x}{\sqrt{2R}} + \frac{\sqrt{2R}}{2kx_1}m\pi N, \quad b^2 = \frac{x^2}{2R} + \frac{mNx}{kx_1} + \frac{R}{2}\left(\frac{m\pi N}{kx}\right)^2$$

$$w_{2_m} = \sqrt{\frac{kR}{\pi}}\left(\frac{x_1 - x}{R} - \frac{m\pi N}{kx_1}\right), \quad w_{1_m} = \sqrt{\frac{kR}{\pi}}\left(\frac{-x_1 - x}{R} - \frac{m\pi N}{kx_1}\right),$$

$$E_m(x, R) = e^{-i\left[\frac{kx^2}{2R} + m\pi N\frac{x}{x_1} + \frac{kR}{2}\left(\frac{m\pi N}{kx_1}\right)^2\right]}\sqrt{\frac{R}{4kx_1^2}}\left[F(w_{2_m}) - F(w_{1_m})\right]$$

The small angle Fresnel zone array factor is given by:

$$E(x,R) = e^{-i\frac{kx^2}{2R}}\sqrt{\frac{\pi R}{4kx_1^2}}\sum_{m=-\infty}^{\infty}(-1)^{m(N-1)}e^{-i\left[mN\pi\frac{x}{x_1} + \frac{kR}{2}\left(\frac{mN\pi}{kx_1}\right)^2\right]}\left[F(w_{2_m}) - F(w_{1_m})\right]$$

By applying equation (67), equation (68) reduces to (65) when $\frac{kx_1^2}{2R}$ is small. Although the physical angle from the array normal $\sin^{-1}(x/R)$ is limited by the inequality $\frac{kx_1^2}{2R}\left(\frac{x}{R}\right)^2 < \frac{\pi}{8}$. the argument of the Fresnel integral is unlimited in m. The angular usefulness of the array factor can be extended to cover the entire Fresnel zone by modifying b^2 and w_m of E_m in accordance

with the phase variable:

$$kR' = kR - \frac{kxx'}{R} - mN\pi \frac{x'}{x_1} + \frac{kx'^2}{2R}\left[1 - \left(\frac{x}{R}\right)^2\right]$$

The factor $\left[1 - (x/R)^2\right]$ was left out of the example to avoid complicating the notation. For this case the Fresnel zone boundary is essentially defined by the inequality:

$$\frac{kxx_1^3}{2R^3} < \frac{\pi}{8} .$$

For the case of an array with linear element density taper, the constant terms in dv/ds will involve Fresnel integrals as shown above, and the slope term will involve a sum of trigonometric functions and Fresnel integrals. Other tabulations are available for particular array ordering.

5. SPURIOUS FREQUENCY CHARACTERISTIC

5.1 Spurious Frequency Response of Electromagnetic Horn Antennas

The analysis of antenna performance at other than design frequencies is complicated by several considerations. The antenna performance becomes more critically dependent on the antenna dimensions as the wavelength decreases and the dimensions become electrically large enough that a multiplicity of higher order modes are generated by the antenna. When antennas are coaxially fed, the radiating efficiency of a coaxial mode is dependent on the impedance characteristics of the coaxial line. In both waveguide and coaxial structures any discontinuity in the structure, such as a connection or a probe, can excite higher order modes whose relative amplitude and phase may be difficult to predict.

Due to these complications previous investigations of spurious frequency response have been essentially experimental. Both Salati[15] and Pullara[16] have investigated experimentally the gain and pattern configuration of coaxially fed L- and S-band horns, respectively, over a 10 to 1 range in frequency. The effect of higher order modes on the radiation pattern of a horn is considerable since the aperture distribution is a function of the vectorial summation of all the modes present according to their phase and amplitude. Determining horn patterns from the individual pattern of each mode is not difficult, but finding the relative amplitude and phase of each of the modes in the aperture is a difficult task when several modes are present.

---

[15] O. M. Salati and D. O. Lewis, "Horn Patterns Are Recorded to the Tenth Harmonic" Electronics. Jan. 19, 1962, pp 56-58

[16] J. C. Pullara, and J. P. Jones, "Radiation Characteristics of Antennas at Other than Design Frequencies," IRE National Convention Record, March 1961.

A method of predicting the mode structure in a probe-fed electromagnetic horn has been suggested.[17] This treatment considers the effects of a probe enclosed by a dielectric rod feeding a horn with a circular taper. The report gives an outline for a proposed computer program for this horn; however, the procedure is quite complex for such a horn and is not easily adapted for other types of horns. Therefore it was felt that it would be more desirable to consider the simpler and more commonly encountered pyramidal horn fed by a probe which is not enclosed in a dielectric. This simplifies the calculations considerably and therefore is a more suitable means of checking the feasibility of this technique by comparison of calculated results with experimental data.

The method described[17] may be used to determine the modes set up by the probe since the equations given simplify to those of a simple probe if E_r, the relative dielectric constant of the dielectric rod, is taken to equal unity. This method may also be used to determine the propagation of the various modes in the horn. The step approximation used there is an adaptation of the technique given by Stevenson who uses the WKB method to find approximate solutions to the equations for propagation of electromagnetic waves in a horn of arbitrary shape. However, it was found that the assumption of a uniform phase front in the aperture did not give a sufficiently good approximation of the patterns of the individual modes radiated by the horn aperture. Therefore, it was assumed that the expressions of the referenced work gave the correct phase and amplitude at the center

17. "Calculations of FreeSpace Radiation Characteristics of Horn Antennas at Spurious Frequencies," Ricerla Scientif ia Applicata." Final Report, Appendix C, Contract No. AF 30(602)-2295 May 1961.

of the aperture and that the phase front in the aperture was of the form $e^{-jk(\xi^2/2\ell_e + \eta^2/2\ell_k)}$. This is the form of the aperture field used by Braun[18] to calculate the radiated fields of the TE_{10} mode of electromagnetic horns. The method of Braun may be modified and used to calculate the patterns of higher order modes resulting from the non-uniform phase in the aperture.

The patterns of a probe-fed pyramidal horn were measured over a wide band of frequencies and these measured patterns are shown in figure 33 and 34. The primary patterns of this horn were calculated in the principal planes at the fundamental frequency by the method described above and a comparison of the calculated and measured patterns is shown in figure 35. Calculation of the patterns at frequencies above the design band were restricted to the H-plane since computation of the H-plane pattern is simplified by the fact that only the TE_{on} modes affect the pattern in this plane. Thus at the third harmonic only two of the four modes need be calculated and at the sixth harmonic only four of the nineteen modes present need be calculated. It should be noted that this is not strictly the case if one takes into account the phase variation in the aperture although it is expected that the H-plane field due to the TE_{mn} (m≠o) modes is negligible compared to that of the TE_{on} modes. The pattern calculation at the third harmonic (7.5 gc) is in relatively close agreement with the measured results as may be seen in figure 36; however, the calculated sixth harmonic (15 gc) pattern shown in figure 37 deviated considerably from the measured pattern.

---

[18] E. H. Braun, "Gain of Electromagnetic Horns", Proc IRE, Jan. 1953, pp 109-115.

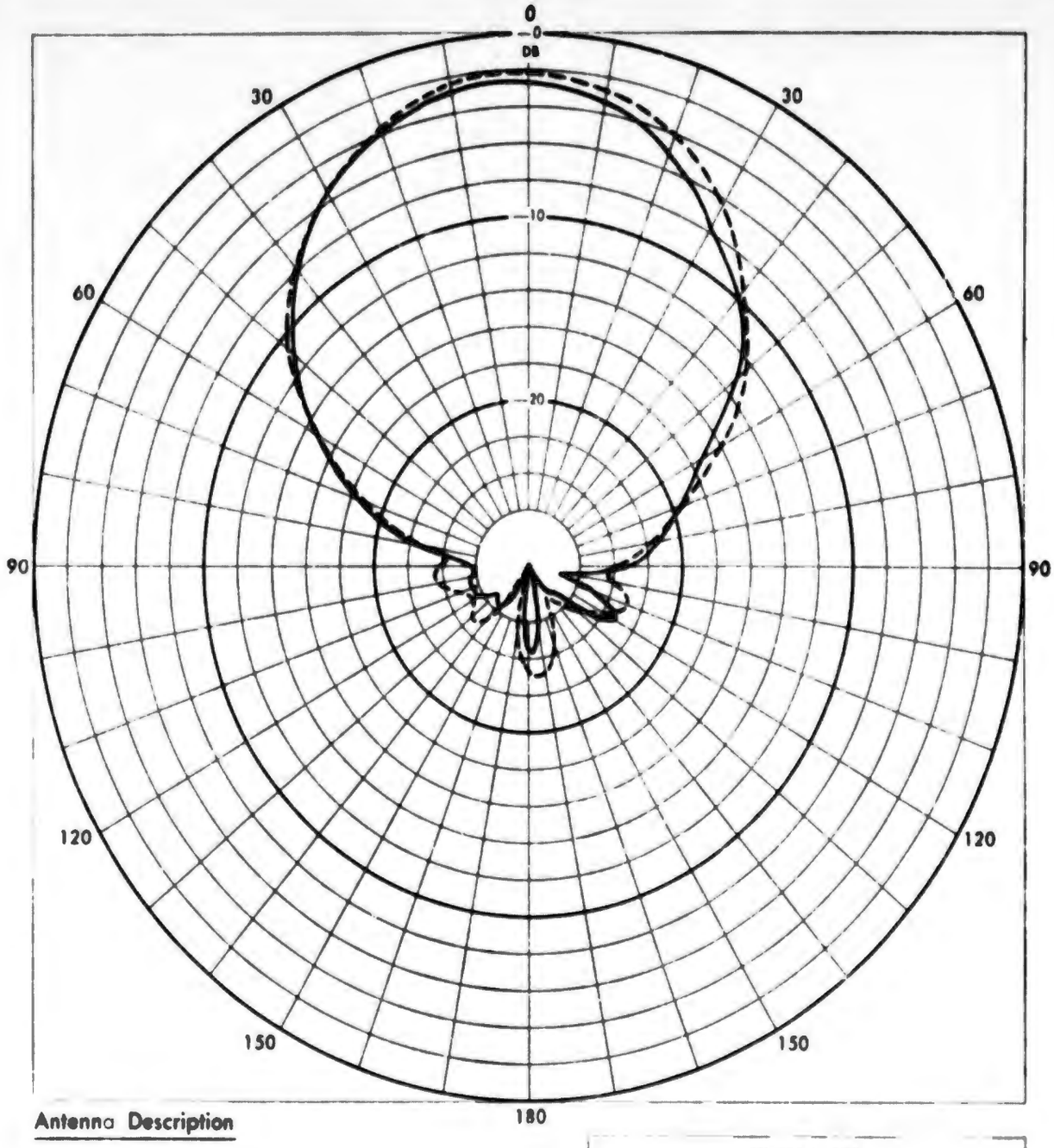

Figure 33. Far Field Radiation Patterns of a Probe-Fed S-Band Electromagnetic Horn at 2.5, 5, 7.5, 10, and 12.5Gc (Sheet 1 of 5)

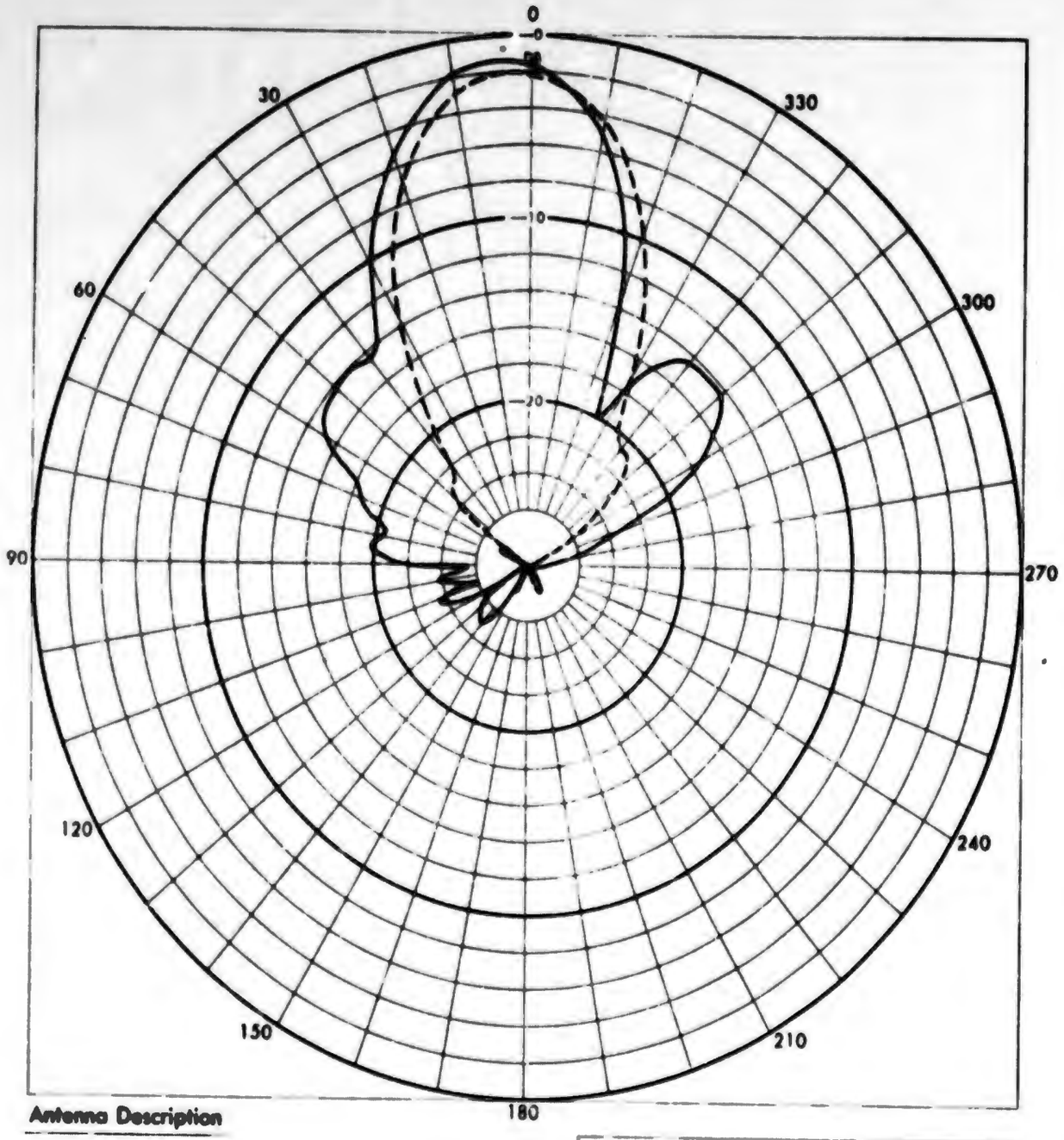

Figure 33. Far Field Radiation Patterns of a Probe-Fed S-Band Electromagnetic Horn at 2.5, 5, 7.5, 10, and 12.5 Gc (Sheet 2 of 5)

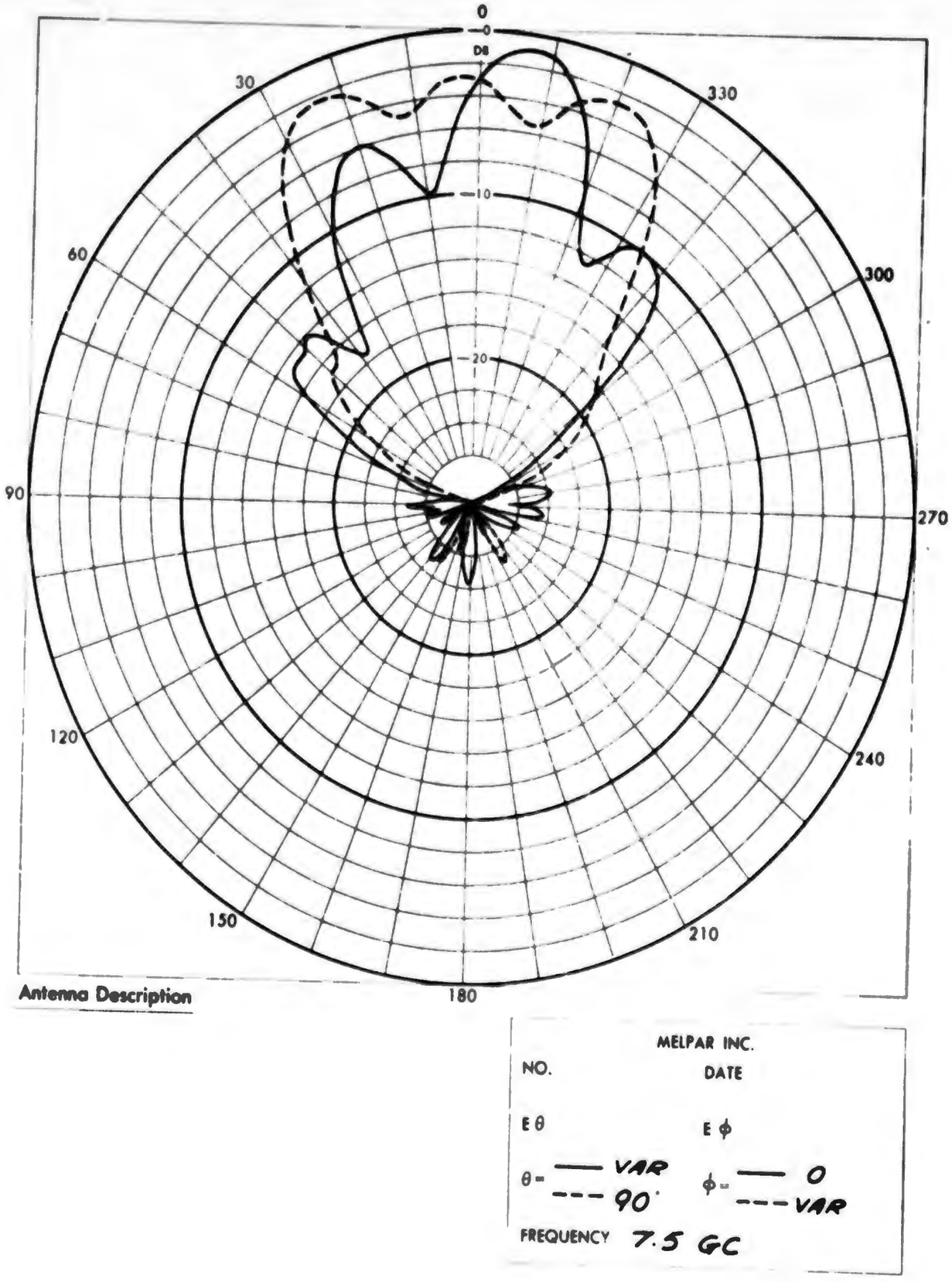

Figure 33. Far Field Radiation Patterns of a Probe-Fed S-Band Electromagnetic Horn at 2.5, 5, 7.5, 10, and 12.5 Gc (Sheet 3 of 5)

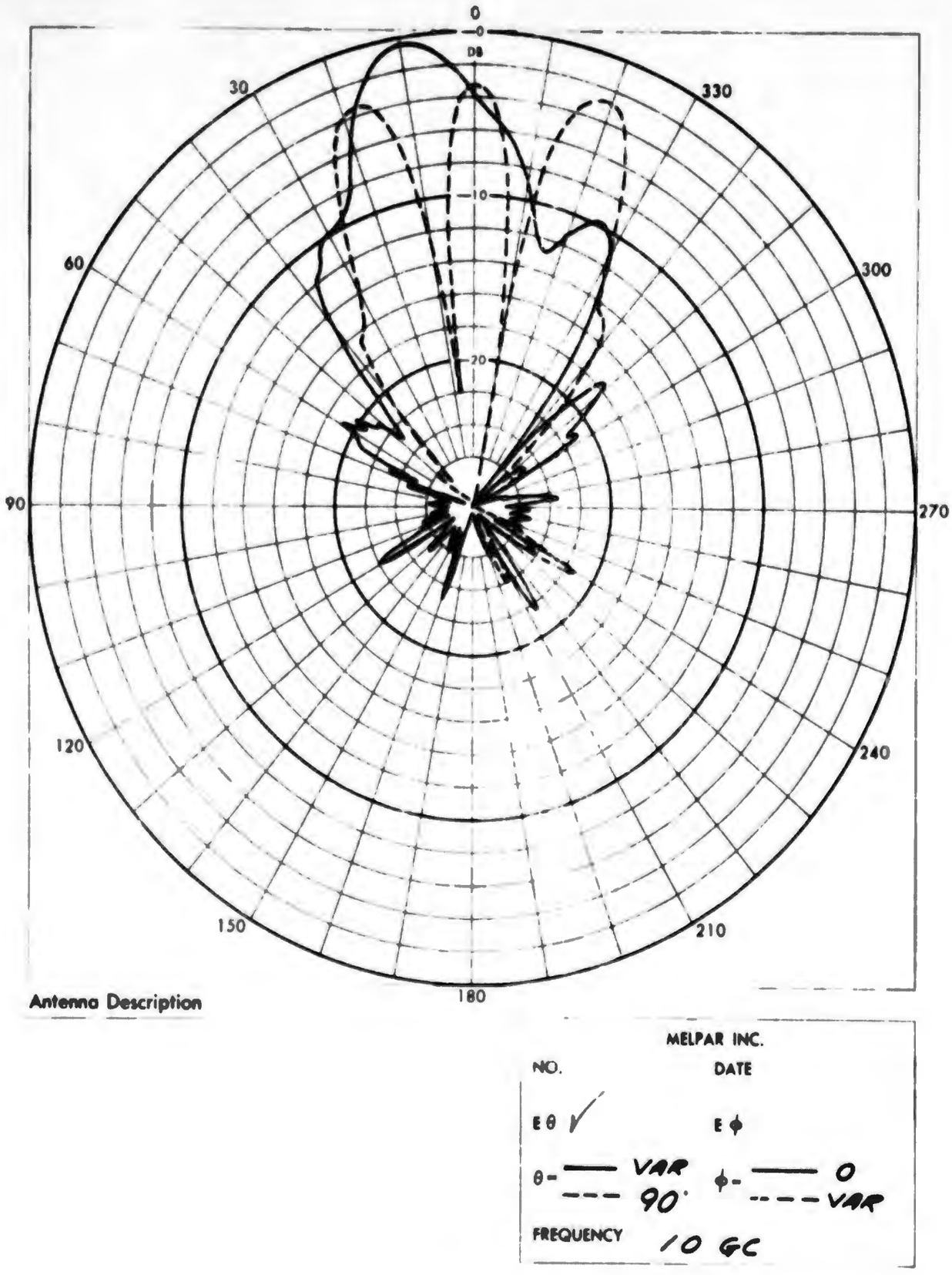

Figure 33. Far Field Radiation Patterns of a Probe-Fed S-Band Electromagnetic Horn at 2.5, 5, 7.5, 10, and 12.5 Gc (Sheet 4 of 5)

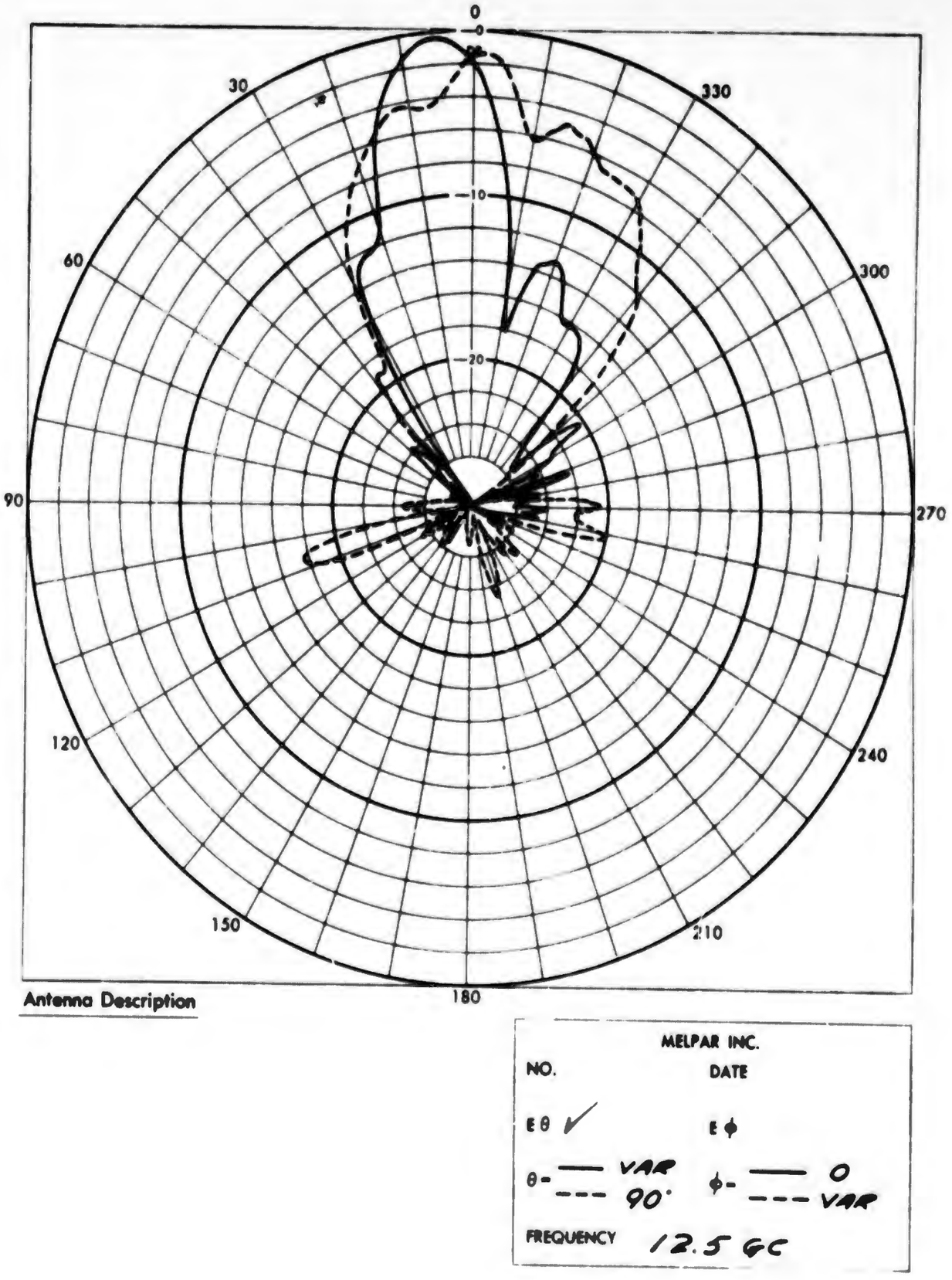

Figure 33. Far Field Radiation Patter of a Probe-Fed S-Band Electromagnetic Horn at 2.5, 5, 7.5, 10, and 12.5 Gc (Sheet 5 of 5)

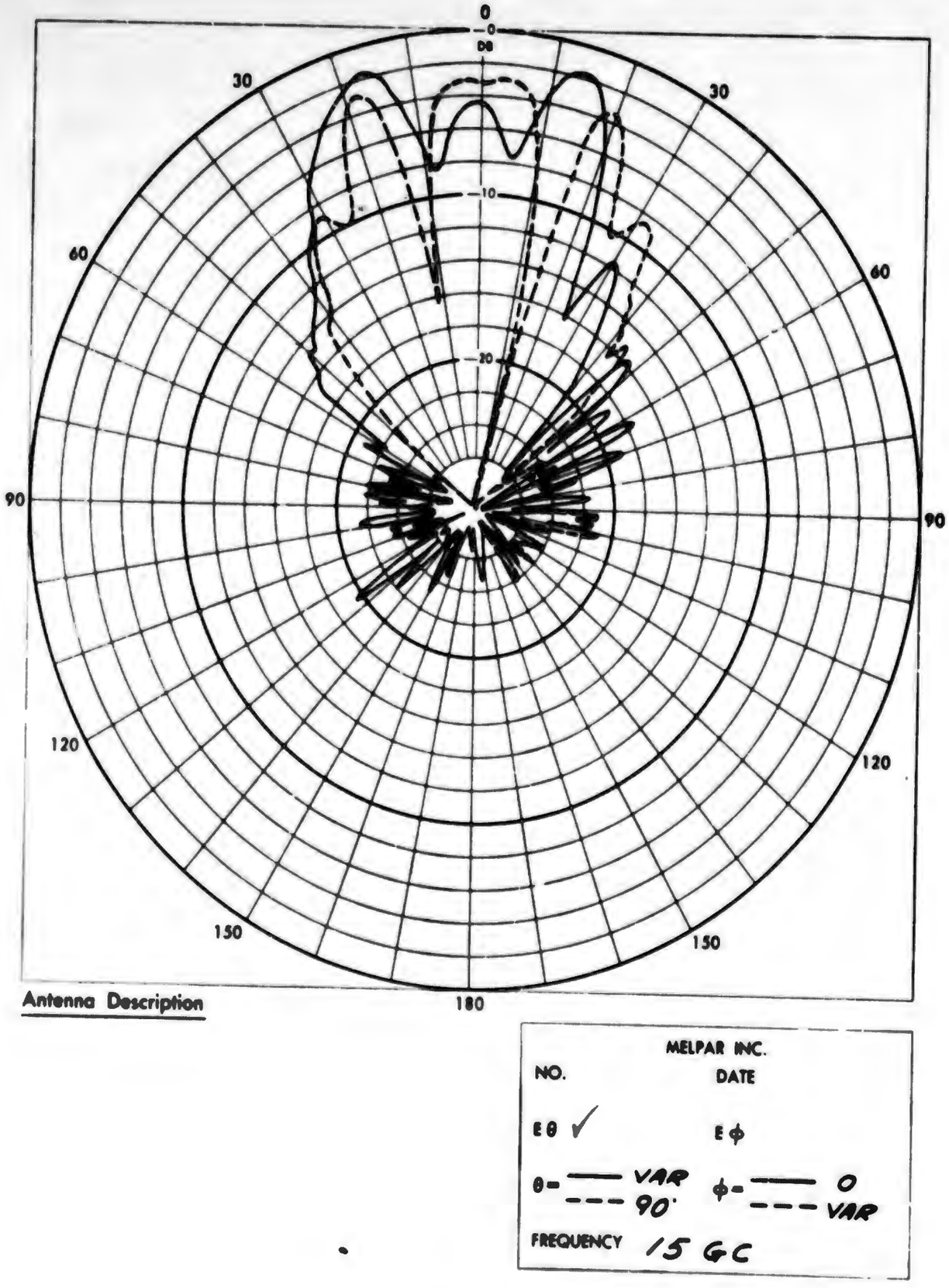

Figure 34. Far Field Radiation Patterns of a Probe-Fed S-Band Electromagnetic Horn at 15, 17.5, 20, and 20.5 Gc (Sheet 1 of 4)

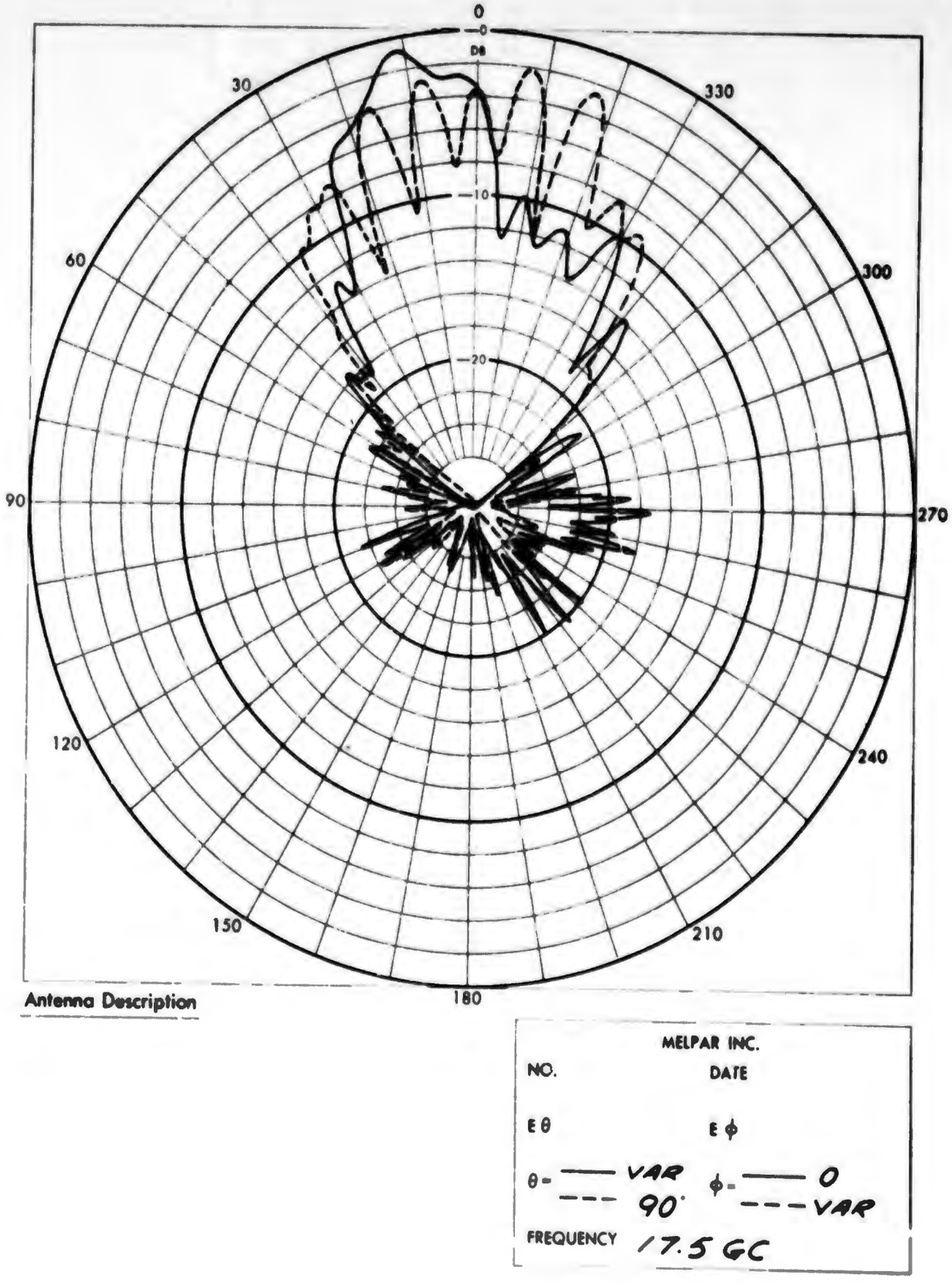

Figure 34. Far Field Radiation Patterns of a Probe-Fed S-Band Electromagnetic Horn at 15, 17.5, 20, and 20.5 Gc (Sheet 2 of 4)

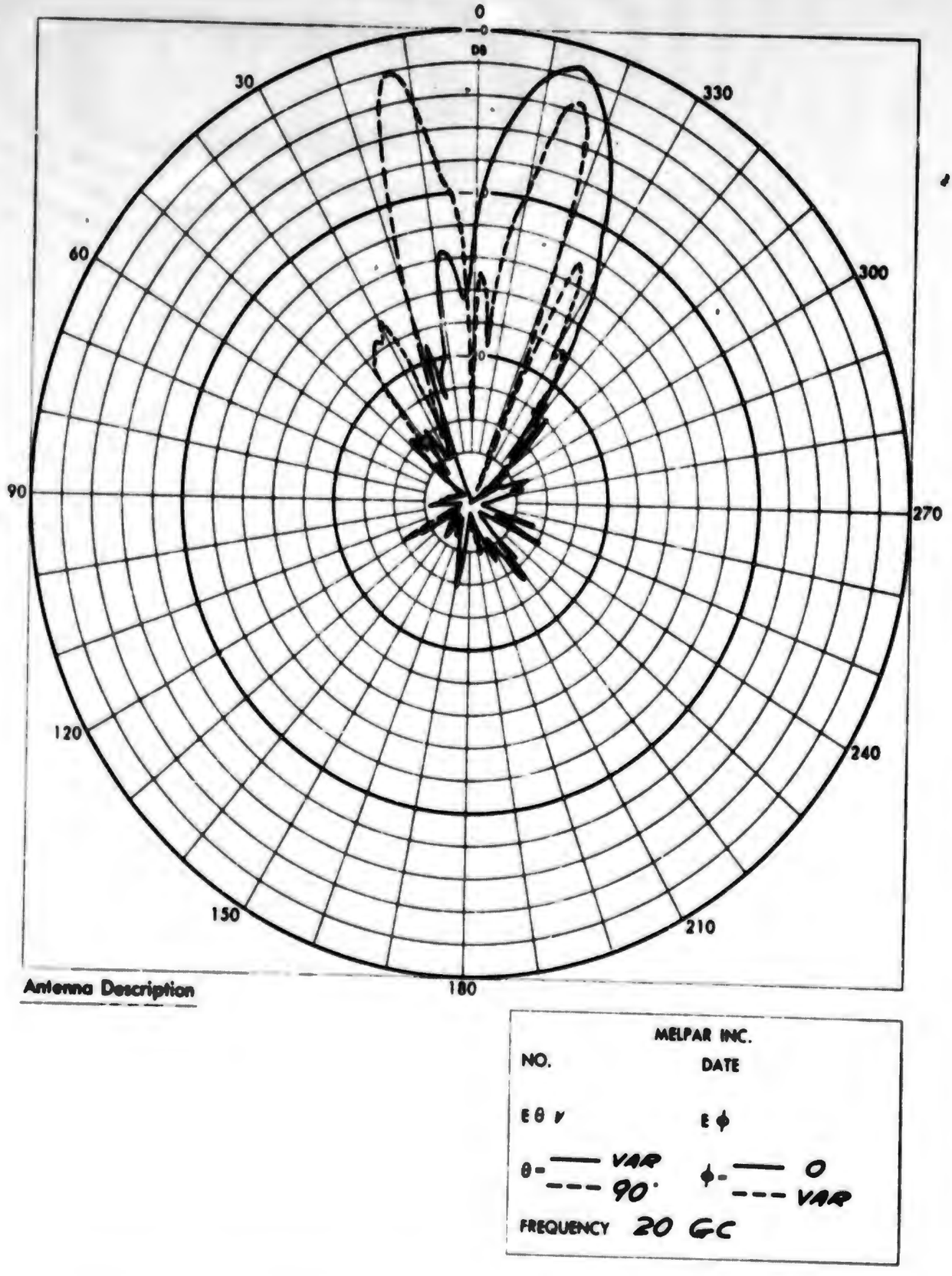

Figure 34. Far Field Radiation Patterns of a Probe-Fed S-Band Electromagnetic Horn at 15, 17.5, 20, and 20.5 Gc (Sheet 3 of 4)

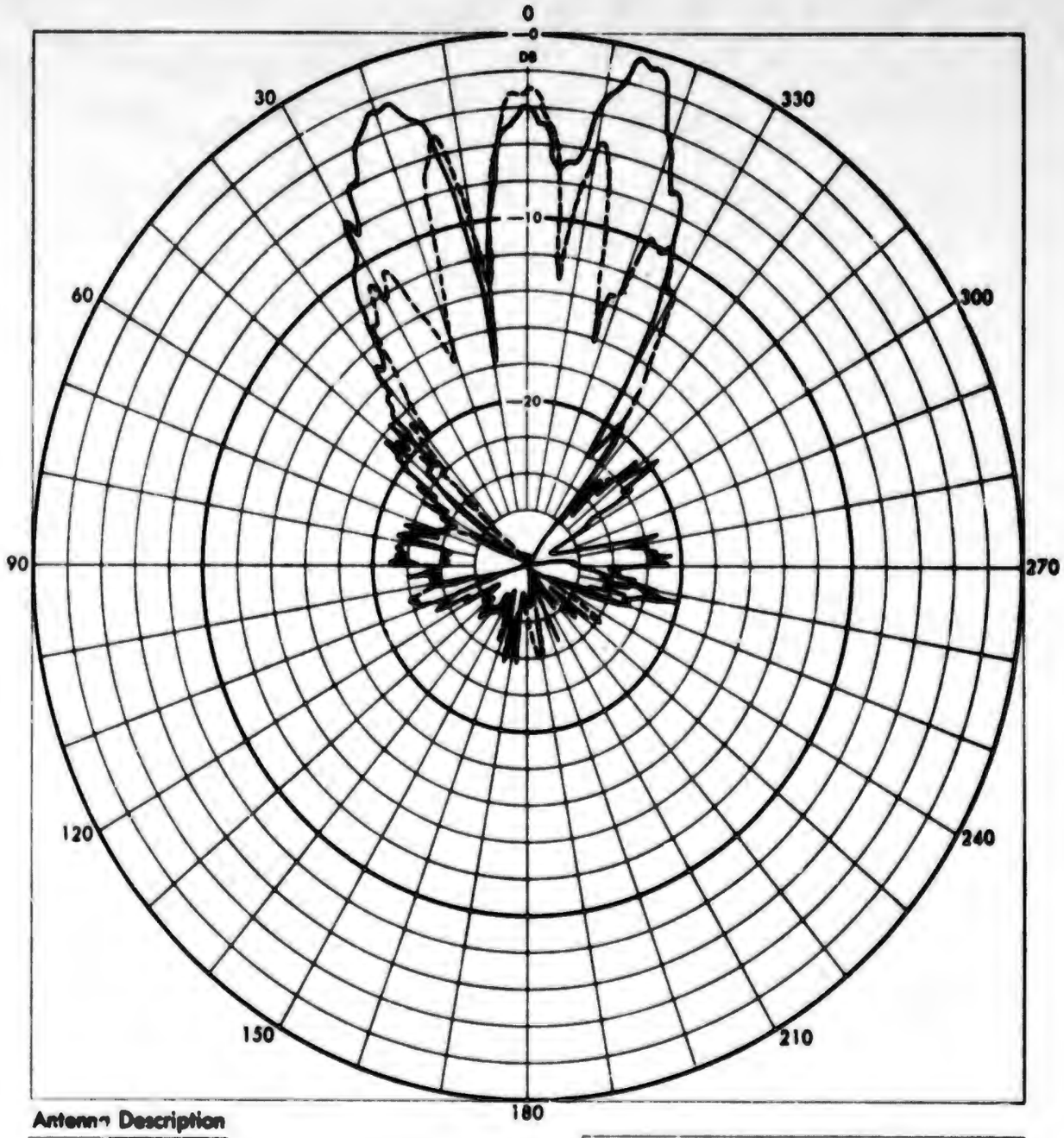

Antenna Description

MELPAR INC.

NO. DATE

Eθ ✓ Eϕ

θ- —— VAR --- 90° ϕ- —— 0 --- VAR

FREQUENCY 22.5 GC

Figure 34. Far Field Radiation Patterns of a Probe-Fed S-Band Electromagnetic Horn at 15, 17.5, 20, and 20.5 Gc (Sheet 4 of 4)

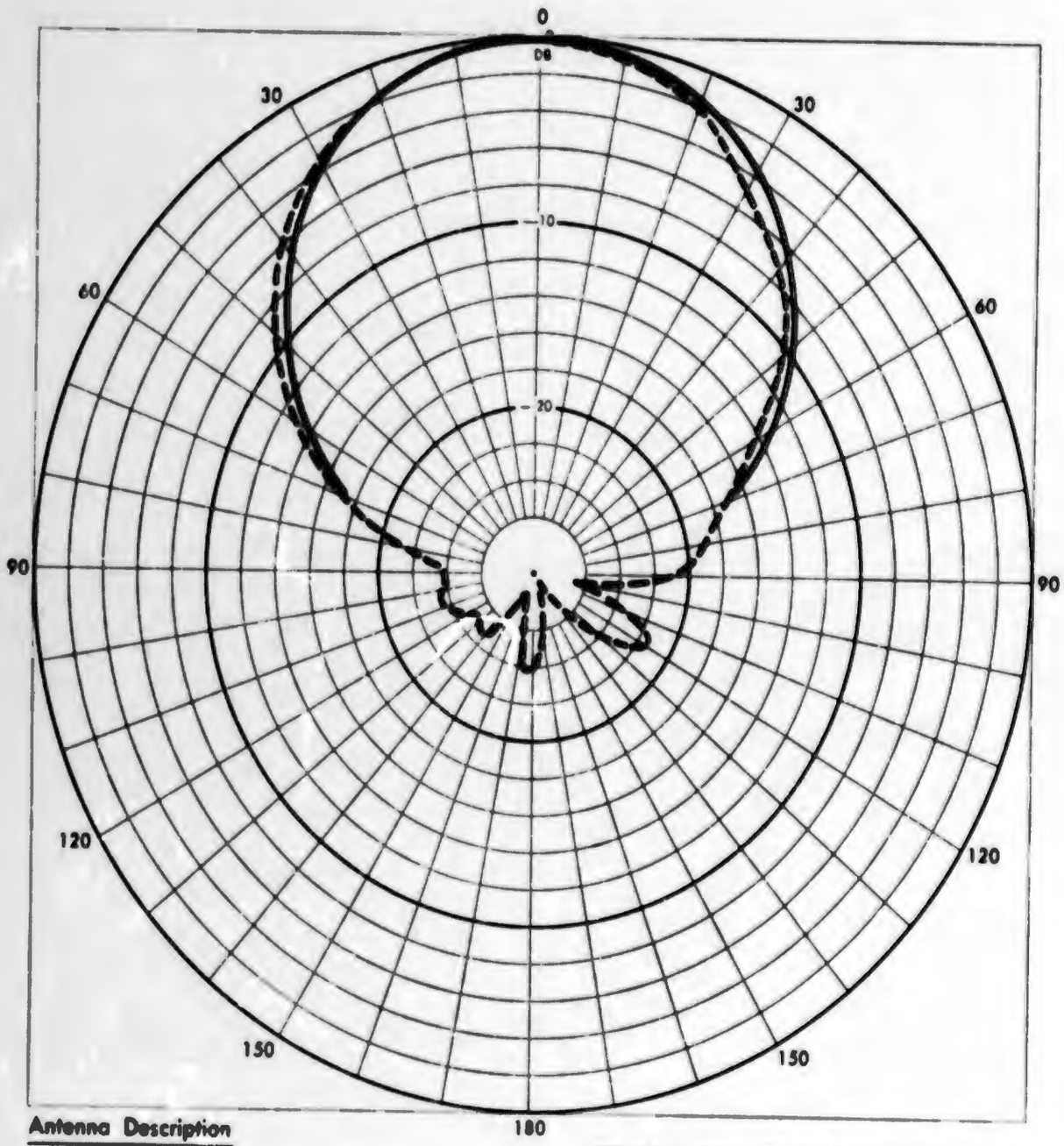

Figure 35. E and H-Plane Pattern of S-Band Horn at the Fundamental Frequency (2.5 Gc) (Sheet 1 of 2)

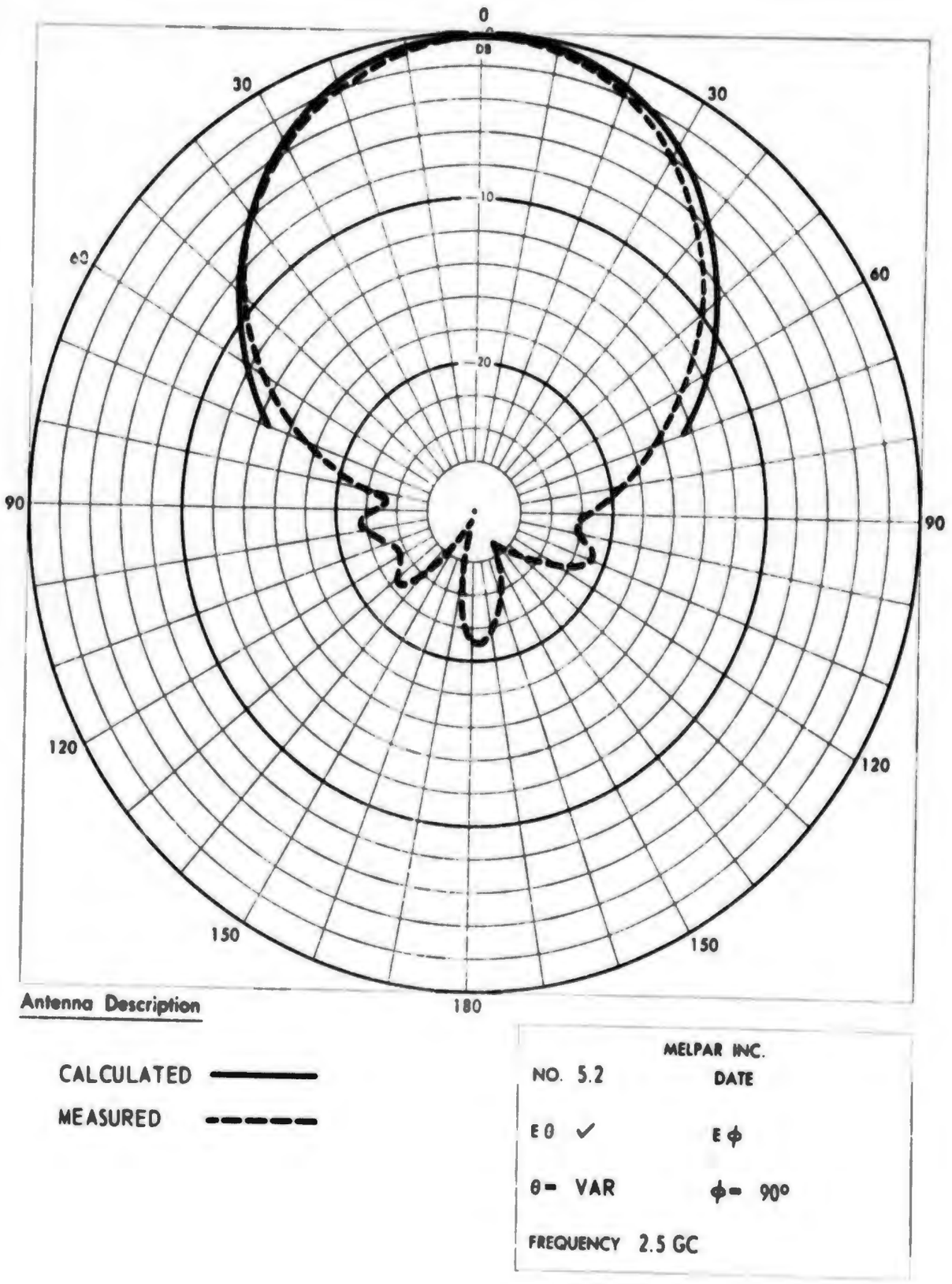

Figure 35. E and H-Plane Pattern of S-Band Horn at the Fundamental Frequency (2.5 Gc) (Sheet 2 of 2)

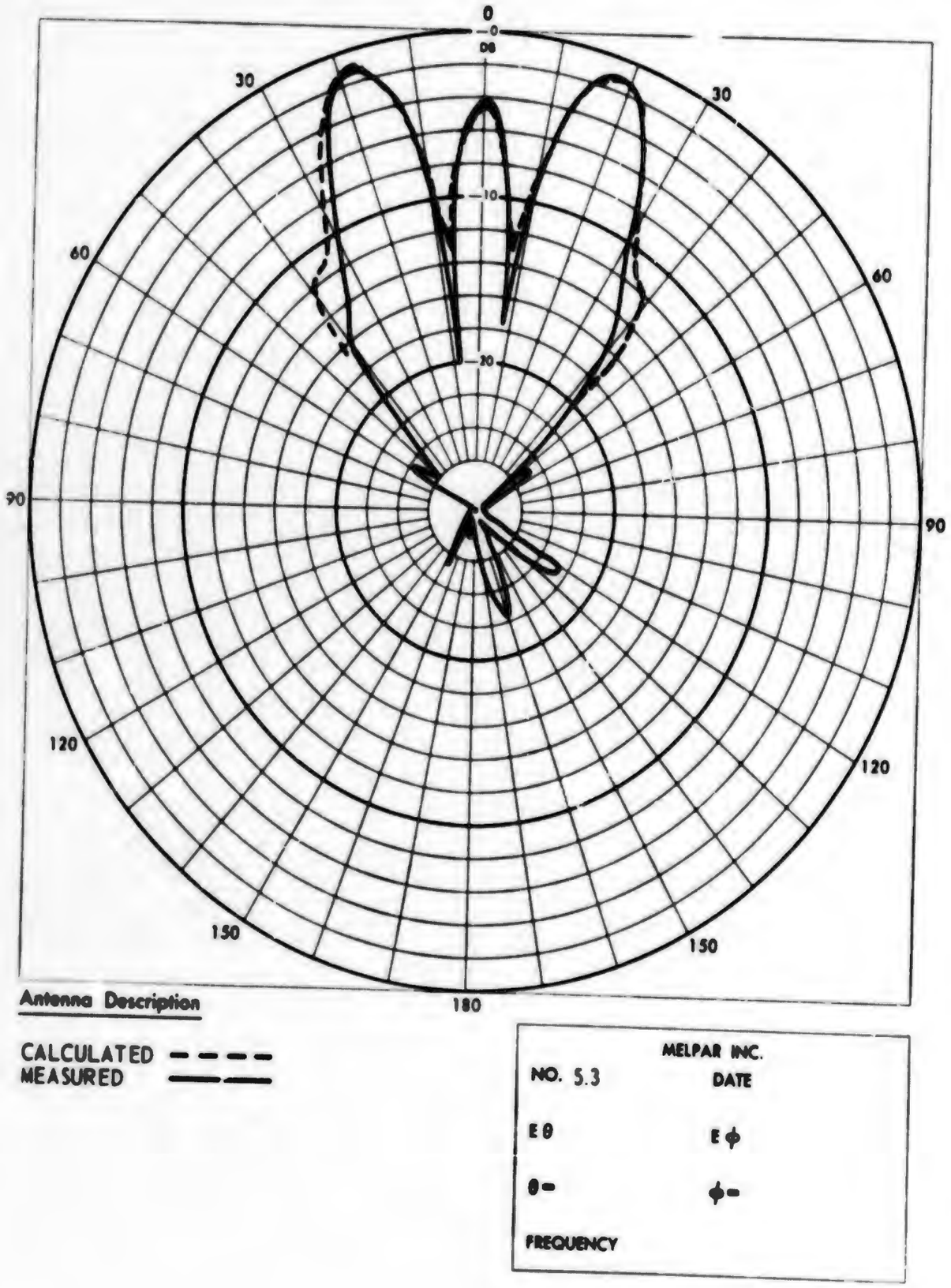

Figure 36. H-Plane Patterns of S-Band Horn at the Third Harmonic (7.5 Gc)

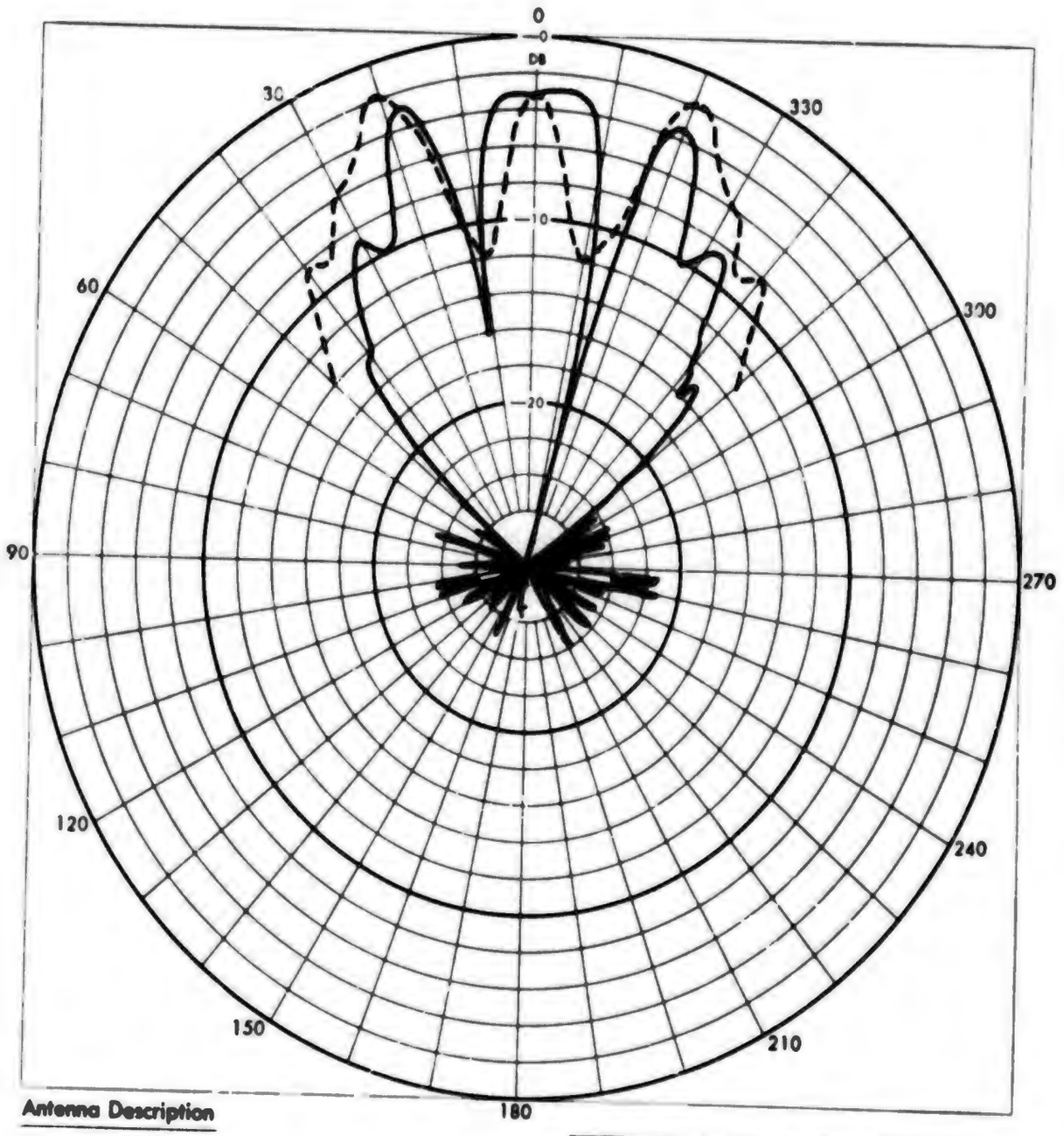

Figure 37. H-Plane Patterns of S-Band Horn at the Sixth Harmonic (15.Gc)

Thus the method suggested[17] seems to be a satisfactory means of calculating the spurious frequency response of this experimental horn at frequencies up to the 3rd harmonic, but the results deteriorate at higher frequencies. It should be noted that the dimensions of the horn are rather critical and this introduces one source of error. Figures 38 and 39 show a series of comparative patterns of two different probe-fed horns which were both built to the same specifications; however, there is a significant difference in the patterns of the two horns at the higher frequencies. Another source of error may be the existence of higher order modes in the coaxial feed section at frequencies above 9 gc.

It should be noted that the modes used[17] as the normal modes of the horn are only approximations to the actual modes and that a slight error in the propagation constants of the modes in the horn could cause a significant error in the horn patterns. It should also be noted that there exists some coupling between modes at the throat and within the horn itself, which is neglected and may be significant.

5.2 Far-Field - Fresnel Region Boundary for Harmonically Related Frequencies

A rather general statement is made many times, namely, that the far-field pattern shape is independent of range. Investigation into this basic statement logically suggests a few basic questions such as:

a. What is meant by the "far-field"? and

b. Are any other conditions assumed when making the statement?

The answer to the first question can be quite varied but the use of the $2D^2/\lambda$ criteria is generally utilized by the antenna design engineer when various design parameters may be tightly controlled. This definition

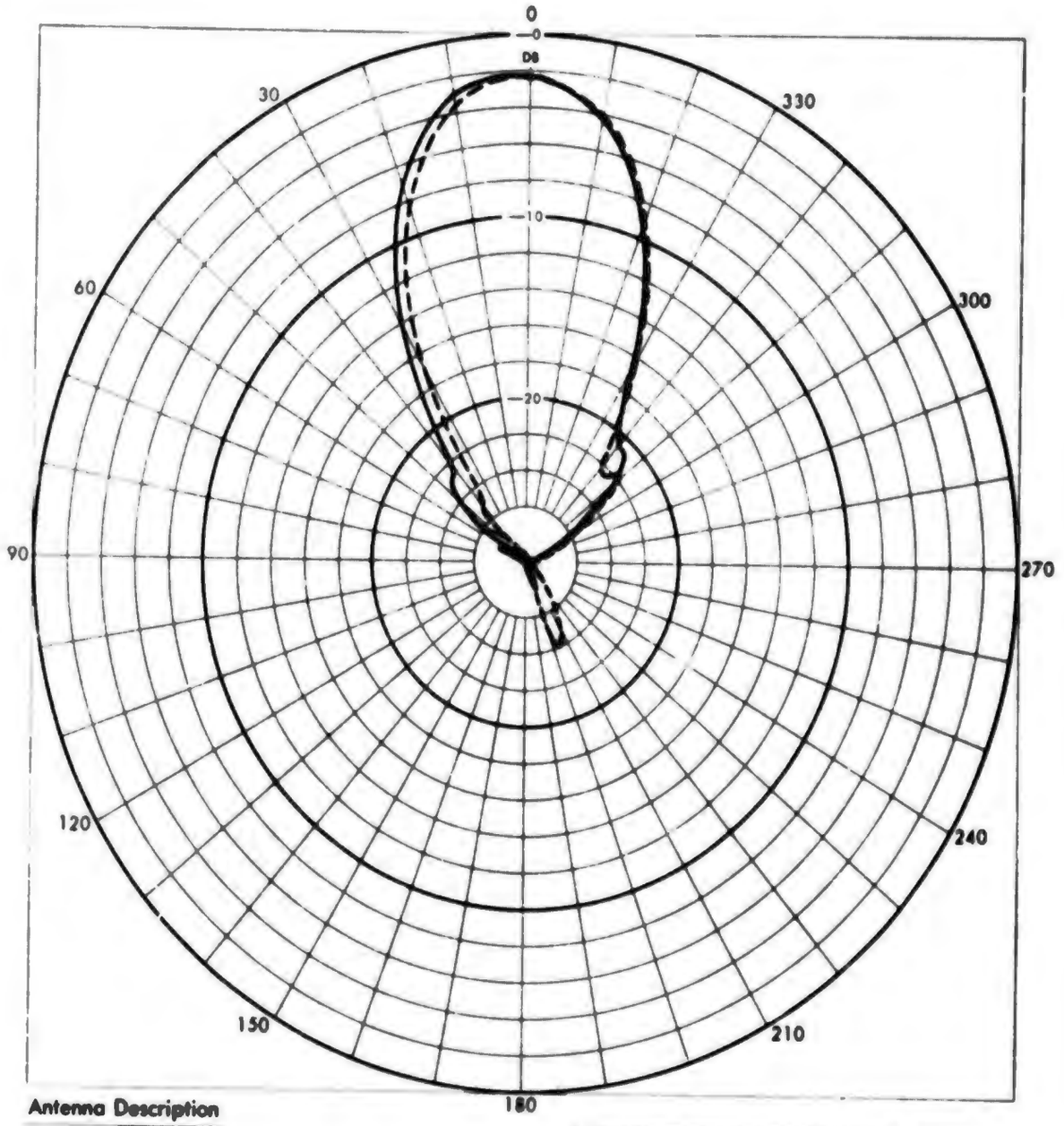

Figure 38. E and H-Plane Patterns of Identical S-Band Horns at 2nd (5.0 Gc) and 4th (10 Gc) Harmonics (Sheet 1 of 4)

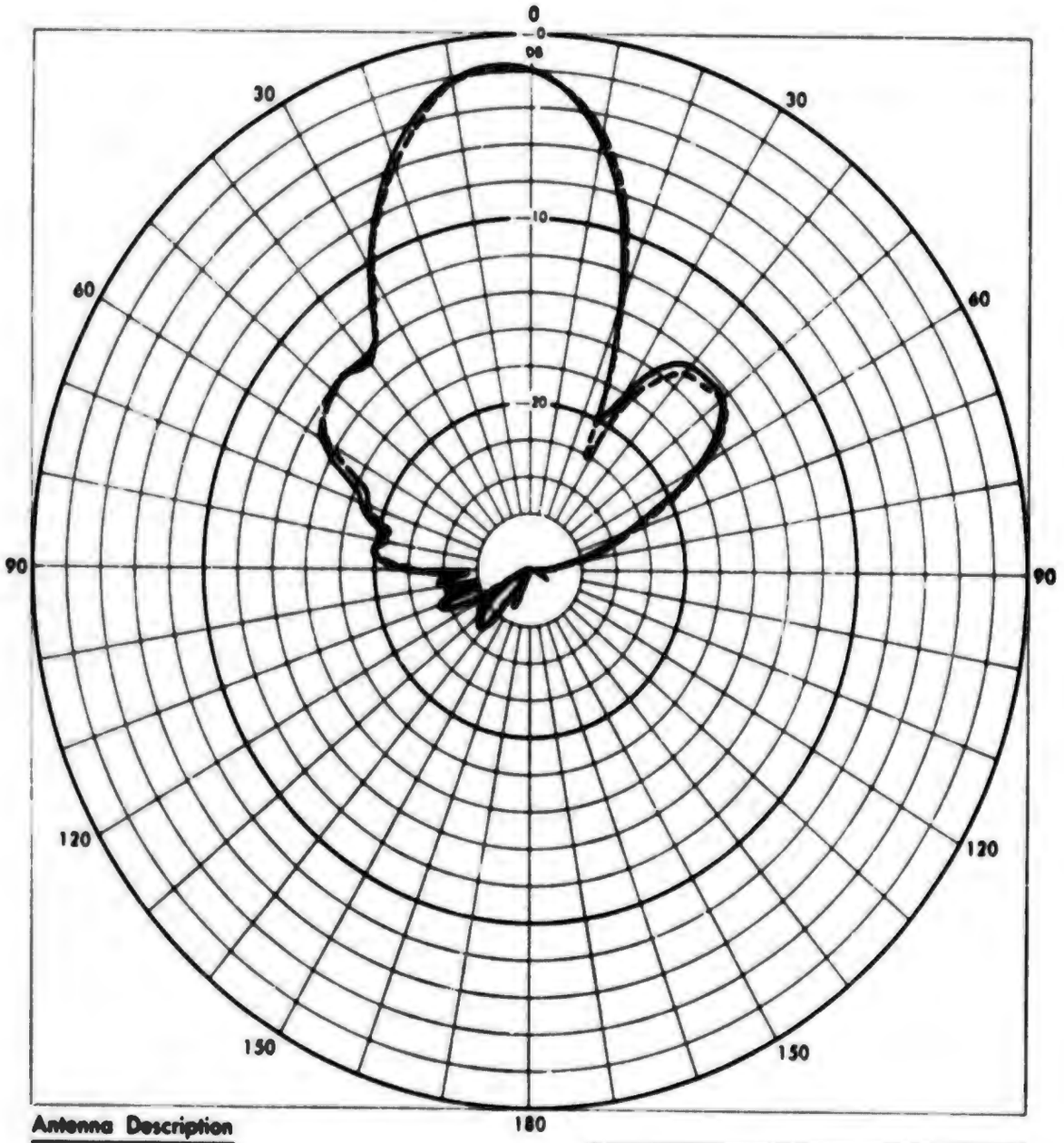

Figure 38. E and H-Plane Patterns of Identical S-Band Horns at 2nd (5.0 Gc) and 4th (10 Gc) Harmonics (Sheet 2 of 4)

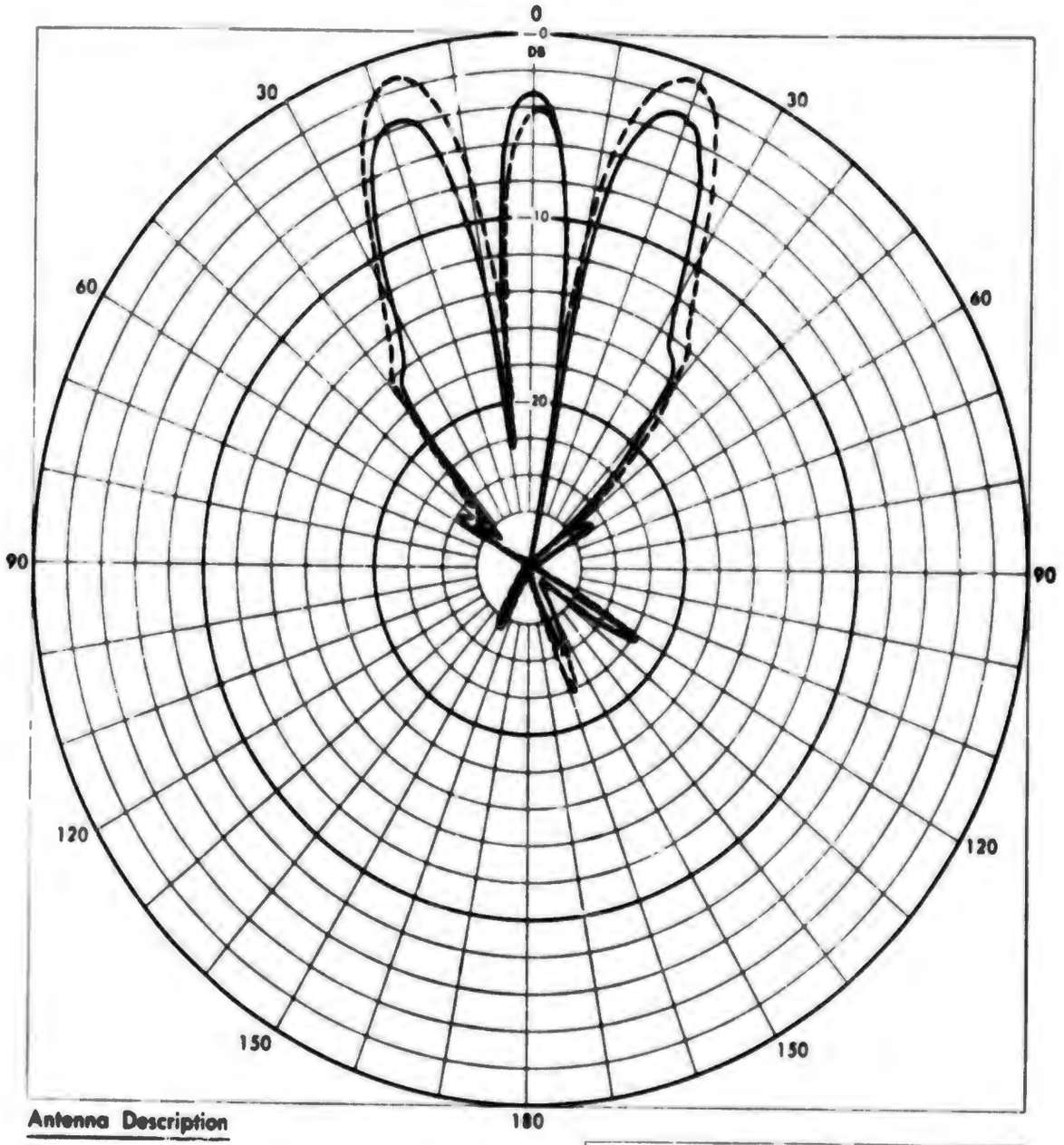

Figure 38. E and H-Plane Patterns of Identical S-Band Horns at 2nd (5.0 Gc) and 4th (10 Gc) Harmonics (Sheet 3 of 4)

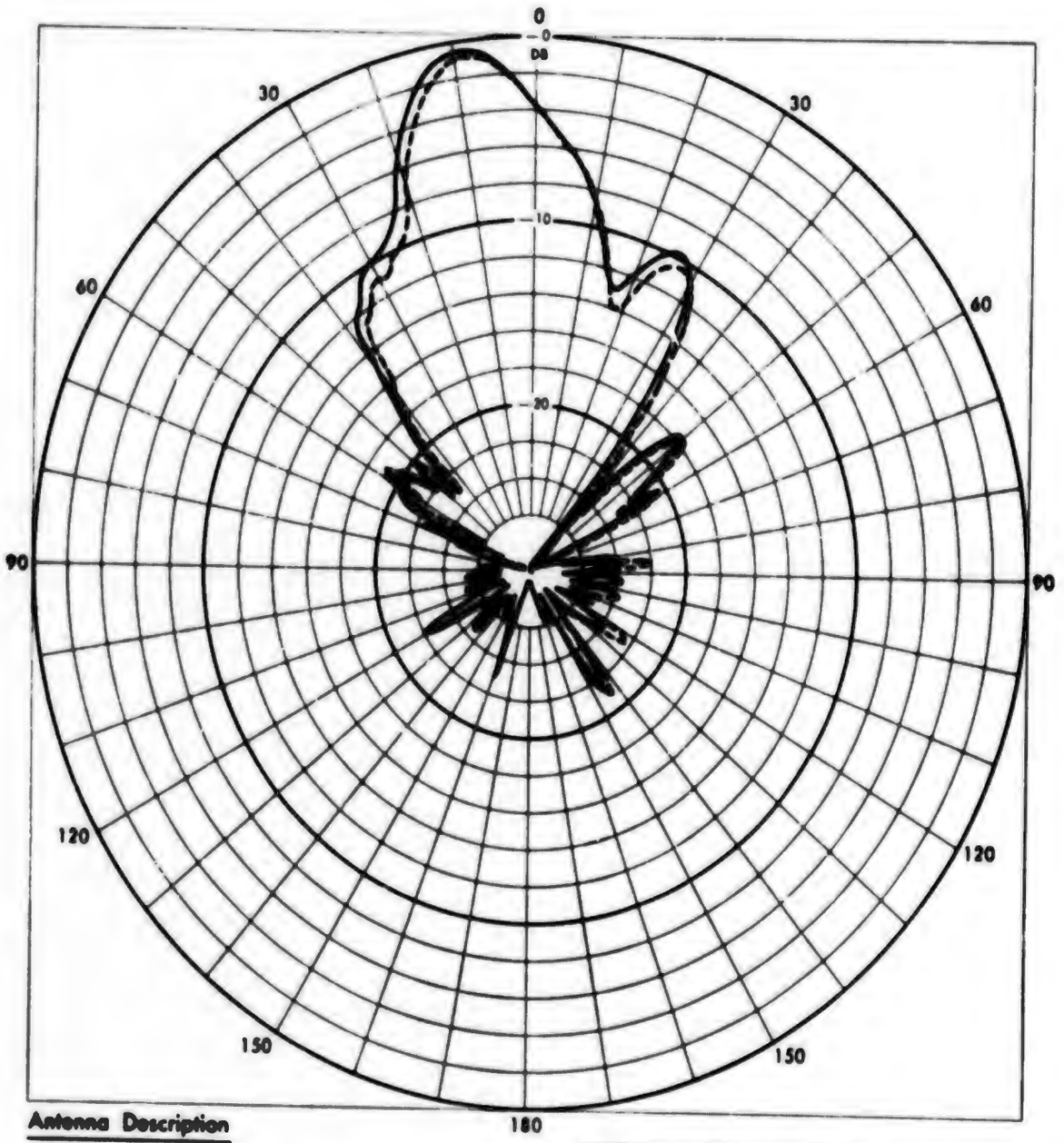

Figure 38. E and H-Plane Patterns of Identical S-Band Horns at 2nd (5.0 Gc) and 4th (10 Gc) Harmonics (Sheet 4 of 4)

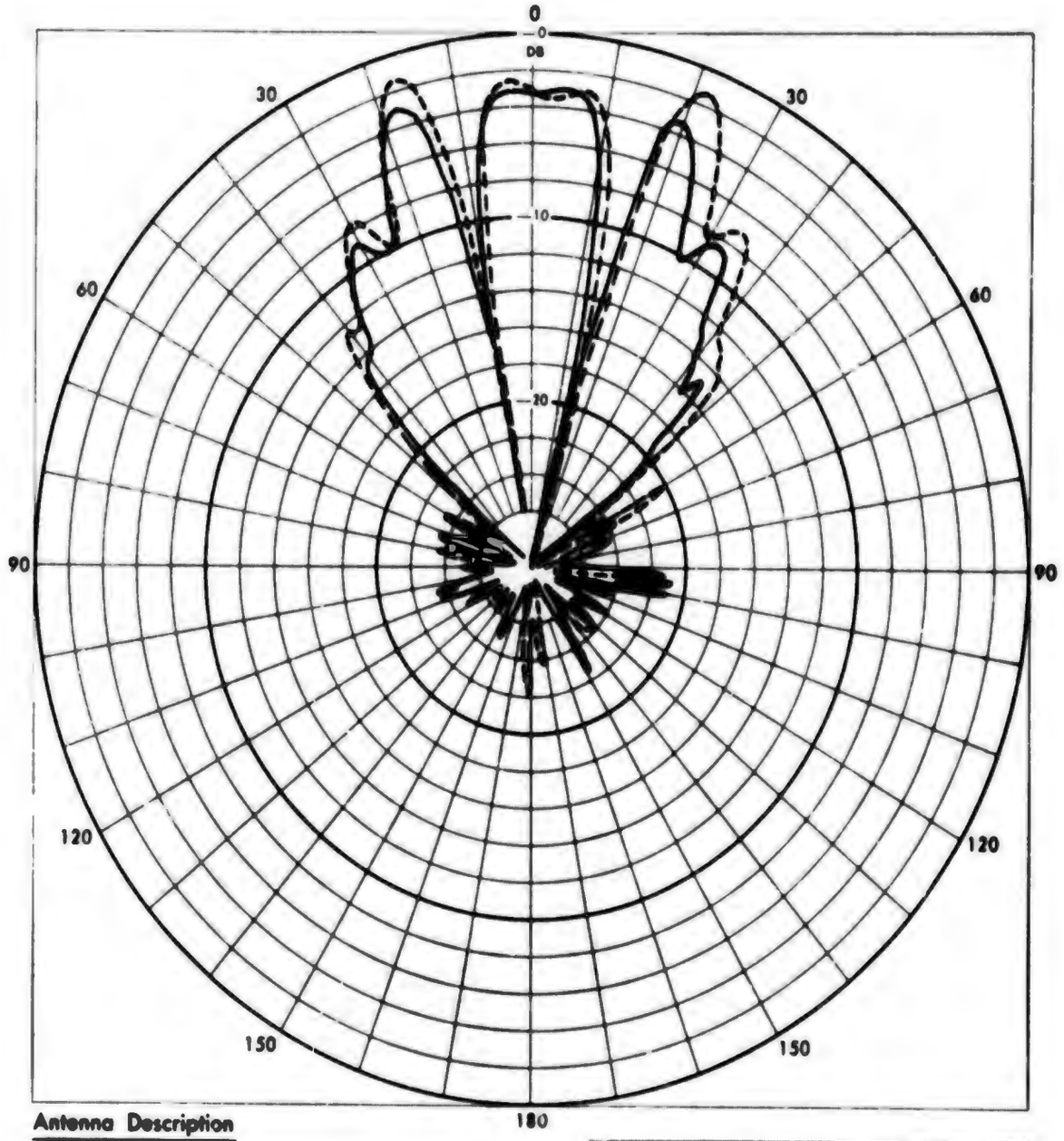

Antenna Description

	HORN	ADAPTER
NO. 1	– – –	NO. 1 – – –
NO. 2	———	NO. 2 ———

MELPAR INC

NO. DATE

Eθ ✓ Eφ

θ= 90° φ= VAR

FREQUENCY 15 GC

Figure 39. E and H-Plane Patterns of Identical S-Band Horns at 6th (15 Gc) and 8th (20 Gc) Harmonics (Sheet 1 of 4)

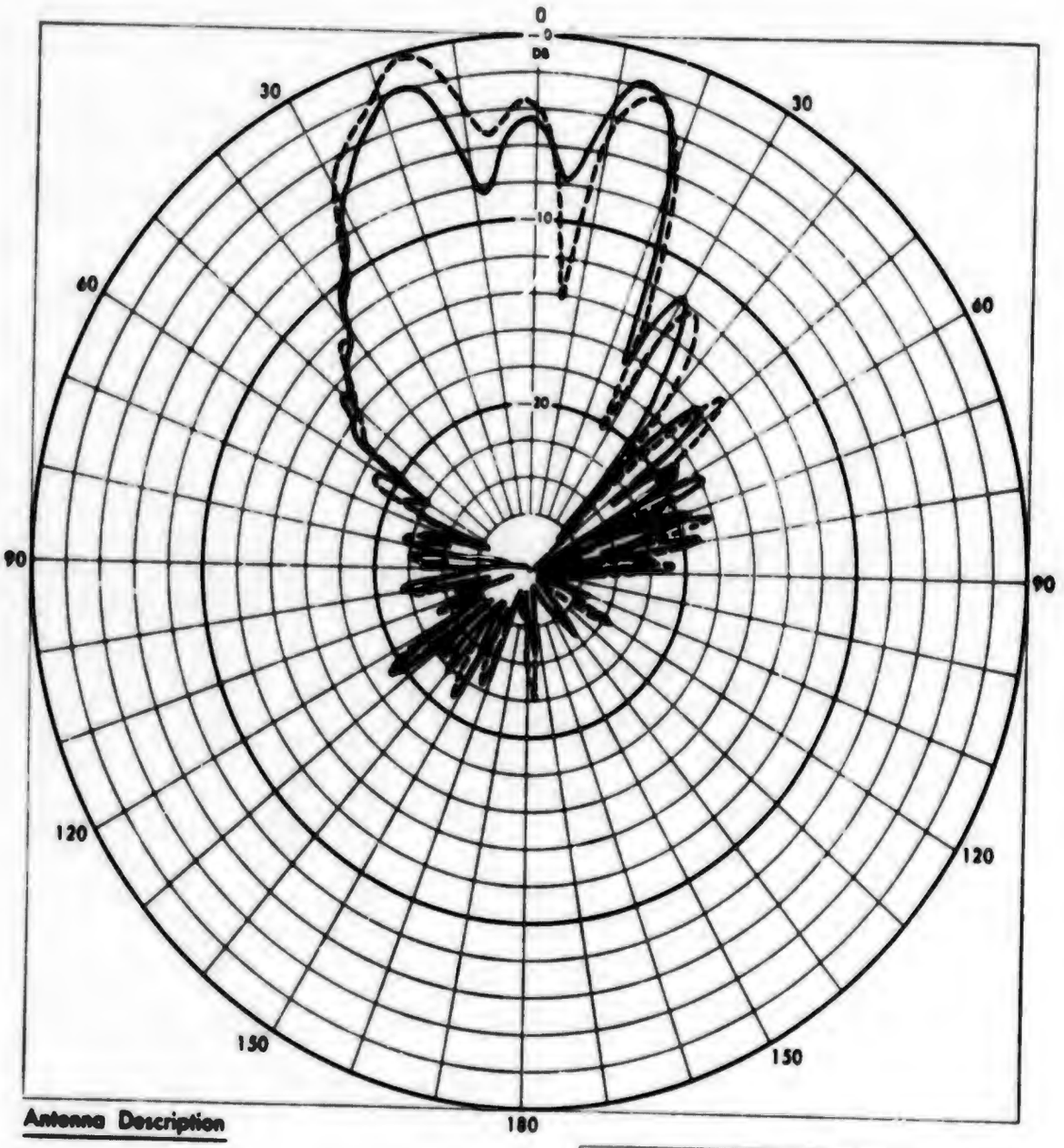

Figure 39. E and H-Plane Patterns of Identical S-Band Horns at 6th (15 Gc) and 8th (20 Gc) Harmonics (Sheet 2 of 4)

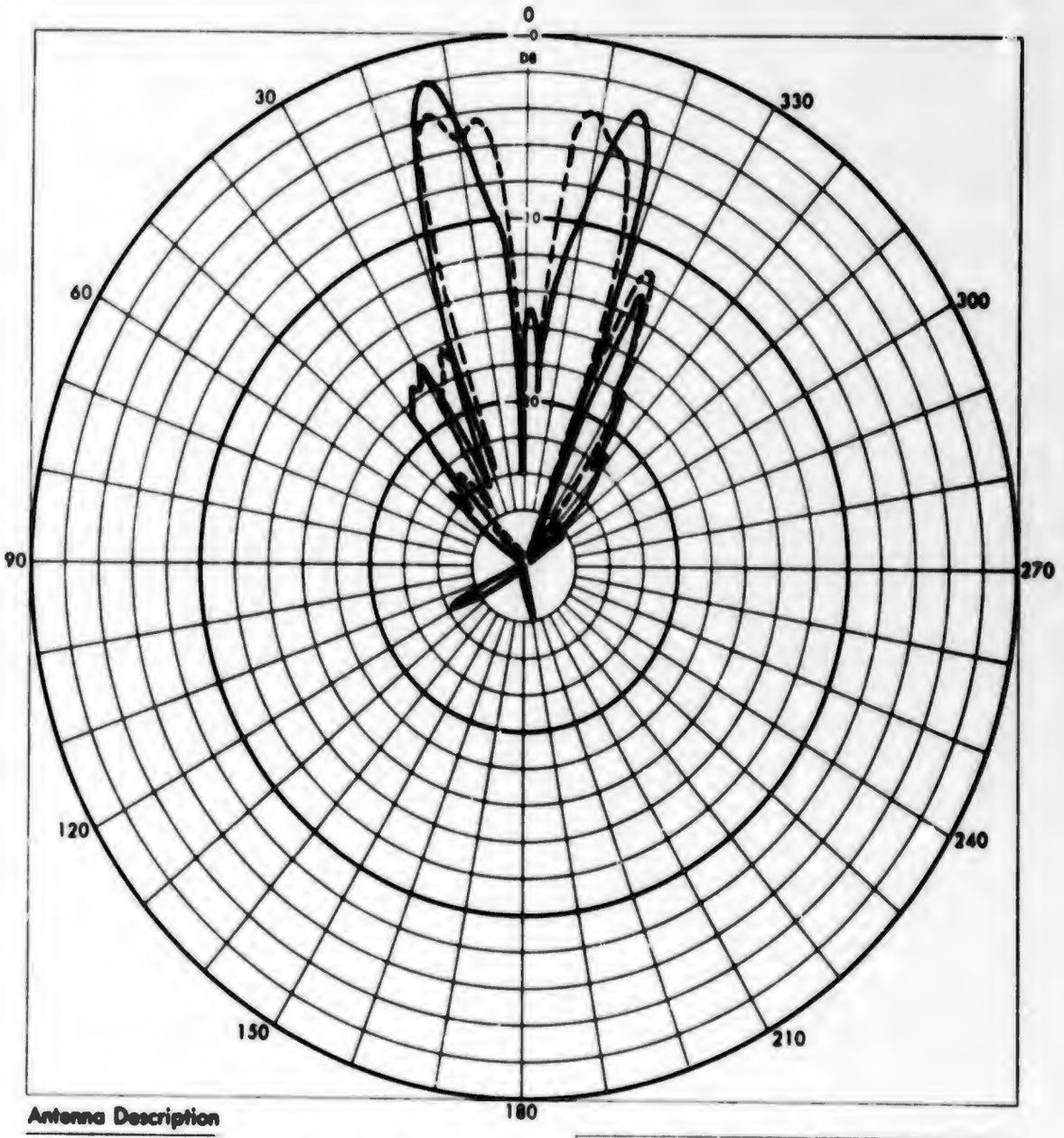

Antenna Description

Horn Adapter

NO. 1 ——— NO. 2 ———

NO. 2 ——— NO. 1 ———

MELPAR INC.

NO. DATE

Eθ ✓ Eϕ

θ- 90° ϕ- VAR

FREQUENCY 20.0 GC

Figure 39. E and H-Plane Patterns of Identical S-Band Horns at 6th (15 Gc) and 8th (20 Gc) Harmonics (Sheet 3 of 4)

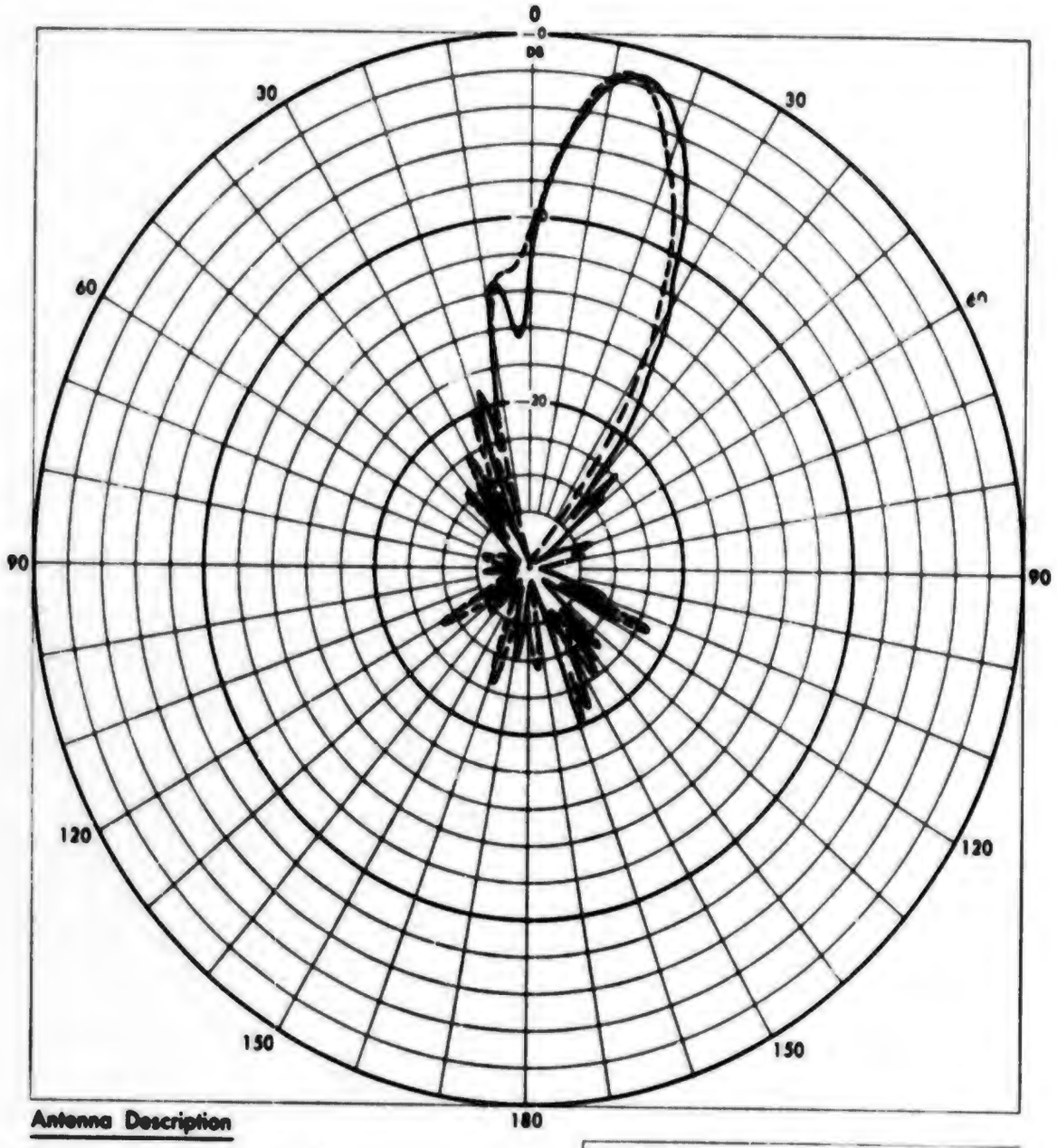

Figure 39. E and H-Plane Patterns of Identical S-Band Horns at 6th (15 Gc) and 8th (20 Gc) Harmonics (Sheet 4 of 4)

describes the far-field range as that distance at which the phase of the received field from a point source across the subject aperture varies no more than $\lambda/16$. However, for the individual concerned with electromagnetic compatibility, the distance at which the antenna pattern shape ceases to change may be the definition. This portion of the report illustrates the results obtained when investigating the effects of range upon the radiation pattern characteristics of an antenna when operating at harmonics of the fundamental frequency. This investigation was conducted to determine the far-field-Fresnel region boundary for an antenna operating at other than the design frequency. This boundary is defined as that range from the subject antenna at which no further change in the radiation pattern shape is noted.

One of the assumptions made is that the subject antenna is not altered by external reflections. Since the characteristics of the measurement range were important from this aspect, the receiving site was investigated by measuring the amplitude variation within the volume that would be occupied by the subject antenna, with the transmitter at a range of 1300 feet. This process resulted in measurements within a four-foot cubed space above the antenna rotator which determined that the power received was within the limits expected. The most severe reflections ($\pm$ 6.5 db), as expected, occurred at the lowest frequency and decreased at higher frequencies. Above the second harmonic, the amplitude variation was no more that $\pm$ 2.0 db in the area of interest when transmitting from the 1300-foot distance.

Another question is introduced when the subject antenna is operating at a frequency harmonically related to the fundamental frequency. The previous discussion in Section 5.1 has shown that the characteristics of the feed pattern produced by an electromagnetic horn change rather drastically when operating over a wide range of frequencies. A program was conducted to determine the far-field-Fresnel region boundary as a function of harmonic frequency when using a large aperture antenna. The subject antenna, is a four-foot diameter paraboloidal reflector fed with a simple pyramidal electromagnetic horn (used as the spurious response model) which is designed to operate at 2.5 Gc. The electrical aperture size varies from 10λ to 100λ when operating over a 10 to 1 frequency range, therefore, the 1300-foot range was necessary to provide a distance of $2D^2/\lambda$ at the 10th harmonic. Radiation patterns of the E- and H-planes for this antenna were measured at this range for the purpose of acting as comparison patterns against those taken at specific frequencies at other distances. Figures 40 through 43 illustrate the E- and H-plane patterns obtained at 2.5, 5.0, 10.0, and 15 Gc at the 1300-foot range. The above frequencies, which are the fundamental, second, fourth, and sixth harmonics, were chosen as the frequencies at which to investigate the far-field-Fresnel region boundary. Their respective $2D^2/\lambda$ distances are 81, 162, 324, and 486 feet. Patterns were obtained for the fundamental at each of these ranges while the second harmonic patterns were taken at all but the 486-foot range. The fourth harmonic patterns were measured at 163 and 324 and the sixth harmonic patterns were measured only at the 486-foot range. The original patterns taken at 1300 feet together with the variable range patterns were compared

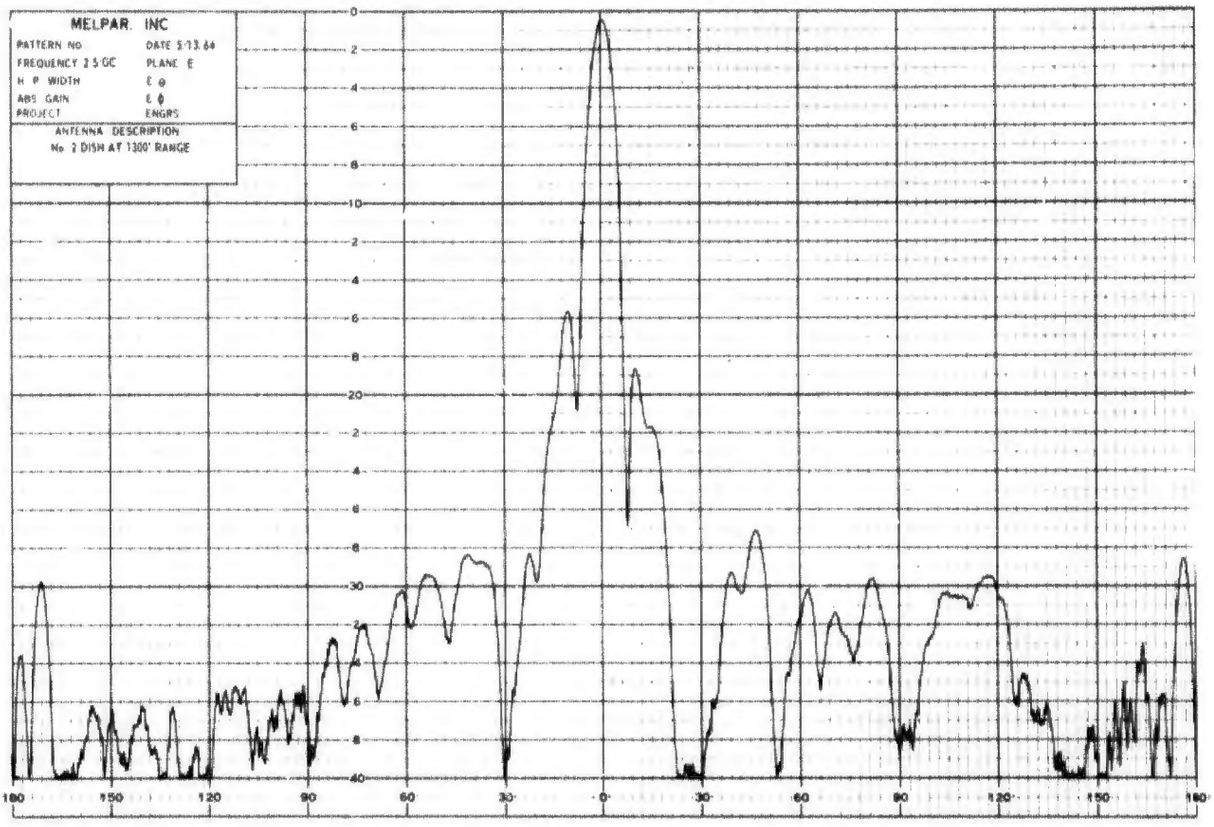

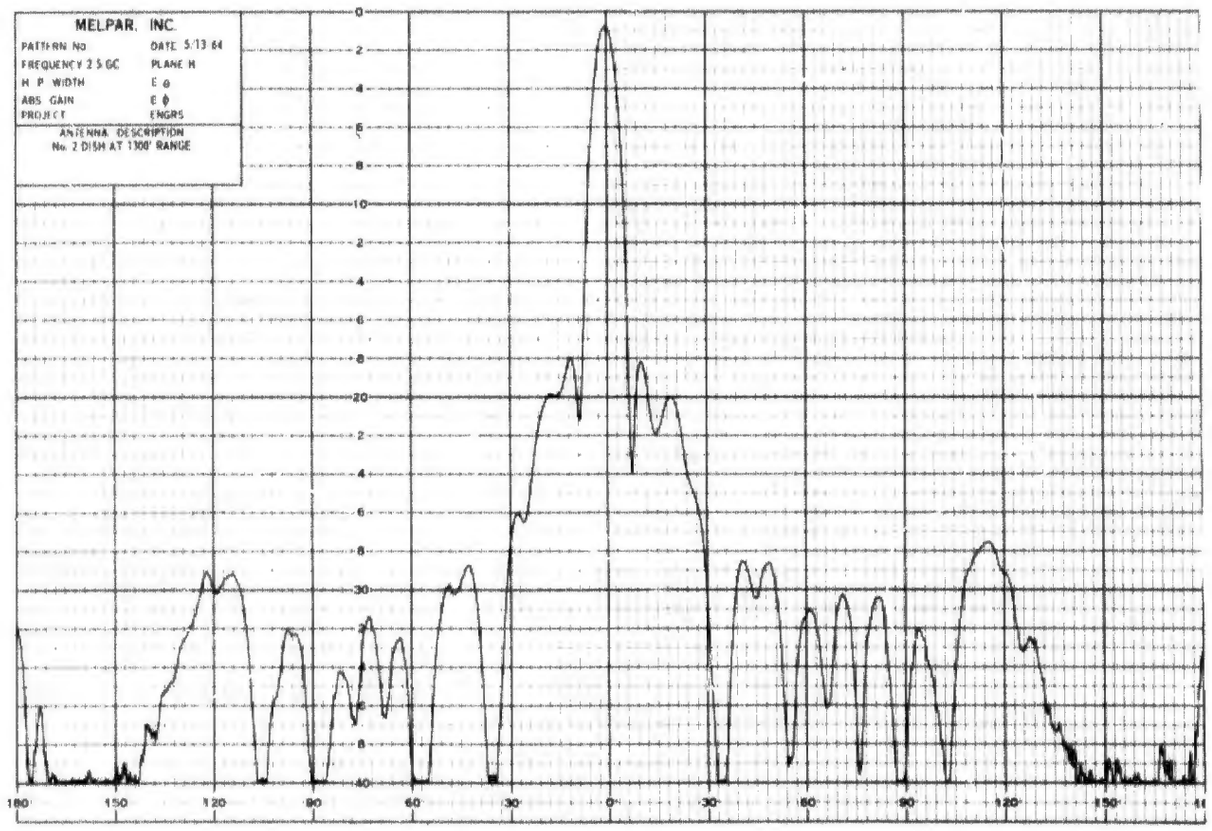

Figure 40. E and H-Plane Pattern of 4-Foot Paraboloid at 2.5 Gc

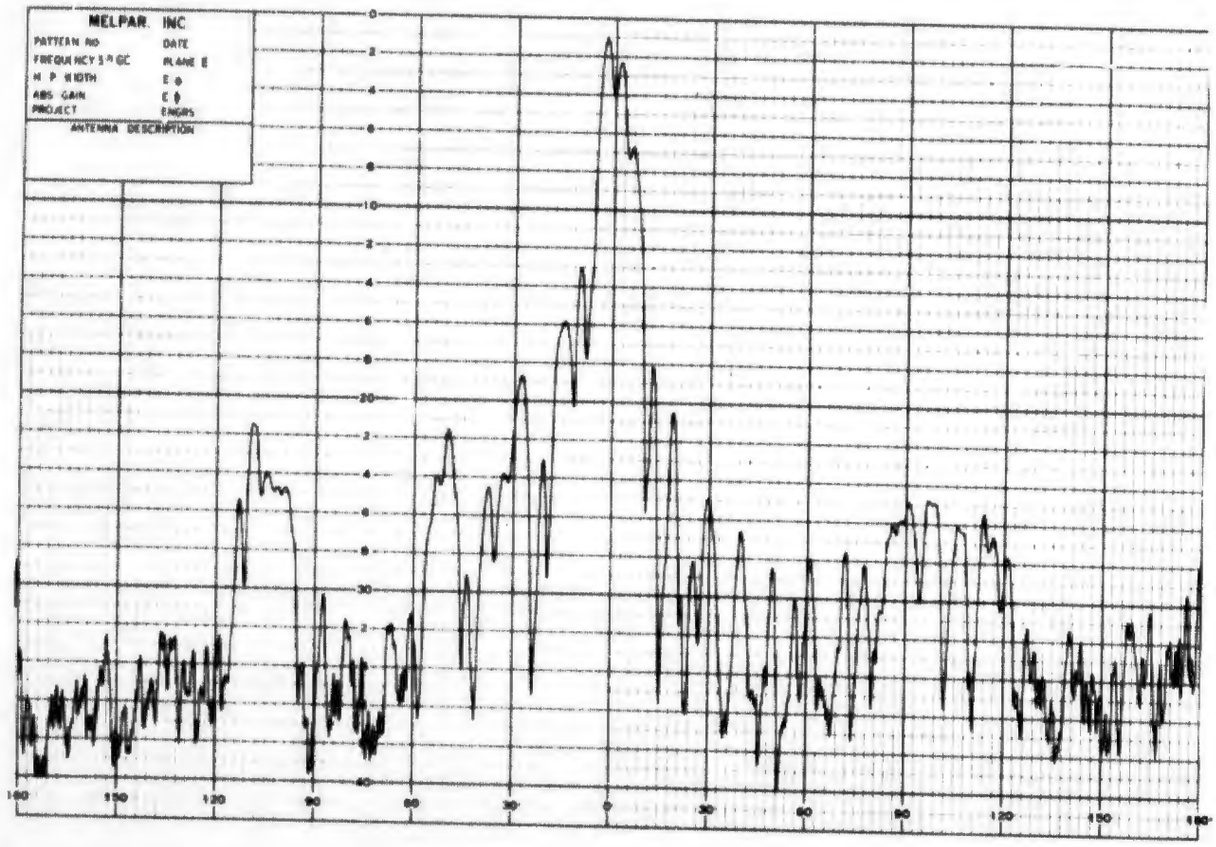

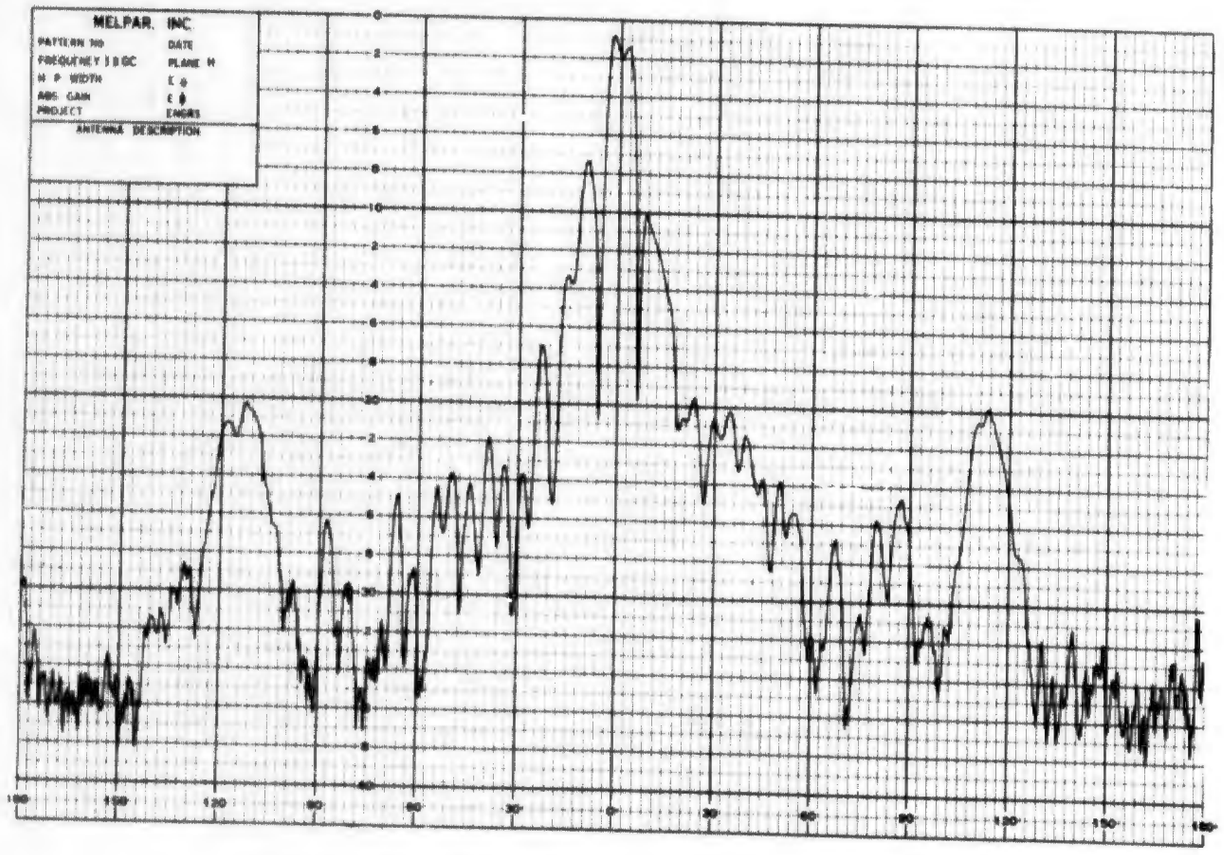

Figure 41. E and H-Plane Pattern of 4-Foot Paraboloid at 5.0 Gc

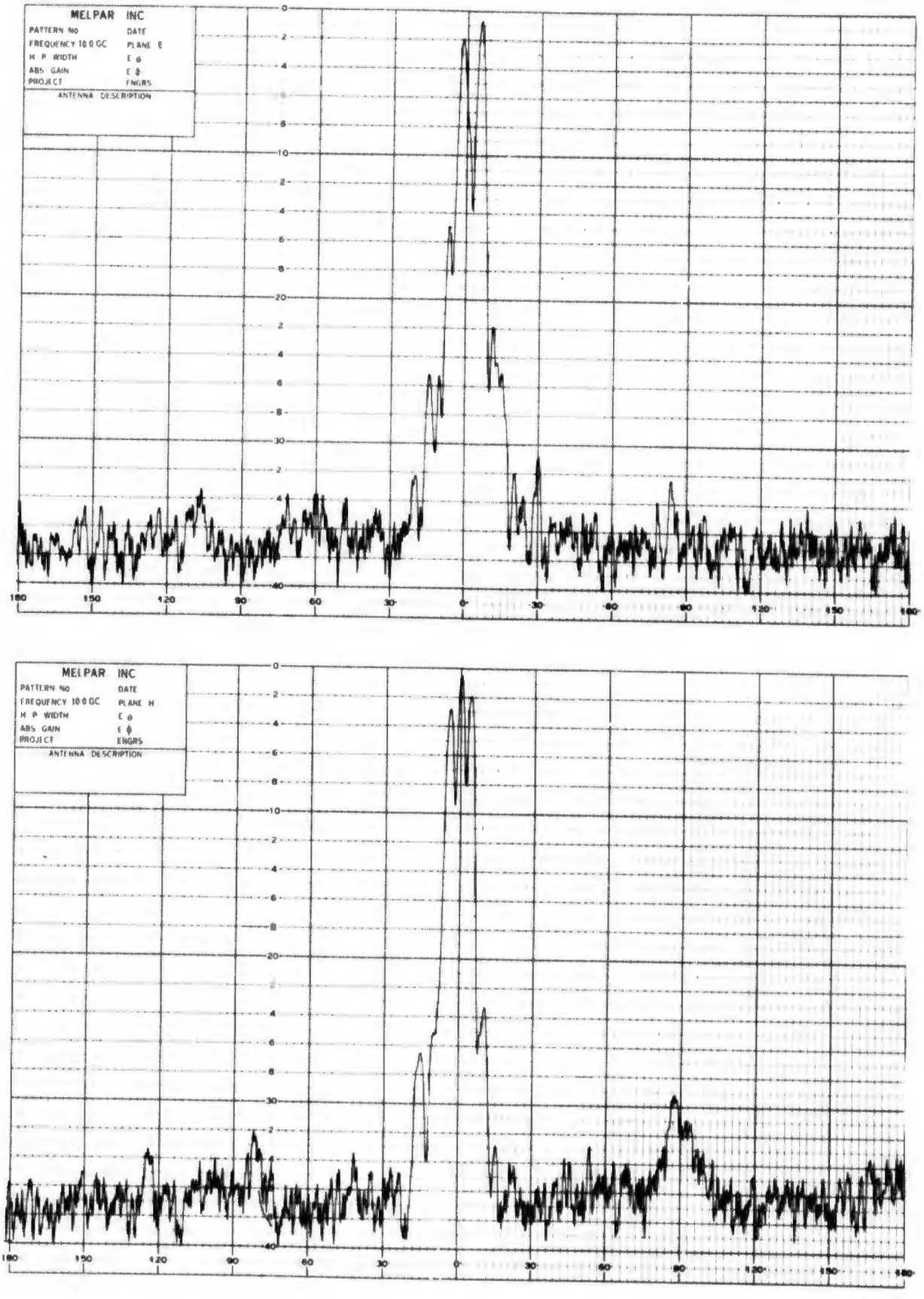

Figure 42. E and H-Plane Pattern of 4-Foot Paraboloid at 10.0 Gc

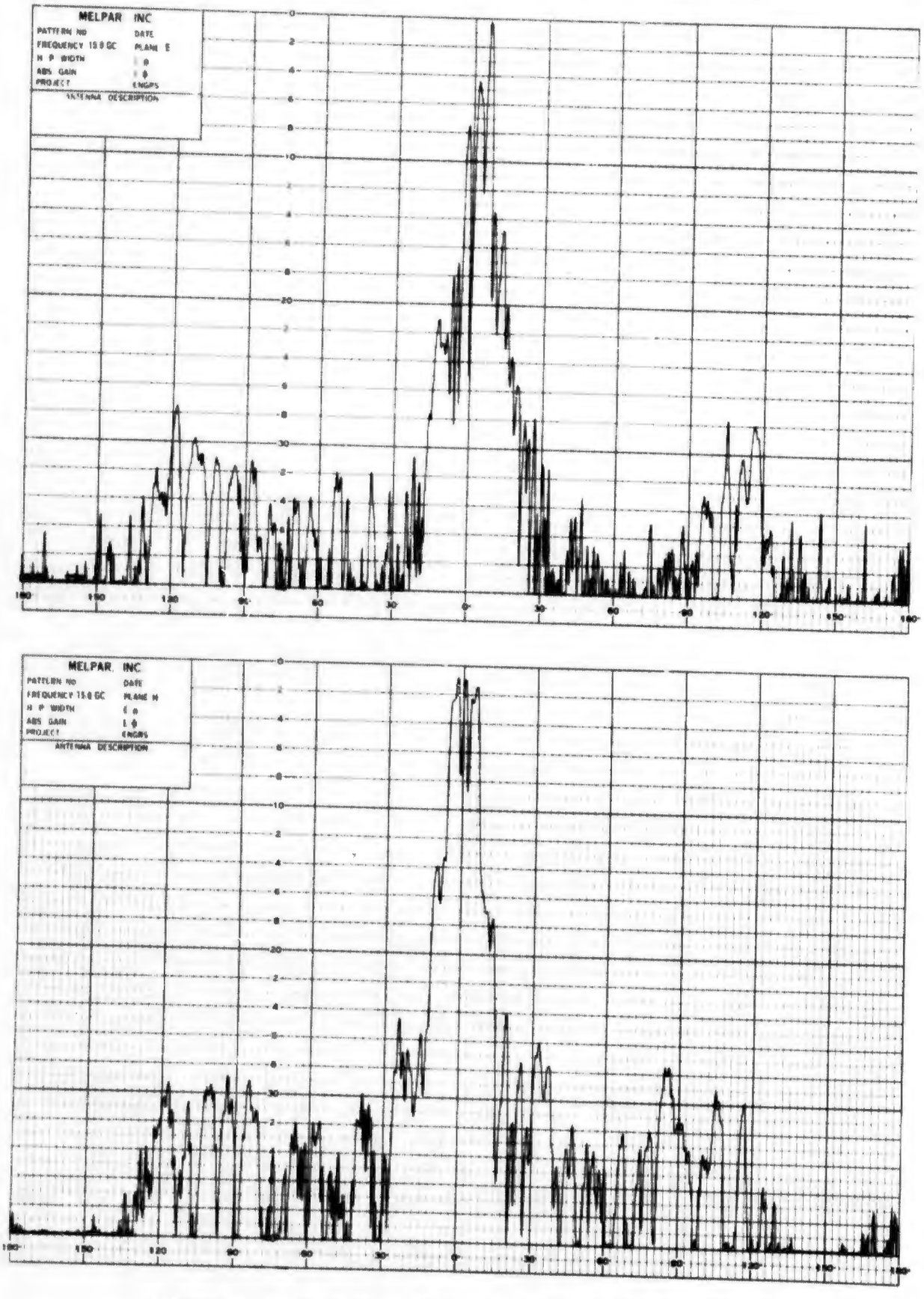

Figure 43. E- and H-Plane Pattern of 4-Foot Paraboloid at 15.0 Gc

to illustrate at what range the far-field-Fresnel zone boundary occurred for each harmonic frequency.

Comparison of the patterns obtained at the fundamental frequency indicates that little variation is noted with an increase of range beyond $2D^2/\lambda$ although some low level effects can be noted in the sidelobes. Low level reflections can cause such effects and were expected. Since the main interest was directed toward operation at harmonic frequencies, the E- and H-plane patterns obtained are contained in figures 44 through 49. The general conclusions that may be drawn seem to indicate a trend toward reproduction of pattern characteristics beyond the $2D^2/\lambda$ range even when operating at higher harmonics. Some discrepancies are noted but since the major differences are noted when the patterns include deep nulls in one or both planes of the patterns such deviations could be expected. Even with the use of a transit to align the antenna for patterns such effects occurred. Further investigation in this area will require an extremely low level of reflections, preferably no reflections, and extremely close tolerances on positioning the subject antenna.

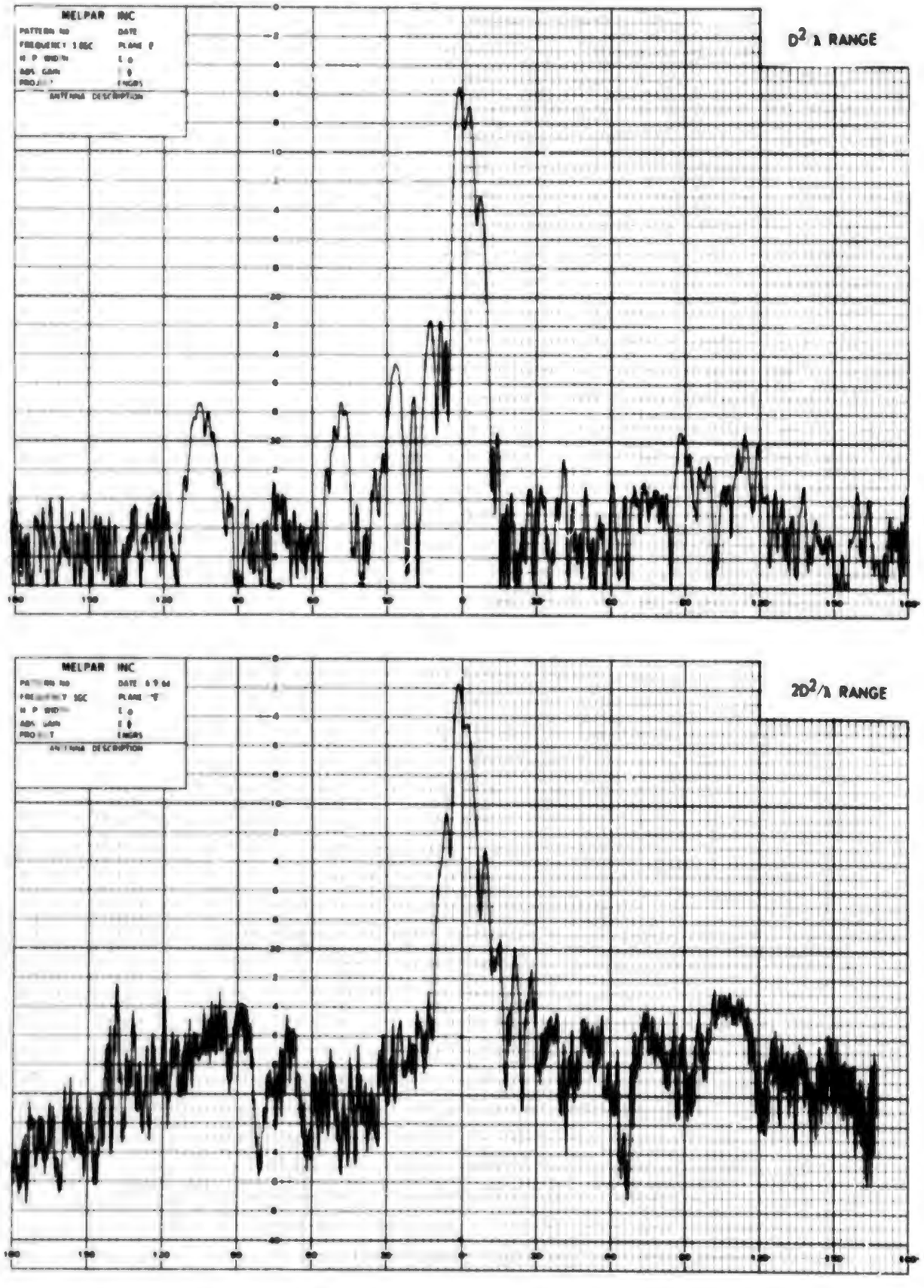

Figure 44. E- Plane Pattern of 4-Foot Paraboloid at 5.0 Gc (D^2/λ , $2D^2/\lambda$)

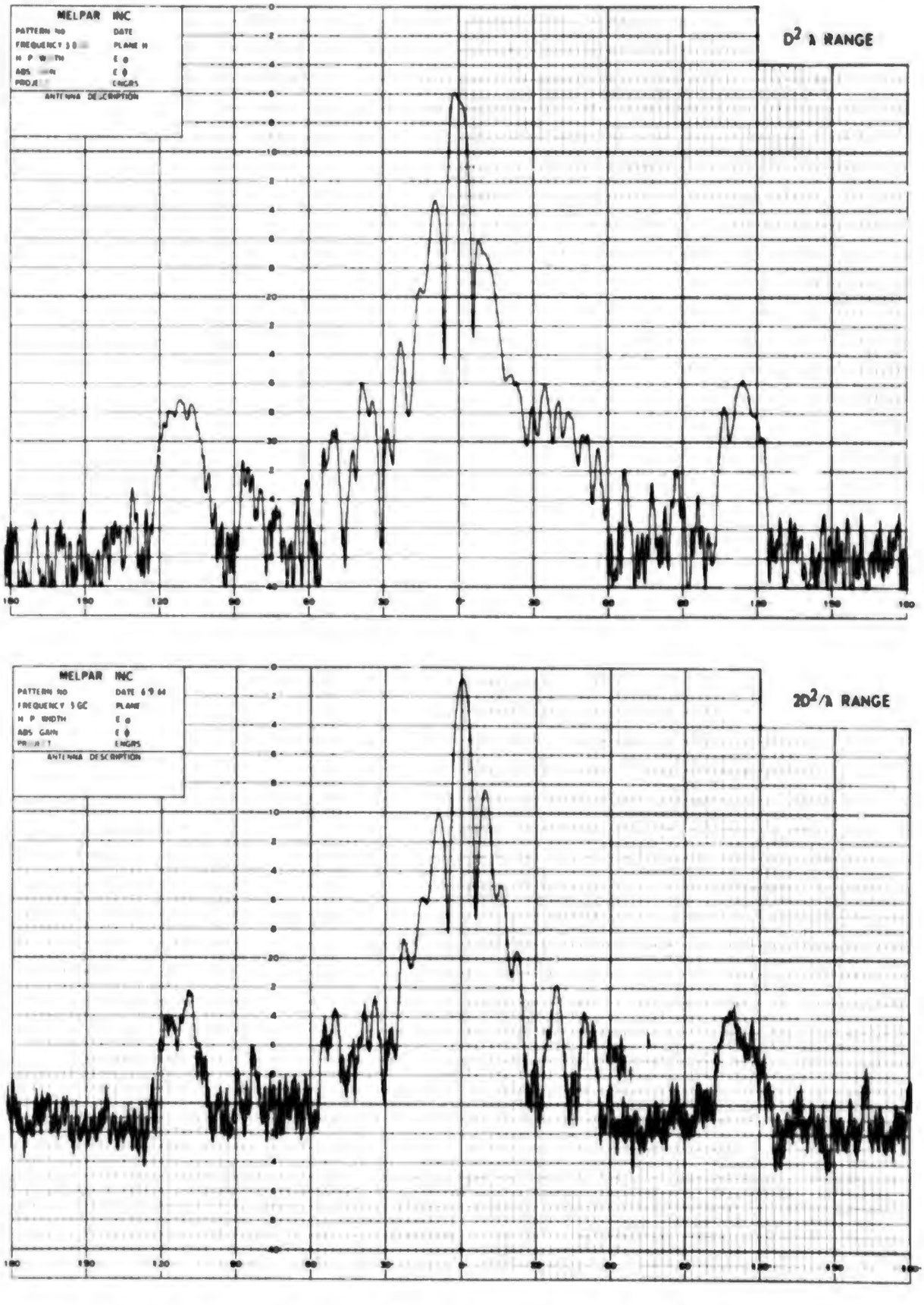

Figure 45. H-Plane Pattern of 4-Foot Paraboloid at 5.0 Gc (D^2/λ, $2D^2/\lambda$)

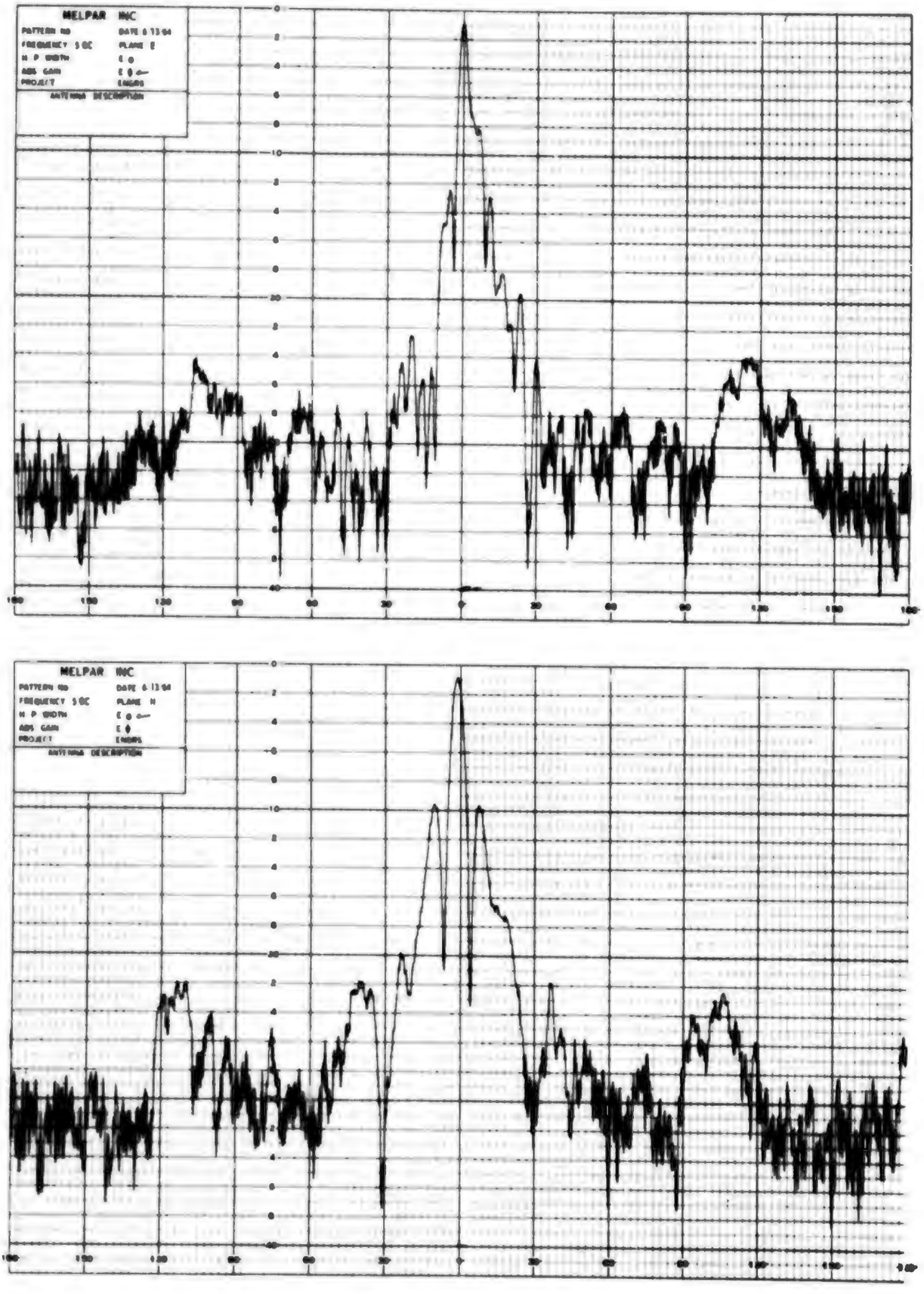

Figure 46. E- and H-Plane Pattern of 4-Foot Paraboloid at 5.0 Gc ($4D^2/\lambda$)

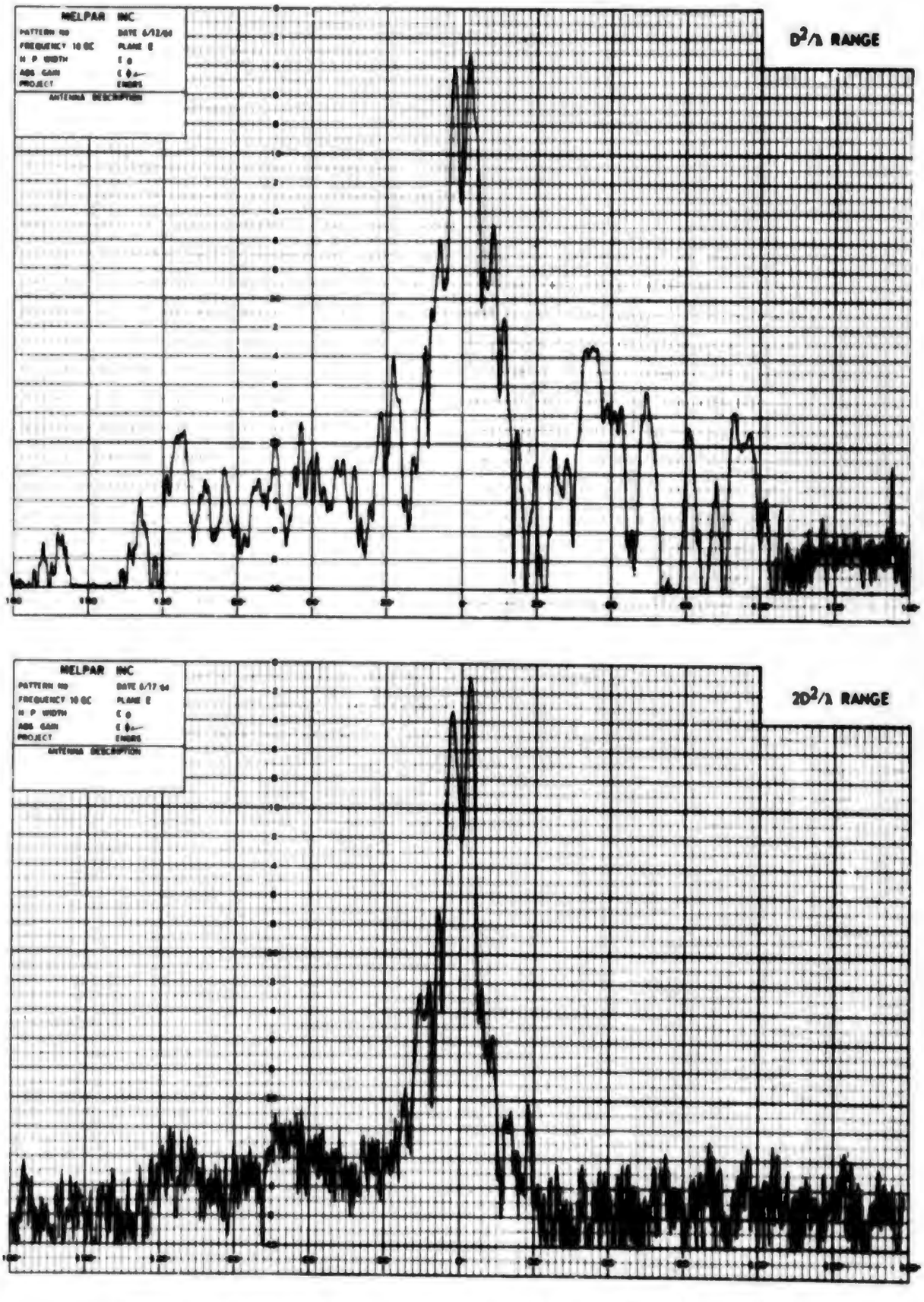

Figure 47. E-Plane Pattern of 4-Foot Paraboloid at 10 Gc (D^2/λ, $2D^2/\lambda$)

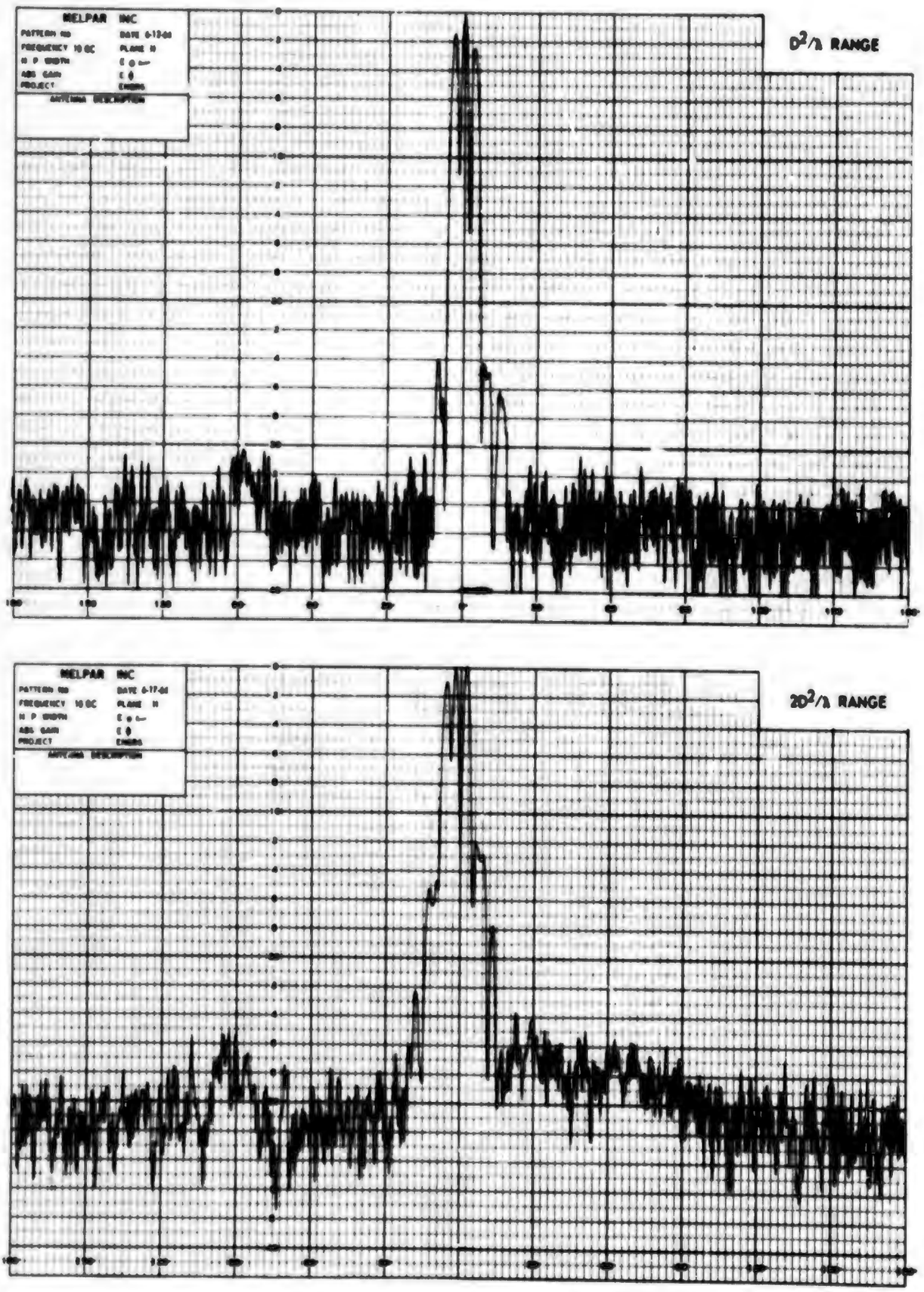

Figure 48. H-Plane Pattern of 4-Foot Paraboloid at 10 Gc (D^2/λ, $2D^2/\lambda$)

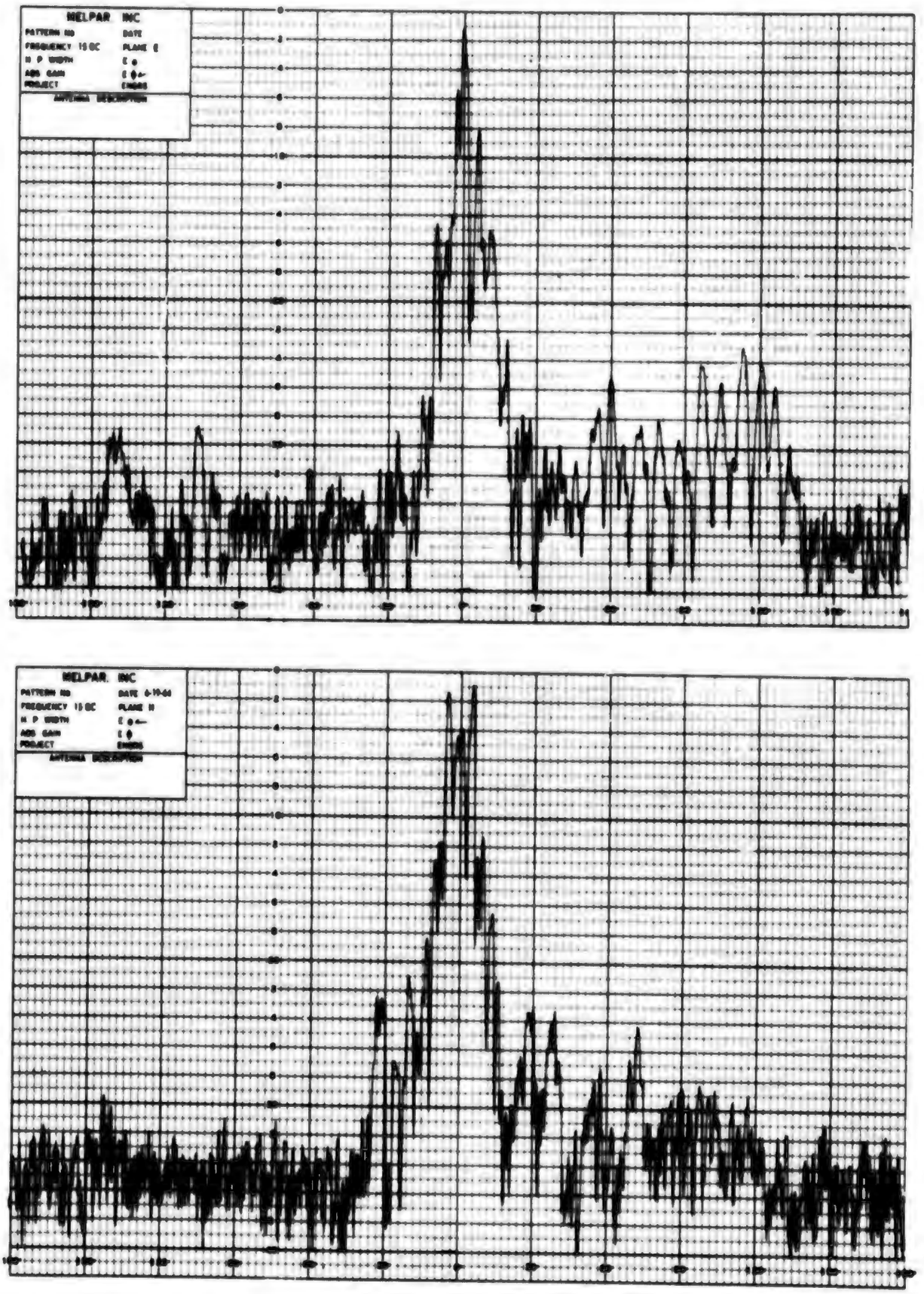

Figure 49. E- and H-Plane Pattern of 4-Foot Paraboloid at 15 Gc ($2D^2/\lambda$)

6. REFLECTIONS IN THE FRESNEL ZONE

Because of the extreme ranges required for pattern measurement of large antennas at $R = 2D^2/\lambda$, and the practical limitations of height, the elevation angle of a field probe subtended from the base of a large antenna may be relatively small. In situations of this nature, propagation reflections are bound to occur in the measurement. By virtue of the image antenna concept, some concern has been expressed as to whether reflections extend the Fresnel zone. A better range criterion is sometimes taken to be $R > 2\,(2h + D)^2/\lambda$.

It is the purpose of this section of the report to examine the effects of propagation reflections on a ground plane for this sort of condition. The meaning of $2D^2/\lambda$ in terms of the worst case of power pattern deviation from the pattern at infinite range is analyzed, and this deviation is used to develop an approximately equivalent criterion for azimuth pattern measurement over a ground plane. The procedure is to illustrate the phenomena by comparing the difference between transmission from a field probe to an aperture antenna, and transmission from a field probe to an aperture antenna over a ground plane. An integral formulation of the Fresnel zone patterns of an aperture antenna for transmission to a field probe over an isotropic homogeneous ground plane with varying reflections is developed.

The definition of the far-field range of an antenna is generally taken to be the minimum range beyond which the radiation power pattern is independent of range as determined by transmission between the antenna in question and a field probe. For typical equipment and operations, this is the range at which the spherical wave front from the field probe illuminates the test antenna's finite aperture with less total phase deviation than $\pi/8$ radians

or 1/16 wavelength from a plane wave illumination traveling along the radius vector from the field probe to the test antenna's effective radiation center. This is the basis for the $2D^2/\lambda$ criterion. Obviously, for an antenna aperture having a source distribution with less weight on the periphery of the aperture than at the center, the criterion will require a condition with less deviation from the plane wave case than for an antenna that is uniformly excited. Moreover, it is immaterial whether the maximum phase difference between the spherical wave and plane wave is weighted at the aperture center or periphery; the uniformly weighted aperture presents the case requiring the greatest control of tolerance of the phase dispersion across the aperture. Since the aperture dimension of $2D^2/\lambda$ is traditionally taken to be the maximum one, for the same reasons the circular aperture presents the most stringent case. The meaning of $2D^2/\lambda$ in terms of altered field strength can be determined by computing the scalar Fresnel zone pattern of a circular aperture with uniform illumination. Putting the source distribution in primed spherical coordinates, the diffraction integral is given by:

$$E(\vec{R}) = \frac{i\,k\,(1+\cos\theta)}{4\pi} \int_0^a \int_0^{2\pi} E_o \frac{e^{ikR''}}{R''} \, R'dR'd\phi'$$

where

$$R'' = \sqrt{R' + R'^2 - 2RR'\cos\Psi}$$

and $\cos\Psi = \sin\theta\cos(\phi-\phi')$

$$R'' = R\left\{1 + \frac{1}{2}\left[\left(\frac{R'}{R}\right)^2 - \frac{2R'\cos\Psi}{R}\right] - \frac{1}{8}\left[\;\right]^2 + \frac{1}{16}\left[\;\right]^3 - \text{----}\right\}$$

$\frac{1}{8}\left[\;\right]^2 \ll \frac{1}{2}\left(\frac{R'}{R}\right)^2$, $\frac{1}{R''} \simeq \frac{1}{R}$, and $\cos\theta \simeq 1$

$$\therefore\; E(\vec{R}) \simeq \frac{ika^2 e^{ikR}}{R} \int_0^1 e^{\frac{ika^2}{2}t^2} J_o(Zt)tdt \text{ where } Z = ka\sin\theta$$

thus

$$E(R) = i\ e^{ikR}\, e^{-ika^2/2R} \left\{ U_1\left(\frac{ka^2}{R}, z\right) - i\, U_2\left(\frac{ka^2}{R}, z\right) \right\}$$

where

$$U_1(W,Z) = \sum_0^\infty (-1)^n \left(\frac{W}{Z}\right)^{n+1} J_{n+1}(Z) \approx \left(\frac{W}{2}\right)^1 \frac{J_1(Z)}{(Z/2)} - \left(\frac{W}{2}\right)^3 \frac{J_3(Z)}{(Z/2)^3}$$

$$U_2(W,Z) = \sum_0^\infty (-1)^n \left(\frac{W}{Z}\right)^{n+2} J_{n+2}(Z) \approx \left(\frac{W}{2}\right)^2 \frac{J_2(Z)}{(Z/2)^2} - \left(\frac{W}{2}\right)^4 \frac{J_4(Z)}{(Z/2)^4}$$

For

$$\frac{W}{2} = \frac{ka^2}{2R} = \frac{\pi}{8} \qquad \text{and} \qquad R = \frac{8a^2}{\lambda}$$

$$\frac{J_n(Z)}{(Z/2)^n} = \frac{\Lambda_n(Z)}{n!} \qquad \text{and} \qquad |\Lambda_n(Z)| \leq 1$$

The far-field pattern is $\Lambda_1(Z)$. Since $\left(\frac{W}{2}\right)^3 \frac{1}{3!} \ll \left(\frac{W}{2}\right)^2 \frac{1}{2!}$, the $2D^2/\lambda$ pattern is given by:

$$E(Z) \simeq \frac{J_1(Z)}{Z/2} - i\frac{\pi}{8} \frac{J_2(Z)}{(Z/2)^2} = \Lambda_1(Z) - i\frac{\pi}{16} \Lambda_2(Z)$$

Thus the "true" axial field strength is modified by another plase quadrature signal, of about 20% the strength of the first signal, but the power deviation is only about 4%. The deviation signal will cause null fill-in of the true pattern, but at the sidelobe peaks of $\Lambda_1(Z)$, $|\Lambda_2(Z)| < |\Lambda_1(Z)|$. The deviation signal will be smaller than that indicated for axial angles greater than about 20^0. This power pattern distortion is the meaning of $2D^2/\lambda$ for probe transmission to a circular aperture. Thus, a power deviation error of less than $(\pi/16)^2$ on lobe peaks is assumed to be the far-field pattern criterion.

For transmission between two directive antennas, a greater range is required. It is known from the reciprocity theorem that the power transfer between two antennas is proportional to the integral:

$$P \sim \left| \int_S (\vec{E}_1 \times \vec{H}_2 - \vec{E}_2 \times \vec{H}_1) \cdot \hat{n} \, dA \right|$$

where E and H are the vector field components of the two antennas and S is an arbitrary surface enclosing one of the antennas with unit normal n. In order to find a surface upon which the far-field components of both antennas are correlated, the distance between the two antennas must be approximately the sum of their far-field ranges.

For the case of a point source over a ground plane, the surfaces of constant relative field strength are surfaces of constant phase difference between the source and its image, and these surfaces are known to be hyperbolas of revolution about the source and image axis. Consequently, when the hyperboloids are sufficiently close to their conical asymptotes, the angular diffraction pattern will be range invariant. The equiphase surfaces of the point source and image are ellipsoids. With increasing range, the ellipsoids rapidly approach their spherical asymptotes. Thus the asymptotic phase structure of a point source over a perfect ground plane is identical to the point source in free space. Their field structure is different due to the amplitude lobe pattern of the point source and image. Consequently, for a range invariant azimuth power pattern for transmission from a field probe to an aperture antenna over a ground plane, the range must be sufficiently great with respect to probe height that the amplitude taper across the vertical antenna aperture is negligible to the same degree that the spherical

phase taper is negligible by the $2D^2/\lambda$ criterion. Let the coordinate system origin be at the midpoint between the source and image, and α be the elevation angle to the field point. The distances between the source or the image and a field point are given respectively by:

$$R_1 = \sqrt{R^2 + h^2 - 2hR \sin\alpha}$$

and $$R_2 = \sqrt{R^2 + h^2 + 2hR \sin\alpha}$$

If $\left(\frac{h}{R}\right)^2 + 2\left(\frac{h}{R}\right)\sin\alpha < 1$,

$$R_1 = R + \frac{h^2}{2R} - h\sin\alpha - \frac{1}{8}\left[\frac{h^4}{R^3} - \frac{4h^3}{R^2}\sin\alpha + \frac{4h^2}{R}\sin^2\alpha\right] + \ldots$$

and $$R_2 = R + \frac{h^2}{2R} + h\sin\alpha - \frac{1}{8}\left[\frac{h^4}{R^3} + \frac{4h^3}{R^2}\sin\alpha + \frac{4h^2}{R}\sin^2\alpha\right] + \ldots$$

$$R_2 - R_1 = 2h\sin\alpha - \frac{h^3}{R^2}\sin\alpha + \ldots$$

$$R_2 + R_1 = 2R + \frac{h^2}{R}\cos^2\alpha - \ldots$$

The potential F at the point (R,α) is given by:

$$F(R,\alpha) = \frac{e^{ikR_1}}{R_1} - \frac{e^{ikR_2}}{R_2} \simeq \frac{e}{R}^{\frac{ik(R_2+R_1)}{2}}\left[e^{\frac{-ik(R_2-R_1)}{2}} - e^{\frac{ik(R_2-R_1)}{2}}\right]$$

$$\simeq -2i\frac{e}{R}^{i\left[kR + \frac{kh^2}{2R}\cos^2\alpha\right]}\sin\left(kR\sin\alpha - \frac{kh^3}{2R^2}\sin\alpha\right)$$

$$\simeq -2i\sin(kh\sin\alpha)\frac{e^{ikR}}{R} \quad \text{where } R \gg h$$

The principal deviation signal from the "true" or asymptotic signal arises from the phase term $\frac{kh^3}{2R^2}\sin\alpha$. Using the criterion developed on the lobe peaks results in the following:

$$\frac{kh^3}{2R^2} < \frac{\pi}{16} \qquad \text{or} \qquad R > 4h\sqrt{h/\lambda}$$

Criteria of this sort do not generally have practical significance without the consideration of transmission between two antennas.

The problem of transmission between a field probe and large aperture antenna over a ground plane is generally calculated by summing the direct and reflected ray from the field probe through the test antenna pattern to the aperture center. This is usually a good procedure if the field probe is in the test antenna's free space far-field range. Consider this case making the assumptions that the propagation terrain is isotropic (not necessarily homogeneous), and that the range is sufficiently large that the reflection coefficient is essentially constant for the correspondence between all aperture points of the test antenna and field probe. (For convenience the reflection coefficient is taken to be $\rho = -1$.) The field probe is at height h_1, an aperture point of the test antenna at h_2, and R is the horizontal range. For this case the reflected ray distance R_2 is given by:

$$R_2 = \sqrt{R^2 + (h_2 + h_1)^2} \qquad R > h_2 + h_1$$

$$R_2 = R\left\{1 + \frac{1}{2}\left[\left(\frac{h_2+h_1}{R}\right)^2\right] - \frac{1}{8}\left[\ \right]^2 + \frac{1}{16}\left[\ \right]^3 + \text{----}\right\}$$

$$R_2 \simeq R + \frac{(h_2+h_1)^2}{2R} = R + \frac{h_1^2+h_2^2}{2R} + \frac{h_1 h_2}{R}$$

Similarly: $R_1 \simeq R + \frac{h_1^2+h_2^2}{2R} - \frac{h_1 h_2}{R}$

Thus the asymtotic field of the probe in this notation varies over the vertical dimension of the aperture antenna as follows:

$$E(R,h_2) = -i\,2E_o \sin\left(\frac{kh_1h_2}{R}\right) e^{ik\left(R + \frac{h_1^2+h_2^2}{2R}\right)}$$

The significance of this field becomes clearer by referring the variation to the aperture center, accounting for the free space range criteria, and dropping the phase constants.

$h_2 = \bar{h} + y$ where $-\frac{w}{2} \leq y \leq \frac{w}{2}$

w - vertical aperture dimension

$\bar{h}$ - vertical aperture midpoint height

$h_2^2 = \bar{h}^2 + 2\bar{h}y + y^2$

$\therefore h_2^2 \approx \bar{h}^2 + 2\bar{h}y$

and $R > \frac{2D^2}{\lambda} \geq \frac{2w^2}{\lambda} \geq \frac{2y^2}{\lambda}$

$\frac{ky^2}{2R} < \frac{\pi}{8}$

$$\therefore E(R,h_2) = -i\,2E_0 \sin\left[\frac{kh_2(\bar{h}+y)}{R}\right] e^{ik\frac{\bar{h}}{R}y} \qquad (69)$$

The development of the expression for amplitude taper in equation (69) is analogous to the phase taper concept for incident field from a probe in the free space problem. If the magnitude of the reflection coefficient is less than one, the amplitude taper expression is more complicated, but less severe. Variations of the reflection coefficient across the vertical aperture dimension should be less than 1.0 of the same order as the required restriction on amplitude taper with constant reflection coefficient. If the aperture antenna is assumed to be very far from the probe, or focused or pointed at the source and image midpoint, then the phase plane "tilt" $e^{ik\frac{\bar{h}}{R}y}$ in equation (69) is cancelled out by the focussing, and the only factor to be summed over the aperture is the vertical amplitude taper.

$$\sin\left[\frac{kh_2(\bar{h}+y)}{R}\right] = \sin\left(\frac{kh_2\bar{h}}{R}\right)\cos\left(\frac{kh_2y}{R}\right) + \cos\left(\frac{kh_2\bar{h}}{R}\right)\sin\left(\frac{kh_2y}{R}\right)$$

If the aperture has symmetric vertical weighting, the antisymmetric taper variation in the incident field cancels out in the integration. However, the antisymmetric component will drop out regardless of the aperture weighting, if $\sin\left(\frac{kh_1\bar{h}}{R}\right)$ is maximized. In general, the aperture weight will be approximately symmetric, and better results will be obtained if the probe height is adjusted for maximum transmission. Normalizing the integration over a uniformly weighted rectangular aperture results in the factor:

$$\sin\left(\frac{kh_1\bar{h}}{R}\right) \cdot \sin\left(\frac{kh_1 w}{2R}\right) \Big/ \left(\frac{kh_1 w}{2R}\right)$$

The corresponding factor for a circular aperture is given by:

$$\sin\left(\frac{k\bar{h}h_1}{R}\right) \cdot J_1\left(\frac{kh_1 w}{2R}\right) \Big/ \left(\frac{kh_1 w}{2R}\right) \frac{1}{2}$$

Thus the usual propagation power transmission factor, $\sin^2(kh_1\bar{h}/R)$ is modified at most by the factor $\sin\left[\left(\frac{kh_1 w}{2R}\right) \Big/ \left(\frac{kh_1 w}{2R}\right)\right]^2$. Consequently, the range requirement for the special case described above can be prescribed from the free space case as follows:

$$1 - \left(\frac{\pi}{16}\right)^2 < \left(\frac{\sin x}{x}\right)^2 \simeq 1 - \frac{x^2}{3}$$

where $x = \frac{kh_1 w}{2R}$

and $\frac{kh_1 w}{\sqrt{3}\,2R} < \frac{\pi}{16}$, $\quad R > \frac{16h_1 w}{\sqrt{3}\,\lambda}$

A more general approach to the problem of range invariant azimuth pattern measurement with less conceptual parallel to the free space problem, but more mathematical precision, is available by the following development. The aperture

antenna is considered to simultaneously receive two plane waves at slightly different elevation angles. Thus the criteria must prescribe a condition for which the elevation angular difference is negligible compared to the elevation angular width of any lobe. The aperture antenna can be considered to be divided into a horizontal series of vertical strips, each strip having the appropriate weighting distribution. The azimuth diffraction is determined by the horizontal weighting on the array of elemental vertical strip antennas. The reflection phenomena perturb the weighting along a vertical strip, from what the resultant weighting would be for a single plane wave. The perturbation of the vertical weighting must be sufficiently negligible that the horizontal weighting of the array is not disturbed. The greater the vertical dimension, and the more rectangular the over all aperture weighting, the sharper the elevation angular resolution, and consequently the more restrictive the elevation angular difference that must be maintained. On the other hand, the more rectangular the overall weighting, the more independent the azimuth pattern becomes of the elevation angle. Thus provided it is kept in mind that the azimuth pattern can change with elevation angle, developing a perturbation criterion from the rectangular aperture is more restrictive than for other apertures. For the uniform circular aperture, for example, the diffraction pattern depends on the axial angle. Since the axial angular difference between the two plane waves is less than or equal to the elevation angular difference, and the diffraction function $\frac{J_1(x)}{x/2}$ is not as sharp as the function $\frac{\sin x}{x}$, the rectangular development is more restrictive.

Referring to equation (69), and putting the amplitude sine factor back into its exponential sum form; the direct and reflected wave components have the following form at the aperture.

Direct Wave:

$$E_1 = E_o\, e^{-ik\frac{h_1\bar{h}}{R}}\; e^{ik\left(\frac{\bar{h}-h_1}{R}\right)y}$$

Reflected Wave:

$$E_2 = \rho\left(\frac{h_1+\bar{h}}{R}\right)\; E_o\, e^{ik\frac{h_1\bar{h}}{R}}\; e^{ik\left(\frac{\bar{h}+h_1}{R}\right)y} \qquad \text{where } h_1 \leq \bar{h}$$

The two elevation angles are defined by:

$$\alpha_1 \simeq \frac{h-h_1}{R}$$

$$\alpha_2 = \tan^{-1}\left(\frac{\bar{h}+h_2}{R}\right) \simeq \frac{\bar{h}+h_2}{R}$$

It is assumed that

$$\rho\left(\frac{h_1+h_1}{R}\right) \simeq \rho\left(\frac{h_1+\bar{h}}{R}\right)$$

where $\rho(\alpha)$ is the reflection coefficient as function of α. For most practical situations when large antennas are used, the range is normally much greater than the heights involved and the criteria concerning the constancy of the reflection coefficient will be less restrictive than that for the free space azimuth pattern variation of the antenna at elevation angles $\frac{\bar{h}-h_1}{R}$ and $\frac{\bar{h}+h_1}{R}$. For a rectangular aperture with uniform weighting, the free space pattern is known to be of the form:

$$E = E_o\, \frac{\sin\left(\frac{kwy}{2}\sin\theta\cos\phi\right)}{\left(\frac{kwy}{2}\sin\theta\cos\phi\right)} \cdot \frac{\sin\left(\frac{kwx}{2}\sin\theta\sin\phi\right)}{\left(\frac{kwx}{2}\sin\theta\sin\phi\right)}$$

where $\sin\theta\begin{Bmatrix}\sin\varphi\\ \cos\varphi\end{Bmatrix}$ are the direction cosines of a field point with respect to the aperture coordinates. Consequently we desire a criterion for the difference of the elevation angles of the direct wave and the reflected wave.

$$g(u_1) = \frac{\sin\left(\frac{kwy}{2}\sin\alpha_1\right)}{\left(\frac{kwy}{2}\sin\alpha_1\right)} \quad \frac{\sin\left(\frac{kwy}{2}\sin\alpha_2\right)}{\left(\frac{kwy}{2}\sin\alpha_2\right)} = g(u_2)$$

$$g(u_2) - g(u_1) = g'(u)\,\delta u$$

$$g(u) = \frac{\sin u}{u}$$

The direct and reflected signals summed in the antenna aperture have the form:

$$E \propto g(u_1)\left[\cos\phi - i\sin\phi\right] - g(u_2)\left[\cos\phi + i\sin\phi\right]$$

$$= \cos\phi\left[g(u_1) - g(u_2)\right] - i\sin\phi\left[g(u_1) - g(u_2)\right]$$

$$\phi = \frac{k\bar{h}h_1}{R}$$

$$EE^* \sim g^2(u_1) + g^2(u_2) + 2g(u_1)\,g(u_2)\left[\sin^2\phi - \cos^2\phi\right]$$

$$= \left[g^2(u) + g(u)\,\delta g(u)\right]4\sin^2\phi + \left[\delta g(u)\right]^2 - 4\sin^2\phi\, g^2(u)$$

If it is prescribed that $\sin^2\phi$ be maximized, then the only requirement is:

$$\frac{\delta g(u)}{g(u)} \ll 1$$

If $\sin^2\phi$ is not maximized, then the requirement becomes:

$$\frac{\delta g(u)}{g(u)} \ll 4\sin^2\phi$$

Differentiating the criterion function $\frac{\delta g(u)}{g(u)}$ with respect to α indicates a minimum deviation for $u = 0$. Assuming u is held small (i.e., an "azimuth cut" is taken), $h_1 \leq \bar{h}$, then for the first criterion:

$$\frac{\delta g(u)}{g(u)} = \left(\frac{u \cos u}{\sin u} - 1\right) \frac{\delta u}{u} \simeq \frac{u\delta u}{3} \simeq \frac{(\delta u)^2}{3} < \left(\frac{\pi}{16}\right)^2$$

$$\delta u = \frac{kw}{2} \delta\alpha, \quad \delta\alpha = \frac{\bar{h}+h_1}{R} - \frac{\bar{h}-h_1}{R} = \frac{2h_1}{R}$$

$$\delta u = \frac{kwh_1}{R} < \frac{\sqrt{3}\pi}{16}, \quad R > \frac{32}{\sqrt{3}} \frac{h_1 w}{\lambda}$$

If $\sin^2 \psi$ is small, it is required that:

$$\frac{1}{3}\left(\frac{kwh_1}{R}\right)^2 << 4 \sin^2\psi = \left(\frac{2k\bar{h}h_1}{R}\right)^2$$

$$w^2 << 12\,\bar{h}^2$$

In general it can only be assured that $w < 2\bar{h}$. Thus, the completed criterion is given by:

$$\frac{\delta g(u)}{g(u)}\left(1 + \frac{\delta g(u)}{4g(u)\sin^2\psi}\right) << 1$$

$$\frac{1}{3}\left(\frac{kwh_1}{R}\right)^2\left[1 + \frac{w^2}{12\bar{h}^2}\right] < \left(\frac{\pi}{16}\right)^2 \quad \frac{kwh_1}{R} < \frac{3}{2} \cdot \frac{\pi}{16}$$

$$\left(\frac{4}{3}\right)\frac{16h_1 w}{\lambda} < R$$

It is observed that if it is assumed that $R > \frac{16h_1 w}{\lambda}$, and that $h_1 = \bar{h} = \frac{w}{2}$, then this corresponds to the criterion: $R > 2(2\bar{h}+w)^2/\lambda$. The fields at $\frac{2D^2}{\lambda} < R < \left(\frac{4}{3}\right)\frac{16h_1 w}{\lambda}$ are not Fresnel zone fields. The quantity $\bar{h}$ does not enter into the criterion because only azimuth patterns are considered. Criteria cannot be prescribed for elevation patterns because the pattern of the field probe also changes with elevation.

As a brief summary of the far-field range criterion problem, the following comments are made. Propagation ground plane reflections do not extend the Fresnel zone, but the phenomena may perturb the horizontal weighting

of an aperture antenna, which modifies the azimuth pattern at near ranges. If the aperture is divided into a horizontal array of vertical strip antennas, and the proper far field signal is received from each strip, then the azimuth pattern will have the far field property. A reasonable criterion for "azimuth cuts" that is approximately equivalent to the free space pattern distortion at $R = 2D^2/\lambda$, is $R > 16\, h_1 w/\lambda$, where h_1 is the field probe height, and w is the vertical aperture dimension. Thus a suggested pattern range for large antennas is given as follows:

$R > \frac{2D^2}{\lambda}$ or $16h_1 w/\lambda$, whichever is greater.

To be consistent with the two antenna rule, the asymptotic range of the field probe (which is relatively small), $R = 4h_1\sqrt{h_1/\lambda}$, should be added to the pattern range.

To complete the description of propagation reflections, an integral formulation for varying reflection phenomena in the Fresnel zone is developed. Variation of the reflection coefficient will not complicate the theoretical approach as long as surface wave phenomena is negligible. The Sommerfeld solution to propagation over an arbitrary plane earth can be interpreted assuming over plans waves reflected at varying elevation angles from the earth's surface. In the region of validity of the free space scalar integral, the field components can be formulated in this manner directly. The scalar integral considered for the free-space case at first is reintroduced with an arbitrary illumination function. To facilitate a superposition view, the origin of the coordinate system is placed in the real aperture center. Coordinate point definitions are made as follows:

(R, θ, φ) = field point

$(R, \pi/2, \varphi_o)$ = real aperture point

$(2\bar{h}, \pi/2, -\pi/2)$ = image aperture center

$(R_1', \pi/2, \varphi_1')$ = image aperture point

$(R_o', \pi/2, -\varphi_o)$ = image aperture point relative to image aperture center

$$R_1' = \left\{ (2\bar{h})^2 + R_o'^2 - 2R_o'(2\bar{h}) \cos\left(\frac{\pi}{2} + \varphi_o'\right) \right\}^{1/2}$$

$$= \left\{ (2\bar{h})^2 + R_o'^2 + 2R_o'(2\bar{h}) \sin \varphi_o' \right\}^{1/2}$$

$$R_o'' = \left\{ R^2 + R_o'^2 - 2R_o'R \sin\theta \cos(\varphi - \varphi_o') \right\}^{1/2}$$

(Real aperture point to field point distance)

$$R_1'' = \left\{ R^2 + R_1'^2 - 2R_1'R \sin\theta \cos(\varphi - \varphi_1') \right\}^{1/2}$$

(image aperture point to field point distance)

$$\cos(\varphi - \varphi_1') = \cos\varphi \cos\varphi_1' + \sin\varphi \sin\varphi_1'$$

$$\cos\varphi_1' = \frac{R_o'}{R_1'} \cos\varphi_o', \quad \sin\varphi_1' = -\frac{2\bar{h} + R_o' \sin\varphi_o}{R_1'}$$

$$R_1'' = R \left\{ 1 + \left(\frac{R_o'}{R}\right)^2 - \frac{2R_o'}{R} \sin\theta \cos(\varphi + \varphi_o') + \frac{(2\bar{h})^2 + 2R_o'(2\bar{h}) \sin\varphi_o' + 2R(2h) \sin\theta \sin\varphi}{R^2} \right\}^{1/2}$$

$$R_o'' \simeq \left[R + \frac{R_o'^2}{2R} - R_o' \sin\theta \cos(\varphi - \varphi_o') \right] = [\,]_o$$

$$R_1'' \simeq R + \frac{R_o'^2}{2R} - R_o' \sin\theta \cos(\varphi + \varphi_o') + \frac{(2\bar{h})^2}{2R} + 2\bar{h} \sin\theta \sin\varphi + \frac{2\bar{h}R_o \sin\varphi_o'}{R}$$

E_o = direct ray field, E_1 = image ray field, $f(R_o', \varphi_o')$ = aperture illumination function. $\rho(R,\theta,\varphi; R_o', \varphi_o')$ = reflection coefficient for the reflection angle defined by the reflected ray correspondence between the aperture point (R_o', φ_o') and the field point, (r, θ, φ).

$$E_o = \frac{k}{2\pi R} \iint f(R'_o, \varphi'_o)\, e^{ik[\ ]_o}\, R'_o\, dR'_o\, d\varphi'_o$$

$$E_1 = e^{ik2\bar{h}(\frac{\bar{h}}{R} + \sin\theta \sin\varphi)}\ \frac{k}{2\pi R} \iint \rho(R'_o, -\varphi'_o)\ f(R'_o, -\varphi'_o)$$

$$\cdot\ e^{-ikR'_o \frac{2\bar{h}}{R} \sin\varphi'_o}\ e^{ik[\ ]_o}\ R'_o dR'_o\, d\varphi'_o$$

The field received by a field probe is the sum of these two signals. The aperture illumination can be conceived as the superposition of the two functions:

$$f_1 = e^{ik2\bar{h}(\frac{\bar{h}}{R} + \sin\theta \sin\varphi)} \rho(R'_o, -\varphi'_o)\ f(R'_o, -\varphi'_o)\ e^{-ikR'_o \frac{2\bar{h}}{R} \sin\varphi'_o}$$

and $f_o = f(R'_o, \varphi'_o)$ where $e^{ik2\bar{h}(\frac{\bar{h}}{R} + \sin\theta \sin\varphi)}$ is a constant phase retardation difference defined by the field point. If $\rho(R'_o, -\varphi'_o)$ is real, and f_o has constant phase, then f_1 has a phase plane that is scanned relative to the constant phase plane of f_o thru the elevation angle $\sin^{-1}\left(\frac{2\bar{h}}{R}\right)$. Thus if f_o is real, the pattern of f_1 is pointed downward from the aperture axis at the elevation angle defined. If the two functions are viewed independently as f_o in its geometric real position, and f_1 in its geometric image position, then the two beams are pointed normal to their apertures, and the field point receives thru the side lobes of the image function. Reversal of the sign of φ'_o is the analogue of optical image inversion. If $\rho(R'_o, -\varphi'_o)$ is real with constant sign, but asymmetric, this amplitude asymmetry will not change the pattern symmetry of the image radiation associated with f_1. For homogeneous smooth dielectric terrain at ranges below the Brewster angle, the magnitude of ρ for an aperture point will decrease with increasing angle of reflection, such that the top of the illumination function in the image aperture will be

more heavily weighted. This will have the effect of lowering the effective radiation center $\bar{h}$. If $f(R_o', \varphi_o')$ is complex, the radiation pattern of f_1 will be modified by $\rho(R_o', -\varphi_o')$ such as to change its symmetry. If f_o is symmetric and defocused by a phase function concave to the field direction, then the main beam in the image aperture will be pointed downward. If f_o is defocused by a convex phase function, the image beam will be pointed upward by the variation of ρ. If f_o is symmetric and focused, and $\rho(R_o', -\varphi_o'$ passes thru the Brewster angle near the midpoint of the aperture, the main beam in the image aperture will tend to split in the elevation pattern.

For large apertures, the variation of ρ for vertical polarization is large in the Fresnel zone. Consider for example, an 85' dish with the radius $a = 100\lambda$. The reflection coefficient for vertical polarization is commonly given as:

$$\rho = \frac{\epsilon' \sin\alpha - \sqrt{\epsilon' - \cos^2\alpha}}{\epsilon' \sin\alpha + \sqrt{\epsilon' - \cos^2\alpha}}$$

where ϵ' is the complex dielectric constant and α is the elevation angle. For S-band frequencies, it is often a good assumption that the conduction current in the flat terrain is very small compared to the displacement current. For this case at small elevation angles:

$$\rho \simeq \frac{\epsilon \sin\alpha - \sqrt{\epsilon - 1}}{\epsilon \sin\alpha + \sqrt{\epsilon - 1}}, \qquad \rho(\alpha_B) \simeq 0$$

$$\sin\alpha_B \simeq \frac{1}{\sqrt{\epsilon + 1}} \quad \text{(Brewster angle)}$$

For $\epsilon = 3 \sim 8$, the Brewster angle is $30^\circ \sim 20^\circ$, and in most cases will not be involved. If the height of the vertical dish antenna assumed is 2a, the

variation of ρ for a field point at the same elevation is from -1.0 to +.2 thruout the Fresnel zone. At a range of 4250', which is the distance for one Fresnel ring $\left(\frac{1}{8}\frac{2D^2}{\lambda}\right)$, the reflection coefficient variation across the vertical aperture is -.9 to -.7. At a range of 425', which is the distance for 10 Fresnel rings, $\rho = -0.3t_0 + 0.2$. At this range ρ varies thru the Brewster angle. Smaller ranges carry into the near field.

From the form of the superposed fields E_0 and E_1, it is clear that the Fresnel zone field structure cannot be extended by propagation over a ground plane. The field structure within the Fresnel zone, however, is sufficiently modified in some cases due to the variation in reflections, that the Fresnel field for large apertures cannot be analyzed by the retarded superposition of two field components of one pattern. For the example cited, this would only be possible at R > 4250', where ρ is essentially constant. It can also be shown that arbitrary first terrain (ρ complex) cannot extend the Fresnel zone, but in this case the phenomena cannot be illustrated by the simple procedure undertaken above. In the event of surface-wave phenomena, however, the antenna will most likely not be large with respect to wavelength.

7. RADIAL E FIELD

7.1 Theoretical Investigation of Radial Electric Field

Some interest has been expressed in the magnitude of the other field components in the Fresnel field relative to the principal component of the field. It is a simple matter to calculate the radical electric field, E, using the integrated vector wave equation given by Silver.[1]

$$\vec{E} = \frac{+j\eta}{4\pi} \iint_A \left\langle (\vec{J}\cdot\nabla)\nabla\psi + k^2\vec{J}\psi \right\rangle da + \frac{1}{4\pi} \iint_A \vec{K} \times \nabla\psi \, da$$

where $\vec{J} = -\hat{n}\times\vec{H}$ is the electric current in the aperture and $\vec{K} = \hat{n}\times\vec{E}$ is the magnetic current in the aperture, and $\psi = \frac{e^{-jkr}}{kr}$ is the free space scalar Greens function.

In the following, we shall consider a planar aperture illuminated by a plane wave, as shown in figure 50. This simplifies the analysis since then $E = -\eta\hat{n}\times\vec{H}$ (where n is the outward normal from the aperture)

Then the vector operators are given by 8 (p. 87)

$$\nabla \frac{e^{-jkr}}{kr} = +\left(j + \frac{1}{kr}\right) \frac{e^{-jkr}}{kr} \hat{r}$$

$$(\vec{J}\cdot\nabla)\nabla \frac{e^{-jkr}}{kr} = \left[\left(-1 + \frac{3j}{kr} + \frac{3}{(kr)^2} \right) (\vec{J}\cdot\hat{r})\,\hat{r} - \frac{1}{kr}\left(j + \frac{1}{kr}\right)\vec{J} \right] \psi$$

$$\vec{K} \times \nabla\psi = \left(j + \frac{1}{kr}\right) \frac{e^{-jkr}}{kr} \vec{K} \times \hat{r}$$

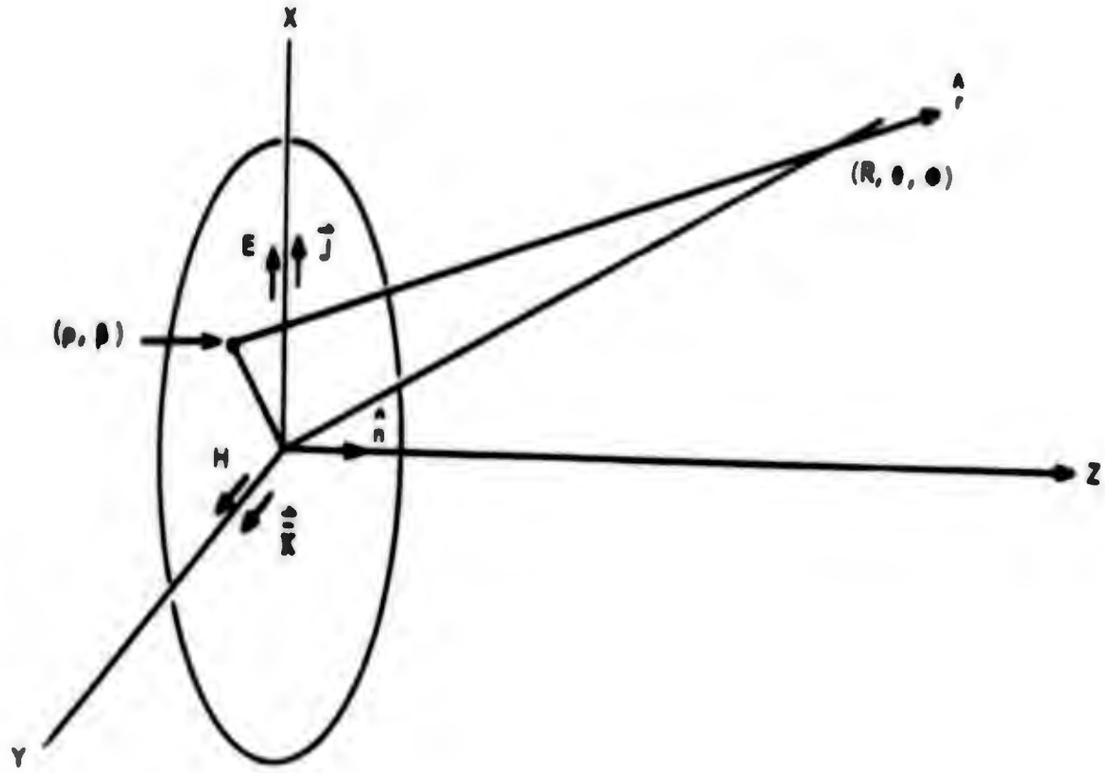

Figure 50. Coordinate System and Surface Currents in the Circular Aperture

Assuming $H = H_y \hat{Y}$

$$\vec{J} \cdot \hat{r} = \left[\frac{R}{r} \sin\theta \cos\varphi - \frac{\rho}{r} \cos\beta \right] H_y$$

$$\hat{R} \cdot (\vec{K} \times \hat{r}) = \left[\frac{\rho}{r} \cos\theta \cos\beta \right] \eta H_y$$

Since the algebra is shortened by consideration of the pattern in one plane and we are primarily interested in the order of magnitude of the radial E field we shall consider only the radial field in the E-plane ($\varphi = 0$) of the aperture. Thus

$$E_R = \vec{E} \cdot \hat{R}$$

$$= \frac{j\eta H_y}{4\pi} \iint_A \left[\left(-1 + \frac{3j}{kr} + \frac{3}{(kr)^2} \right) \left(\frac{R}{r} \sin\theta - \frac{\rho}{r} \cos\beta \right) \left(\frac{R}{r} - \frac{\rho}{r} \sin\theta \cos\beta \right) \right.$$

$$\left. + \left(1 - \frac{j}{kr} - \frac{1}{(kr)^2} \right) \sin\theta \right] \Phi \, da + \frac{\eta H_y}{4\pi} \iint \left(j + \frac{1}{kr} \right) \frac{\rho}{r} \cos\theta \cos\beta \, da$$

expanding the integrand of the first integral one obtains

$$I_1 = \left(\frac{\rho^2}{r^2} - \frac{R\rho \sin\theta \cos\beta}{r^2} \right) \sin\theta + \frac{1}{kr} \left(\frac{3R^2}{r^2} - 1 \right) \sin\theta + \frac{R\rho}{r^2} \cos\beta$$

$$- \frac{3j\rho}{kr^3} \sin\theta \cos\beta \, (R \sin\theta + \rho \cos\beta)$$

It was found by calculation of the remaining terms that the $\frac{R\rho}{r^2}$ powers predominate over the other terms in the Fresnel zone. Thus

$$E_r \simeq \frac{j\eta H_y}{4\pi} \int_0^{2\pi} \int_0^{ka} \frac{R\rho}{r^2} (-\sin^2\theta \cos\beta + \cos\beta) \, k\rho \, dk\rho \, d\beta$$

$$+ \frac{j\eta H_y}{4\pi} \iint \left| \frac{\rho}{r} \cos\theta \cos\beta \right| k\rho \, dk\rho \, d\beta$$

Then

$$E_r \simeq \frac{j\eta H_y}{r\pi} \int_0^{2\pi} \int_0^{ka} \left| \frac{R\rho}{r^2} + \frac{\rho}{r} \cos\theta \right| \cos\beta \, \frac{e^{-jkr}}{kr} \, k\rho \, dk\rho \, d\beta$$

We shall use the Fresnel approximation namely $kr \simeq kR - ka\rho \sin\theta \cos\beta + \frac{\rho^2}{2R}$ is the exponential and $r \simeq R$ in the denominator. Now if the usual change of variables[11] are made, E_r may be expressed as a generalised Lommel function

$$E_r \simeq \frac{j\eta H_y \cos\theta (1 + \cos\theta)}{4\pi k^2 R^2} \left[2\pi (ka)^3 (-j) e^{-jkR - j\frac{\gamma}{2}} W_1^0 (\gamma, u) \right]$$

or

$$E_r \simeq \frac{\eta H_y \gamma_a \cos\theta (1 + \cos\theta)}{2R} e^{-jkR - j\frac{\gamma}{2}} W_1^0 (\gamma, u)$$

where $\gamma = \frac{ka^2}{2}$ and $u = ka \sin\theta$ and W_1^0 are the functions tabulated in table 1, of the Appendix.

$$E_r = \frac{j\eta H_y \gamma (1 + \cos\theta)}{2} e^{-jkR - j\frac{\gamma}{2}} W_0^0 (\gamma, u)$$

and the ratio of the two components of the field are given by

$$\frac{E_r}{E_\theta} = \frac{a \cos\theta \, W_1^0 (\gamma, u)}{jR \, W_0^0 (\gamma, u)}$$

Thus in the Fresnel zone $|E_r|$ is of the same order of magnitude as $\frac{a}{R}|E_\theta| \cos\theta$ and if $R \gg a$ the radial E field is negligible compared to the E_θ component. Figure 51 shows a plot of both the principal field component and the radial field component at a distance of 200λ for a 40λ aperture ($\gamma=4\pi$). Thus it may be seen that the radial field is significant compared to the principal component, only at distances a few antenna radii away from the aperture.

7.2 Measurement of the Radial Field Component

The experimental determination of an arbitrarily polarized field is a difficult problem requiring a large number of measurements at each point to determine the polarization ellipse at that point. However the problem is greatly simplified if only the relative amplitudes of two orthogonal components such as E_r and E_θ are of interest. In this case a thin dipole oriented in the direction of the desired component has a voltage induced across the terminals which is proportional to the component of the field oriented along the dipole. However the dipole must be short enough that there is no significant variation in the amplitude of the field along the dipole.

For the case of the fields radiated by a large aperture antenna the measurement problem is further simplified since the fields vary sufficiently slowly in the Fresnel zone that a resonant dipole may be used. However, a serious problem is introduced by the effect of the transmission line connecting the probe to the detection equipment. Several methods[19] [20] have

19. K. Iizuka, "How to Measure Field Pattern with Photo-Sensitive Probes," Electronics, Vol. 36, pp 39-43, Jan. 25, 1963.

20. Hu, M. K. "Measurements of Microwave E and H Field Distributions by using Modulated Scattering Techniques," IRE Transactions Vol. MTT 8, May 1960.

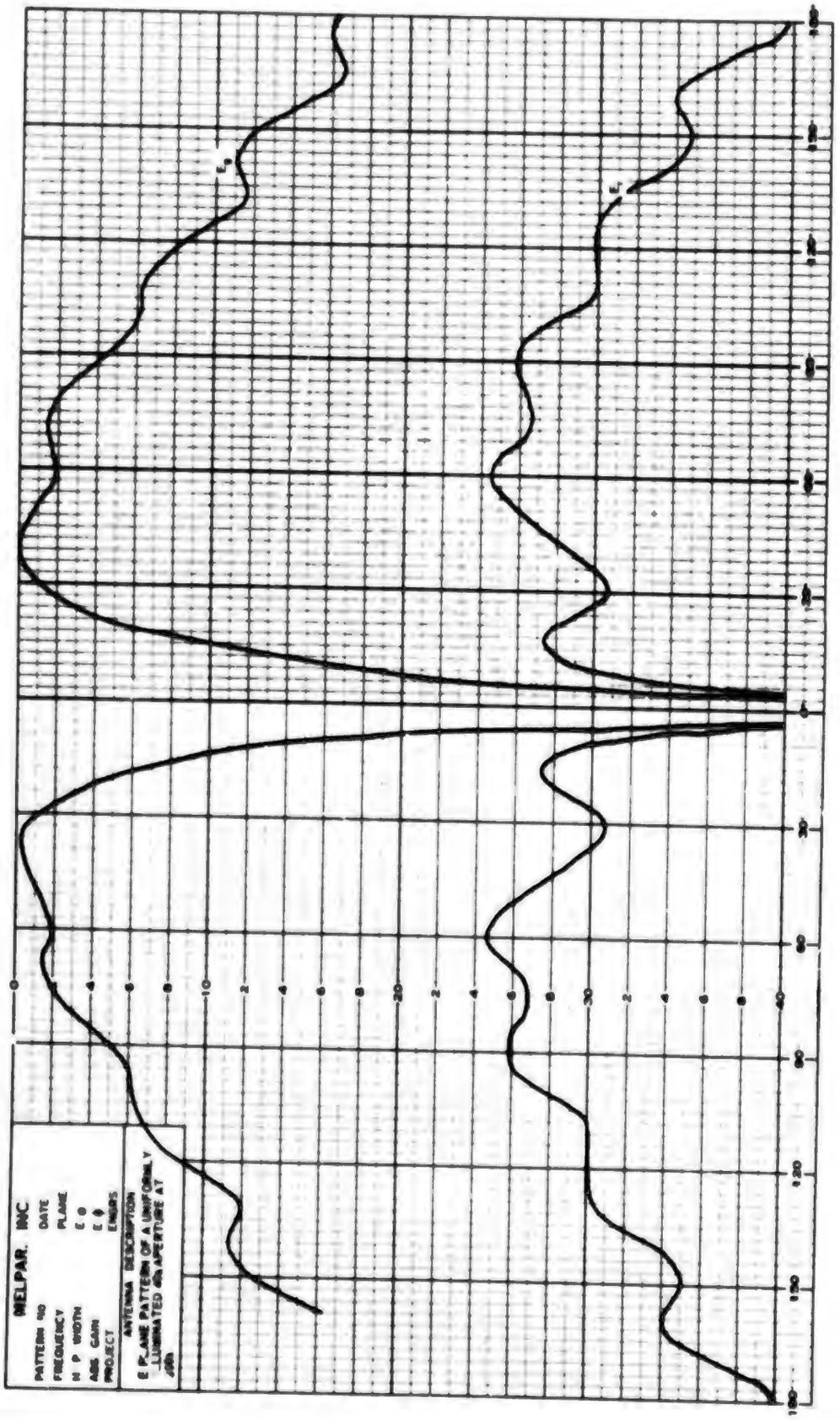

Figure 51. E-Plane E_r and E_θ Field Components of a Uniformly Illuminated Aperture Plotted Versus $u = ka\sin\theta$ at a Distance $\rho = 4\pi$

been used to eliminate the transmission line. These methods use a scatterer, such as a dipole, loaded with a diode. The back scattered signal from the scatterer is amplitude modulated by application of an audio frequency signal to the diode. The back scattered signal is received by the transmitting antenna and detected by a coherent detection system. In the method proposed by Hu[2] a germanium diode is modulated by a bias voltage applied through a thin, poorly conducting thread coated with aquadag. The probe used by Iizuka[19] eliminates lead wires entirely. It consists of a dipole loaded with a photocell which is modulated by a chopped light beam. The modulated scattering technique will give good results for radial field measurement if the diode and dipole cross section can be kept thin enough to provide the dynamic range required to measure the radial field. However, it should be noted that this is primarily a laboratory technique and requires a rather elaborate receiving system.

8. FRESNEL REGION MEASUREMENTS OF A CIRCULAR APERTURE

To determine the degree which theoretically derived radiation patterns for a circular aperture, discussed in Section 2.1 of this report, may be realised in an actual antenna, experimental patterns were taken on a 40λ circular aperture paraboloidal reflector at X-band. Figure 52 shows the test antenna consisting of a 4-foot dish with a focal length of 22-1/8 inches and an adjustable waveguide-fed feed horn. The measured primary pattern of the horn shown in figure 53 determined that the amplitude distribution across the circular aperture was circularly symmetric with a 12 db taper. A comparison of the theoretically predicted and experimental E- and H-plane far-field patterns of the test antenna are shown in figure 54. To minimise the effect of ground reflections in the Fresnel zone the test antenna was mounted on a 38-foot high model rotator consisting of a fiberglass tower assembly which can be moved along concrete tracks to vary the test range.

Radiation patterns were taken in both the E- and H-planes of the test antenna at a frequency of 9835 mcs. To insure that the signal source antenna far field requirement was extremely small, an open-end waveguide mounted on a wooden tower was used. Experimental patterns are compared with those theoretically predicted by the method of Hu[5] for normalised distances in the Fresnel Region in figures 55 through 58. On inspection of these patterns it becomes evident that while the envelope of the main lobe of the radiation patterns can be predicted with fairly good accuracy using mathematical techniques, the physical limitations of the antenna and the measurement facility introduce unpredictable details in the actual patterns.

Figure 52. X-Band Test Antenna

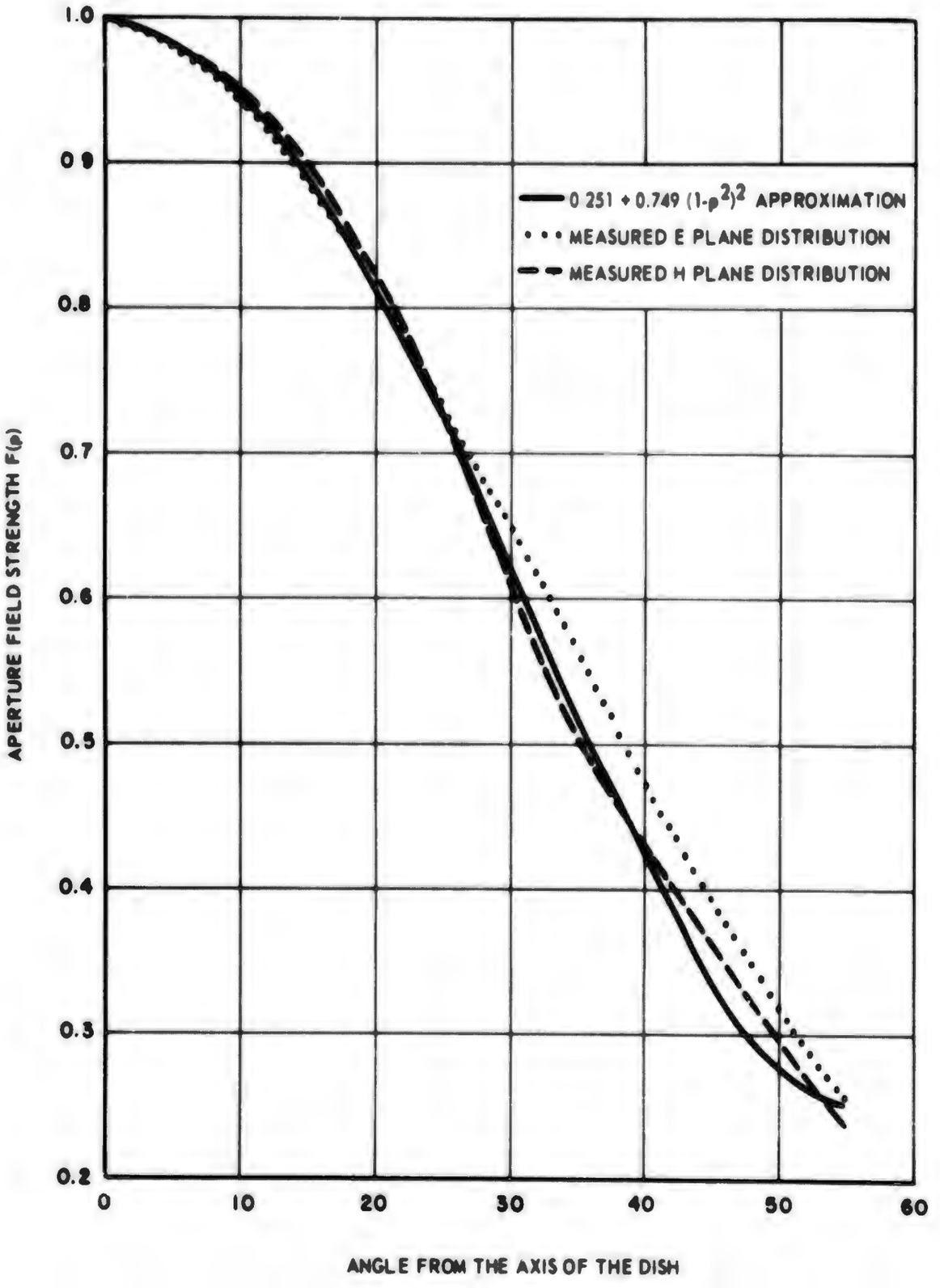

Figure 53. Aperture Field of Experimental Paraboloidal Reflector (D = 40λ)

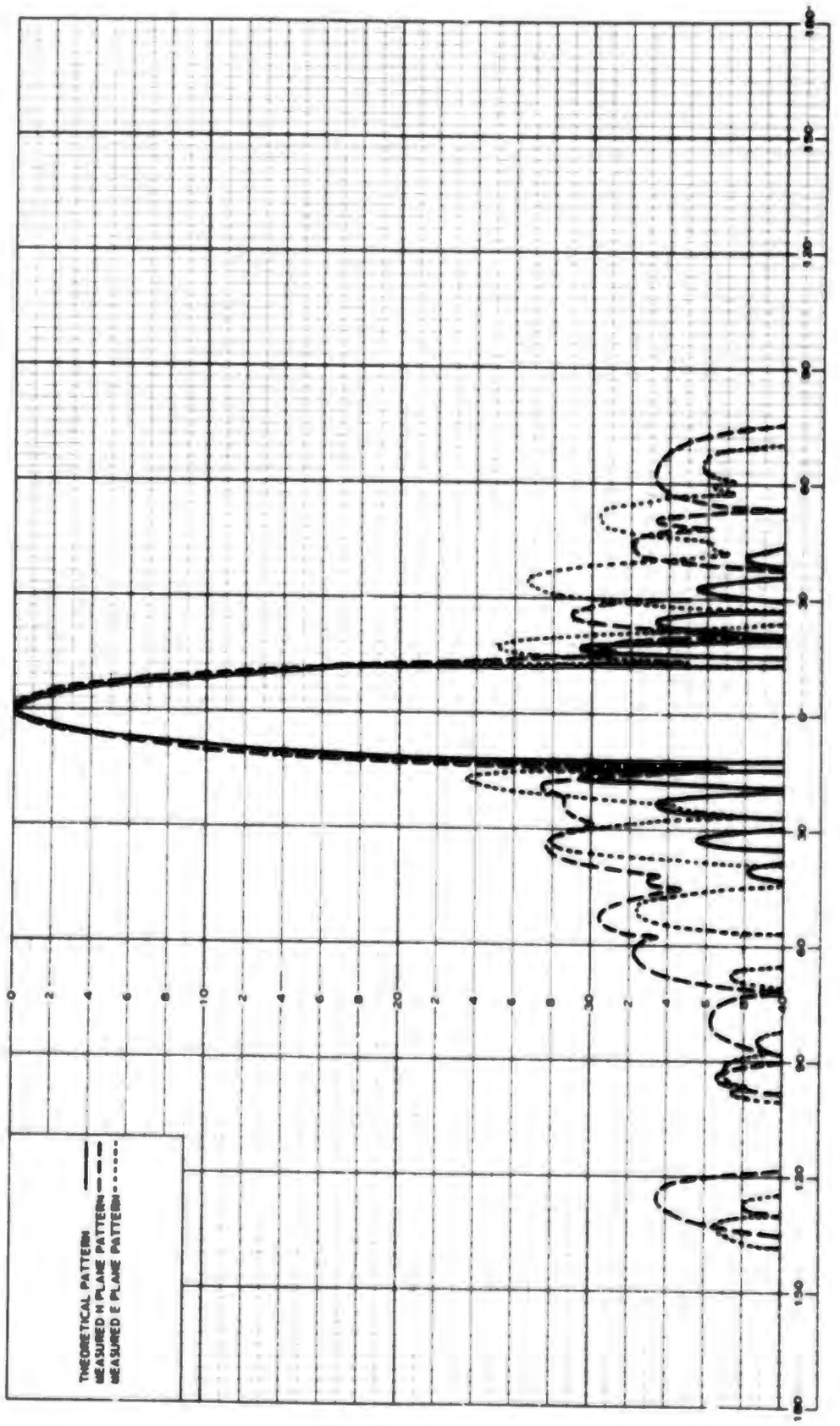

Figure 54. Patterns of Horn-Fed 4-Foot Diameter Paraboloidal Reflector at 9835 mc (Far Field)

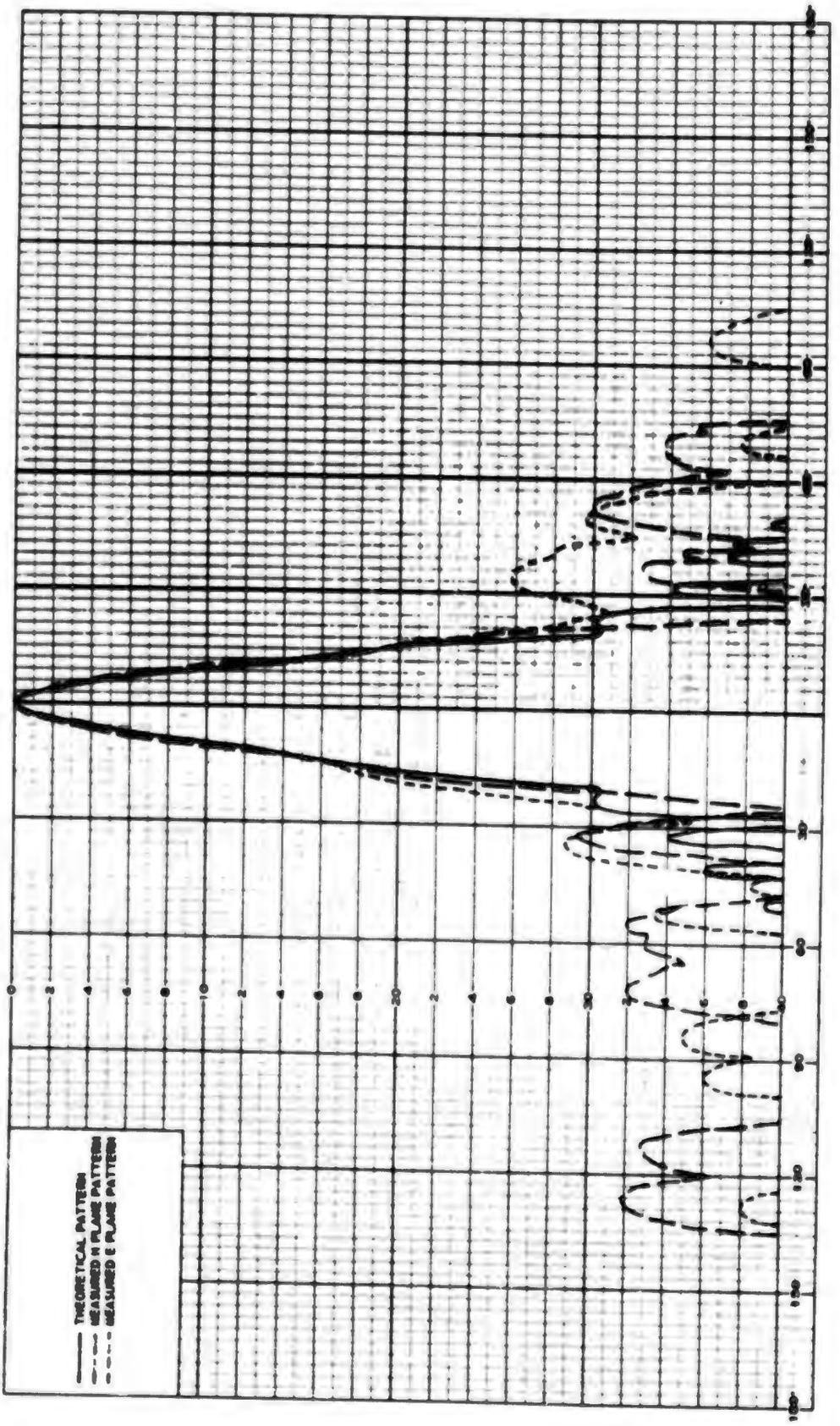

Figure 55. Patterns of Horn-Fed 4-Foot Diameter Paraboloidal Reflector at 9835 mc ($D^2/2\lambda = 80$)

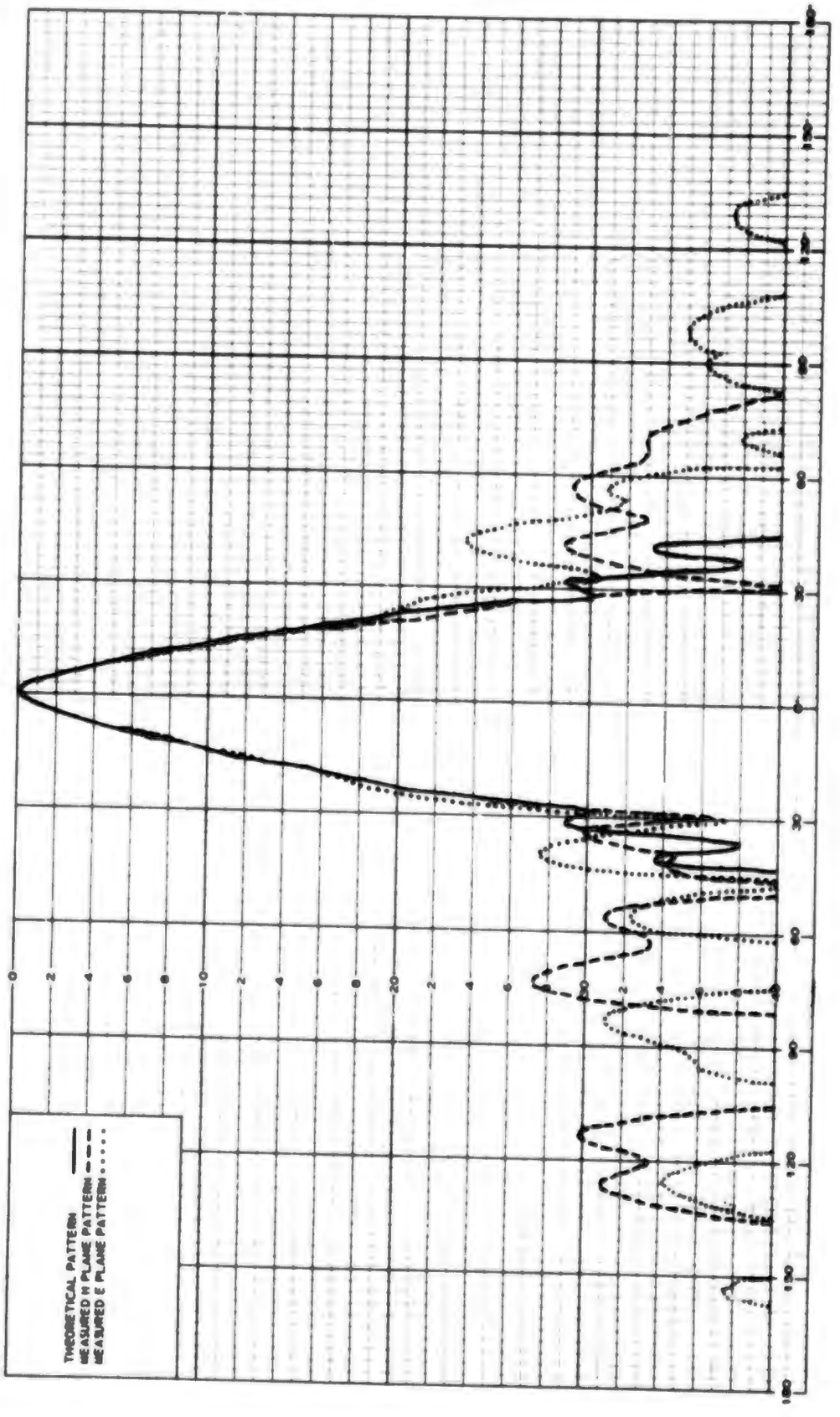

Figure 56. Patterns of Horn-Fed 4-Foot Diameter Paraboloidal Reflector at 9835 mc ($D^2/4\lambda = 40$)

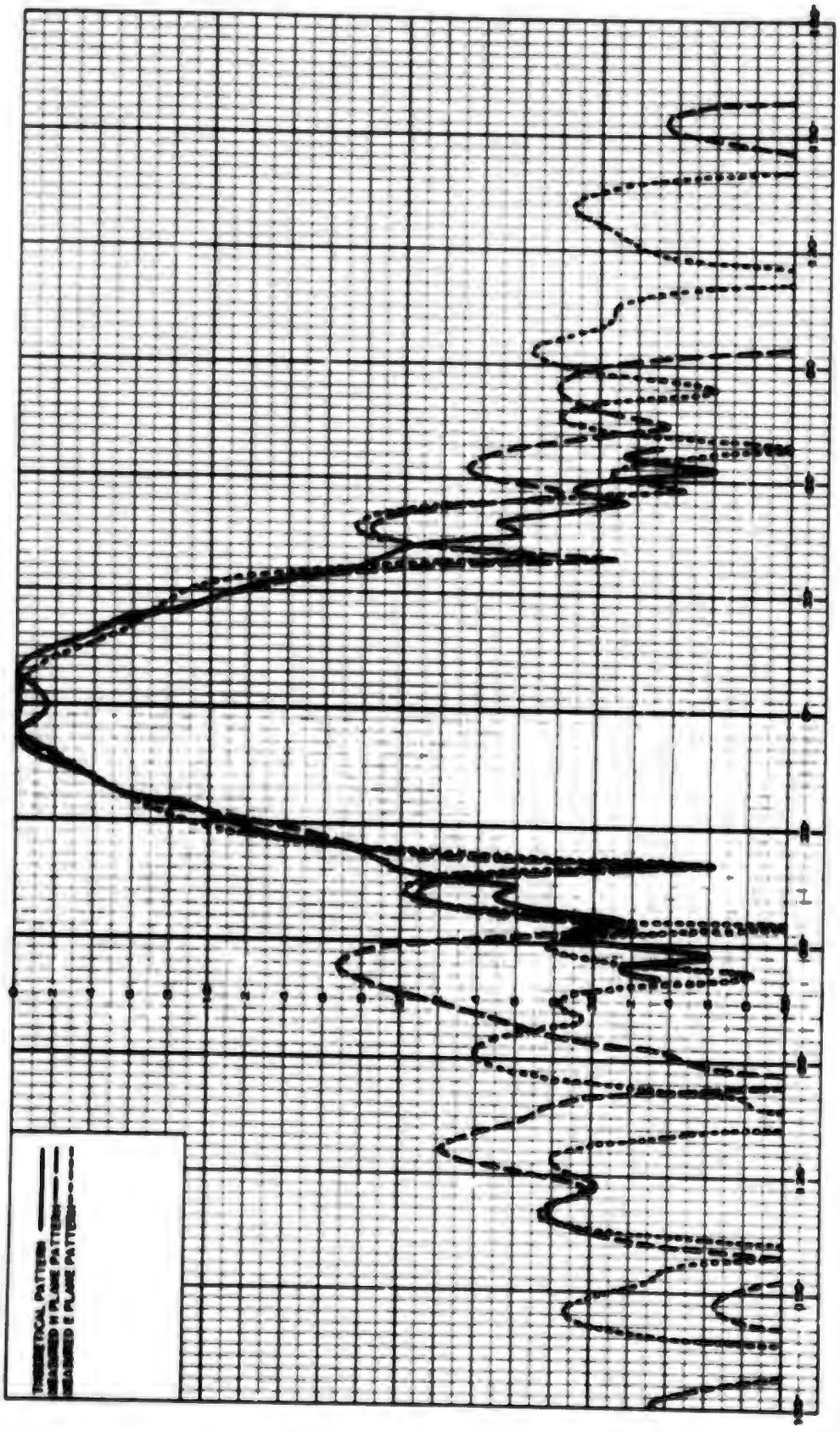

Figure 57. Patterns of Horn-Fed 4-Foot Diameter Paraboloidal Reflector at 9835 mc ($D^2/8\lambda = 20$)

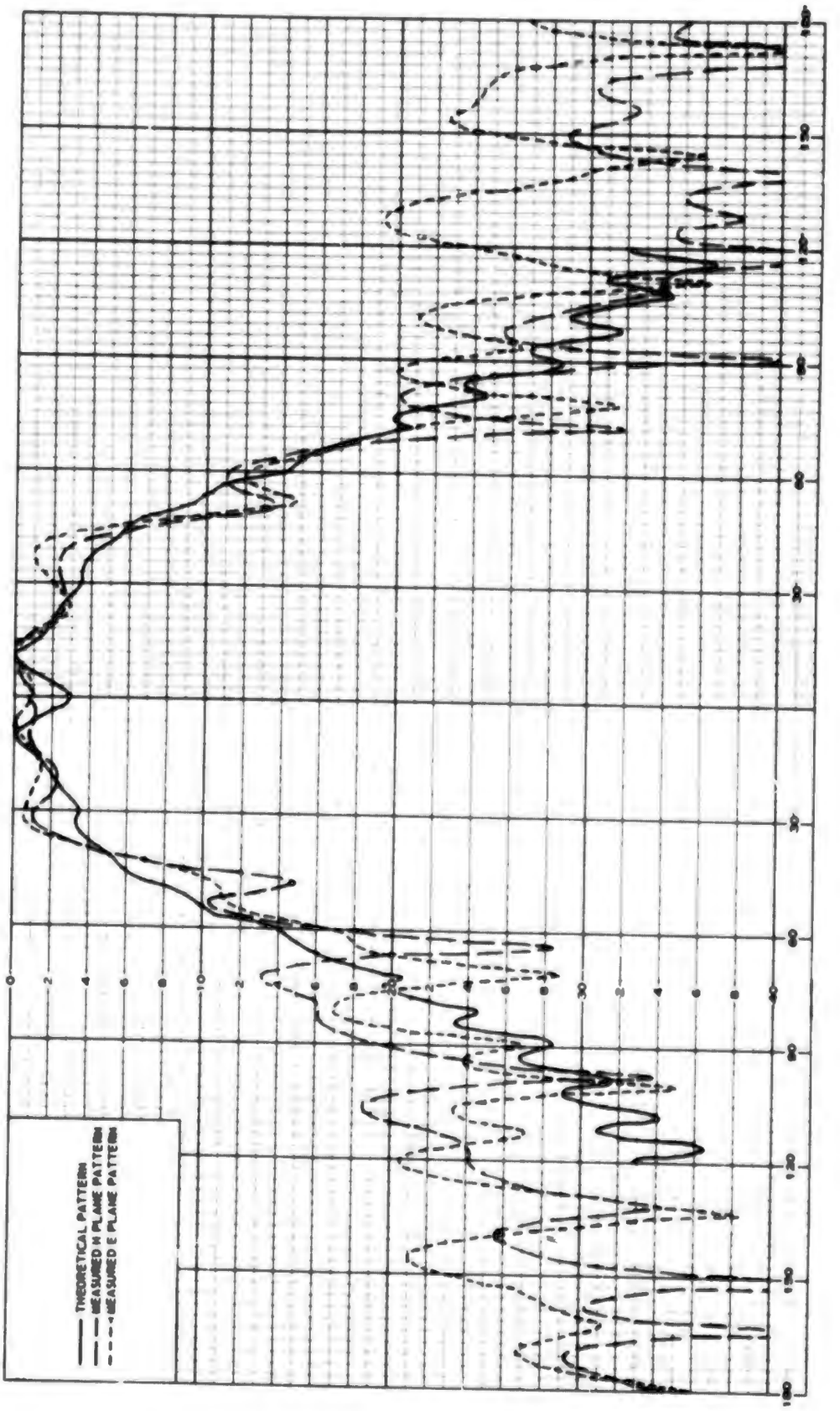

Figure 58. Patterns of Horn-Fed 4-Foot Diameter Paraboloidal Reflector at 9835 mc ($D^2/16\lambda = 10$)

Specifically, at ranges in the Fresnel Region where the separation between the signal source and the test antenna is very small, reflections from the tower structure supporting the signal source may cause some of the lobing in the patterns. In addition the reflector tolerances, feed defocus, and aperture blocking by the feed may have a significant effect on the lower level sidelobes.

9. ANTENNA COUPLING IN THE FRESNEL REGION

The on-axis power transfer between rectangular apertures in the Fresnel region has been treated by Jacobs[21]; therefore, the effort in this area has been directed toward developing an expression to describe the power transfer or coupling between circular apertures.

The use of a Fresnel region gain expression (such as the one derived by Hu[22]) can be incorporated in the Friis transmission formula to calculate the power transfer between two antennas when the ratio of their aperture areas is sufficiently large that one of the antennas appears as a point source. An example of an application would be where a probe is used in measurements of the field on axis near a large aperture antenna.

$$\frac{P_r}{P_t} = \frac{G_p\, G_{fr}\, \lambda^2}{(4\pi R)^2}$$

where

P_r = the power received

P_t = the power transmitted

G_p = the far field gain of the probe

G_{fr} = the Fresnel region gain of the large aperture as defined by [22]

λ = the wavelength

R = the separation distance

Unfortunately as the apertures approach the same size this expression rapidly becomes invalid in the Fresnel region. The introduction of an additional Fresnel region gain expression for the second aperture will not increase the validity of the Friis transmission formula because the concept

---

21. E. Jacobs, 15 Sept. 1960, Final Rept. AF 30-602-1785 University of Pennsylvania. "Maximum Power Transfer Between Large Aperture Antennas in the Fresnel Region."

22. M.K. Hu, IRE Natl. Conv. "Near Zone Power Transmission Formular," Record Part 8, pp 128-135, March 1958.

of gain has meaning only when the field of one antenna is essentially a uniform plane wave over the second antenna. This condition is not approximated in the Fresnel region unless one antenna is much smaller than the other.

Hu[22] has developed a quite general formula for power transmission between two antennas. However, evaluation of the coupling under these general conditions without simplifying approximations is difficult. This formula simplifies considerably when the following assumptions can be made

a. Both antennas are matched lossless planar aperture type antennas with linearly polarized uniform phase wavefronts in the aperture.

b. The Fresnel approximation holds for r, the distance between arbitrary points on each aperture.

c. Multiple reflection can be neglected.

Under these restrictions the following Fresnel region coupling formula holds. Where the field of the transmitting aperture weighted by the aperture illumination of the receiving aperture is integrated over the receiving aperture

$$\frac{P_r}{P_t} = \frac{\left| \frac{jk}{4\pi} \int_{A_1} \int_{A_2} F_1 F_2 \frac{e^{-j\,kr}}{r} \left(1 - \frac{R}{r} \cos\theta \right) dA_1\, dA_2 \right|^2}{\left\{ \int_{A_1} |F_1|^2\, dA_1 \right\} \left\{ \int_{A_2} |F_2|^2\, dA_2 \right\}} \qquad (70)$$

where F_1 and F_2 represent the illuminations of A_1 and A_2 respectively and R and r are shown in figure 59. This power transfer formula may be reduced to a form amenable to specific calculations in the Fresnel region by assuming the usual small angle Fresnel approximations

$$\frac{1}{r} \left(1 + \frac{R}{r} \cos\theta \right) \simeq \frac{2}{R}$$

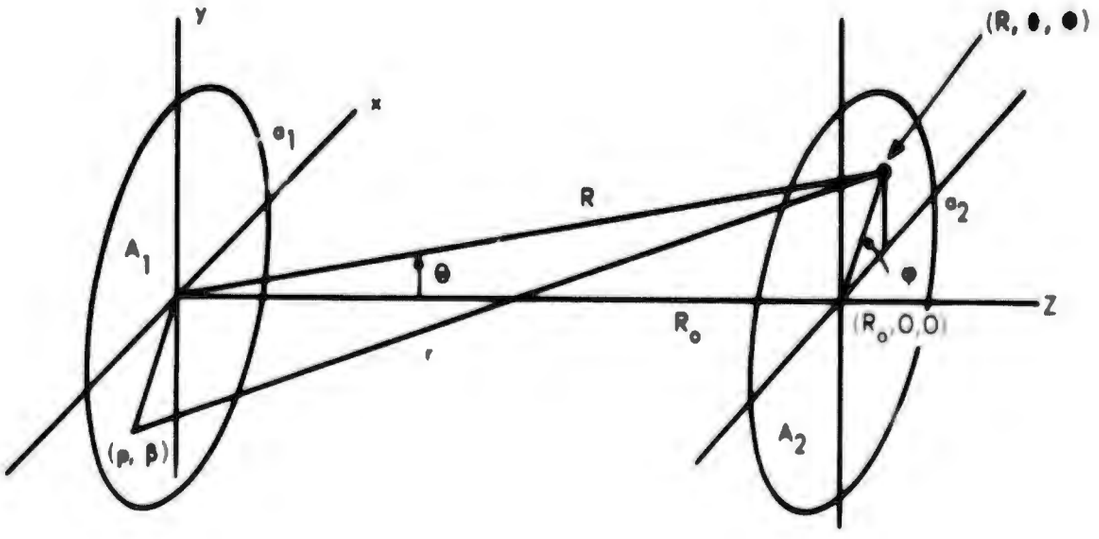

Figure 59. Coordinate for Transmitting and Receiving Antennas

and

$$r \simeq R - \rho \sin\theta \cos(\theta - \beta) + \frac{\rho^2}{2R} \tag{70}$$

in this case E_1, the Fresnel region field radiated by A_1, is given by

$$\frac{\lambda R}{j} E_1 = \int_{A_1} F_1 e^{-jkr} \, dA_1 \tag{71}$$

Thus we may rewrite (70) as

$$\frac{P_r}{P_t} = \frac{\left| \int_{A_2} E_1 F_2 \, dA_2 \right|^2}{\left\{ \int_{A_1} |F_1|^2 \, dA_1 \right\} \left\{ \int_{A_2} |F_2|^2 \, dA_2 \right\}} \tag{72}$$

For uniformly illuminated circular apertures, one with a radius a_1 and the other with radius a_2, it was shown in Section 2.1, that we may write

$$E_1 = e^{-jkR} \, v \, e^{-j\left(\frac{u}{2} + \frac{v}{2}\right)} W_0^0(v,u)$$

where

$$u = ka_1 \sin\theta \text{ and } v = \frac{ka_1^2}{R}$$

Thus for antennas having uniform illumination $F(\rho,\beta) = 1$, Hu's power transfer formula may be rewritten as

$$\frac{P_r}{P_t} = \frac{\left| \int_{A_2} \left\{ U_1(v,u) + j\, U_2(v,u) \right\} e^{-jkR - j\frac{v}{2}} \, dA_2 \right|^2}{\pi \, a_1^2 \, a_2^2} \tag{73}$$

where $U_1(v,u)$ and $U_2(v,u)$ are Lommel functions having the form

$$U_k(v,u) = \sum_{n=0}^{\infty} (-1)^n \left(\frac{v}{u}\right)^{2n+k} J_{2n+k}(u)$$

$$= \sum_{n=0}^{\infty} (-1)^n \left(\frac{v}{2}\right)^{2n+k} \frac{\Lambda_{2n+k}(u)}{(2n+k)!} \tag{74}$$

where $\Lambda_\rho(u)$ are the Lambda functions tabulated by Jaknke and Emde this expression may be reduced to the following radial integral because of the circular symmetry of the two apertures:

$$\frac{P_r}{P_t} = 4 \frac{\left| \int_0^{a_1} e^{-j(kR + \frac{\gamma}{2})} \left\{ U_1 + jU_2 \right\} \rho d\rho \right|^2}{a_1^2 a_2^2} \qquad (75)$$

This integral may be evaluated by a numerical integration. It is evident that γ and u refer to the coordinate system of the first antenna and must therefore be calculated for various values of ρ. For these calculations, γ may be assumed to be a constant over the second aperture in the Lommel function U_n. Use of the Fresnel approximation

$$R = \sqrt{R_o^2 - \rho^2} \simeq R_o + \frac{\rho^2}{2R_o}$$

where R_o is the antenna aperture separation on axis, letting $\gamma = \frac{ka_1^2}{R}$ where $\gamma \simeq \gamma_o = \frac{ka_1^2}{R_o}$, and $\rho = a_1\zeta$ results in

$$kR + \frac{\gamma}{2} = kR_o + \frac{ka_1^2 \zeta}{2R_o} + \frac{\gamma}{2} \simeq kR_o + \frac{\gamma_o}{2}(1-\zeta^2)$$

which expresses the phase term quite simply as a function of the coordinates of the aperture ζ and the separation distance γ_o. Thus

$$\frac{P_r}{P_t} = \frac{4 \left| \int_0^1 e^{-j\frac{\gamma_o}{2}(1-\zeta^2)} \left(U_1(\gamma_o, u) + j\, U_2(\gamma_o, u) \right) u\, d\zeta \right|^2}{a_2^2} \qquad (76)$$

one may use the relationships

$$U_1(v,u) = V_1(v,u) + \sin\left(\frac{v^2+u^2}{2v}\right)$$

$$U_2(v,u) = V_0(v,u) - \cos\left(\frac{v^2+u^2}{2v}\right) \qquad (77)$$

to conveniently calculate the Lommel functions U_n, where

$$V_n(v,u) = (-1)^n \sum_{k=0}^{\infty} (-1)^k \left(\frac{u}{v}\right)^{2k+n} J_{2k+n}(U) \qquad (78)$$

is a Lommel function of second kind. These are more convenient than the original expressions for the U_n (v, u) functions since u is rather small ($u \leq 12$) even at the closest distances considered and therefore the series (74) is slowly convergent.

The above formulae were used to calculate the integrand, graphs were drawn and a planimeter was used to perform the integration. By this method several sets of curves were obtained showing the coupling between two antennas in the Fresnel region for various distances. These curves are plotted in figure 60 using a generalised abscissa $(\pi\frac{D^2}{v})$ so that the curves may be used to estimate the coupling between apertures of arbitrary diameter D.

One interesting result was obtained by comparing the results of these Fresnel calculations with the far-field Friis transmission formula as shown in figure 61. Whereas no correlation is expected in the Fresnel region, since Friis formula assumes point source antennas, it should be noted that even at $2D^2/\lambda$ there is a slight error in the Friis formula. For example, it was found that for a uniformly illuminated aperture the Fresnel formula gave a result 0.45 db above the Friis formula. Braun[18] has shown that a similar result applies to electromagnetic horns and that there may be an error

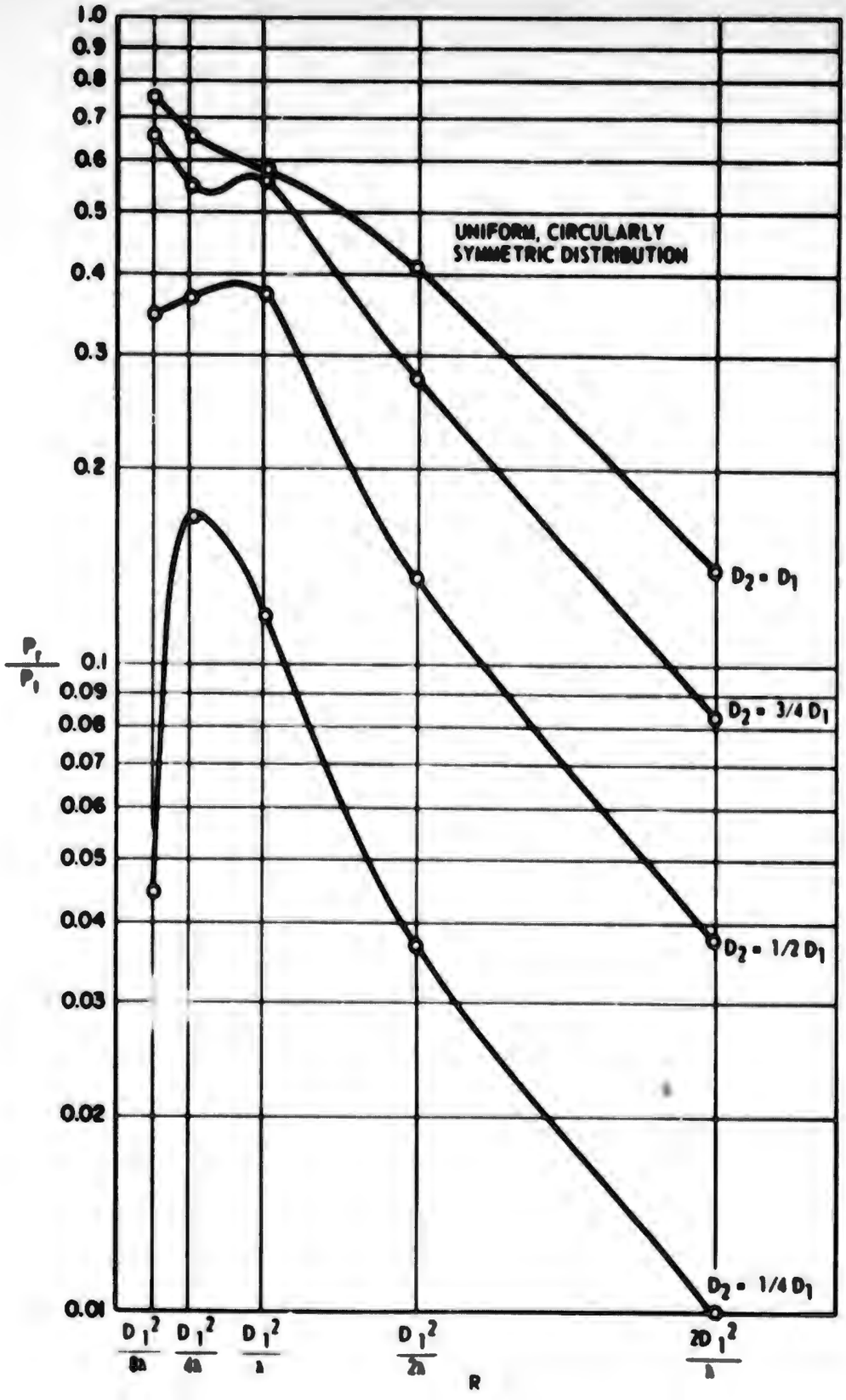

Figure 60. Aperture - Aperture Coupling as a Function of Range for Different Values of the Diameter of the Receiving Antenna

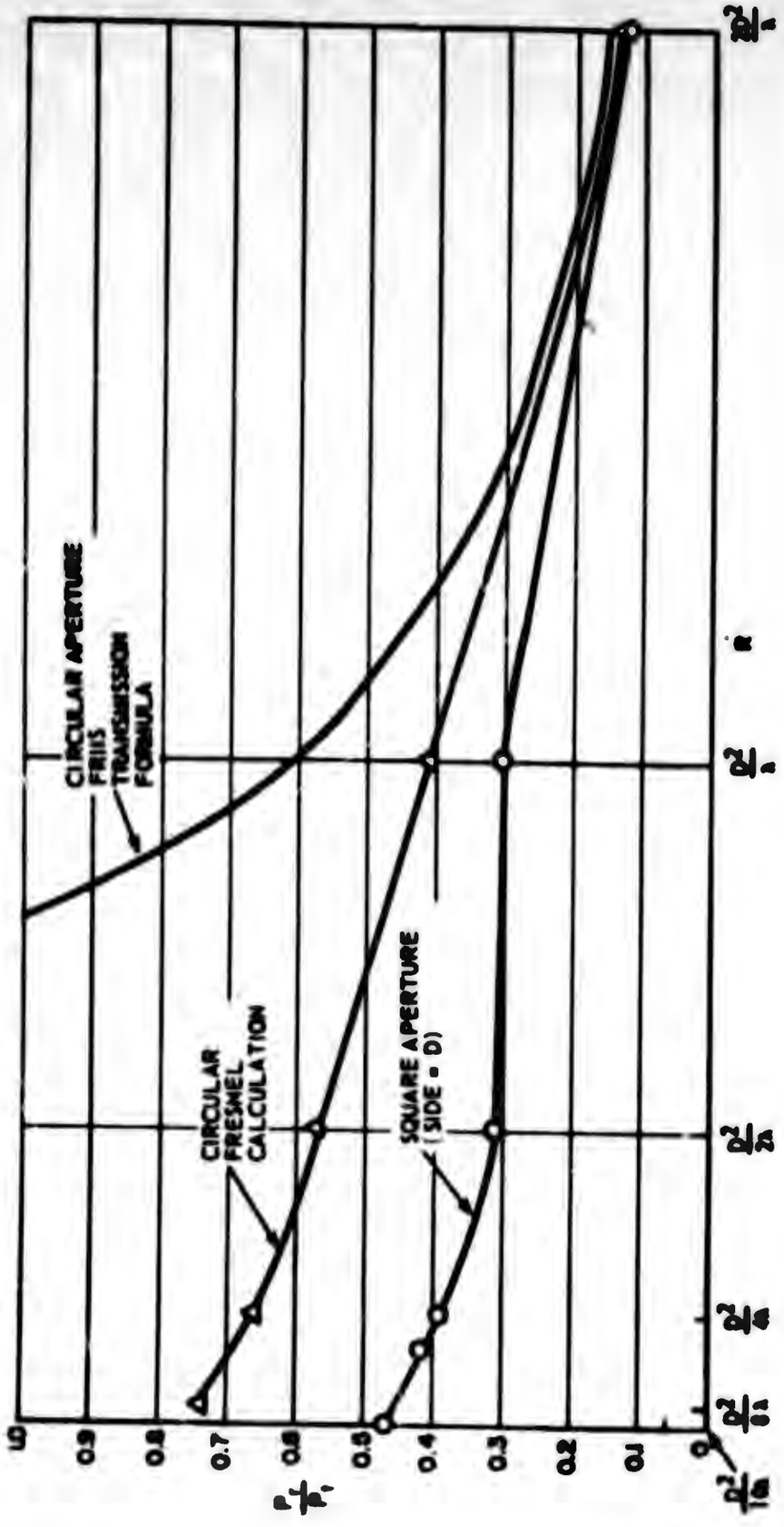

Figure 61. Comparison of Pr/Pt in Fresnel Zone for Circular and Rectangular Apertures with Pr/Pt by Friis Transmission Formula for Equal Size Apertures

of the order of 1 db in measuring the gain of a horn at a distance of $2D^2/\lambda$. A set of correction curves were prepared by Braun to indicate the magnitude of the error, and to enable the addition of a correction factor to obtain the true gain of the horn. From the calculations which were made during this quarter, it has been shown that there is also an error in measuring the gain of a circular aperture at $2D^2/\lambda$ although it is somewhat smaller than for a horn of similar size (only 0.2 db for a uniform circular aperture). An intuitive reason for the larger deviation for coupling between apertures can be seen by observing that, at $2D^2/\lambda$, the maximum phase deviation between the two apertures is not $\pi/8$ as is the case for a single point and an aperture. It is rather $\lambda/4$ phase error between the center to center phase and the phase from the edge of one aperture to the opposite edge of the other aperture.

Figure 62 shows the coupling between two apertures with a parabolic $1-(\rho/a.)^2$ distribution. Here the field from the first antenna may be reduced to the first and second order Lommel functions since,

$$\frac{\lambda R}{j} E_1 = \int_{A_2} F_1 e^{-jkr} dA_1 = \frac{\lambda R}{j} e^{-j(kR+\frac{\gamma}{2})} \nu W_o^1(\nu,u)$$

$$= \frac{\lambda R}{j} e^{-j(kR+\frac{\gamma}{2})} \nu \frac{2}{j}\left[\frac{\partial}{\partial \nu}\left[\frac{U_1}{\nu} + j\frac{U_2}{\nu}\right]\right]$$

may be reduced by differentiation to:

$$E_1 = j e^{-j(kR+\frac{\gamma}{2})}\left\{\left[1-(\frac{u}{\nu})^2+j(\frac{2}{\nu})\right]\left[U_1 + j U_2\right] + \frac{u}{\nu} J_1(u) - j J_o(u)\right\}$$

and the previously calculated functions U_1 and U_2 may be used.

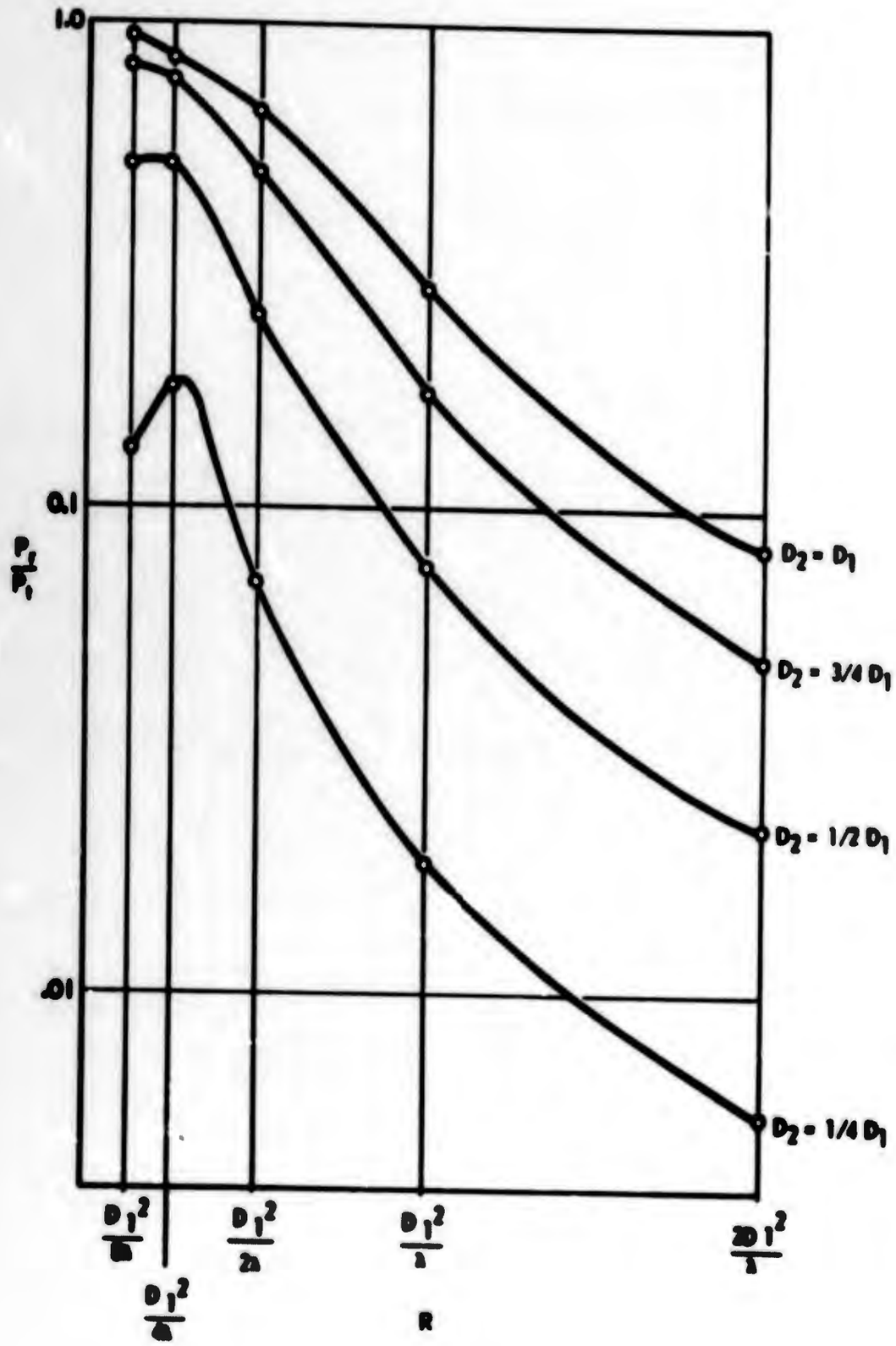

Figure 62. Aperture to Aperture Coupling as a Function of Range for Different Values of the Receiving Antenna $(1 - \zeta^2)$ Circularly Symmetric Distribution

We may then calculate the coupling between two apertures with parabolic illumination from

$$\frac{P_r}{P_t} = \frac{(2\pi)^2 \left| \int_0^{a_2} (1-\zeta^2)\, E_1(r,\theta)\, \rho\, d\rho \right|^2}{\left(\frac{\pi a_1^2}{3}\right)\left(\frac{\pi a_2^2}{3}\right)}$$

$$= \frac{36 \left| \int_0^{a_2} (1-\zeta^2)\, E_1(r,\theta)\, \rho\, d\rho \right|^2}{a_1^2\, a_2^2}$$

In figures 63 and 64 the ratio P_r/P_t is plotted as a function of the ratio a_2/a_1 for uniform and parabolic illuminations, respectively.

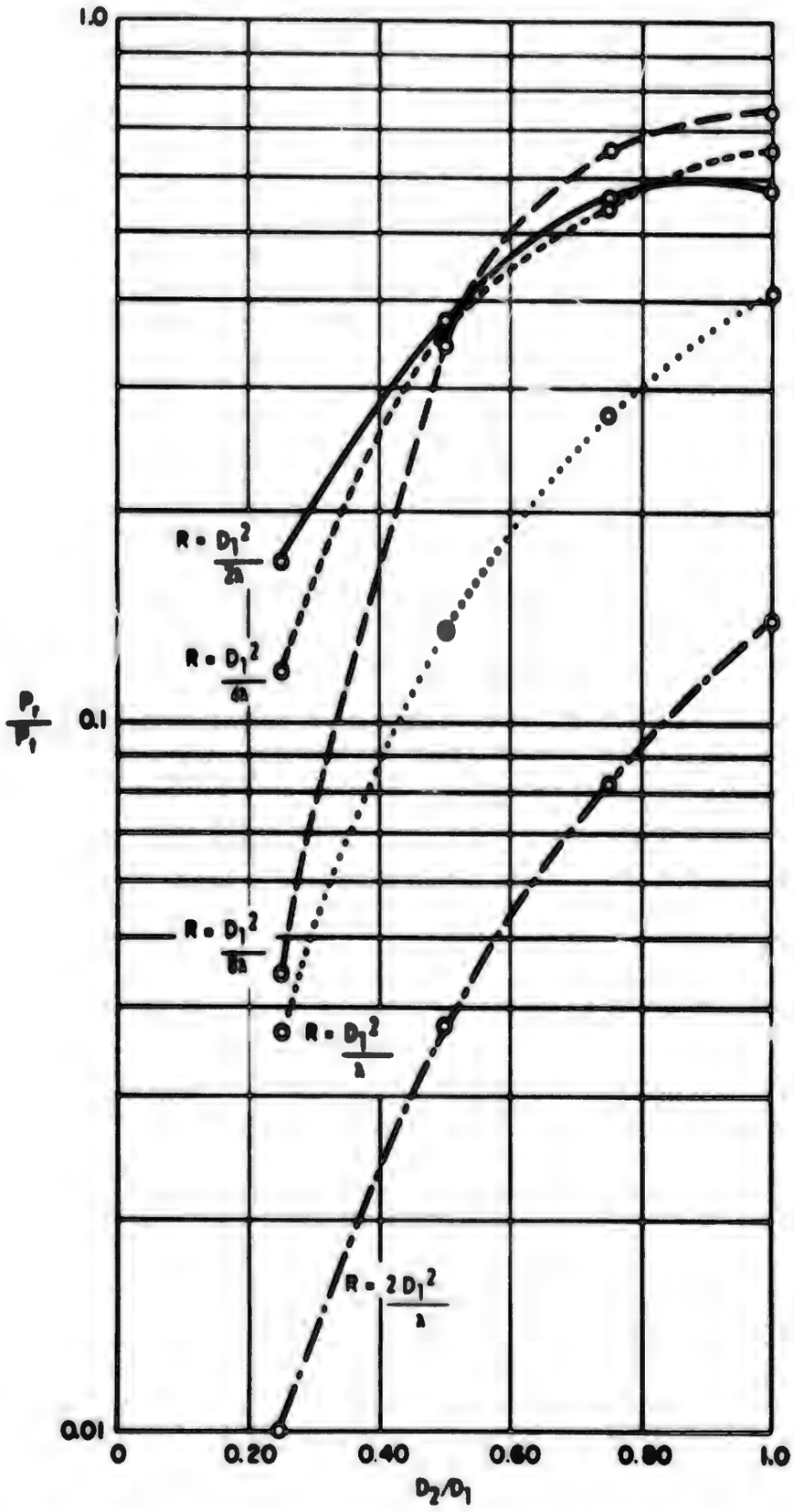

Figure 63. Aperture to Aperture Coupling as a Function of the Ratio of the Diameter of the Receiving Antenna to the Diameter of the Transmitting Antenna for Different Ranges (Uniform, Circularly Symmetric Distribution)

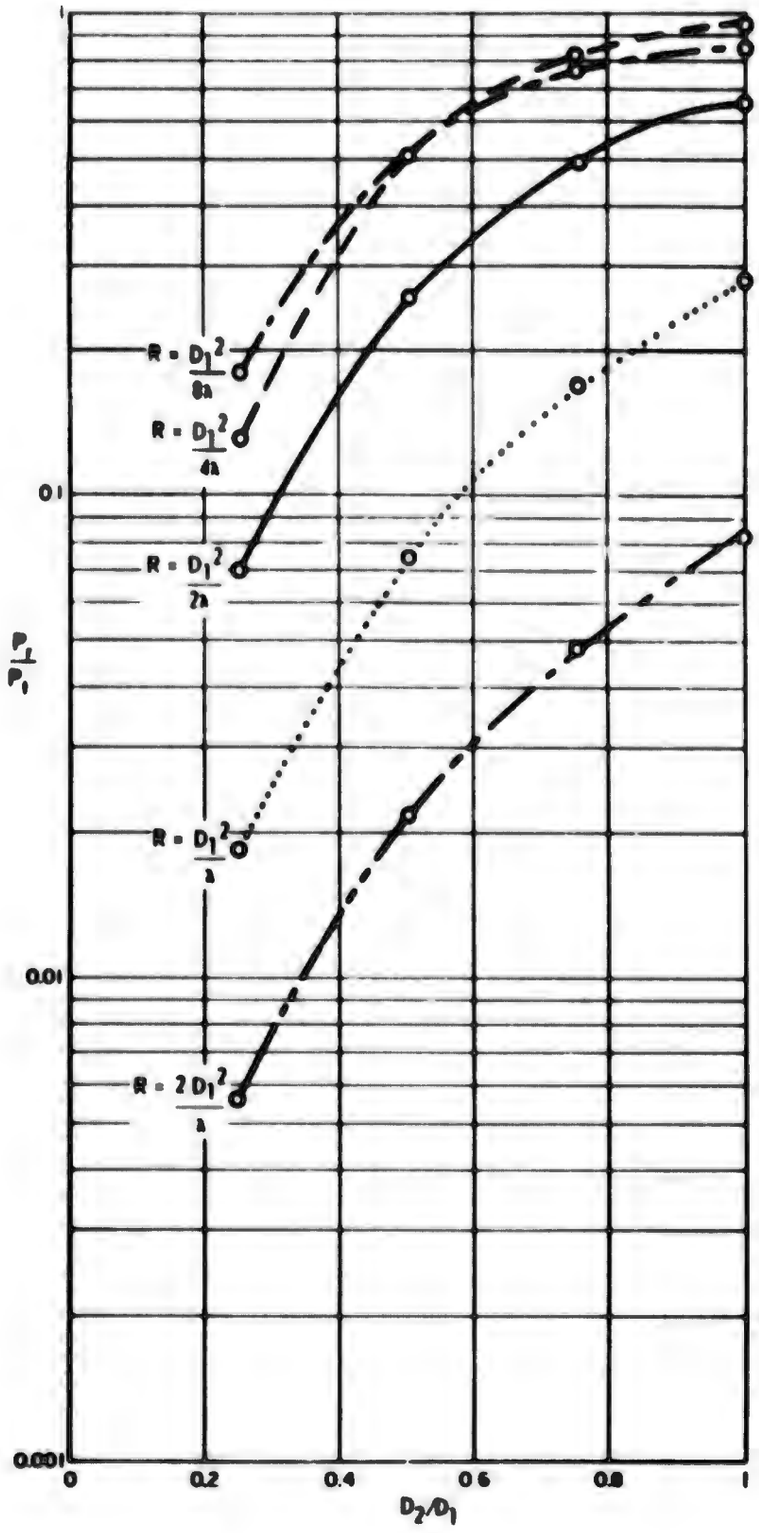

Figure 64. Aperture to Aperture Coupling as a Function of the Ratio of the Diameter of the Receiving Antenna to the Diameter of the Transmitting Antenna for Different Ranges $(1 - \zeta^2)$ Circularly Symmetric Distribution

10. DEFOCUSING TECHNIQUES

10.1 Displacement of the Feed

Several authors have discussed methods of defocusing large aperture antennas to simulate Fraunhofer-field patterns in the Fresnel zone. The technique commonly used for reflectors is to displace the primary source of the antenna slightly from the focal point in a direction away from the antenna. This has the effect of focusing the aperture at a point in the Fresnel zone. If the antenna can be perfectly focused at a point in the Fresnel zone without changing the aperture illumination then a perfect small angle far-field pattern can be obtained by measuring the field in the focal plane.[23]

It is well known that, for a point source excitation of a paraboloidal reflector, the best Fraunhofer pattern is obtained with the point source at the focus of the antenna. Thus, the paraboloid has the property that the path length from the focus to a distant point along the axis of the paraboloid results in an additive in-phase condition and a maximum gain along the axis. To focus the antenna at some intermediate point, the path length differences from the aperture plane to the field point must be minimised in order to approximate the far-field pattern. Since the amount of on-axis defocus is the only variable which is available, one cannot hope to equate the path lengths from each point of the paraboloidal reflector. One conventional technique is to equate the path length along the axis of

---

[23] J. W. Sherman, "Properties of Focused Apertures in the Fresnel Zone," IRE Transactions, Vol. AP-10, July 1962, p 403.

the paraboloid with that at the edges of the aperture. Using this technique, the amount of displacement (ε) which the primary source must be moved away from the reflector is given by $$\varepsilon = \frac{f^2}{R}\left[\frac{R}{R-f} + \left(\frac{D^2}{4f}\right)^2\right]$$

where f = is the focal length

R = is the distance from the aperture to the field point

D = is the aperture diameter

The amount of defocus increases as R decreases and when D increases.

Another technique, called the ellipsoidal reflector method, is available for calculating the required defocus. This technique uses the property that an ellipsoid focuses energy emanating from one focal point at the other focal point. Thus, one chooses one focal point of the ellipsoid as the focal point of the antenna and the other as the desired point of focus of the reflector. Then the defocus distance is chosen to give the best approximation of the elliptical surface by the parabolic surface. With this method the defocus distance is given by $\varepsilon = \frac{f^2}{R-f}$ and is somewhat less than that calculated from the geometric method for identical focal length (f) and radius (R).

To check these techniques, experimentally, patterns have been taken with a defocused 40λ parabolic reflector at distances $\frac{D^2}{2\lambda}$, $\frac{D^2}{4\lambda}$, and $\frac{D^2}{8\lambda}$. Both the above methods have been used to calculate the defocus distance (ε). The defocused sum and difference monopulse patterns were compared with the far-field patterns in figures 65 through 69. The ellipsoidal reflector method gives somewhat better results since the approximation from which this (ε) is derived is very good and its correctness is not restricted to only the edge of the reflector.

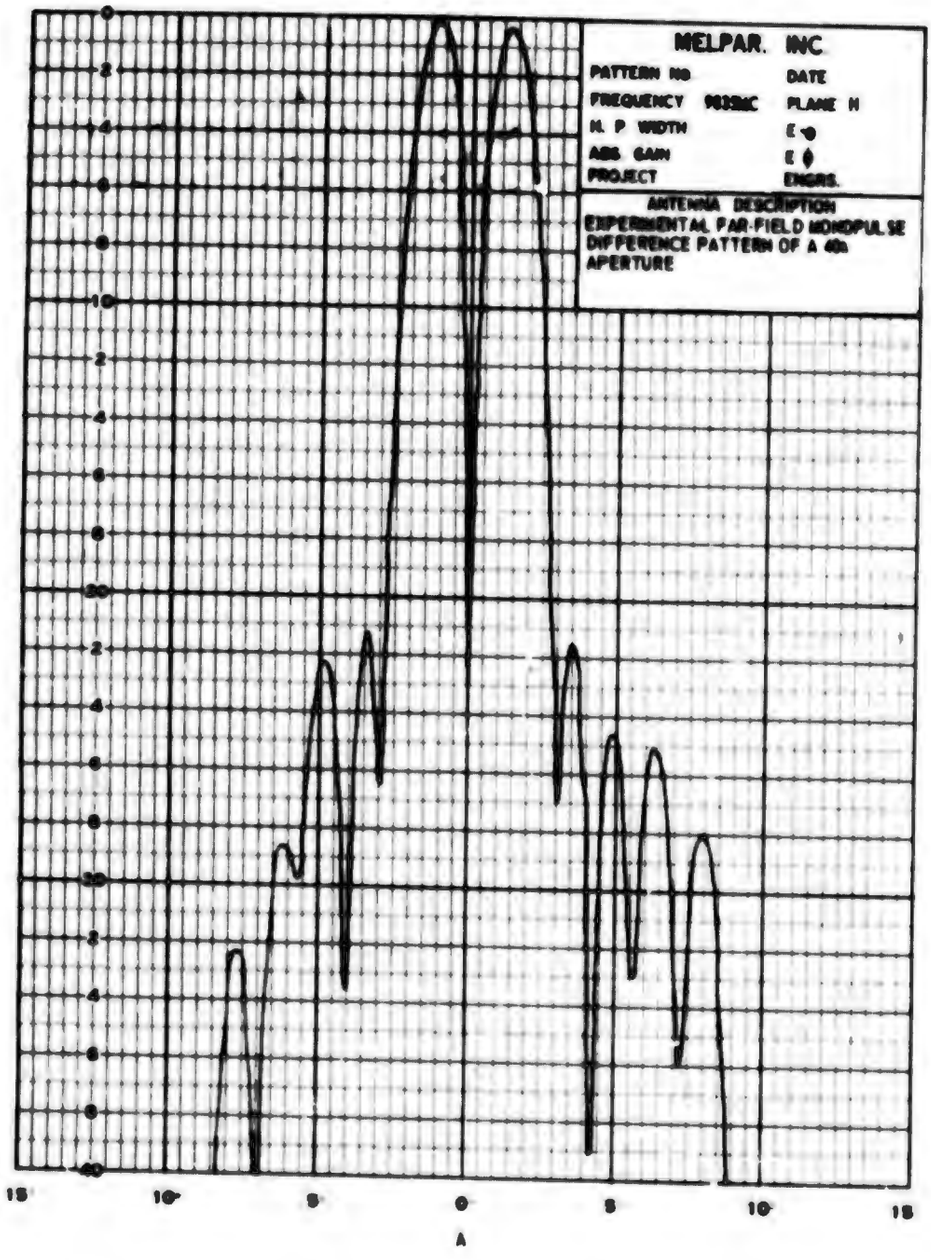
MELPAR. INC.
PATTERN NO
DATE
FREQUENCY 9035MC
PLANE H
H. P WIDTH
E θ
ABS GAIN
E φ
PROJECT
ENGRS.
ANTENNA DESCRIPTION
EXPERIMENTAL FAR-FIELD MONOPULSE DIFFERENCE PATTERN OF A 40λ APERTURE
15
10
5
0
5
10
15
A

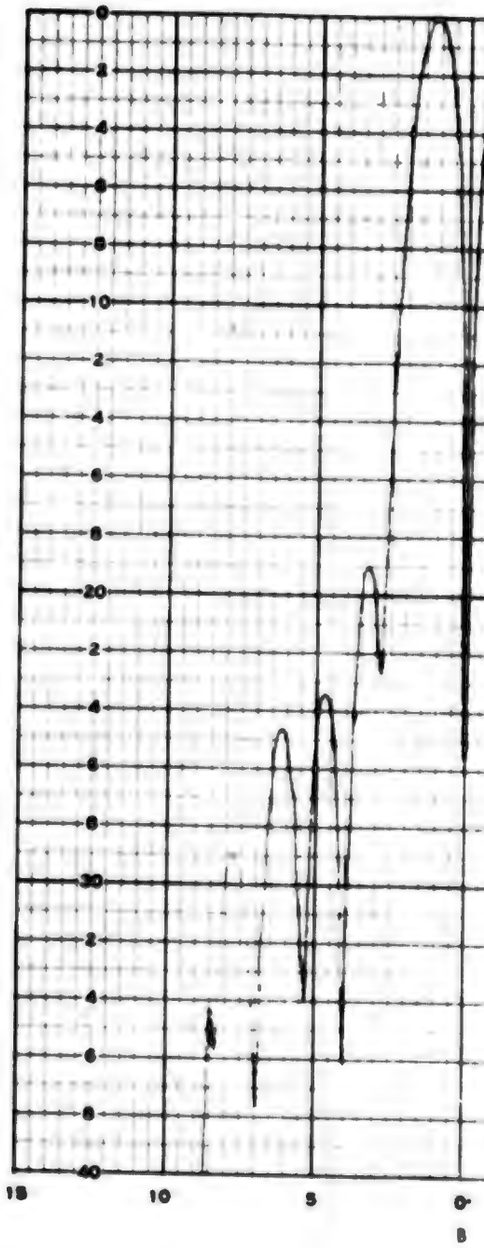
15
10
5
0
B

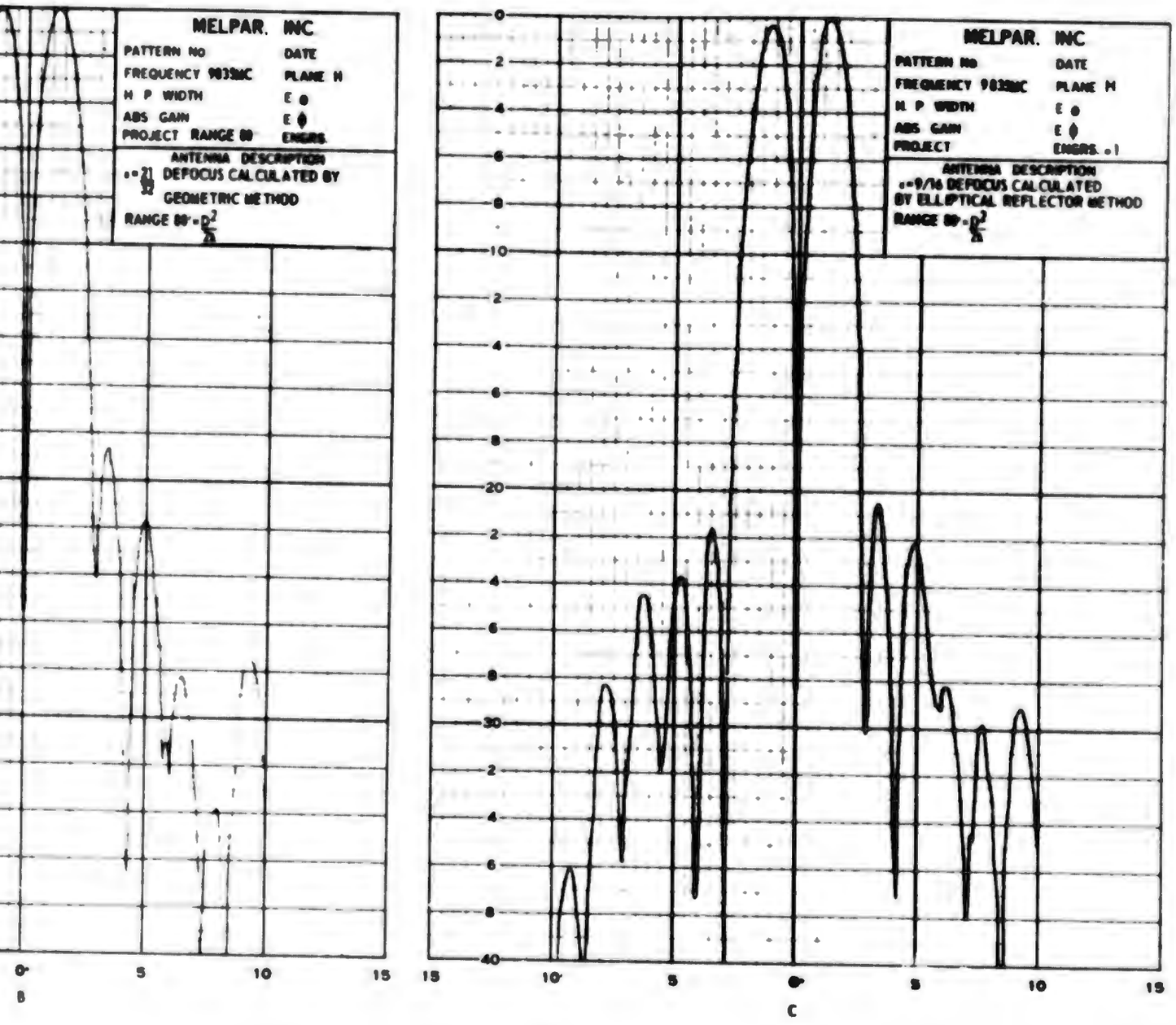

Figure 65. Comparison of Measured Far-Field and Defocused Near Field ($D^2/2\lambda$) Difference Patterns of Monopulse Antenna

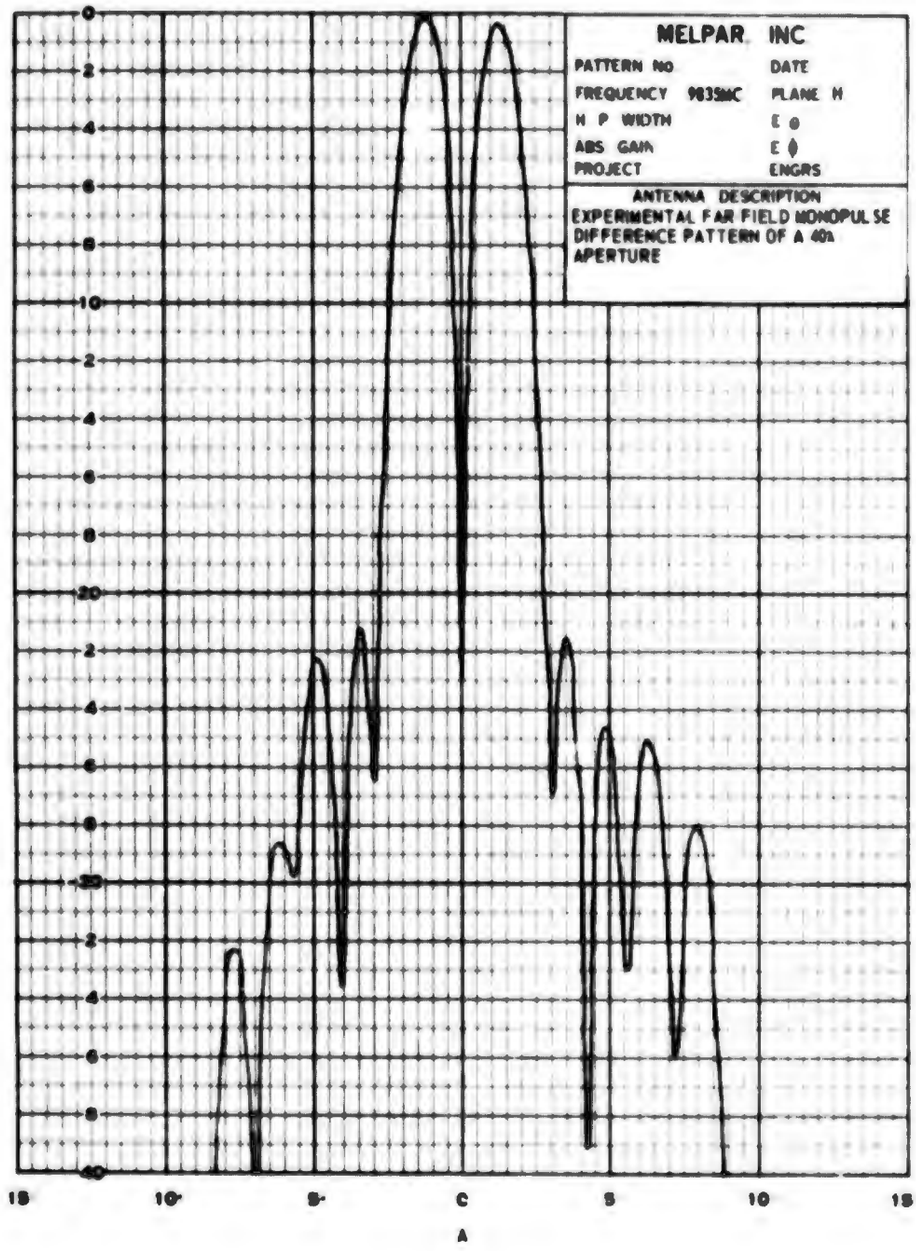
MELPAR INC
PATTERN NO
DATE
FREQUENCY 9835MC
PLANE H
H P WIDTH
E θ
ABS GAIN
E ϕ
PROJECT
ENGRS
ANTENNA DESCRIPTION
EXPERIMENTAL FAR FIELD MONOPULSE DIFFERENCE PATTERN OF A 40λ APERTURE
15
10
5
0
5
10
15
A

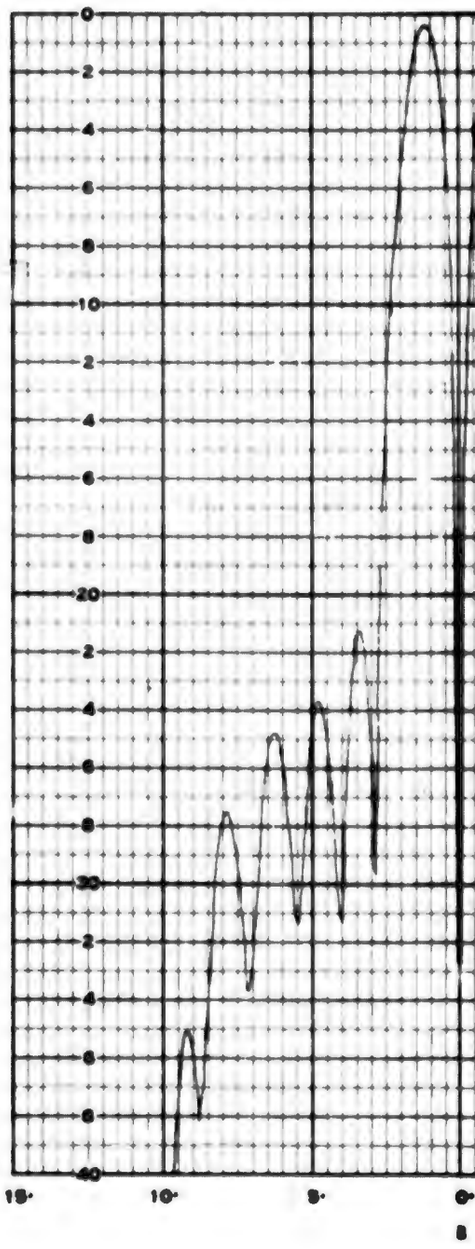
15
10
5
0
B

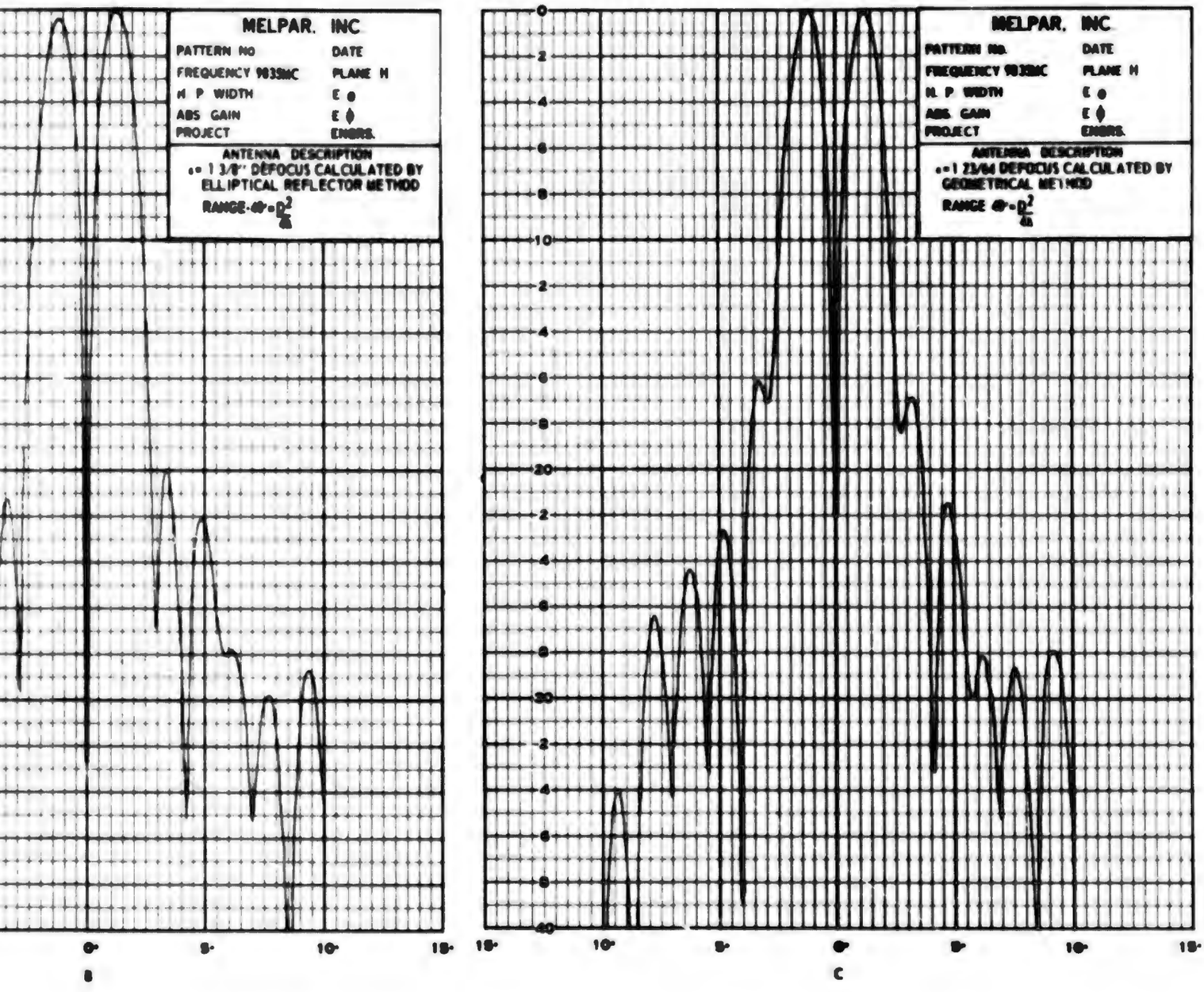

Figure 66. Comparison of Measured Far-Field and Defocused Near Field ($D^2/4\lambda$) Difference Patterns of Monopulse Antenna

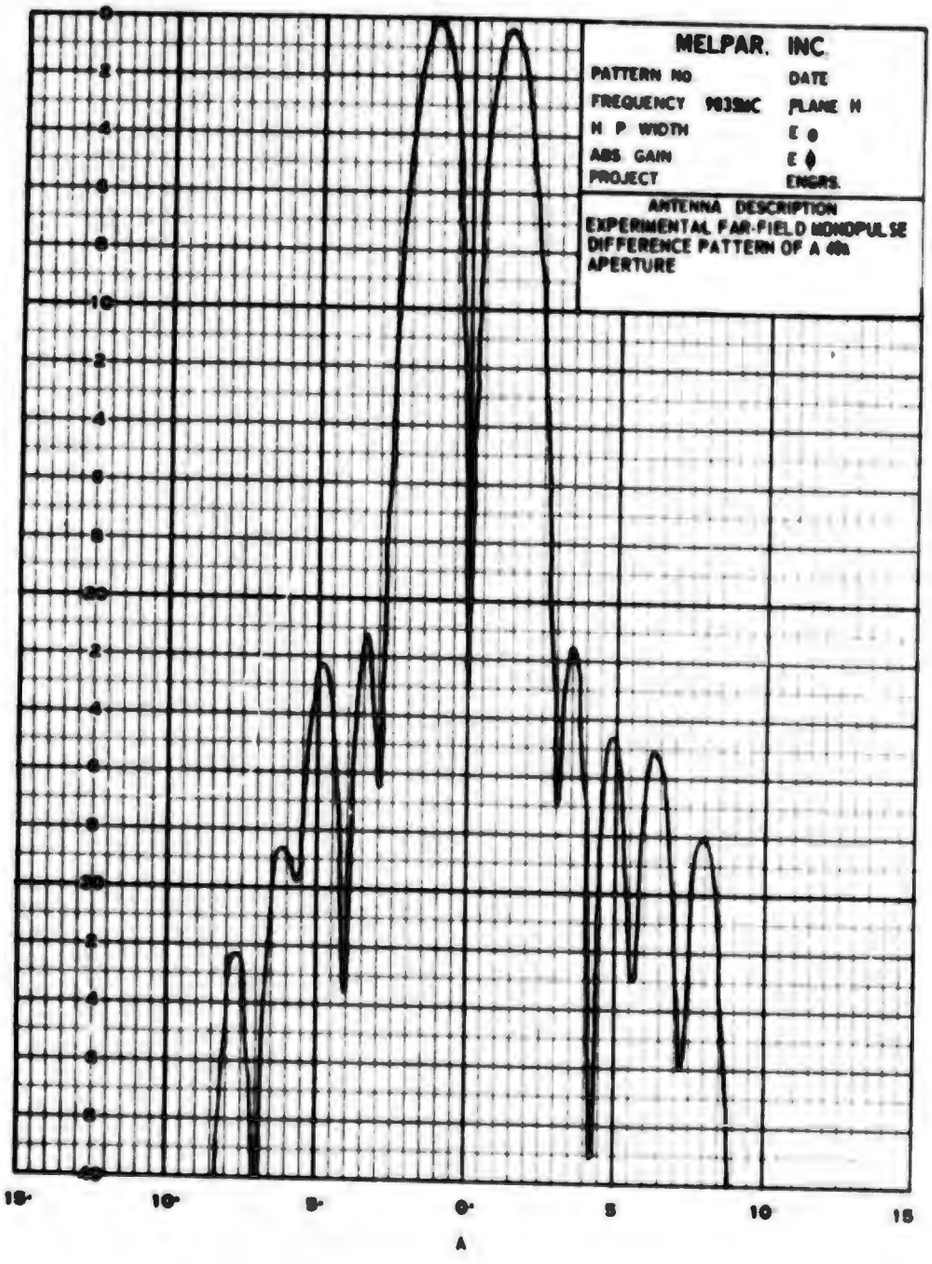
MELPAR, INC.
PATTERN NO
DATE
FREQUENCY 9039MC
PLANE H
H P WIDTH
E θ
ABS GAIN
E φ
PROJECT
ENGRS.
ANTENNA DESCRIPTION
EXPERIMENTAL FAR-FIELD MONOPULSE DIFFERENCE PATTERN OF A 40λ APERTURE
15°
10°
5°
0°
5
10
15

A

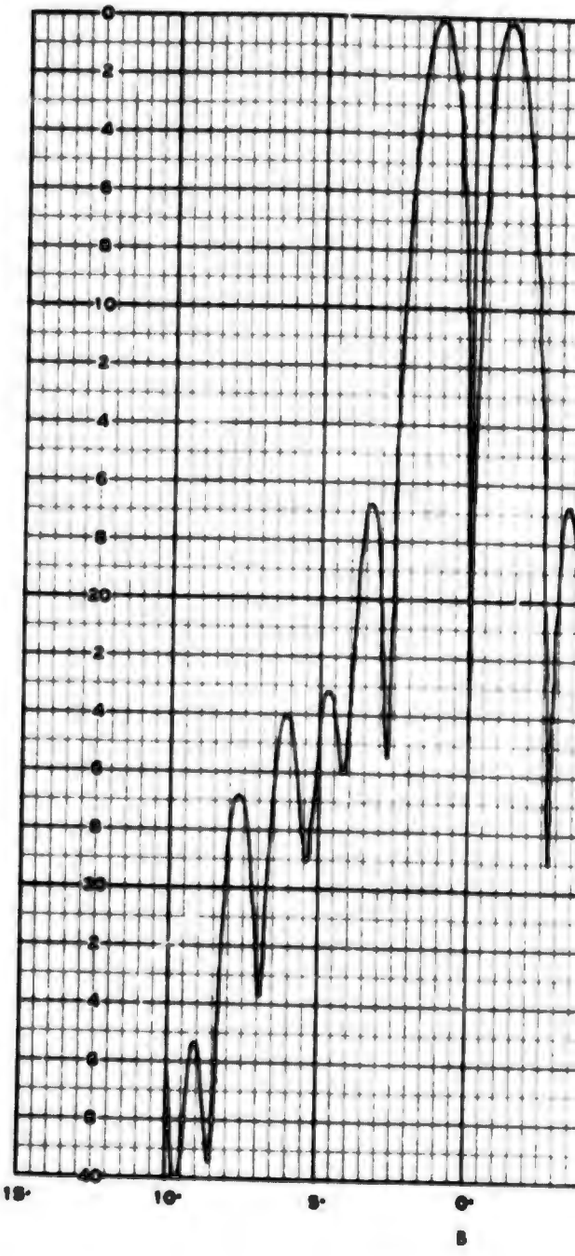
15°
10°
5°
0°

B

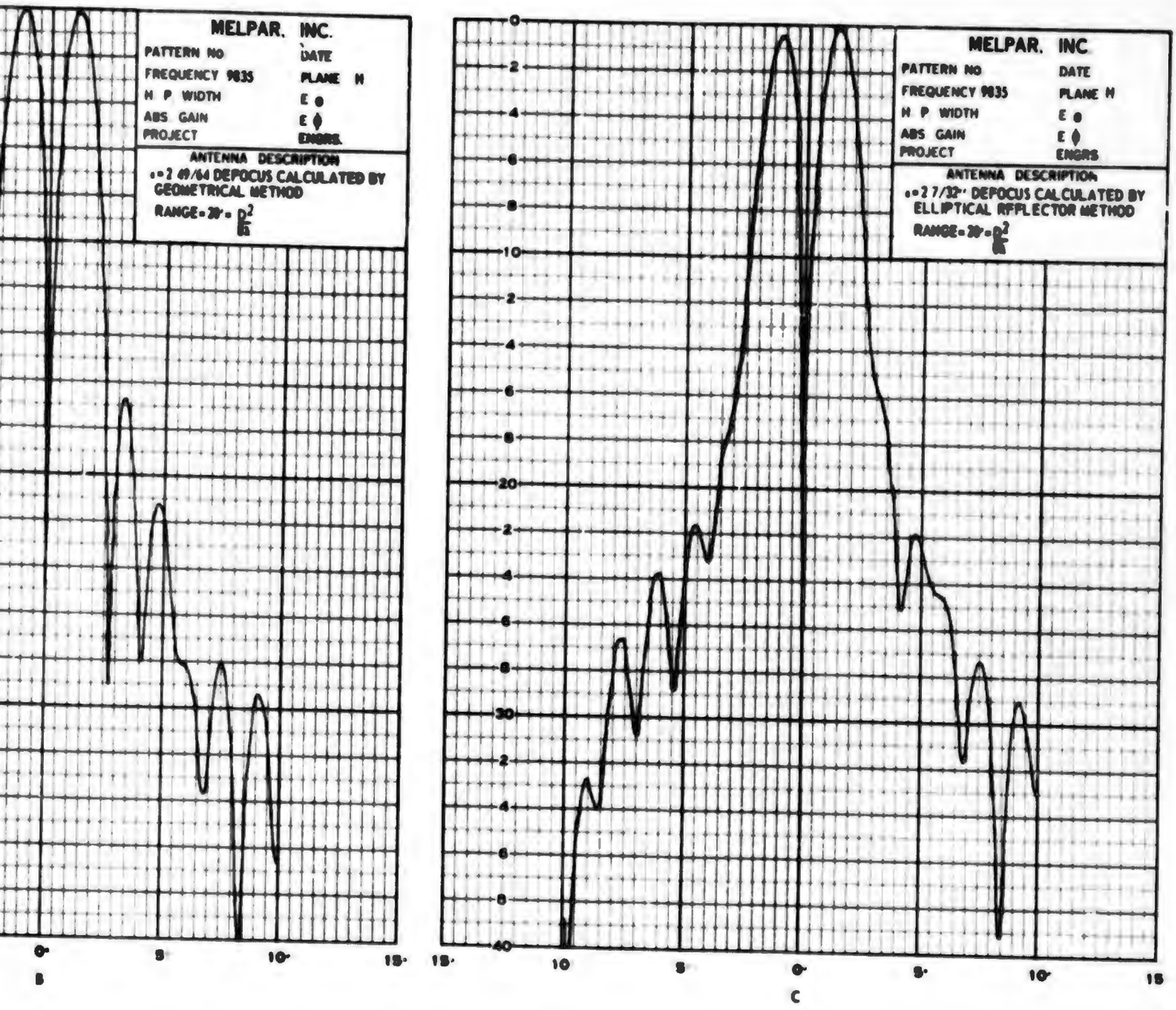

Figure 67. Comparison of Measured Far-Field and Defocused Near Field ($D^2/8\lambda$) Difference Patterns of Monopulse Antenna

BLANK PAGE

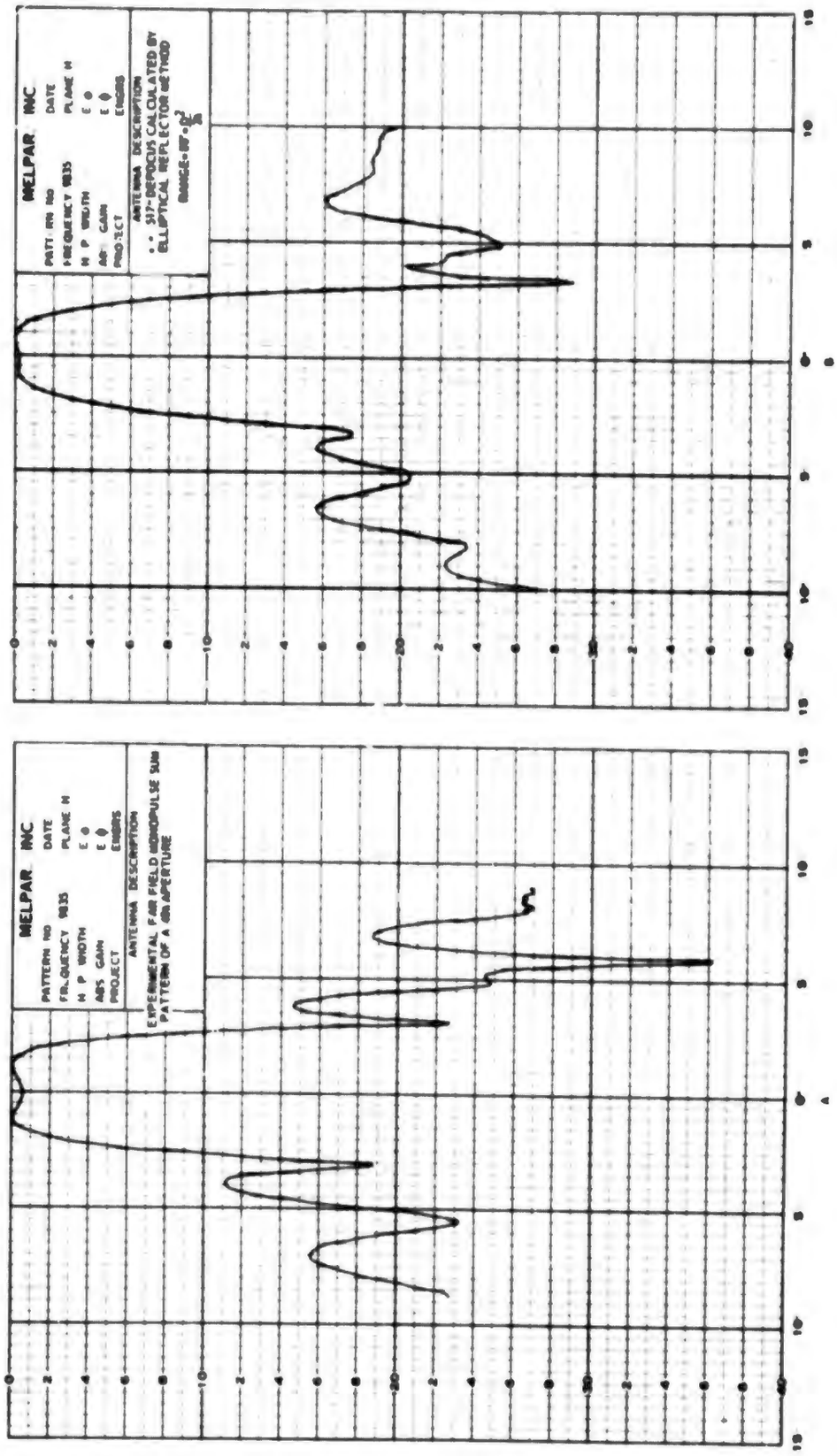

Figure 68. Comparison of Measured Far-Field and Defocused Near Field ($D^2/2\lambda$) Sum Patterns of Monopulse Antenna

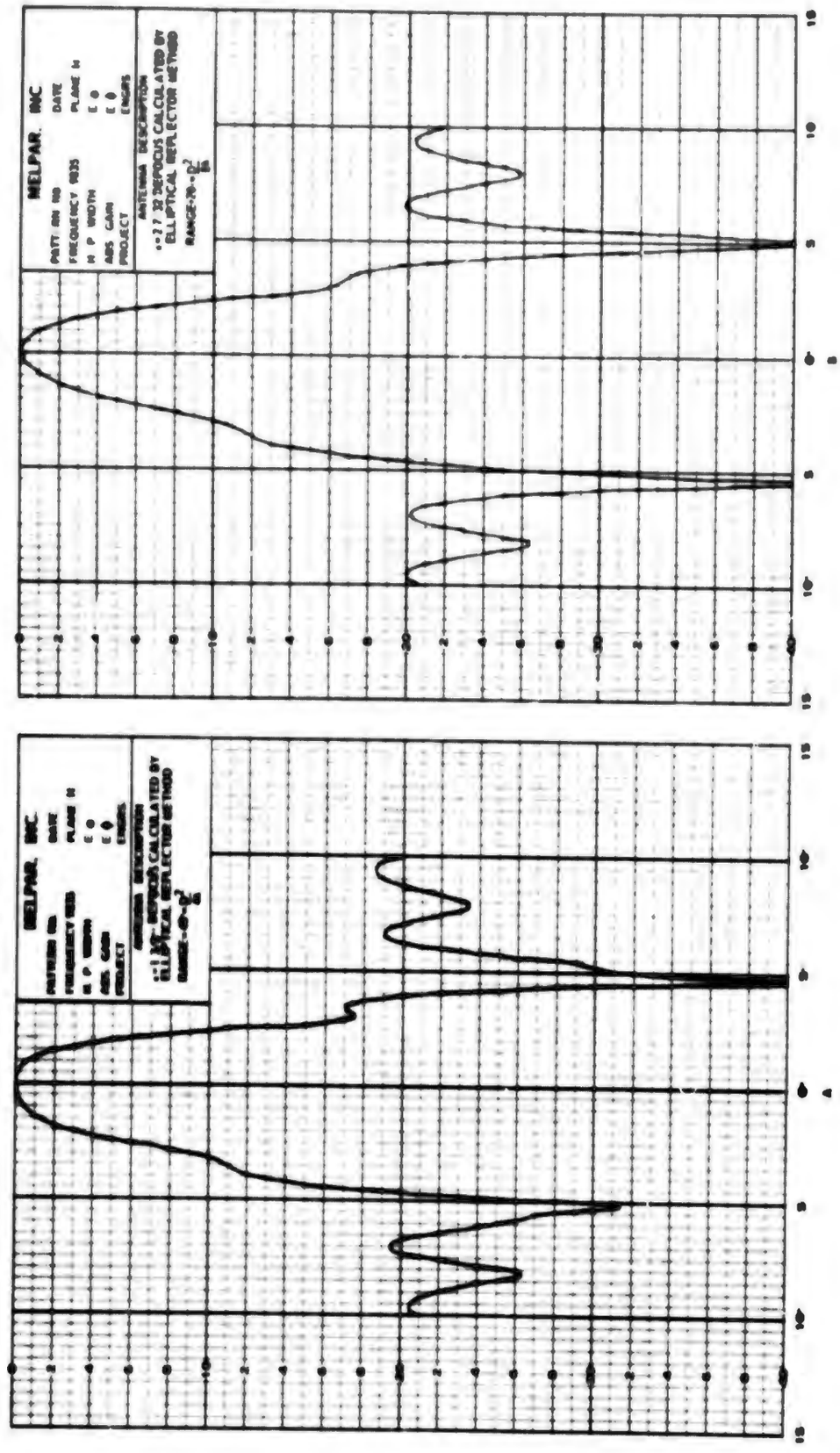

Figure 69. Comparison of Measured Defocused Near Field ($D^2/4\lambda$ and $D^2/8\lambda$) Sum Patterns of Monopulse Antenna

10.2 Lens Defocusing

The method of defocusing a reflector by laterally displacing the feed along the axis has several disadvantages. The feed must be designed so that it is movable, and several common types of antennas do not have this feature. In addition, a different amount of defocus may be needed in the two principal planes. This is true for elliptically shaped and beam-shaping reflectors. The use of a lens placed between the feed and the reflector to accomplish defocusing has neither of these disadvantages. Different profiles may be used in the two principal planes to achieve simultaneous focusing at the same point in both planes; however, some method, such as a tripod, must be devised to hold the lens in position.

The simplest lens to design is the single surface lens (see figure 70) which can be computed from the following conditions where the coordinates of the inner surface are those of a sphere about the actual focal point.

$$\overline{xx'} + n\overline{x'x''} + \overline{x''x'''} = c$$

(c = constant and n = relative dielectric constant)

This type of lens focuses a spherical wave, whose center is the desired image point, on the focal point of the feed. Thus, rays which come from a finite point converge on the focus of the parabola. For the aperture distribution to be the same in the presence and the absence of the lens, the rays should converge at the same angle. Thus a single lens will give some distortion of the pattern due to the changed aperture illumination.

This difficulty may be overcome by designing a double surface lens, so that the incident and refracted rays are parallel, (see figure 71). If

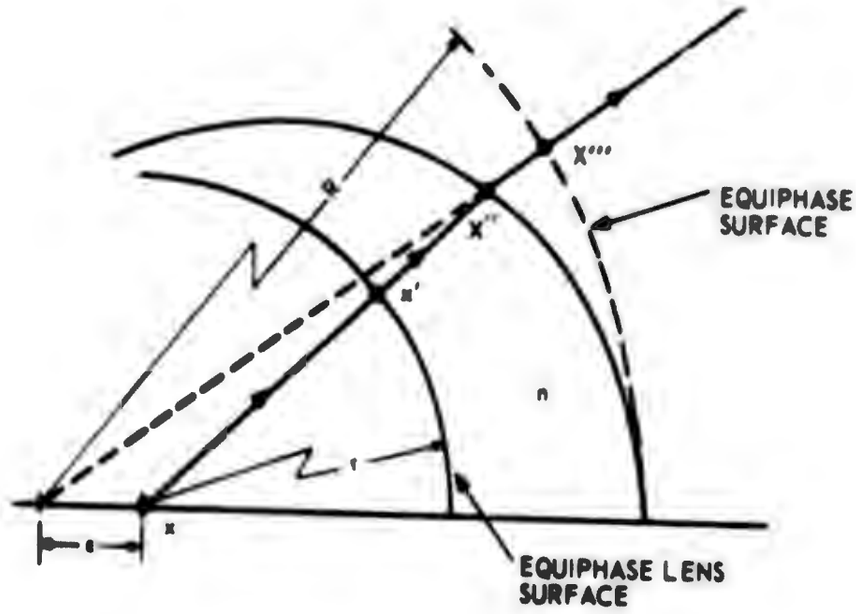

Figure 70. Single Surface Lens for Defocusing a Reflector

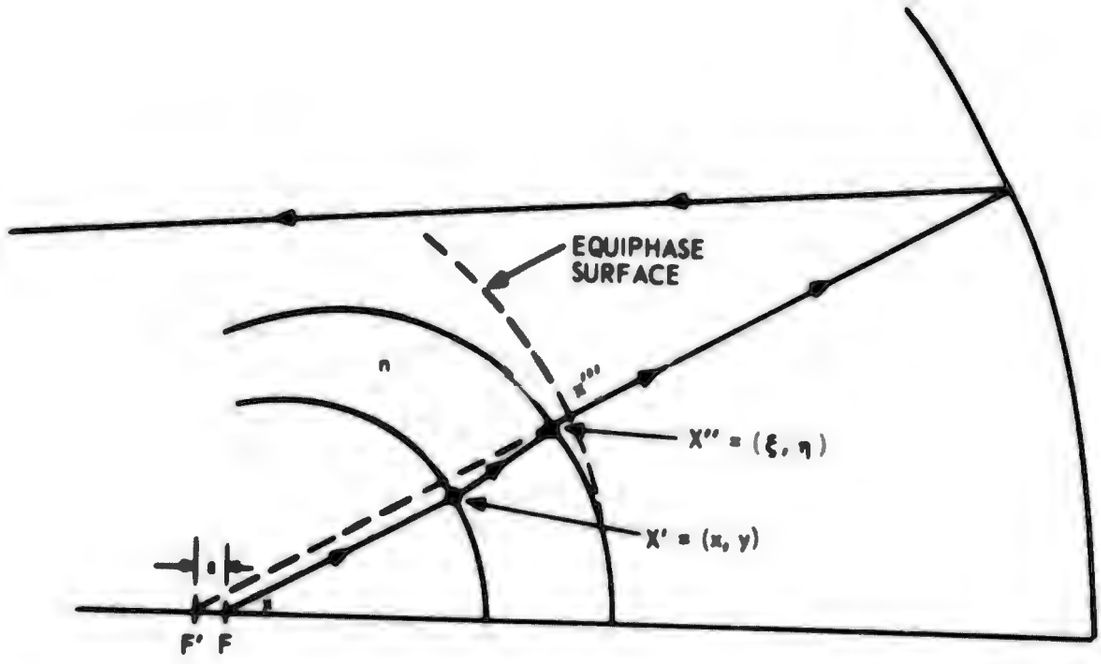

Figure 71. Double Surface Lens for Antenna Focusing

two requirements are made for the shape of the lens, both surfaces are uniquely defined by the two conditions. The desired double surface lens must satisfy the two conditions

a. $\overline{xx'} + \overline{nx'x''} + \overline{x''x'''} = c$

b. $\frac{x}{y} = \frac{\xi+\delta}{\eta}$

The first condition gives the desired displacement of the image point and the second condition gives the parallel property of the incident and refracted rays.

The lens method of defocusing has the disadvantage that to achieve focusing at distances very close to the antenna the lens must be sufficiently large that the angles of incidence do not become large enough to cause severe reflections from the lens surfaces, i.e., the lens must be larger if the antenna is to be focused closer to the aperture since a larger defocus distance (δ) is required. Thus the lens may become so large that its aperture blockage and weight are significant disadvantages.

The double surface lens, shown in figure 72, was fabricated from Plexiglass (polymethyl methacrylate). This lens was designed to focus the four-foot diameter reflector ($f/D = .4$) at a distance of sixty feet or $(3/8)\ D^2/\lambda$. The experimental measurements were performed using the monopulse feed and the measurements are shown in figures 73 and 75 for the difference and sum patterns, respectively. Although the lens defocus patterns are not in complete agreement with the far-field patterns, it can be seen that the lens has a definite focusing property by comparison of the lens pattern with the corresponding 60' Fresnel zone difference and sum patterns shown in figures 74 and 76.

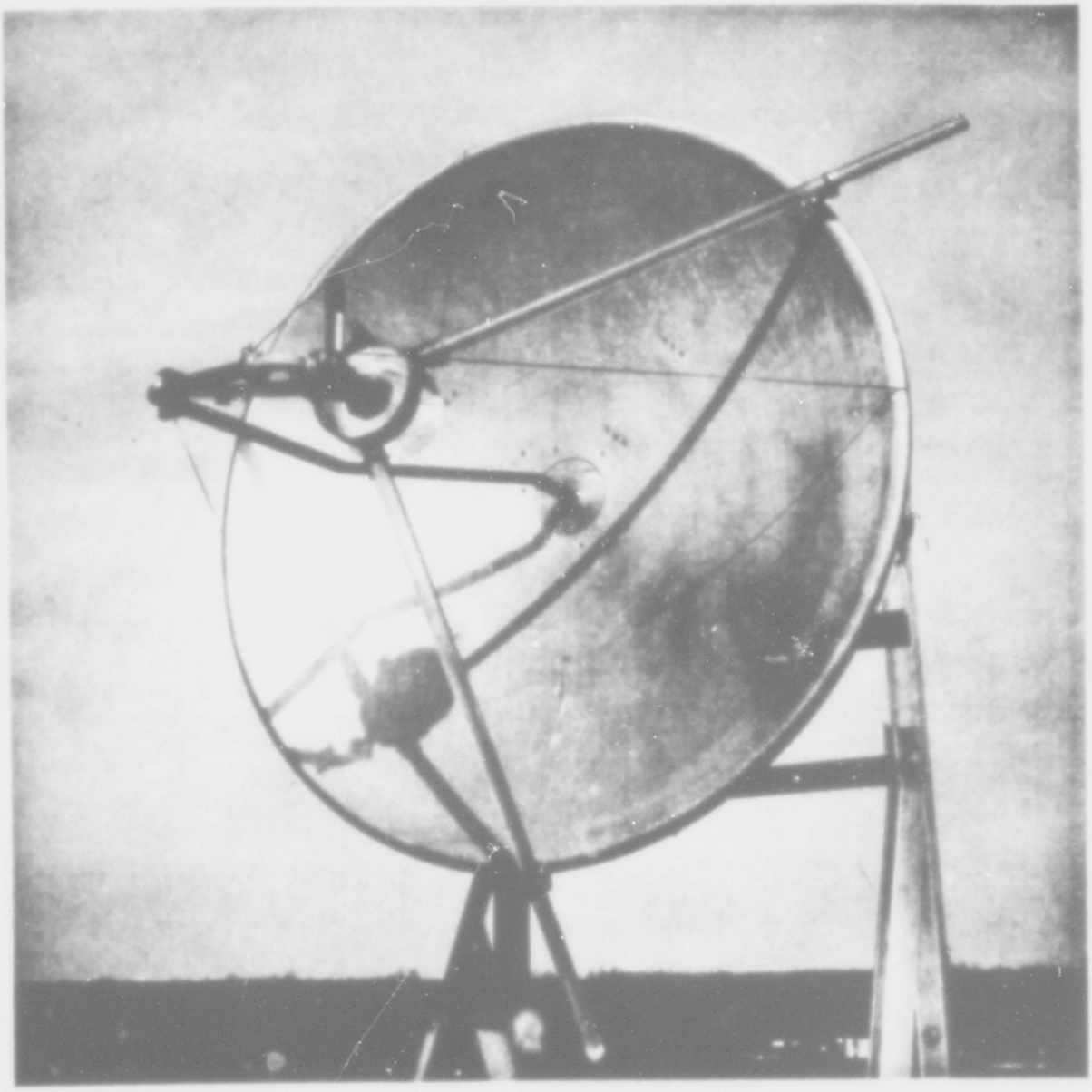

Figure 72. Monopulse Antenna with Defocusing Lens in Position

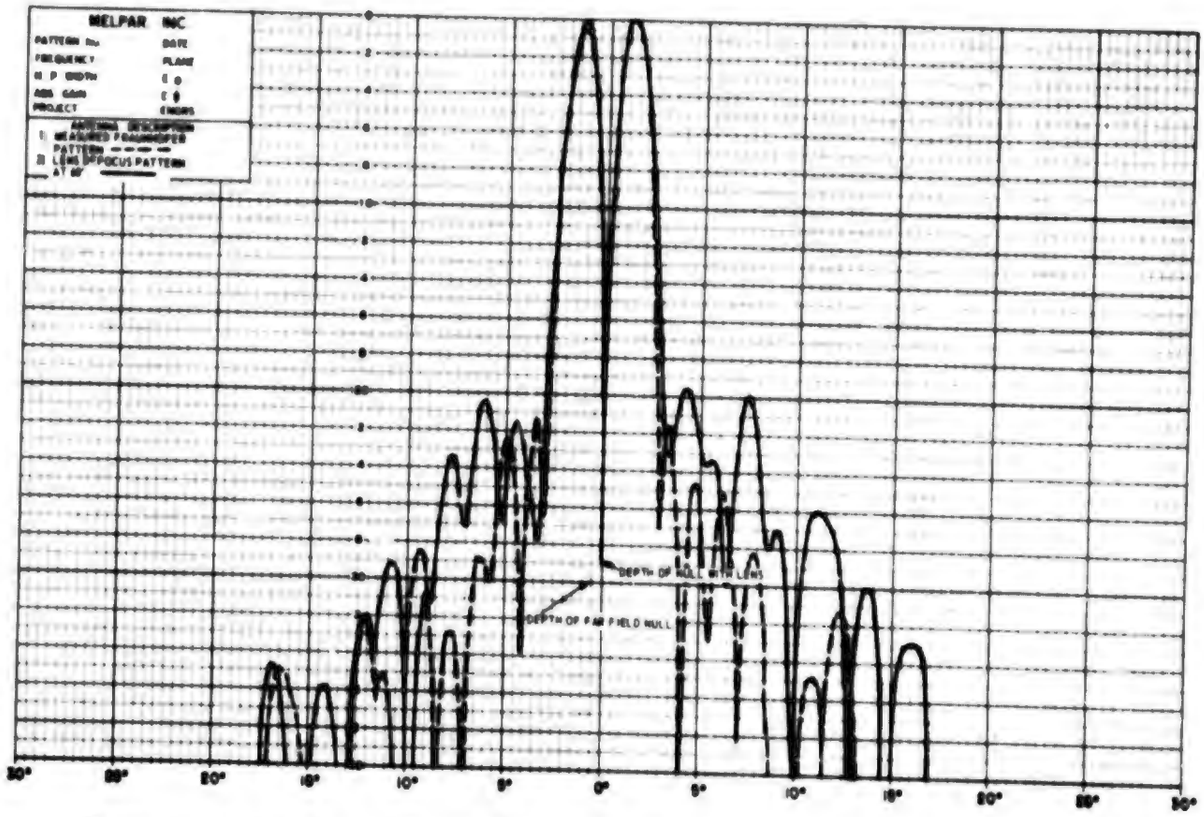

Figure 73. Comparison of Fraunhofer Difference Pattern with Lens Defocus Pattern

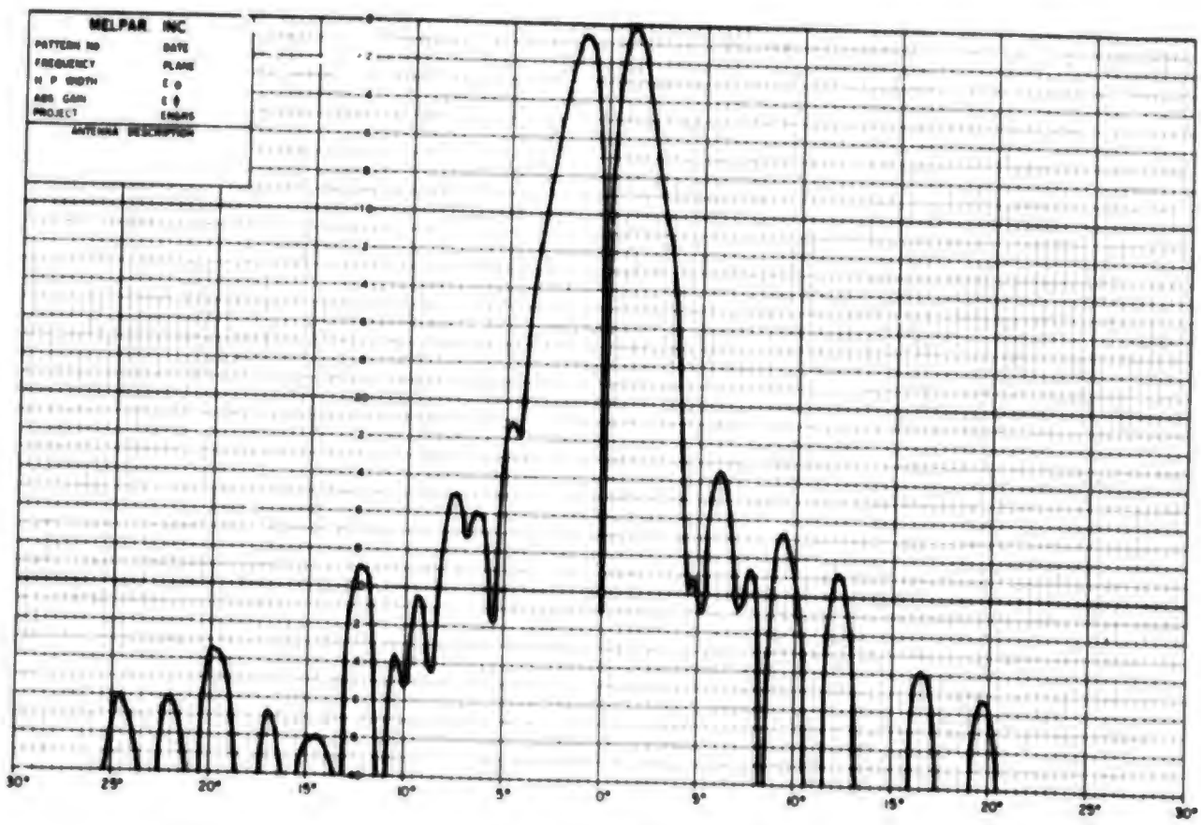

Figure 74. Measured 60-Foot Range Fresnel Zone Difference Pattern

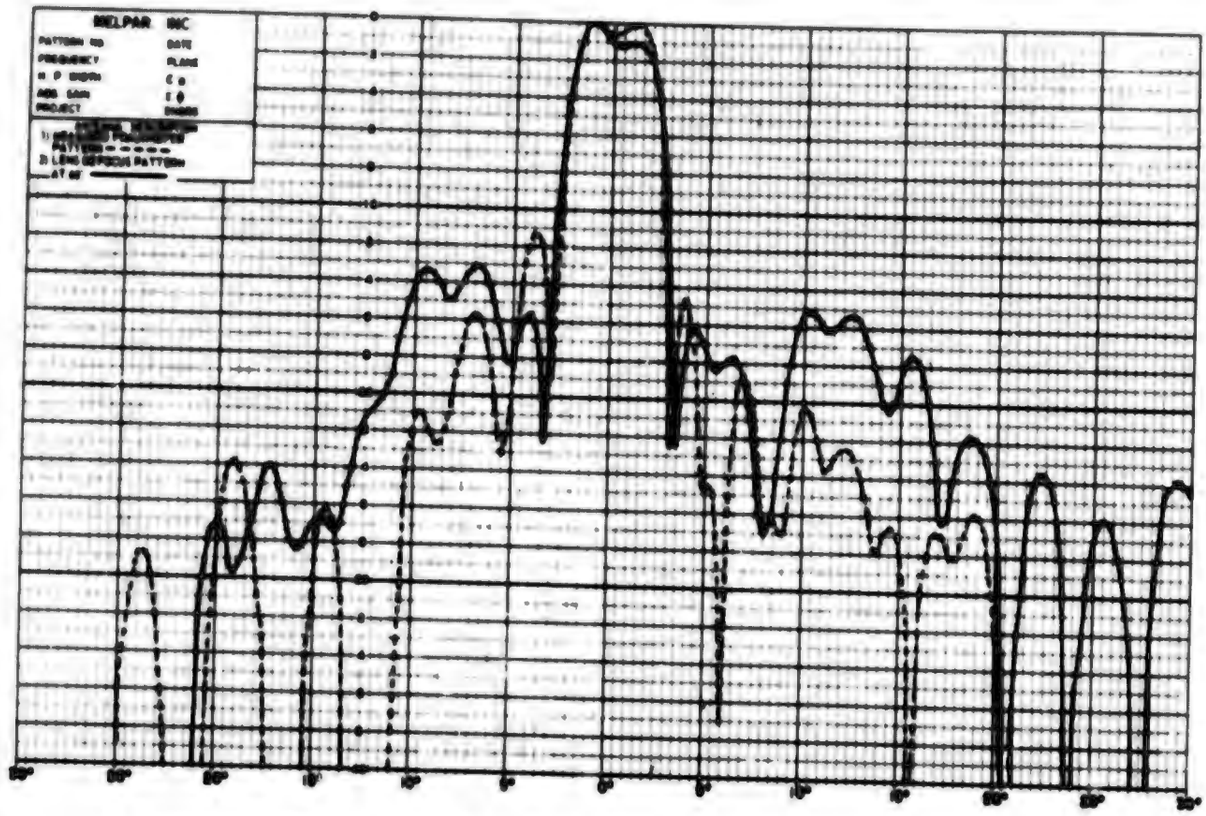

Figure 75. Comparison of Fraunhofer Sum Pattern with Lens Defocus Pattern

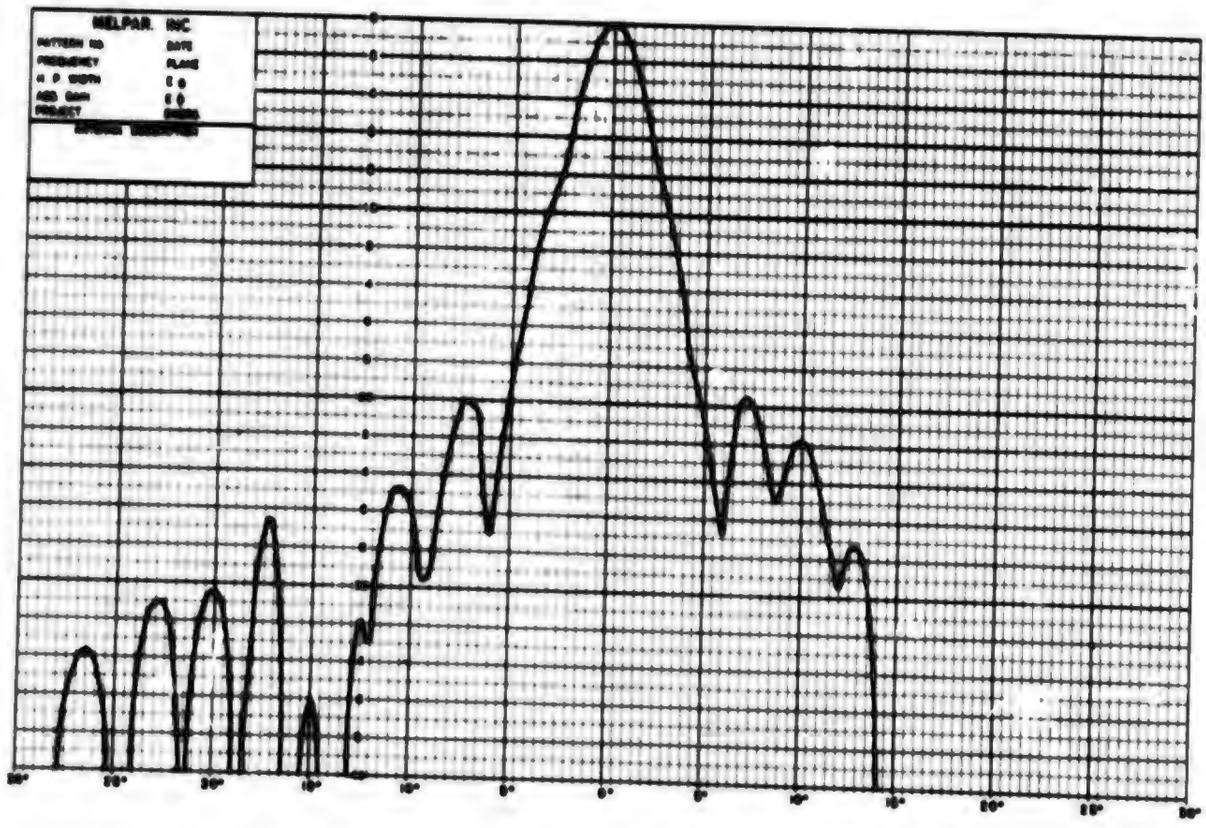

Figure 76. Measured 60-Foot Range Fresnel Zone Sum Pattern

One obvious disadvantage of the lens defocusing method is the effect of aperture blocking by the lens supports and by the lens itself. The effect of this blocking is to lower the gain and raise the sidelobe level of the focused pattern. The increase in sidelobe level for the supports used on the experimental antenna is indicated by Gray[24] to be on the order of 1.5 db for a 20-db sidelobe level, and much greater for lower sidelobe levels. Thus, it would seem that where it is possible, defocusing by longitudinal movement of the feed is a more desirable method of far-field pattern measurement in the Fresnel region.

---

[24]C. L. Gray, "Estimating the Effect of Feed Support Member Blocking on Antenna Gain and Side Lobe Level," Microwave Journal, March 1964, p. 88-91.

11. CONCLUSIONS

This report presents a description of the study and evaluation of various techniques to define interference aspects of Fresnel region phenomena for a variety of antenna types. A general statement may be made regarding the mathematical approaches for determination of the adequacy of the phenomena description, namely that the more precise the definition required, the more complex the mathematical procedures become. Mathematical rigor or exactness is also often accompanied by a more complex procedure than those methods utilizing simplification approximations. The procedures discussed in this report relate to large apertures and are generally limited to small angles on each side of the antenna axis, except for the Fresnel ring focusing technique which may be used over the complete volume if desired.

New approaches have been developed which enable desk calculations of the Fresnel zone radiation for certain types of monopulse antennas, elliptical or irregular shaped aperture antennas, and simple phased array antennas. A new technique was developed which enables determination of the far field pattern of a large aperture antenna with Fresnel region measurements. This method was subject to a great deal of theoretical analysis and appears to be a feasible method of obtaining an adequate far-field pattern of an antenna.

A preliminary analysis of a novel array or sampling model for obtaining the far-field diffraction pattern of very large antennas at ranges deep in the Fresnel zone has been presented in Section 1.2 and shown to be feasible.

The model is based on a Fresnel ring focusing technique, which focuses the quadratic phase variable in a series approximation to unity of the following general form.

$$1 \simeq \left(\frac{z}{z_o}\right)^{\alpha} \sum_{n=0}^{N} \frac{\alpha(\alpha+1)\ldots(\alpha-1+n)}{n!}\left(1-\frac{z}{z_o}\right)^{n}, \quad |z-z_o| < r_w, \quad |z_c| > |z|$$

"z" is the quadratic phase variable in the focal domain (which is defined by z_o) and "z_o" is a design parameter. When "α" is an integer, the array is spaced in harmonic multiples of "1/R". When "α" is non-integral, the spacing is anharmonic. A sample calculation for a spherical focal domain with a diameter of 200λ has been shown for the case of $\alpha = 1$. It was found that for this problem very good convergence characteristics of the focusing function, as compared to the $(2D^2/\lambda)$ criterion, are available with 7 elements. The maximum pattern range here was about $1/6(2D^2/\lambda)$ for total pattern coverage. By restricting the pattern coverage and increasing the number of elements, the pattern range for aperture antennas can be further reduced. The number of available elements is limited by the inner boundary of the Fresnel zone and the maximum usable range. The larger the antenna (i.e. the greater the number of available Fresnel rings) the greater the available number of elements, and consequently there is more flexibility in array design. By varying the parameter "α", the array weighting function (and also the array spacing) may be changed for the same focal domain. The array weighting function for the case of $\alpha = 1$ was derived with the following result.

$$C_n = \frac{(-1)^{n+1}\, N!\, e^{-ikR_n}}{(N-n)!\, n!}\left(\frac{1}{n\, z_o^{\,n}}\right), \quad n = 1 \to N, \quad |z_o| > |.$$

It was shown in the sample problem that C_n converges rapidly to negligible quantities. The maximum value of C_n, however, was 4.4 relative to the unit focusing function. For this element, an error signal is multiplied by 4.4. It was also shown that the distant elements, with the largest array weight, are the most insensitive to positioning accuracy. With uniform weight and position tolerance, the error signal on the farthest element of a 10 element array is only 1.0% to 10.% of the error signal on the nearest element. An error signal corresponding to the $2\ D^2/\lambda$ error for the sample problem on the distant element permits a position tolerance in the form δR(radial) x l_s(angular) of ($\pm$)1,144.λ x 4.23λ. The corresponding near element tolerance is approximately ($\pm$) 23.4λ x 0.60λ. Consequently, the required order of position tolerance is quite feasible. However, due to the array weight, relative to the unit focusing function, and the fact that the element signals are summed, the element error signal tolerance must be at least an order of magnitude more stringent than usual in order to obtain the usual tolerance in array output. This requirement, plus the required phase stability over a very long array (e.g. 13,000λ, which is within the state-of-the-art) are the most serious problems inherent in the system. It was shown than an (end-fire) element gain of up to 15.db is permissible for the sample problem. Due to wide element spacing, mutual interaction is negligible. It was aso shown that mutual coupling between the array and the test antenna is negligible. Other sources of error that should be considered in a rigorous evaluation with statistical error analysis are calibration errors and higher order near-field components. Although the

higher order near-field compcnents are negli itle compared to the Fresnel field, they might have a small effect on the error statistics relative to the unit focusing function. These components also have the fortunate characteristic of becoming more negligible as the array weight becomes larger. The variation of the error distribution with the array weighting function constitutes a complicated problem that requires further study. A statistical error analysis is essential to evaluating the dynamic range of the system. The potential results are promising. Such a system might even discriminate against spurious reflected signals, by cross-correlating the outputs of different array weighting functions.

Considerable past effort has been expended on this problem. Prior work has been primarily based on the Sommerfeld series representation of the multipole expansion of radiation. The Sommerfeld series was used by H. H. Hougardy[1] in the "Time/Frequency" scheme, anc by V. Galindo[4] in his extrapolation study. These approaches require truncation of the Sommerfeld expansion, and consequently they are confined to the outer fringes of the Fresnel zone. For this reason, it would be highly impractical, if not impossible, to use the Sommerfeld series as an analytical tool for evaluating the unusual array design above. It is instructive, however, to compare the results of the two approaches to the problem. The array analyzed by Galindo was uniformly spaced (end-fire) with the following coefficients (relative approximately to unity[4]).

$$C_n = \frac{(-1)^n \left(\frac{R}{\Delta R}\right)^N e^{-ikR_n}}{(N-1-n)!\, n!} \left(1+n\frac{\Delta R}{R}\right)^N, \quad (R > \Delta R), n = o \rightarrow N-1.$$

These coefficients become quite large, and the error magnification for each element is greater than one. In order to decrease the pattern range, the number of elements must be increased for this array also. For the array to have any utility, at least 4 elements are required. For this case Galindo indicates the statistical error magnification[4] is greater than 130. The maximum element error magnification factor is about 62.5. For a seven element array, it would be about 1.5×10^5. By contrast, the maximum element error magnification in the suggested seven element array is 4.4. The coefficients of the last three elements are less than one. Thus the suggested array constitutes a considerable improvement over the earlier approaches to the problem. Recommendations for future investigation of the Fresnel ring focusing technique are contained in Section 12.

Investigations have also been performed to provide basic techniques to define the Fresnel region radiation fields of monopulse antennas, elliptical apertures, and phased arrays. Section 2 gives a procedure for calculating the Fresnel zone field of a monopulse antenna consisting of a four-antenna primary feed structure and a circular aperture secondary antenna. Section 2.2 describes the calculation procedure involved and shows that the experimental data on a test antenna compares favorably with the calculated data. This technique provides an adequate tool for prediction of the small angle Fresnel region pattern for such an antenna as illustrated by the figures in Section 2.2.6.

The procedure formulated for calculating the Fresnel region field for an elliptically or irregularly shaped aperture is described in Section 3.

The method used is similar to the strip approximation process used in basic integral calculus and comparison of experimental, and calculated data for a circular aperture was good. Calculated and measured data comparison using the AN/TPS-1D antenna as an example results in significant differences as shown in Section 3.2. It is not suggested that this difference indicates a limitation of the technique but that more accurate prediction may require a more precise description of the illumination function and adequate detailed design data for the antenna. Extreme care must also be exercised in measurement techniques to assure satisfaction of problem criteria for comparison. The method developed is a powerful tool and use of a computer for problems requiring a large number of summation strips may become necessary.

Section 4 presents a discussion of a technique that may be utilized with phased arrays. The general field problem for an arbitrary array with known excitation can be summed by computer but, for many arrays of interest, this is a difficult problem. For determining the Fresnel zone field of very large arrays with simple configurations, however, the computer is not the only resort. The array transformation theory by Ishimaru can be used for some arrays to obtain relatively simple expressions in terms of already tabulated functions. A small angle Fresnel zone array factor for rectangular arrays of uniform elements and linear weighing (or linear element density taper), for example, can be obtained from tabulations of trigonometric functions and Fresnel integrals. The method is illustrated by calculating the array factor for uniform line arrays.

A simple probe fed horn is utilized as an example of the problem of determining the spurious frequency response of an antenna at harmonically and non-harmonically related frequencies. The response of such an antenna is complicated by the higher order modes produced at frequencies other than the fundamental operating range. A method of predicting the mode structure in a probe fed electromagnetic horn has been investigated resulting in a favorable prediction as shown in Section 5.1 at the fundamental and 3rd harmonic frequencies. Results at the 6th harmonic were not too favorable and suggest a severe limitation of spurious frequency response prediction at frequencies higher than the 3rd harmonic by the method used.

The results of an experimental investigation to determine the definition of the far-field Fresnel region boundary for harmonically related frequencies is presented in Section 5.2. Resultant experimental data indicates that the pattern repetition beyond the $2D^2/\lambda$ range, by in large, is evident even with operation at higher harmonic frequencies. Extreme care must be excercised when acquiring data.

Section 6 presents the results of a theoretical investigation of the effects of terrain reflections in the Fresnel region upon the far-field Fresnel region boundary. It is concluded that the Fresnel region is not extended by propagation over a ground plane. In some cases, the field structure in the Fresnel region could be sufficiently modified because of reflections such that the Fresnel region patterns for large apertures could not be analyzed by the superposition of two field components as presented.

Theoretical investigations of antenna-to-antenna coupling of energy in the Fresnel region were conducted and graphs are presented in Section 9 to illustrate the power transfer as functions of range, diameter, and aperture distribution.

The radial E-field (Er) is defined in Section 7 as having the same order of magnitude as: $\frac{a}{R} |E_\theta| \cos \theta$

The principal field component (E_θ) and the radial field for a 40λ aperture are plotted for a Fresnel region range of 200λ. Investigation of measurement problems associated with the radial E-field suggests use of a thin radial dipole and the modulated dipole, scattering technique. The success of these techniques depends largely upon the ability to maintain the field probe extremely small so as not to disturb the radiating source antenna.

The defocusing techniques investigated utilize a monopulse model antenna and results of feed positioning indicate that the ellipsoidal reflector method give better results as shown in Section 10 than that defining the feed displacement by equating path lengths at the edge of the reflector. Lens defocusing was also examined, but the practical application of such techniques indicate that the problems encountered to provide a lens support, and pattern distortion caused by aperture blocking would be severe with large apertures.

It may be concluded from the summaries above that adequate techniques are available to define the Fresnel region small angle radiation patterns of various types of apertures including circular, rectangular, and elliptical apertures along with monopulse antennas, and phased arrays. For the purposes

of interference prediction, employment of such analytical techniques can be initiated with the understanding, that, only at small angles from the axis of the antenna will adequate description in the Fresnel region be obtained with the present state-of-the-art. Further investigation into this area is not recommended except as it pertains to specific examples such as shaped beam antennas or specific phased arrays.

Other areas are suggested as areas for future investigation as recommended in the next section of this report.

12. RECOMMENDATIONS

Based upon the conclusions drawn from investigation of the Fresnel ring focusing technique, it is recommended that a study be performed to evaluate the effectiveness of Fresnel ring focusing systems as practical measurement devices of far-field patterns in the Fresnel zone. The study should be oriented toward applying state-of-the-art equipment to test antennas with apertures greater than 100λ at maximum pattern ranges of less than $\frac{1}{5}(2D^2/\lambda)$. A statistical error analysis is first required, which should be based on the possible range of array weighting functions within the class described in this report. To facilitate this study, the theoretical test antenna might consist of a uniformly illuminated circular aperture, which would have a pattern requiring the most stringent system tolerance for a given aperture diameter. For the small angle "true" Fresnel field, this would require tabulations of the 1st and 2nd order Lommel functions of two variables at ranges down to about $\frac{1}{50}(2D^2/\lambda)$, or to ranges of the two variables (w,α) to about 20π. The error signal distribution would be determined from the equipment calibration tolerance, the array element position tolerance, and an estimation of the magnitude and range distribution of the higher order near field components. The error distribution would be summed statistically with the array weighting functions, giving attention to system dynamic range and band-width.

Consideration should also be given to the possibility of cross correlating the outputs of different array weighting functions for increasing dynamic range, and discriminating against relatively large reflected signals.

It is further recommended that additional investigation concerning Fresnel region antenna-to-antenna coupling be conducted with specific problem application. Experimental measurements should accompany any such exploration and may well include the effects of a high-powered surveillance or tracking radar at other locations within the Fresnel region where antennas are located.

Since it has been concluded in Section 11 that this study and previous work has provided sufficient additional tools to describe circular, rectangular and elliptical apertures along with monopulse antennas and phased arrays, the only additional program that should be initiated is the application of these techniques to specific problems. Further study in the field of radial E-field measurements should be conducted but with relation to specific problems. This application should include an investigation of coupling characteristics in the near field with an attempt to determine how the energy content may be measured.

It is not recommended that far field pattern determination produced by movement of the virtual feed point of a paraboloid defocusing techniques be investigated further, since the Fresnel ring focusing approach seems to employ more powerful techniques. The investigation of spurious frequency response has indicated a limitation in application of the approach taken and no recommendations for further investigation of analytical techniques are suggested in this area.

APPENDIX I

GENERALIZED LOMMEL FUNCTIONS $W^{\nu}_{m}(\nu,u)$

TABLE 1

GENERALIZED LOMMEL FUNCTIONS $W_m^\nu(\nu,u)$

The following tables may be calculated from the series expansion

$$W_m^\nu(\nu,u) = \frac{2^\nu}{u^{\nu+1}} \sum_{n=0}^{\infty} (j)^n \frac{(n+\nu)!}{n!} \left(\frac{\nu}{u}\right)^n J_{n+\nu+m+1}(u)$$

The following is a list of the computer notation used in the tables for the variables in the above equation

WR = The real part of $W_m^\nu(\nu,u)$, $(\mathrm{Re}(W_m^\nu))$

WI = The imaginary part of $W_m^\nu(\nu,u)$, $(\mathrm{Im}(W_m^\nu))$

U = u

G = ν

The tables are arranged with a fixed value of U and G on a given page. The values of U and G are given in the upper lefthand corner of the page. The Lommel functions are listed as shown on the following page.

BLANK PAGE

TABLE 1

GENERALIZED LOMMEL FUNCTION

U = u, G = γ

$\mathrm{Im}(w_m^{\nu}(\gamma,u))/\mathrm{Re}(w_m^{\nu}(\gamma,u))$ = WI/WR

(ν=4)	0.	0.	0.	0.	0.
	0.	0.	0.	0.	0.
(ν=3)	0.	0.	0.	0.	0.
	0.	0.	0.	0.	0.
(ν=2)	0.	0.	0.	0.	$\mathrm{Im}(w_5^2(\gamma,u))$
	0.	0.	0.	0.	$\mathrm{Re}(w_5^2(\gamma,u))$
(ν=1)	0.	0.	$\mathrm{Im}(w_7^1(\gamma,u))$	$\mathrm{Im}(w_6^1(\gamma,u))$	$\mathrm{Im}(w_5^1(\gamma,u))$
	0.	0.	$\mathrm{Re}(w_7^1(\gamma,u))$	$\mathrm{Re}(w_6^1(\gamma,u))$	$\mathrm{Re}(w_5^1(\gamma,u))$
(ν=0)	$\mathrm{Im}(w_9^0(\gamma,u))$	$\mathrm{Im}(w_8^0(\gamma,u))$	$\mathrm{Im}(w_7^0(\gamma,u))$	$\mathrm{Im}(w_6^0(\gamma,u))$	$\mathrm{Im}(w_5^0(\gamma,u))$
	$\mathrm{Re}(w_9^0(\gamma,u))$	$\mathrm{Re}(w_8^0(\gamma,u))$	$\mathrm{Re}(w_7^0(\gamma,u))$	$\mathrm{Re}(w_6^0(\gamma,u))$	$\mathrm{Re}(w_5^0(\gamma,u))$
	m = 9	m = 8	m = 7	m = 6	m = 5

TIONS $w_m^{\nu}(\gamma,u)$

0.	0.	0.	$\mathrm{Im}(w_1^4(\gamma,u))$	$\mathrm{Im}(w_0^4(\gamma,u))$
0.	0.	0.	$\mathrm{Re}(w_1^4(\gamma,u))$	$\mathrm{Re}(w_0^4(\gamma,u))$
0.	$\mathrm{Im}(w_3^3(\gamma,u))$	$\mathrm{Im}(w_2^3(\gamma,u))$	$\mathrm{Im}(w_1^3(\gamma,u))$	$\mathrm{Im}(w_0^3(\gamma,u))$
0.	$\mathrm{Re}(w_3^3(\gamma,u))$	$\mathrm{Re}(w_2^3(\gamma,u))$	$\mathrm{Re}(w_1^3(\gamma,u))$	$\mathrm{Re}(w_0^3(\gamma,u))$
$\mathrm{Im}(w_4^2(\gamma,u))$	$\mathrm{Im}(w_3^2(\gamma,u))$	$\mathrm{Im}(w_2^2(\gamma,u))$	$\mathrm{Im}(w_1^2(\gamma,u))$	$\mathrm{Im}(w_0^2(\gamma,u))$
$\mathrm{Re}(w_4^2(\gamma,u))$	$\mathrm{Re}(w_3^2(\gamma,u))$	$\mathrm{Re}(w_2^2(\gamma,u))$	$\mathrm{Re}(w_1^2(\gamma,u))$	$\mathrm{Re}(w_0^2(\gamma,u))$
$\mathrm{Im}(w_4^1(\gamma,u))$	$\mathrm{Im}(w_3^1(\gamma,u))$	$\mathrm{Im}(w_2^1(\gamma,u))$	$\mathrm{Im}(w_1^1(\gamma,u))$	$\mathrm{Im}(w_0^1(\gamma,u))$
$\mathrm{Re}(w_4^1(\gamma,u))$	$\mathrm{Re}(w_3^1(\gamma,u))$	$\mathrm{Re}(w_2^1(\gamma,u))$	$\mathrm{Re}(w_1^1(\gamma,u))$	$\mathrm{Re}(w_0^1(\gamma,u))$
$\mathrm{Im}(w_4^0(\gamma,u))$	$\mathrm{Im}(w_3^0(\gamma,u))$	$\mathrm{Im}(w_2^0(\gamma,u))$	$\mathrm{Im}(w_1^0(\gamma,u))$	$\mathrm{Im}(w_0^0(\gamma,u))$
$\mathrm{Re}(w_4^0(\gamma,u))$	$\mathrm{Re}(w_3^0(\gamma,u))$	$\mathrm{Re}(w_2^0(\gamma,u))$	$\mathrm{Re}(w_1^0(\gamma,u))$	$\mathrm{Re}(w_0^0(\gamma,u))$
$m = 4$	$m = 3$	$m = 2$	$m = 1$	$m = 0$

U= 1 G= 0.78539816

MI/MR

0.	0.	0.	0.	0.	0.	0.	0.	0.00223	0.03096
0.	0.	0.	0.	0.	0.	0.	0.	0.00771	0.09062
0.	0.	0.	0.	0.	0.	0.00001	0.00022	0.00311	0.03697
0.	0.	0.	0.	0.	0.	0.00007	0.00098	0.01155	0.11274
0.	0.	0.	0.	0.00000	0.00000	0.00003	0.00039	0.00465	0.04588
0.	0.	0.	0.	0.00000	0.00001	0.00016	0.00195	0.01920	0.14918
0.	0.	0.00000	0.00000	0.00000	0.00000	0.00007	0.00078	0.00770	0.06050
0.	0.	0.00000	0.00000	0.00000	0.00004	0.00049	0.00488	0.03821	0.22072
0.00000	0.00000	0.00000	0.00000	0.00000	0.00002	0.00020	0.00193	0.01524	0.08905
0.00000	0.00000	0.00000	0.00000	0.00002	0.00025	0.00246	0.01941	0.11338	0.42808

U= 2 G= 0.78539816

MI/MR

0.	0.	0.	0.	0.	0.	0.	0.	0.00406	0.02777
0.	0.	0.	0.	0.	0.	0.	0.	0.01382	0.07967
0.	0.	0.	0.	0.	0.	0.00010	0.00082	0.00559	0.03254
0.	0.	0.	0.	0.	0.	0.00051	0.00351	0.02032	0.09648
0.	0.	0.	0.	0.00000	0.00003	0.00020	0.00140	0.00819	0.03933
0.	0.	0.	0.	0.00002	0.00017	0.00118	0.00688	0.03289	0.12249
0.	0.	0.00000	0.00000	0.00001	0.00007	0.00047	0.00274	0.01320	0.04979
0.	0.	0.00000	0.00001	0.00009	0.00060	0.00348	0.01672	0.06285	0.16862
0.00000	0.00000	0.00000	0.00000	0.00003	0.00024	0.00138	0.00664	0.02510	0.06825
0.00000	0.00000	0.00001	0.00009	0.00060	0.00351	0.01691	0.06393	0.17381	0.27850

V= 3 G= 0.70229010

ml/mR

0.	0.	0.	0.	0.	0.	0.	0.	0.00519	0.02308
0.	0.	0.	0.	0.	0.	0.	0.	0.01721	0.06390
0.	0.	0.	0.	0.	0.	0.00030	0.00156	0.00697	0.02616
0.	0.	0.	0.	0.	0.	0.00148	0.00655	0.02447	0.07366
0.	0.	0.	0.	0.00002	0.00011	0.00059	0.00263	0.00990	0.03012
0.	0.	0.	0.	0.00014	0.00074	0.00332	0.01244	0.03774	0.00638
0.	0.	0.00000	0.00001	0.00006	0.00030	0.00132	0.00497	0.01518	0.03528
0.	0.	0.00002	0.00011	0.00056	0.00251	0.00945	0.02882	0.06673	0.10205
0.00000	0.00000	0.00001	0.00004	0.00022	0.00099	0.00374	0.01145	0.02671	0.04163
0.00000	0.00003	0.00016	0.00085	0.00379	0.01428	0.04375	0.10204	0.15903	0.10603

V= 4 G= 0.70229010

ml/mR

0.	0.	0.	0.	0.	0.	0.	0.	0.00349	0.01767
0.	0.	0.	0.	0.	0.	0.	0.	0.01754	0.04628
0.	0.	0.	0.	0.	0.	0.00039	0.00221	0.00711	0.01902
0.	0.	0.	0.	0.	0.	0.00278	0.00891	0.02368	0.04920
0.	0.	0.	0.	0.00007	0.00029	0.00111	0.00358	0.00958	0.02024
0.	0.	0.	0.	0.00050	0.00187	0.00662	0.01607	0.03373	0.04999
0.	0.	0.00001	0.00005	0.00020	0.00074	0.00239	0.00643	0.01361	0.02062
0.	0.	0.00012	0.00050	0.00188	0.00608	0.01629	0.03444	0.05188	0.04150
0.00000	0.00001	0.00005	0.00020	0.00074	0.00240	0.00646	0.01371	0.02067	0.01734
0.00005	0.00023	0.00101	0.00378	0.01223	0.03288	0.06981	0.10628	0.00834	-0.02061

[illegible] = 2 [illegible]

0.	0.	0.	0.	0.	0.	0.	0.	0.00906	0.01234
								0.01527	0.02069
0.	0.	0.	0.	0.	0.	0.00088	0.00294	0.00681	0.01229
						0.00400	0.00972	0.01909	0.02759
0.	0.	0.	0.	[illegible]	[illegible]	[illegible]	[illegible]	[illegible]	[illegible]
0.	0.	0.	0.	0.00017	[illegible]	[illegible]	[illegible]	[illegible]	[illegible]
				0.00116					
0.	0.	[illegible]	[illegible]	[illegible]	[illegible]	[illegible]	[illegible]	[illegible]	[illegible]
0.00001	0.00005	0.00017	0.00050	0.00167	0.00410	0.00816	0.01819	0.01126	0.00116
0.00029	0.00110	0.00367	0.01065	0.02812	0.05107	0.07760	0.07168	0.00748	-0.06728

[illegible] = 4 [illegible]

0.	0.	0.	0.	0.	0.	0.	0.	0.00411	0.00773
								0.01143	0.01626
0.	0.	0.	0.	0.	0.	0.00108	0.00248	0.00467	0.00681
						0.00467	0.00875	0.01260	0.01171
0.	0.	0.	0.	[illegible]	[illegible]	[illegible]	[illegible]	[illegible]	[illegible]
				0.00207	0.00472	0.00889	0.01292	0.01232	0.00200
0.	0.	[illegible]	[illegible]	[illegible]	[illegible]	[illegible]	[illegible]	[illegible]	[illegible]
		0.00119	0.00312	0.00714	0.01350	0.01975	0.01917	0.00535	-0.01449
0.00004	0.00015	0.00044	0.00120	0.00282	0.00534	0.00783	0.00771	0.00237	-0.00543
0.00116	0.00352	0.00840	0.02154	0.04801	0.05066	0.05691	0.01010	-0.04149	-0.04642

M= 7 G= 0.79820816

MI/MR

0. 0.	0. 0.	0. 0.	0. 0.	0. 0.	0. 0.	0. 0.	0. 0.	0.00293 0.00720	0.00420 0.00696
0. 0.	0. 0.	0. 0.	0. 0.	0. 0.	0. 0.	0.00113 0.00452	0.00206 0.00646	0.00297 0.00637	0.00299 0.00232
0. 0.	0. 0.	0. 0.	0. 0.	0.00046 0.00244	0.00108 0.00354	0.00181 0.00760	0.00307 0.00771	0.00268 0.00326	-0.00113 -0.00351
0. 0.	0. 0.	0.00021 0.00250	0.00094 0.00519	0.00117 0.00644	0.00213 0.01365	0.00308 0.01584	0.00313 0.00502	0.00127 -0.00757	-0.00101 -0.01284
0.00013 0.00336	0.00038 0.00648	0.00094 0.01824	0.00205 0.03326	0.00373 0.04823	0.00541 0.04928	0.00553 0.02104	0.00246 -0.02456	-0.00276 -0.04334	-0.00486 -0.00036

M= 8 G= 0.79820816

MI/MR

0. 0.	0. 0.	0. 0.	0. 0.	0. 0.	0. 0.	0. 0.	0. 0.	0.00188 0.00358	0.00184 0.00164
0. 0.	0. 0.	0. 0.	0. 0.	0. 0.	0. 0.	0.00101 0.00362	0.00145 0.00371	0.00158 0.00182	0.00078 -0.00161
0. 0.	0. 0.	0. 0.	0. 0.	0.00058 0.00344	0.00102 0.00498	0.00164 0.00587	0.00152 0.00262	0.00081 -0.00195	-0.00043 -0.00471
0. 0.	0. 0.	0.00037 0.00342	0.00077 0.00693	0.00136 0.00998	0.00195 0.01033	0.00203 0.00352	0.00110 -0.00389	-0.00069 -0.00926	-0.00101 -0.00343
0.00021 0.00758	0.00074 0.01576	0.00185 0.02766	0.00274 0.03992	0.00292 0.04193	0.00212 0.02284	0.00224 -0.01557	-0.00133 -0.03461	-0.00289 -0.01399	-0.00137 0.02960

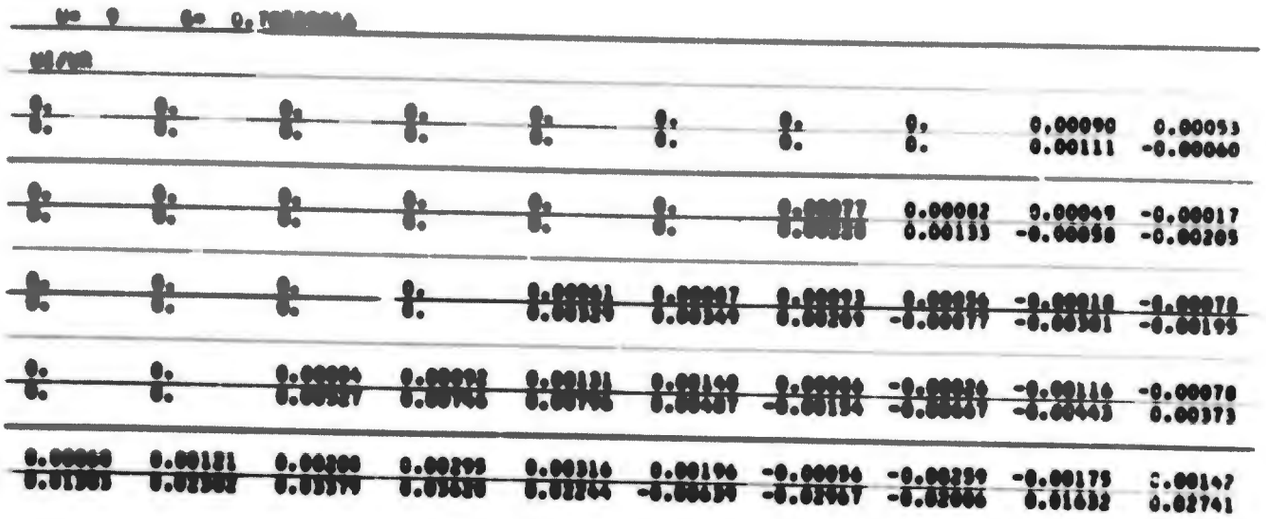

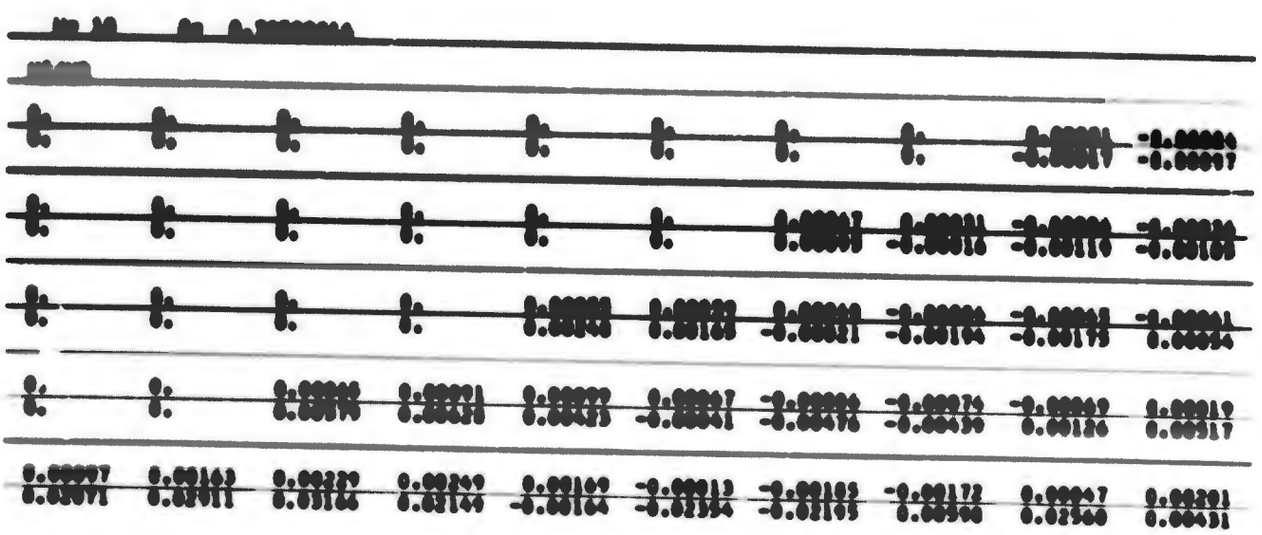

MP 11 θ= 0.78539816

MI/MR

0. 0.	0. 0.	0. 0.	0. 0.	0. 0.	0. 0.	0. 0.	0. 0.	0.00001 -0.00052	-0.00018 -0.00057
0. 0.	0. 0.	0. 0.	0. 0.	0. 0.	0. 0.	0.00020 0.00001	0.00001 -0.00010	-0.00019 -0.00078	-0.00022 -0.00001
0. 0.	0. 0.	0. 0.	0. 0.	0.00020 0.00150	0.00020 0.00005	0.00002 -0.00129	-0.00024 -0.00143	-0.00021 -0.00005	-0.00001 0.00141
0. 0.	0. 0.	0.00066 0.00309	0.00072 0.00365	0.00052 0.00023	0.00004 -0.00330	-0.00048 -0.00344	-0.00036 -0.00026	-0.00003 0.00182	0.00054 0.00256
0.00130 0.02944	0.00162 0.02798	0.00200 0.02032	0.00145 0.00193	0.00011 -0.01845	-0.00132 -0.02167	-0.00155 -0.00127	-0.00009 0.02078	0.00148 0.01265	0.00000 -0.01618

MP 12 θ= 0.78539816

MI/MR

0. 0.	0. 0.	0. 0.	0. 0.	0. 0.	0. 0.	0. 0.	0. 0.	-0.00009 -0.00038	-0.00012 -0.00010
0. 0.	0. 0.	0. 0.	0. 0.	0. 0.	0. 0.	0.00002 -0.00042	-0.00011 -0.00057	-0.00015 -0.00015	-0.00004 0.00045
0. 0.	0. 0.	0. 0.	0. 0.	0.00021 0.00017	0.00004 -0.00002	-0.00014 -0.00113	-0.00022 -0.00032	-0.00004 0.00007	0.00017 0.00001
0. 0.	0. 0.	0.00054 0.00313	0.00041 0.00057	0.00000 -0.00241	-0.00021 -0.00339	-0.00044 -0.00099	-0.00013 0.00250	0.00024 0.00272	0.00036 -0.00121
0.00147 0.02497	0.00163 0.01910	0.00125 0.00365	0.00024 -0.01427	-0.00003 -0.02033	-0.00122 -0.00006	-0.00040 0.01930	0.00100 0.01629	0.00107 -0.00714	-0.00047 -0.01049

0. 0.	0. 0.	0. 0.	0. 0.	0. 0.	0. 0.	0. 0.	0. 0.	-0.00008 -0.00011	-0.00004 0.00015
0. 0.	0. 0.	0. 0.	0. 0.	0. 0.	0. 0.	-0.00006 -0.00041	-0.00010 -0.00019	-0.00005 0.00024	0.00006 0.00038
0. 0.	0. 0.	0. 0.	0. 0.	0.00004 -0.00053	-0.00009 -0.00088	-0.00016 -0.00042	-0.00008 0.00050	0.00009 0.00081	0.00015 0.00000
0. 0.	0. 0.	0.00033 0.00075	0.00009 -0.00170	-0.00020 -0.00286	-0.00034 -0.00138	-0.00017 0.00159	0.00019 0.00261	0.00031 0.00002	0.00000 -0.00261
0.00156 0.01701	0.00108 0.00507	0.00031 -0.01032	-0.00064 -0.01852	-0.00112 -0.00004	-0.00055 0.01019	0.00062 0.01690	0.00102 0.00022	0.00001 -0.01681	-0.00102 -0.00941

0. 0.	0. 0.	0. 0.	0. 0.	0. 0.	0. 0.	0. 0.	0. 0.	-0.00003 0.00007	0.00002 0.00016
0. 0.	0. 0.	0. 0.	0. 0.	0. 0.	0. 0.	-0.00007 -0.00018	-0.00004 0.00011	0.00002 0.00028	0.00004 0.00009
0. 0.	0. 0.	0. 0.	0. 0.	-0.00004 -0.00063	-0.00011 -0.00043	-0.00007 0.00025	0.00004 0.00063	0.00011 0.00022	0.00004 -0.00053
0. 0.	0. 0.	0.00010 -0.00119	-0.00013 -0.00230	-0.00027 -0.00153	-0.00017 0.00005	0.00009 0.00226	0.00025 0.00077	0.00009 -0.00183	-0.00020 -0.00156
0.00004 0.00681	0.00034 -0.00822	-0.00046 -0.01654	-0.00093 -0.01075	-0.00060 0.00585	0.00033 0.01578	0.00008 0.00543	0.00030 -0.01268	-0.00071 -0.01088	-0.00061 0.00957

V= 15 G= 0.78539816

WI/WR

0. 0.	0. 0.	0. 0.	0. 0.	0. 0.	0. 0.	0. 0.	0. 0.	0.00001 0.00011	0.00003 0.00007
0. 0.	0. 0.	0. 0.	0. 0.	0. 0.	0. 0.	-0.00003 0.00004	0.00001 0.00020	0.00004 0.00012	0.00003 -0.00012
0. 0.	0. 0.	0. 0.	0. 0.	-0.00008 -0.00041	-0.00006 0.00009	0.00001 0.00050	0.00000 0.00031	0.00003 -0.00029	-0.00005 -0.00046
0. 0.	0. 0.	-0.00009 -0.00196	-0.00021 -0.00154	-0.00016 0.00032	0.00003 0.00185	0.00019 0.00116	0.00012 -0.00107	-0.00011 -0.00173	-0.00018 0.00038
0.00035 -0.00585	-0.00032 -0.01469	-0.00077 -0.01158	-0.00061 0.00234	0.00012 0.01378	0.00072 0.00869	0.00046 -0.00798	-0.00042 -0.01266	-0.00068 0.00276	0.00015 0.01371

V= 16 G= 0.78539816

WI/WR

0. 0.	0. 0.	0. 0.	0. 0.	0. 0.	0. 0.	0. 0.	0. 0.	0.00002 0.00006	0.00001 -0.00002
0. 0.	0. 0.	0. 0.	0. 0.	0. 0.	0. 0.	-0.00000 0.00014	0.00003 0.00012	0.00002 -0.00005	-0.00001 -0.00015
0. 0.	0. 0.	0. 0.	0. 0.	-0.00003 -0.00061	-0.00000 0.00036	0.00005 0.00033	0.00005 -0.00012	-0.00002 -0.00040	-0.00004 -0.00008
0. 0.	0. 0.	-0.00016 -0.00148	-0.00015 -0.00004	-0.00000 0.00144	0.00014 0.00130	0.00013 -0.00046	-0.00004 -0.00159	-0.00016 -0.00034	-0.00003 0.00147
-0.00021 -0.01290	-0.00063 -0.01184	-0.00058 -0.00041	-0.00002 0.01144	0.00056 0.01042	0.00051 -0.00362	-0.00018 -0.01269	-0.00062 -0.00273	-0.00013 0.01167	0.00057 0.00966

M= 17 G= 0.7053816

M1/M8

0. 0.	0. 0.	0. 0.	0. 0.	0. 0.	0. 0.	0. 0.	0. 0.	0.00001 -0.00000	-0.00005 -0.00005
0. 0.	0. 0.	0. 0.	0. 0.	0. 0.	0. 0.	0.00002 0.00011	0.00002 -0.00000	-0.00000 -0.00011	-0.00002 -0.00006
0. 0.	0. 0.	0. 0.	0. 0.	-0.00001 0.00025	0.00004 0.00031	0.00004 -0.00000	-0.00000 -0.00031	-0.00004 -0.00018	-0.00002 0.00022
0. 0.	0. 0.	-0.00013 -0.00089	-0.00003 0.00107	0.00010 0.00138	0.00012 -0.00066	0.00000 -0.00138	-0.00012 -0.00077	-0.00007 0.00064	0.00004 0.00110
-0.00000 -0.01171	-0.00004 -0.00238	-0.00012 0.00087	0.00042 0.01164	0.00031 0.00842	0.00000 -0.01103	-0.00031 -0.00651	-0.00030 0.00746	0.00037 0.00333	0.00043 -0.00376

M= 18 G= 0.7053816

M1/M8

0. 0.	0. 0.	0. 0.	0. 0.	0. 0.	0. 0.	0. 0.	0. 0.	0.00000 -0.00003	-0.00001 -0.00003
0. 0.	0. 0.	0. 0.	0. 0.	0. 0.	0. 0.	0.00002 0.00002	0.00000 -0.00007	-0.00001 -0.00007	-0.00001 0.00003
0. 0.	0. 0.	0. 0.	0. 0.	0.00002 0.00027	0.00004 0.00007	0.00001 -0.00022	-0.00001 -0.00021	-0.00001 0.00010	0.00001 0.00026
0. 0.	0. 0.	-0.00004 0.00076	0.00007 0.00121	0.00011 0.00031	0.00003 -0.00097	-0.00008 -0.00096	-0.00008 0.00044	0.00004 0.00116	0.00010 -0.00005
-0.00049 -0.00405	-0.00018 0.00404	0.00030 0.01084	0.00048 0.00284	0.00012 -0.00068	-0.00038 -0.00844	-0.00038 0.00389	0.00017 0.01037	0.00045 -0.00043	-0.00002 -0.01046

N= 19 G= 0.70539816

WI/WR

0. 0.	0. 0.	0. 0.	0. 0.	0. 0.	0. 0.	0. 0.	0. 0.	-0.00000 -0.00003	-0.00001 0.00000
0. 0.	0. 0.	0. 0.	0. 0.	0. 0.	0. 0.	0.00001 -0.00004	-0.00001 -0.00007	-0.0000. 0.00000	0.00000 0.00007
0. 0.	0. 0.	0. 0.	0. 0.	0.00003 0.00011	0.00001 -0.00014	-0.00002 -0.00021	-0.00001 0.00001	0.00000 0.00021	0.00002 0.00000
0. 0.	0. 0.	0.00004 0.00108	0.00009 0.00051	0.00004 -0.00045	-0.00005 -0.00099	-0.00008 0.00002	0.00000 0.00101	0.00008 0.00040	0.00003 -0.00088
-0.00021 0.00484	0.00020 0.01076	0.00042 0.00488	0.00020 -0.00615	-0.00025 -0.00942	-0.00039 0.00020	0.00001 0.00952	0.00039 0.00381	0.00016 -0.00832	-0.00034 -0.00557

N= 20 G= 0.70539816

WI/WR

0. 0.	0. 0.	0. 0.	0. 0.	0. 0.	0. 0.	0. 0.	0. 0.	-0.00000 -0.00001	-0.00000 0.00002
0. 0.	0. 0.	0. 0.	0. 0.	0. 0.	0. 0.	-0.00000 -0.00006	-0.00001 -0.00002	-0.00000 0.00005	0.00001 0.00004
0. 0.	0. 0.	0. 0.	0. 0.	0.00001 -0.00008	-0.00001 -0.00019	-0.00002 -0.00005	-0.00001 0.00015	0.00002 0.00013	0.00002 -0.00010
0. 0.	0. 0.	0.00007 0.00062	0.00005 -0.00037	-0.00003 -0.00002	-0.00007 -0.00027	-0.00002 0.00076	0.00006 0.00065	0.00005 -0.00050	-0.00004 -0.00000
0.00012 0.00933	0.00037 0.00625	0.00025 -0.00371	-0.00015 -0.00922	-0.00036 -0.00275	-0.00011 0.00757	0.00030 0.00654	0.00026 -0.00496	-0.00019 -0.00003	-0.00032 0.00335

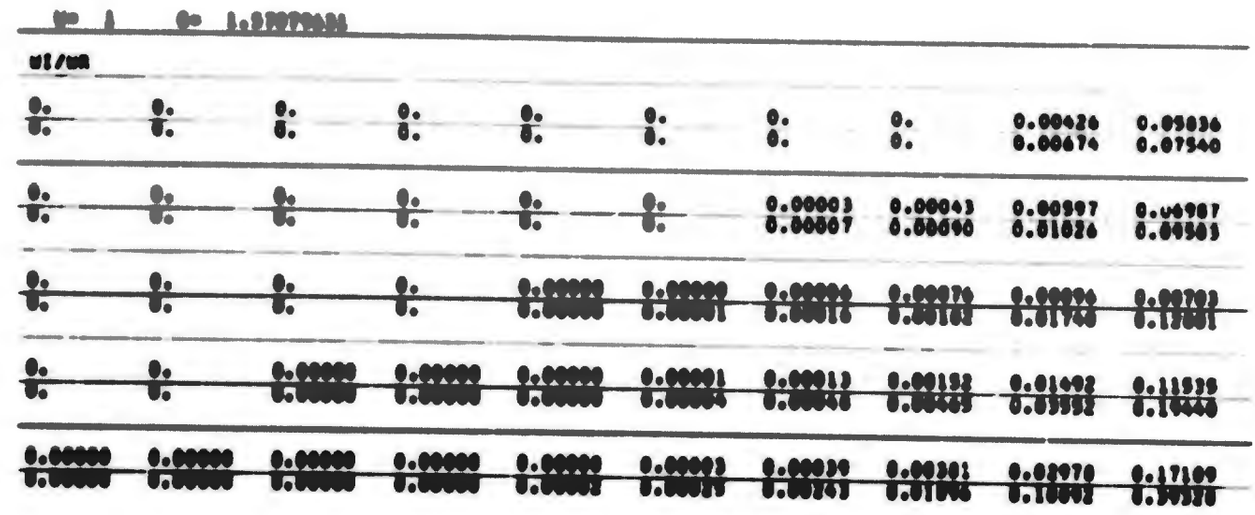

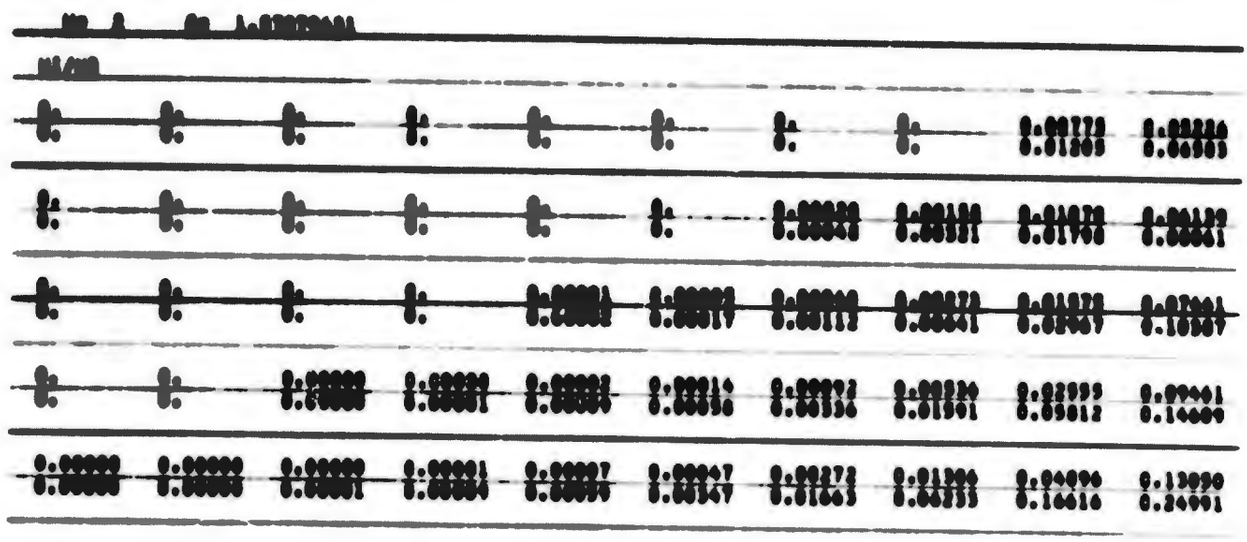

U= 3 G= 1.57079631

MI/MR

0. 0.	0. 0.	0. 0.	0. 0.	0. 0.	0. 0.	0. 0.	0. 0.	0.00988 0.01490	0.04332 0.05213
0. 0.	0. 0.	0. 0.	0. 0.	0. 0.	0. 0.	0.00059 0.00138	0.00302 0.00597	0.01332 0.02149	0.04918 0.06049
0. 0.	0. 0.	0. 0.	0. 0.	0.00004 0.00014	0.00022 0.00071	0.00115 0.00314	0.00510 0.01184	0.01096 0.03373	0.05673 0.07144
0. 0.	0. 0.	0.00000 0.00002	0.00002 0.00011	0.00011 0.00055	0.00058 0.00244	0.00259 0.00910	0.00969 0.02730	0.02930 0.06103	0.06657 0.08402
0.00000 0.00000	0.00000 0.00003	0.00001 0.00016	0.00009 0.00084	0.00044 0.00375	0.00197 0.01411	0.00739 0.04298	0.02251 0.09915	0.05192 0.15025	0.07867 0.08504

U= 4 G= 1.57079631

MI/MR

0. 0.	0. 0.	0. 0.	0. 0.	0. 0.	0. 0.	0. 0.	0. 0.	0.01044 0.01503	0.03303 0.03694
0. 0.	0. 0.	0. 0.	0. 0.	0. 0.	0. 0.	0.00114 0.00258	0.00426 0.00807	0.01356 0.02092	0.03595 0.03914
0. 0.	0. 0.	0. 0.	0. 0.	0.00014 0.00048	0.00058 0.00179	0.00214 0.00568	0.00693 0.01488	0.01833 0.02964	0.03778 0.03916
0. 0.	0. 0.	0.00002 0.00012	0.00009 0.00049	0.00039 0.00184	0.00146 0.00591	0.00470 0.01565	0.01251 0.03236	0.02614 0.04636	0.03834 0.02998
0.00000 0.00005	0.00002 0.00023	0.00009 0.00100	0.00039 0.00376	0.00148 0.01212	0.00476 0.03244	0.01274 0.06841	0.02687 0.10294	0.04027 0.08048	0.03161 -0.03232

[redacted]

[redacted]

U= 7 G= 1.57079631

wl/wR

0.	0.	0.	0.	0.	0.	0.	0.	0.00547	0.0079
0.	0.	0.	0.	0.	0.	0.	0.	0.00564	0.00415
0.	0.	0.	0.	0.	0.	0.00219	0.00393	0.00552	0.00523
0.	0.	0.	0.	0.	0.	0.00409	0.00553	0.00471	-0.00004
0.	0.	0.	0.	0.00090	0.00195	0.00351	0.00500	0.00486	0.00162
0.	0.	0.	0.	0.00282	0.00504	0.00703	0.00652	0.00140	-0.00416
0.	0.	0.00043	0.00106	0.00230	0.00417	0.00598	0.00595	0.00228	-0.00360
0.	0.	0.00235	0.00508	0.00918	0.01307	0.01279	0.00441	-0.00887	-0.01310
0.00027	0.00075	0.00180	0.00406	0.00739	0.01067	0.01078	0.00452	-0.00991	-0.00989
0.00334	0.00836	0.01811	0.03295	0.04754	0.04804	0.02015	-0.02636	-0.04407	0.00066

U= 0 G= 1.57079631

wl/wR

0.	0.	0.	0.	0.	0.	0.	0.	0.00331	0.00322
0.	0.	0.	0.	0.	0.	0.	0.	0.00251	0.00015
0.	0.	0.	0.	0.	0.	0.00195	0.00273	0.00272	0.00117
0.	0.	0.	0.	0.	0.	0.00320	0.00298	0.00080	-0.00263
0.	0.	0.	0.	0.00113	0.	0.00280	0.00285	0.00134	-0.00135
0.	0.	0.	0.	0.00328	0.	0.00449	0.00179	-0.00279	-0.00511
0.	0.	0.00074	0.00153	0.00269	0.00382	0.00393	0.00198	-0.00160	-0.00373
0.	0.	0.00386	0.00677	0.00957	0.00976	0.00468	-0.00446	-0.00970	-0.00307
0.00063	0.00148	0.00308	0.00543	0.00775	0.00808	0.00426	-0.00290	-0.00731	-0.00266
0.00795	0.01967	0.02784	0.03947	0.04113	0.02170	-0.01476	-0.03723	-0.01356	0.03076

[illegible] 9 [illegible] 1.07079631

ui/ue

0.	0.	0.	0.	0.	0.	0.	0.	0.00161	0.00081
0.	0.	0.	0.	0.	0.	0.	0.	0.00047	-0.00124
0.	0.	0.	0.	0.	0.	0.00144	0.00151	0.00081	-0.00052
0.	0.	0.	0.	0.	0.	0.00193	0.00084	-0.00108	-0.00233
0.	0.	0.	0.	0.00120	0.00168	0.00176	0.00100	[illegible]	[illegible]
0.	0.	0.	0.	0.00310	0.00317	0.00165	[illegible]	[illegible]	[illegible]
0.	0.	0.00106	0.00102	0.00256	0.00271	0.00160	-0.00064	-0.00239	-0.00152
0.	0.	0.00517	0.00725	0.00761	0.00437	-0.00207	-0.00648	-0.00431	0.00420
0.00120	0.00240	0.00413	0.00584	0.00622	0.00378	-0.00126	-0.00526	-0.00347	0.00297
0.01376	0.02367	0.03348	0.03566	0.02168	-0.00728	-0.03016	-0.01988	0.01701	0.02786

[illegible] 10 [illegible] 1.[illegible]

ui/ue

0.	0.	0.	0.	0.	0.	0.	0.	0.00091	-0.00020
0.	0.	0.	0.	0.	0.	0.	0.	-0.00047	-0.00116
0.	0.	0.	0.	0.	0.	0.00088	0.00095	-0.00016	-0.00078
0.	0.	0.	0.	0.	0.	0.00071	-0.00043	-0.00135	-0.00101
0.	0.	0.	0.	0.00106	0.00113	0.00073	[illegible]	[illegible]	[illegible]
0.	0.	0.	0.	0.00230	0.00140	-0.00048	-0.00211	-0.00172	0.00076
0.	0.	0.00128	0.00100	0.00193	0.00127	-0.00019	-0.00153	-0.00137	0.00044
0.	0.	0.00564	0.00405	0.00391	-0.00075	-0.00498	-0.00435	0.00153	0.00542
0.00192	0.00323	0.00494	0.00491	0.00329	-0.00035	-0.00376	-0.00344	0.00101	0.00408
0.02059	0.02888	0.03128	0.02096	-0.00222	-0.02392	-0.02191	0.00643	0.02600	0.00419

M= 11 G= 1.57079631

MI/MR

0.	0.	0.	0.	0.	0.	0.	0.	-0.00004	-0.00039
0.	0.	0.	0.	0.	0.	0.	0.	-0.00063	-0.00056
0.	0.	0.	0.	0.	0.	0.00037	-0.00002	-0.00042	-0.00045
0.	0.	0.	0.	0.	0.	-0.00014	-0.00080	-0.00078	0.00010
0.	0.	0.	0.	0.00076	0.00053	-0.00001	-0.00056	-0.00061	-0.00000
0.	0.	0.	0.	0.00115	-0.00011	-0.00137	-0.00143	0.00007	0.00194
0.	0.	0.00130	0.00142	0.00101	0.00003	-0.00099	-0.00113	-0.00003	0.00112
0.	0.	0.00490	0.00344	-0.00000	-0.00355	-0.00395	-0.00004	0.00400	0.00231
0.00259	0.00361	0.00396	0.00285	0.00016	-0.00267	-0.00310	-0.00014	0.00301	0.00181
0.02527	0.02771	0.01994	0.00111	-0.01873	-0.02168	-0.00099	0.02111	0.01266	-0.01650

M= 12 G= 1.57079631

MI/MR

0.	0.	0.	0.	0.	0.	0.	0.	-0.00020	-0.00025
0.	0.	0.	0.	0.	0.	0.	0.	-0.00038	-0.00004
0.	0.	0.	0.	0.	0.	0.00002	-0.00023	-0.00030	-0.00007
0.	0.	0.	0.	0.	0.	-0.00048	-0.00058	-0.00010	0.00052
0.	0.	0.	0.	0.00039	0.00005	-0.00033	-0.00049	-0.00012	0.00036
0.	0.	0.	0.	0.00067	-0.00009	-0.00114	-0.00025	0.00046	0.00093
0.	0.	0.00107	0.00080	0.00013	-0.00065	-0.00089	-0.00025	0.00049	0.00072
0.	0.	0.00301	0.00042	-0.00252	-0.00341	-0.00089	0.00271	0.00276	-0.00131
0.00293	0.00324	0.00246	0.00044	-0.00190	-0.00267	-0.00077	0.00204	0.00214	-0.00096
0.02476	0.01882	0.00333	-0.01451	-0.02037	-0.00587	0.01556	0.01636	-0.00734	-0.01890

[illegible]

w1/wA

0. 0.	0. 0.	0. 0.	0. 0.	0. 0.	0. 0.	0. 0.	0. 0.	-0.00015 -0.00009	-0.00006 0.00019
0. 0.	0. 0.	0. 0.	0. 0.	0. 0.	0. 0.	-0.00013 -0.00042	-0.00020 -0.00016	-0.00009 0.00028	0.00012 0.00040
0. 0.	0. 0.	0. 0.	0. 0.	0.00007 [illegible]	[illegible] [illegible]	-0.00032 -0.00038	-0.00015 0.00056	0.00019 0.00083	0.00030 -0.00003
0. 0.	0. 0.	0.00005 [illegible]	0.00017 -0.00179	-0.00042 -0.00288	-0.00069 -0.00132	-0.00033 0.00168	0.00040 0.00265	0.00064 -0.00003	-0.00000 -0.00269
0.00269 0.01769	0.00214 0.00483	0.00058 -0.01111	-0.00134 -0.01856	-0.00224 -0.00892	-0.00108 0.01646	0.00126 0.01700	0.00205 0.00610	0.00001 -0.01700	-0.00205 -0.00541

[illegible]

w1/wA

0. 0.	0. 0.	0. 0.	0. 0.	0. 0.	0. 0.	0. 0.	0. 0.	-0.00006 0.00009	0.00004 0.00018
0. 0.	0. 0.	0. 0.	0. 0.	0. 0.	0. 0.	-0.00013 -0.00017	-0.00008 0.00014	0.00005 0.00030	0.00013 0.00008
0. 0.	0. 0.	0. 0.	0. 0.	-0.00012 -0.00069	-0.00023 -0.00041	-0.00014 0.00029	0.00009 0.00067	0.00022 0.00020	0.00007 -0.00057
0. 0.	0. 0.	0.00018 -0.00126	-0.00028 -0.00240	-0.00054 -0.00149	-0.00034 0.00092	0.00020 0.00231	0.00051 0.00074	0.00017 -0.00189	-0.00042 -0.00158
0.00106 0.00582	0.00065 -0.00037	-0.00094 -0.01664	-0.00107 -0.01067	-0.00120 0.00601	0.00067 0.01588	0.00178 0.00537	0.00060 -0.01283	-0.00144 -0.01093	-0.00123 0.00969

M= 15 G= 1.37979631

MI/MA

0.	0.	0.	0.	0.	0.	0.	0.	0.00001	0.00006
0.	0.	0.	0.	0.	0.	0.	0.	0.00012	0.00006
0.	0.	0.	0.	0.	0.	-0.00007	0.00002	0.00009	0.00005
0.	0.	0.	0.	0.	0.	0.00006	0.00021	0.00012	-0.00014
0.	0.	0.	0.	-0.00017	-0.00013	0.00003	0.00016	0.00010	-0.00009
0.	0.	0.	0.	-0.00040	0.00012	0.00052	0.00030	-0.00032	-0.00048
0.	0.	-0.00018	-0.00041	-0.00032	0.00007	0.00039	0.00024	-0.00023	-0.00037
0.	0.	-0.00108	-0.00152	0.00037	0.00108	0.00115	-0.00112	-0.00176	0.00041
0.00068	-0.00065	-0.00154	-0.00121	0.00026	0.00145	0.00091	-0.00085	-0.00136	0.00030
-0.00618	-0.01474	-0.01153	0.00246	0.01307	0.00867	-0.00810	-0.01303	0.00286	0.01302

M= 16 G= 1.37979631

MI/MA

0.	0.	0.	0.	0.	0.	0.	0.	0.00004	0.00003
0.	0.	0.	0.	0.	0.	0.	0.	0.00006	-0.00003
0.	0.	0.	0.	0.	0.	0.00000	0.00006	0.00005	-0.00002
0.	0.	0.	0.	0.	0.	0.00015	0.00012	-0.00006	-0.00016
0.	0.	0.	0.	-0.00011	-0.00008	0.00011	0.00010	-0.00004	-0.00012
0.	0.	0.	0.	0.00001	0.00038	0.00033	-0.00013	-0.00041	-0.00008
0.	0.	-0.00032	-0.00029	-0.00000	0.00029	0.00026	-0.00009	-0.00032	-0.00007
0.	0.	-0.00146	-0.00001	0.00147	0.00130	-0.00049	-0.00162	-0.00033	0.00150
-0.00043	-0.00127	-0.00116	-0.00003	0.00113	0.00102	-0.00036	-0.00125	-0.00027	0.00115
-0.01295	-0.01180	-0.00031	0.01152	0.01042	-0.00370	-0.01277	-0.00270	0.01176	0.00568

[illegible]

wl/wn

0. 0.	0. 0.	0. 0.	0. 0.	0. 0.	0. 0.	0. 0.	0. 0.	0.00002 -0.00001	-0.00000 -0.00006
0. 0.	0. 0.	0. 0.	0. 0.	0. 0.	0. 0.	0.00003 0.00011	0.00004 -0.00001	-0.00000 -0.00012	-0.00004 -0.00006
0. 0.	0. 0.	0. 0.	0. 0.	-0.00004 0.00027	0.00007 0.00031	0.00002 -0.00001	-0.00008 -0.00032	-0.00002 -0.00018	-0.00002 0.00024
0. 0.	0. 0.	-0.00025 -0.00026	-0.00005 0.00110	0.00020 0.00131	0.00024 -0.00002	-0.00000 -0.00133	-0.00024 -0.00077	-0.00014 0.00097	0.00010 0.00112
-0.00105 -0.01164	-0.00100 -0.00242	-0.00022 0.00014	0.00004 0.01105	0.00102 -0.00004	-0.00000 -0.01110	-0.00103 -0.00651	-0.00060 0.00003	0.00074 0.00937	0.00007 -0.00581

[illegible]

[illegible]

0. 0.	0. 0.	0. 0.	0. 0.	0. 0.	0. 0.	0. 0.	0. 0.	[illegible] -0.00004	-0.00001 -0.00003
0. 0.	0. 0.	0. 0.	0. 0.	0. 0.	0. 0.	0.00003 0.00002	0.00001 -0.00000	-0.00003 -0.00007	-0.00003 0.00004
0. 0.	0. 0.	0. 0.	0. 0.	0.00005 0.00027	0.00007 0.00006	0.00002 -0.00023	-0.00004 -0.00022	-0.00004 0.00011	0.00003 0.00027
0. 0.	0. 0.	-0.00000 0.00074	0.00014 0.00122	0.00021 0.00036	0.00005 -0.00099	-0.00017 -0.00097	-0.00017 0.00045	0.00000 0.00117	0.00020 -0.00006
-0.00009 -0.00399	-0.00035 0.00601	0.00060 0.01092	0.00095 0.00260	0.00024 -0.00075	-0.00076 -0.00065	-0.00076 0.00394	0.00034 0.01042	0.00091 -0.00045	-0.00004 -0.01052

M= 19 G= 1.57079631

WI/WR

0.	0.	0.	0.	0.	0.	0.	0.	-0.00001	-0.00001
0.	0.	0.	0.	0.	0.	0.	0.	-0.00003	0.00000
0.	0.	0.	0.	0.	0.	0.00001	-0.00002	-0.00002	0.00000
0.	0.	0.	0.	0.	0.	-0.00005	-0.00007	0.00000	0.00007
0.	0.	0.	0.	0.00006	0.00003	-0.00003	-0.00005	0.00000	0.00005
0.	0.	0.	0.	0.00010	-0.00015	-0.00021	0.00001	0.00022	0.00008
0.	0.	0.00009	0.00018	0.00008	-0.00011	-0.00016	0.00000	0.00017	0.00007
0.	0.	0.00109	0.00050	-0.00067	-0.00100	0.00003	0.00102	0.00040	-0.00089

M= 20 G= 1.57079631

WI/WR

0.	0.	0.	0.	0.	0.	0.	0.	-0.00001	-0.00000
0.	0.	0.	0.	0.	0.	0.	0.	-0.00001	0.00002
0.	0.	0.	0.	0.	0.	-0.00001	-0.00002	-0.00000	0.00001
0.	0.	0.	0.	0.	0.	-0.00006	-0.00002	0.00005	0.00004
0.	0.	0.	0.	0.00003	-0.00002	-0.00004	-0.00001	0.00004	0.00003
0.	0.	0.	0.	-0.00008	-0.00019	-0.00005	0.00016	0.00013	-0.00010
0.	0.	0.00015	0.00010	-0.00006	-0.00015	-0.00004	0.00012	0.00010	-0.00008
0.	0.	0.00062	-0.00039	-0.00093	-0.00027	0.00077	0.00066	-0.00051	-0.00081
0.00025	0.00074	0.00049	-0.00029	-0.00073	-0.00021	0.00060	0.00051	-0.00039	-0.00063
0.00936	0.00624	-0.00375	-0.00925	-0.00273	0.00762	0.00655	-0.00499	-0.00006	0.00337

								0.00704 0.00334	0.00074 0.00395
						0.00005 0.00005	0.00076 0.00060	0.01003 0.00569	0.11005 0.03412

								0.01275 0.00579	0.00068 0.01060
						0.00036 0.00035	0.00275 0.00212	0.01790 0.00968	0.09583 0.02624
		0.00000 0.00000	0.00000 0.00001	0.00003 0.00008	0.00026 0.00052	0.00172 0.00291	0.00977 0.01287	0.04469 0.04003	0.15277 0.06777
0.00000 0.00000	0.00000 0.00000	0.00000 0.00001	0.00002 0.00008	0.00013 0.00057	0.00090 0.00331	0.00520 0.01558	0.02447 0.05630	0.08844 0.13797	0.21672 0.14945

U= 3 G= 3.14159262

wl/wR

0. 0.	0. 0.	0. 0.	0. 0.	0. 0.	0. 0.	0. 0.	0. 0.	0.01615 0.00680	0.06602 0.01225
0. 0.	0. 0.	0. 0.	0. 0.	0. 0.	0. 0.	0.00106 0.00100	0.00525 0.00305	0.02209 0.01094	0.07949 0.01569
0. 0.	0. 0.	0. 0.	0. 0.	0.00007 0.00012	0.00043 0.00060	0.00210 0.00248	0.00982 0.00823	0.03282 0.01941	0.08782 0.02041
0. 0.	0. 0.	0.00001 0.00002	0.00004 0.00010	0.00022 0.00091	0.00110 0.00219	0.00482 0.00781	0.01756 0.02164	0.05062 0.04046	0.10400 0.02574
0.00000 0.00000	0.00000 0.00003	0.00003 0.00016	0.00017 0.00082	0.00086 0.00362	0.00379 0.01344	0.01408 0.04004	0.04193 0.08828	0.09244 0.11812	0.12369 0.01621

W= 4 G= 3.14159262

wl/wR

0. 0.	0. 0.	0. 0.	0. 0.	0. 0.	0. 0.	0. 0.	0. 0.	0.01688 0.00627	0.04929 0.00560
0. 0.	0. 0.	0. 0.	0. 0.	0. 0.	0. 0.	0.00204 0.00185	0.00735 0.00501	0.02218 0.00943	0.05303 0.00530
0. 0.	0. 0.	0. 0.	0. 0.	0.00026 0.00042	0.00107 0.00149	0.00393 0.00441	0.01217 0.01013	0.03042 0.01515	0.05688 0.00275
0. 0.	0. 0.	0.00004 0.00011	0.00018 0.00046	0.00075 0.00169	0.00276 0.00525	0.00870 0.01322	0.02246 0.02471	0.04418 0.02664	0.05570 -0.00864
0.00001 0.00009	0.00004 0.00023	0.00018 0.00098	0.00077 0.00365	0.00287 0.01167	0.00916 0.03077	0.02417 0.06308	0.04955 0.08856	0.06956 0.05212	0.04093 -0.07114

[illegible]

[illegible]									
0. 0.	0. 0.	0. 0.	0. 0.	0. 0.	0. 0.	0. 0.	0. 0.	0.01523 0.00456	0.03306 0.00011
0. 0.	0. 0.	0. 0.	0. 0.	0. 0.	0. 0.	0.00302 0.00257	0.00834 0.00507	0.01087 0.00605	0.03227 -0.00254
0. 0.	0. 0.	0. 0.	0. 0.	[illegible]	[illegible]	[illegible]	[illegible]	[illegible] 0.00777	[illegible] [illegible]
0. 0.	0. 0.	[illegible]	[illegible]	0.00174 [illegible]	[illegible]	0.01170 [illegible]	0.02227 [illegible]	0.02976 0.00759	0.01033 -0.02578
[illegible]	[illegible]	[illegible]	[illegible]	[illegible]	[illegible]	[illegible]	[illegible]	[illegible] -0.01771	[illegible] [illegible]

[illegible]

[illegible]									
0. 0.	0. 0.	0. 0.	0. 0.	0. 0.	0. 0.	0. 0.	0. 0.	[illegible]	0.01937 -0.00336
0. 0.	0. 0.	0. 0.	0. 0.	0. 0.	0. 0.	[illegible]	[illegible]	[illegible]	[illegible] [illegible]
0. 0.	0. 0.	0. 0.	0. 0.	[illegible] 0.00164	[illegible]	[illegible]	[illegible]	[illegible]	[illegible] -0.01203
0. 0.	0. 0.	[illegible]	[illegible]	[illegible]	[illegible] 0.01122	[illegible] 0.01462	[illegible]	0.01367 -0.00763	[illegible] -0.02514
[illegible]	[illegible]	[illegible]	[illegible] 0.02066	[illegible] 0.03040	0.02015 0.05460	[illegible] 0.04906	0.02949 0.00414	0.00216 -0.05393	-0.02024 -0.04725

U= 7 G= 3.14159262

mi/mR

0.	0.	0.	0.	0.	0.	0.	0.	0.00813	0.00930
0.	0.	0.	0.	0.	0.	0.	0.	0.00034	-0.00466
0.	0.	0.	0.	0.	0.	0.00379	0.00442	0.00801	0.00517
0.	0.	0.	0.	0.	0.	0.00252	0.00226	-0.00089	-0.00718
0.	0.	0.	0.	0.00168	0.00335	0.00416	0.00410	0.00090	-0.00112
0.	0.	0.	0.	0.00234	0.00390	0.00462	0.00232	-0.00419	-0.01070
0.	0.	0.00082	0.00204	0.00435	0.00772	0.01064	0.00955	0.00132	-0.01030
0.	0.	0.00221	0.00466	0.00815	0.01088	0.00891	-0.00092	-0.01362	-0.01367
0.00052	0.00148	0.00367	0.00791	0.01424	0.02015	0.01944	0.00606	-0.01466	-0.02055
0.00329	0.00818	0.01762	0.03172	0.04491	0.04331	0.01350	-0.03266	-0.04578	0.00591

U= 8 G= 3.14159262

mi/mR

0.	0.	0.	0.	0.	0.	0.	0.	0.00457	0.00300
0.	0.	0.	0.	0.	0.	0.	0.	-0.00100	-0.00427
0.	0.	0.	0.	0.	0.	0.00331	0.00426	0.00340	-0.00041
0.	0.	0.	0.	0.	0.	0.00171	0.00048	-0.00247	-0.00536
0.	0.	0.	0.	0.00209	0.00357	0.00478	0.00428	0.00075	-0.00450
0.	0.	0.	0.	0.00266	0.00332	0.00237	-0.00107	-0.00537	-0.00564
0.	0.	0.00142	0.00291	0.00504	0.00696	0.00670	0.00234	-0.00477	-0.00803
0.	0.	0.00359	0.00614	0.00828	0.00794	0.00162	-0.00739	-0.01069	-0.00892
0.00123	0.00291	0.00601	0.01052	0.01491	0.01495	0.00664	-0.00748	-0.01535	-0.00440
0.00741	0.01531	0.02679	0.03771	0.04807	0.01741	-0.01904	-0.03908	-0.01119	0.03536

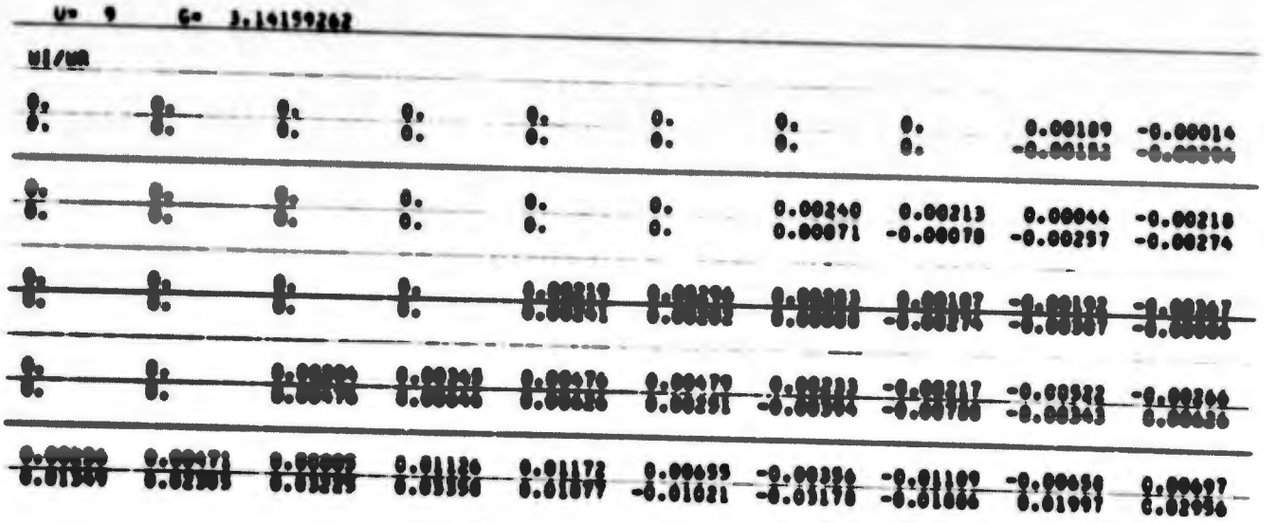

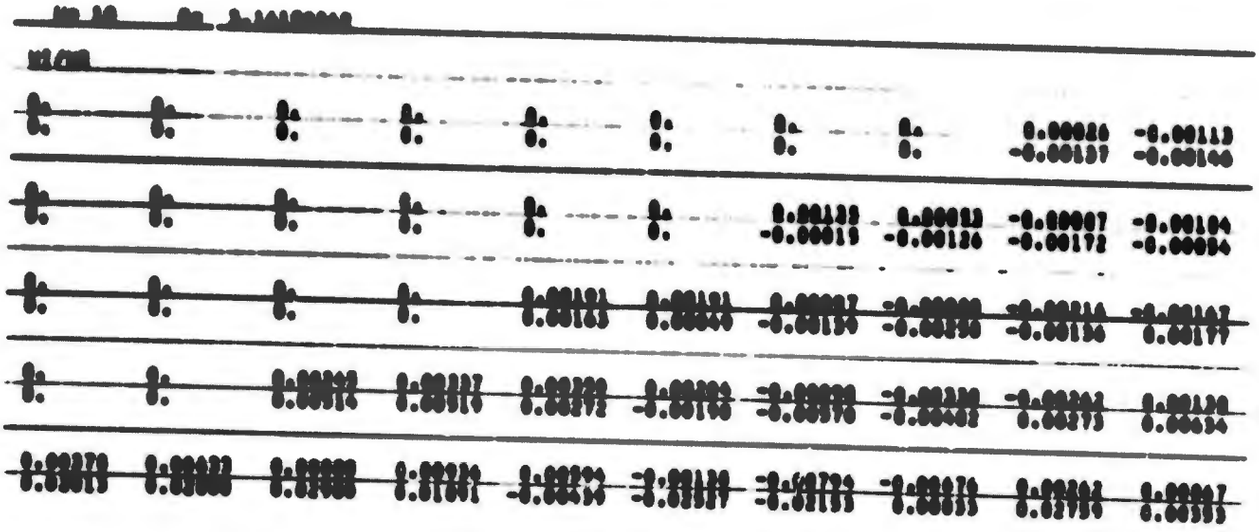

U= 11 G= 3.14159262

MI/MR

0. 0.	0. 0.	0. 0.	0. 0.	0. 0.	0. 0.	0. 0.	0. 0.	-0.00043 -0.00086	-0.00090 -0.00033
0. 0.	0. 0.	0. 0.	0. 0.	0. 0.	0. 0.	0.00045 -0.00062	-0.00034 -0.00107	-0.00101 -0.00062	-0.00062 0.00062
0. 0.	0. 0.	0. 0.	0. 0.	[illegible]	[illegible]	[illegible]	[illegible]	[illegible]	[illegible]
0. 0.	0. 0.	0.00247 0.00433	0.00262 0.00265	0.00171 -0.00084	-0.00027 -0.00410	-0.00220 -0.00386	-0.00222 0.00067	0.00021 0.00471	0.00251 0.00284
0.00000 0.02461	0.00703 0.02683	0.00760 0.01644	0.00527 -0.00850	-0.00014 -0.01985	-0.00566 -0.02162	-0.00618 0.00025	0.00007 0.02243	0.00641 0.01262	0.00360 -0.01700

MR 11 G= 3.14159262

MI/MR

0. 0.	0. 0.	0. 0.	0. 0.	0. 0.	0. 0.	0. 0.	0. 0.	-0.00021 -0.00091	-0.00047 0.00029
0. 0.	0. 0.	0. 0.	0. 0.	0. 0.	0. 0.	-0.00011 -0.00066	-0.00036 -0.00053	-0.00058 0.00017	-0.00001 0.00001
0. 0.	0. 0.	0. 0.	0. 0.	[illegible]	[illegible]	[illegible]	[illegible]	[illegible]	[illegible]
0. 0.	0. 0.	0.00200 0.00347	0.00142 -0.00017	0.00005 -0.00294	-0.00144 -0.00342	-0.00179 -0.00047	-0.00034 0.00334	0.00137 0.00206	0.00147 -0.00170
0.00372 0.02395	0.00427 0.01770	0.00463 0.00212	0.00055 -0.01540	-0.00403 -0.02046	-0.00536 -0.00507	-0.00133 0.01661	0.00435 0.01661	0.00435 -0.00022	-0.00215 -0.01976

[illegible] U= 13 G= 3.14159262

[illegible]

0.	0.	0.	0.	0.	0.	0.	0.	-0.00031	-0.00005
								0.00008	0.00006
0.	0.	0.	0.	0.	0.	-0.00032	-0.00040	-0.00011	0.00033
						-0.00042	-0.00002	0.00046	0.00045
0.	0.	0.	0.	[illegible]	[illegible]	[illegible]	[illegible]	[illegible]	[illegible]
0.	0.	[illegible]	[illegible]	[illegible]	[illegible]	[illegible]	[illegible]	0.00132	-0.00008
								-0.00038	-0.00008
[illegible]	[illegible]	[illegible]	[illegible]	[illegible]	[illegible]	[illegible]	[illegible]	[illegible]	[illegible]

[illegible] U= 14 G= [illegible]

[illegible]

0.	0.	0.	0.	0.	0.	0.	0.	-0.00008	0.00013
								0.00019	0.00002
0.	0.	0.	0.	0.	0.	-0.00027	-0.00013	0.00016	0.00028
						-0.00009	0.00025	0.00035	0.00002
0.	0.	0.	0.	[illegible]	[illegible]	[illegible]	[illegible]	[illegible]	[illegible]
				-0.00072	-0.00032	0.00045	0.00076	0.00012	-0.00012
0.	0.	0.00026	-0.00062	-0.00109	-0.00063	0.00048	0.00107	0.00030	-0.00092
		-0.00150	-0.00246	-0.00133	0.00119	0.00246	0.00062	-0.00216	-0.00166
0.00200	0.00114	-0.00201	-0.00378	-0.00232	0.00149	0.00365	0.00115	-0.00302	-0.00249
0.00568	-0.00097	-0.01603	-0.01032	0.00664	0.01626	0.00911	-0.01345	-0.01112	0.01020

U= 15 G= 3.14159262

WI/WR

0. 0.	0. 0.	0. 0.	0. 0.	0. 0.	0. 0.	0. 0.	0. 0.	0.00006 0.00015	C.00013 0.00004
0. 0.	0. 0.	0. 0.	0. 0.	0. 0.	0. 0.	-0.00012 0.00013	0.00007 0.00026	0.00019 0.00009	C.00009 -0.00021
0. 0.	0. 0.	0. 0.	0. 0.	-0.00024 -0.00054	-0.00029 0.00022	0.00018 0.00054	0.00024 0.00037	0.00018 -0.00042	-0.00023 -0.00054
0. 0.	0. 0.	-0.00041 -0.00205	-0.00085 -0.00142	-0.00061 0.00097	0.00020 0.00203	0.00082 0.00110	0.00047 -0.00131	-0.00051 -0.00187	-0.00076 0.00093
0.00123 -0.00667	-0.00140 -0.01493	-0.00313 -0.01131	-0.00237 0.00295	0.00062 0.01424	0.00298 0.00897	0.00179 -0.00857	-0.00179 -0.01331	-0.00279 0.00315	0.00066 0.01426

WR 16 G= 3.14159262

WI/WR

0. 0.	0. 0.	0. 0.	0. 0.	0. 0.	0. 0.	0. 0.	0. 0.	0.00008 0.00005	0.00006 -0.00007
0. 0.	0. 0.	0. 0.	0. 0.	0. 0.	0. 0.	0.00002 0.00018	0.00012 0.00012	0.00009 -0.00010	-0.00006 -0.00020
0. 0.	0. 0.	0. 0.	0. 0.	-0.00021 0.00000	0.00002 0.00044	0.00024 0.00032	0.00019 -0.00020	-0.00010 -0.00047	-0.00024 -0.00005
0. 0.	0. 0.	-0.00066 -0.00141	-0.00056 0.00014	0.00003 0.00159	0.00060 0.00130	0.00051 -0.00062	-0.00022 -0.00173	-0.00066 -0.00028	-0.00012 0.00165
-0.00094 -0.01313	-0.00258 -0.01166	-0.00229 0.00007	0.00001 0.01186	0.00233 0.01042	0.00205 -0.00405	-0.00080 -0.01307	-0.00257 -0.00258	-0.00051 0.01214	0.00238 0.00575

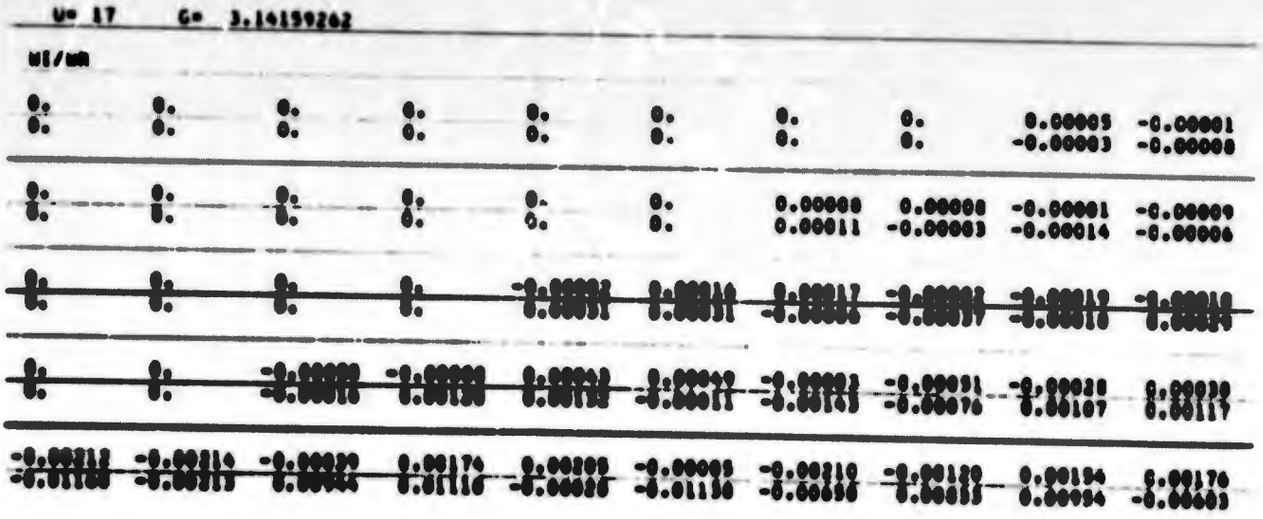
U= 17 G= 3.14159262
MI/MR

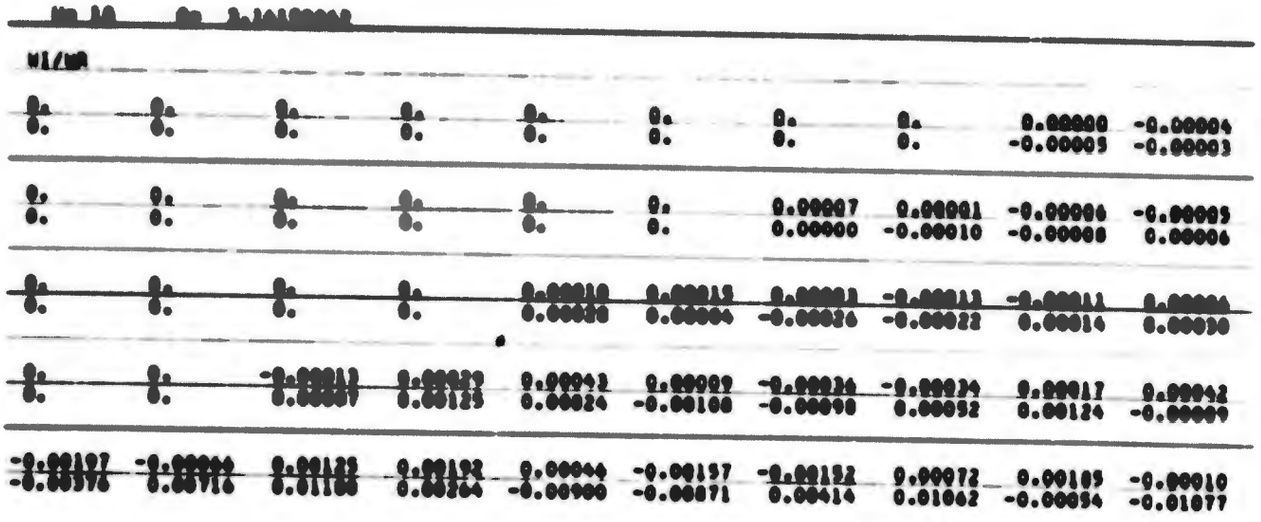
MI/MR

[illegible] 19 [illegible] 3.14159265

ml/mR

0.	0.	0.	0.	0.	0.	0.	0.	-0.00002	-0.00002
0.	0.	0.	0.	0.	0.	0.	0.	-0.00003	0.00001
0.	0.	0.	0.	0.	0.	0.00002	-0.00004	-0.00005	0.00001
0.	0.	0.	0.	0.	0.	-0.00006	-0.00007	0.00001	0.00009
0.	0.	0.	0.	0.00012	0.00003	-0.00008	-0.00011	0.00001	0.00011
0.	0.	0.	0.	0.00004	-0.00017	-0.00022	0.00003	0.00025	0.00008
0.	0.	0.00019	0.00037	0.00016	-0.00023	-0.00024	0.00002	0.00028	0.00013
0.	0.	0.00112	0.00047	-0.00074	-0.00103	0.00046	0.00108	0.00043	-0.00036
-0.00002	0.00005	0.00172	0.00079	-0.00106	-0.00158	0.00004	0.00162	0.00043	-0.00142
0.00311	0.01038	0.00479	-0.00041	-0.00954	0.00036	0.00977	0.00381	-0.00037	-0.00367

[illegible] 20 [illegible] 3.14159265

ml/mR

0.	0.	0.	0.	0.	0.	0.	0.	-0.00002	-0.00000
0.	0.	0.	0.	0.	0.	0.	0.	-0.00000	0.00003
0.	0.	0.	0.	0.	0.	-0.00002	-0.00004	-0.00001	0.00003
0.	0.	0.	0.	0.	0.	-0.00004	-0.00001	0.00006	0.00004
0.	0.	0.	0.	0.00006	-0.00004	-0.00009	-0.00002	0.00008	0.00004
0.	0.	0.	0.	-0.00010	-0.00020	-0.00004	0.00018	0.00014	-0.00012
0.	0.	0.00030	0.00019	-0.00013	-0.00030	-0.00008	0.00023	0.00021	-0.00017
0.	0.	0.00060	-0.00044	-0.00097	-0.00025	0.00083	0.00067	-0.00055	-0.00085
0.00052	0.00149	0.00097	-0.00062	-0.00147	-0.00042	0.00122	0.00104	-0.00001	-0.00128
0.00947	0.00617	-0.00393	-0.00036	-0.00266	0.00779	0.00660	-0.00514	-0.00018	0.00347

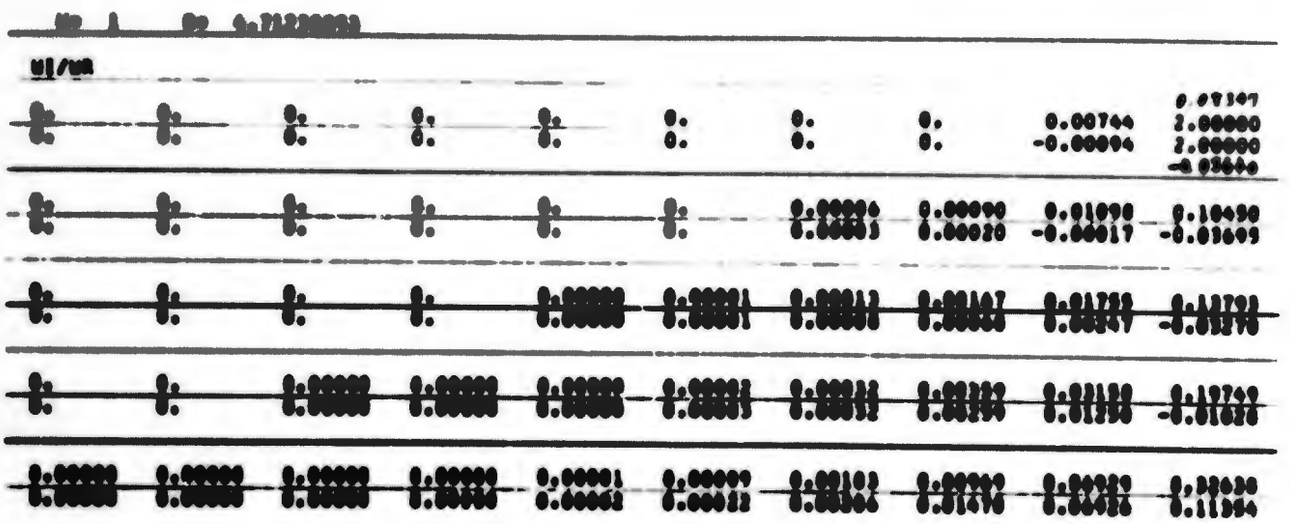

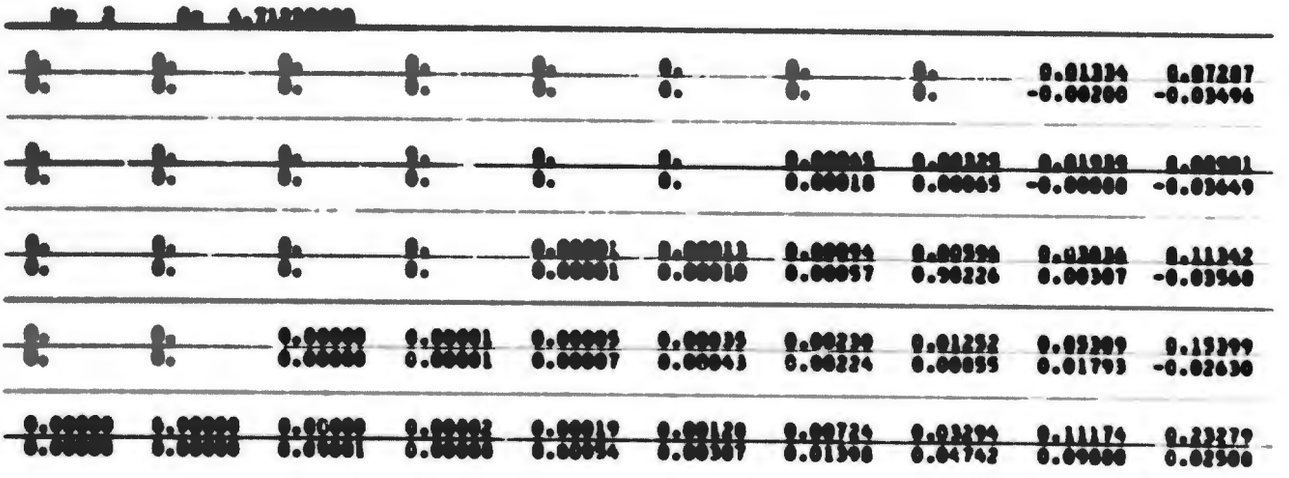

N= 3 θ= 4.71238893

ωI/ωR

0. 0.	0. 0.	0. 0.	0. 0.	0. 0.	0. 0.	0. 0.	0. 0.	0.01663 -0.00320	0.05763 -0.03237
0. 0.	0. 0.	0. 0.	0. 0.	0. 0.	0. 0.	0.00131 0.00046	0.00613 0.00101	0.02350 -0.00234	0.06717 -0.03404
0. 0.	0. 0.	0. 0.	0. 0.	0.00010 0.00010	0.00035 0.00043	0.00262 0.00155	0.01024 0.00565	0.02242 0.00604	0.07082 -0.03742
0. 0.	0. 0.	0.00001 0.00002	0.00005 0.00004	0.00030 0.00044	0.00131 0.00166	0.00041 0.00596	0.02227 0.01565	0.03070 0.01324	0.07062 -0.04272
0.00000 0.00000	0.00001 0.00003	0.00004 0.00015	0.00024 0.00076	0.00123 0.00342	0.00537 0.01241	0.01949 0.03536	0.05509 0.07240	0.11273 0.07424	0.11062 -0.06562

N= 4 θ= 4.71238893

ωI/ωR

0. 0.	0. 0.	0. 0.	0. 0.	0. 0.	0. 0.	0. 0.	0. 0.	0.01694 -0.00441	0.04061 -0.02055
0. 0.	0. 0.	0. 0.	0. 0.	0. 0.	0. 0.	0.00250 0.00003	0.00066 0.00094	0.02290 -0.00430	0.04300 -0.03164
0. 0.	0. 0.	0. 0.	0. 0.	0.00035 0.00032	0.00162 0.00104	0.00492 0.00259	0.01693 0.00378	0.03294 -0.00311	0.04320 -0.03697
0. 0.	0. 0.	0.00005 0.00010	0.00025 0.00041	0.00104 0.00145	0.00376 0.00426	0.01140 0.00966	0.02790 0.01401	0.04094 0.00125	0.04177 -0.05036
0.00001 0.00005	0.00005 0.00022	0.00026 0.00094	0.00111 0.00349	0.00411 0.01096	0.01292 0.02818	0.03320 0.05507	0.06407 0.06043	0.08061 0.01461	0.01721 -0.11140

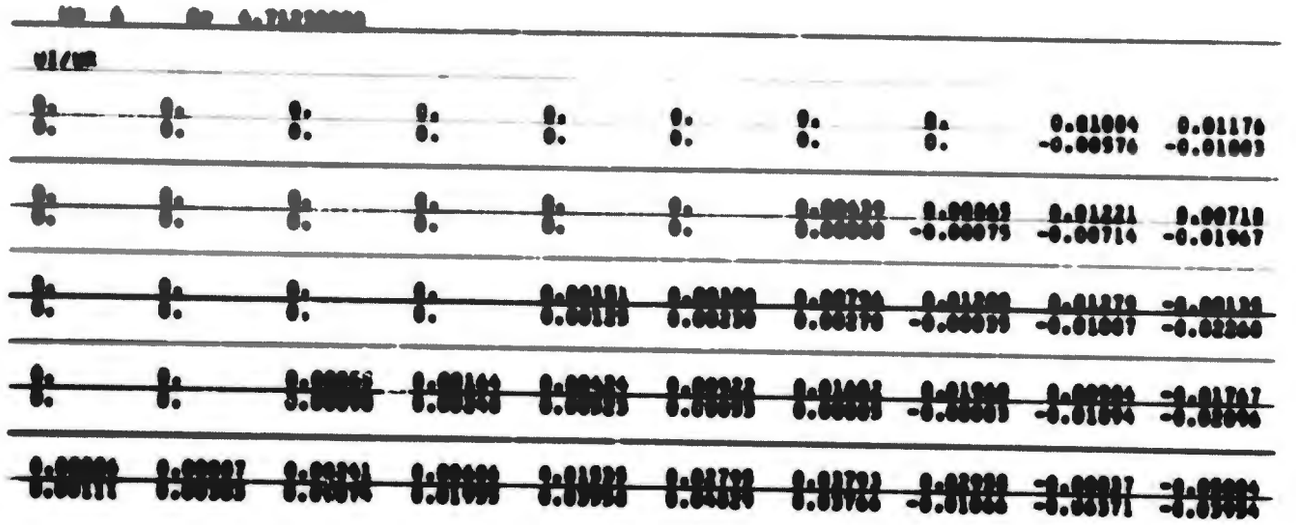

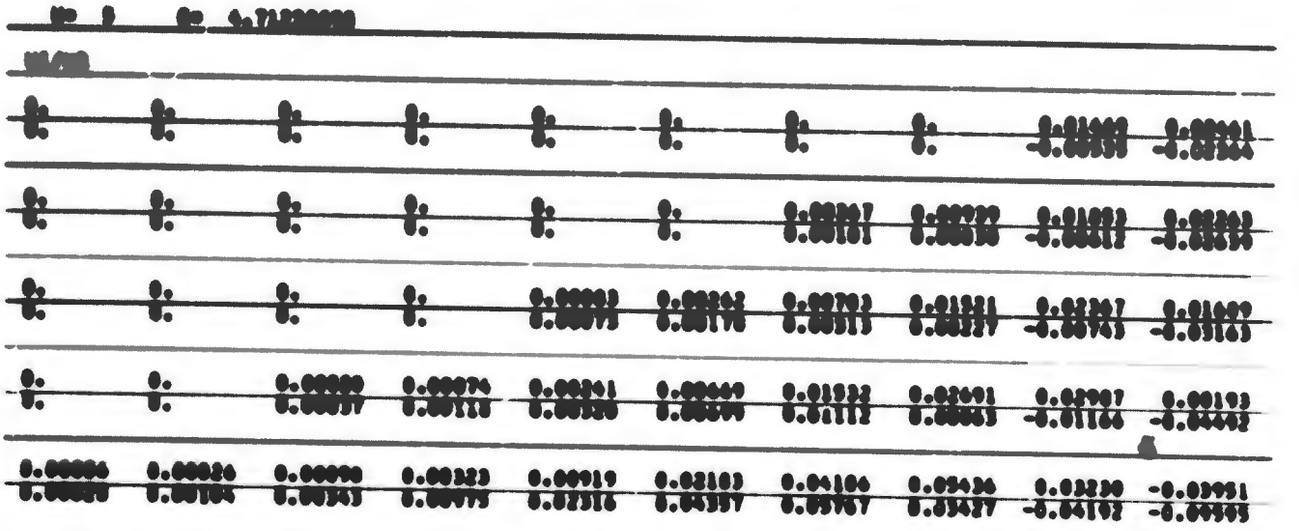

	0.	0.	0.	0.	0.	0.	0.	0.00656	0.00307
	0.	0.	0.	0.	0.	0.	0.	-0.00549	-0.01235
	0.	0.	0.	0.	0.	0.00440	0.00657	0.00592	-0.00181
	0.	0.	0.	0.	0.	0.00042	-0.00102	-0.00604	-0.01252
	0.	0.	0.	0.00223	0.00428	0.00734	0.00833	0.00134	-0.00718
	0.	0.	0.	0.00167	0.00227	0.00133	-0.00204	-0.00946	-0.01242
	0.	0.00117	0.00285	0.00595	0.01017	0.01301	0.00832	-0.00424	-0.01074
	0.	0.00107	0.00482	0.00659	0.00766	0.00350	-0.00761	-0.01760	-0.00660
0.00077	0.00215	0.00532	0.01133	0.02005	0.02749	0.02437	0.00878	-0.02716	-0.02822
0.00320	0.00708	0.01603	0.02976	0.04003	0.03620	0.00464	-0.04034	-0.04480	0.01761

	0.	0.	0.	0.	0.	0.	0.	-0.00284	-0.00184
	0.	0.	0.	0.	0.	0.	0.	-0.00458	-0.00727
	0.	0.	0.	0.	0.	0.00367	0.00388	0.00113	-0.00817
	0.	0.	0.	0.	0.	-0.00024	-0.00290	-0.00959	-0.00617
	0.	0.	0.	0.00270	0.00444	0.00817	0.00367	-0.00288	-0.00824
	0.	0.	0.	0.00177	0.00197	-0.00045	-0.00440	-0.00734	-0.00361
	0.	0.00299	0.00494	0.00688	0.00898	0.00747	0.00018	-0.00988	-0.01191
	0.	0.00317	0.00918	0.00636	0.00434	-0.00247	-0.01059	-0.01017	0.00444
0.00180	0.00424	0.00868	0.01498	0.02060	0.01964	0.00653	-0.01458	-0.02370	-0.00326
0.00719	0.01473	0.02944	0.03496	0.03337	0.01109	-0.02475	-0.04024	-0.00554	0.0[illegible]329

[illegible] 9 [illegible] 4.71238893

wi/wa

0. 0.	0. 0.	0. 0.	0. 0.	0. 0.	0. 0.	0. 0.	0. 0.	0.00033 -0.00327	-0.00305 -0.00311
0. 0.	0. 0.	0. 0.	0. 0.	0. 0.	0. 0.	0.00246 -0.00085	0.00141 -0.00299	-0.00151 -0.00355	-0.00490 -0.00157
[illegible]	[illegible]	[illegible]	[illegible]	[illegible]	[illegible]	[illegible]	[illegible]	[illegible]	[illegible]
0. 0.	0. 0.	0.00206 0.00414	0.00473 0.00324	0.00627 0.00426	0.00576 -0.00009	0.00163 -0.00622	-0.00494 -0.00828	-0.00823 -0.00180	-0.0024 0.00092
0.00345 0.01305	0.00683 0.02207	0.01155 0.03032	0.01507 0.03035	0.01588 0.01439	0.00753 -0.01443	-0.00756 -0.03944	-0.01751 -0.01615	-0.00845 0.02526	0.01323 0.03168

[illegible] 10 [illegible] 4.71238893

wi/wa

0. 0.	0. 0.	0. 0.	0. 0.	0. 0.	0. 0.	0. 0.	0. 0.	-0.00094 -0.00188	-0.00265 -0.00076
0. 0.	0. 0.	0. 0.	0. 0.	0. 0.	0. 0.	0.00115 -0.00117	-0.00028 -0.00200	-0.00220 -0.00151	-0.00280 0.00093
[illegible]	[illegible]	[illegible]	[illegible]	[illegible]	[illegible]	[illegible]	[illegible]	[illegible]	[illegible]
0. 0.	0. 0.	0.00341 0.00433	0.00455 0.00389	0.00442 0.00181	0.00196 -0.00159	-0.00240 -0.00631	-0.00551 -0.00292	-0.00329 0.00496	0.00345 0.02794
0.00551 0.01948	0.00914 0.02659	0.01293 0.02748	0.01295 0.01577	0.00743 -0.00795	-0.00356 -0.02691	-0.01268 -0.02028	-0.00936 0.01181	0.00557 0.02997	0.01412 0.00172

U= 11 G= 4.71238893

MI/MR

0. 0.	0. 0.	0. 0.	0. 0.	0. 0.	0. 0.	0. 0.	0. 0.	-0.00118 -0.00072	-0.00152 0.00050
0. 0.	0. 0.	0. 0.	0. 0.	0. 0.	0. 0.	0.00011 -0.00112	-0.00102 -0.00112	-0.00167 -0.00000	-0.00000 0.00162
0. 0.	0. 0.	0. 0.	0. 0.	-0.00155 -0.00016	-0.00042 -0.00158	-0.00099 -0.00197	-0.00217 -0.00081	-0.00147 0.00167	0.00110 0.00273
0. 0.	0. 0.	0.00338 0.00345	0.00342 0.00168	0.00189 -0.00164	-0.00188 -0.00468	-0.00344 -0.00358	-0.00309 0.00285	0.00187 0.00379	0.00319 0.00176
0.00739 0.02355	0.01009 0.02401	0.01067 0.01615	0.00691 -0.00298	-0.00124 -0.02134	-0.00918 -0.02115	-0.00985 0.00354	0.00189 0.02455	0.01022 0.01317	0.00322 -0.00868

U= 12 G= 4.71238893

MI/MR

0. 0.	0. 0.	0. 0.	0. 0.	0. 0.	0. 0.	0. 0.	0. 0.	-0.00086 0.00003	-0.00047 0.00081
0. 0.	0. 0.	0. 0.	0. 0.	0. 0.	0. 0.	-0.00047 -0.00077	-0.00098 -0.00027	-0.00072 0.00071	0.00039 0.00120
0. 0.	0. 0.	0. 0.	0. 0.	0.00060 -0.00079	-0.00041 -0.00138	-0.00134 -0.00091	-0.00123 0.00045	0.00023 0.00104	0.00144 0.00006
0. 0.	0. 0.	0.00267 0.00165	0.00169 -0.00100	-0.00038 -0.00344	-0.00244 -0.00324	-0.00261 0.00037	-0.00009 0.00408	0.00280 0.00284	0.00221 -0.00275
0.00827 0.02265	0.00890 0.01595	0.00626 0.00026	0.00010 -0.01665	-0.00654 -0.02035	-0.00799 -0.00356	-0.00140 0.01835	0.00720 0.01681	0.00660 -0.00991	-0.00389 -0.02121

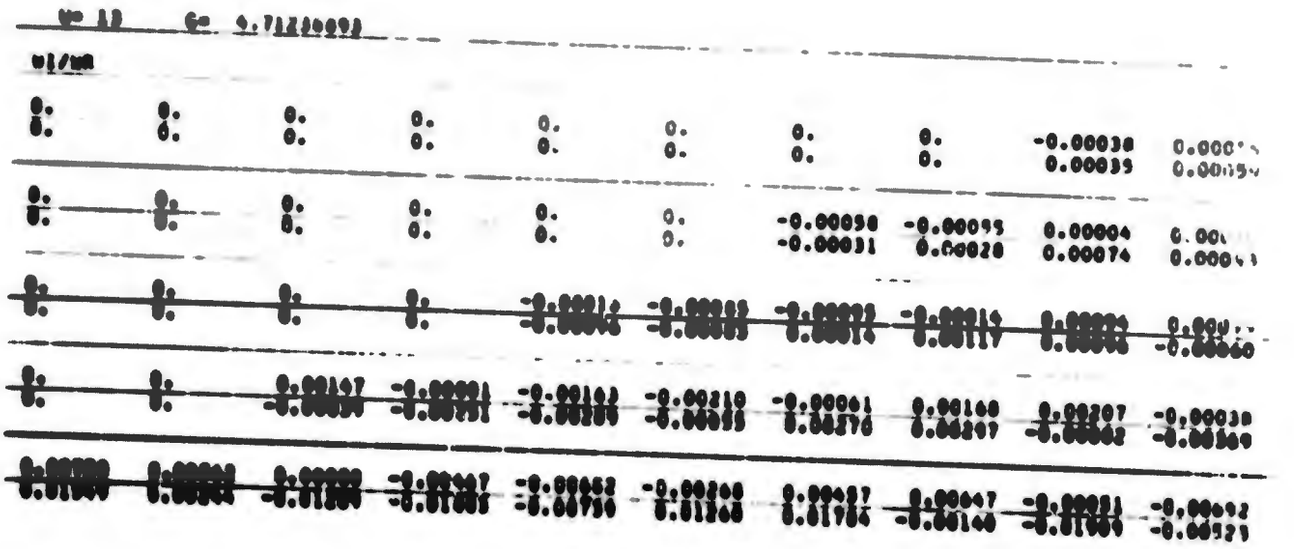

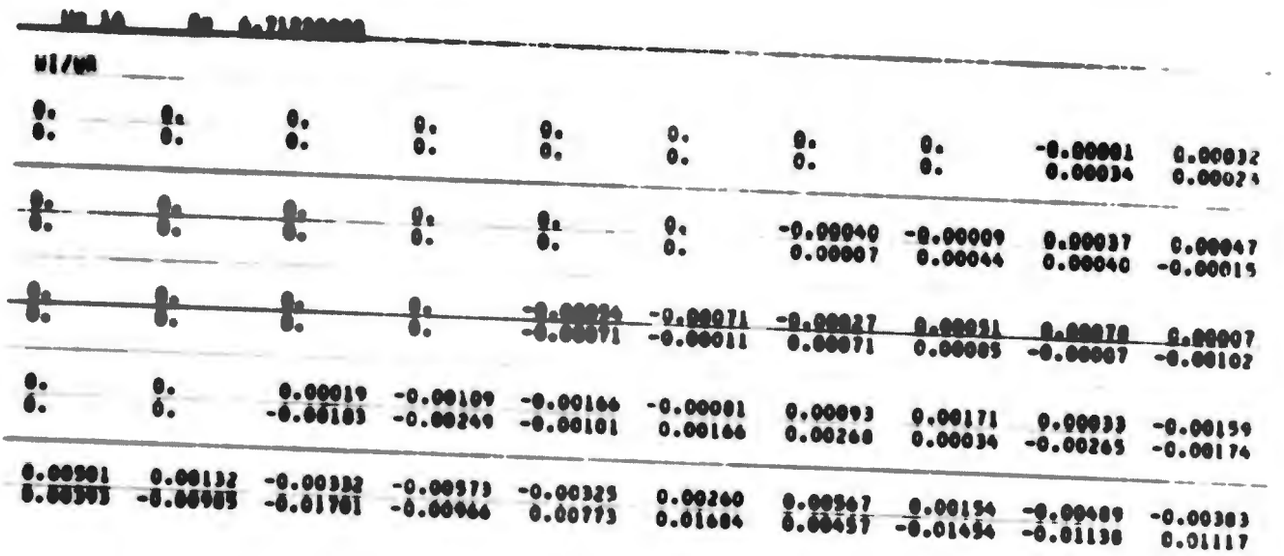

M= 15 G= 4.71238893

MI/MR

0. 0.	0. 0.	0. 0.	0. 0.	0. 0.	0. 0.	0. 0.	0. 0.	0.00016 0.00018	0.00023 -0.00004
0. 0.	0. 0.	0. 0.	0. 0.	0. 0.	0. 0.	-0.00012 0.00025	0.00018 0.00031	0.00033 0.00002	0.00010 -0.00035
0. 0.	0. 0.	0. 0.	0. 0.	-0.00023 -0.00052	-0.00029 0.00041	0.00025 0.00049	0.00007 0.00018	0.00013 -0.00042	-0.00004 -0.00042
0. 0.	0. 0.	-0.00073 -0.00211	-0.00130 -0.00122	-0.00004 0.00091	0.00045 0.00224	0.00132 0.00097	0.00065 -0.00167	-0.00092 -0.00204	-0.00122 0.00078
0.00155 -0.00741	-0.00233 -0.01516	-0.00476 -0.01087	-0.00341 0.00376	0.00119 0.01482	0.00465 0.00832	0.00261 -0.00441	-0.00296 -0.01376	-0.00482 0.00370	0.00116 0.01503

M= 16 G= 4.71238893

MI/MR

0. 0.	0. 0.	0. 0.	0. 0.	0. 0.	0. 0.	0. 0.	0. 0.	0.00015 0.00002	0.00007 -0.00014
0. 0.	0. 0.	0. 0.	0. 0.	0. 0.	0. 0.	0.00008 0.00023	0.00022 0.00008	0.00013 -0.00019	-0.00013 -0.00025
0. 0.	0. 0.	0. 0.	0. 0.	-0.00027 0.00021	0.00010 0.00053	0.00044 0.00020	0.00027 -0.00034	-0.00021 -0.00056	-0.00043 0.00002
0. 0.	0. 0.	-0.00101 -0.00128	-0.00080 0.00039	0.00014 0.00178	0.00098 0.00125	0.00075 -0.00087	-0.00043 -0.00192	-0.00106 -0.00017	-0.00013 0.00192
-0.00160 -0.01338	-0.00394 -0.01137	-0.00335 0.00072	0.00021 0.01239	0.00365 0.01036	0.00305 -0.00467	-0.00137 -0.01356	-0.00399 -0.00234	-0.00069 0.01281	0.00377 0.00585

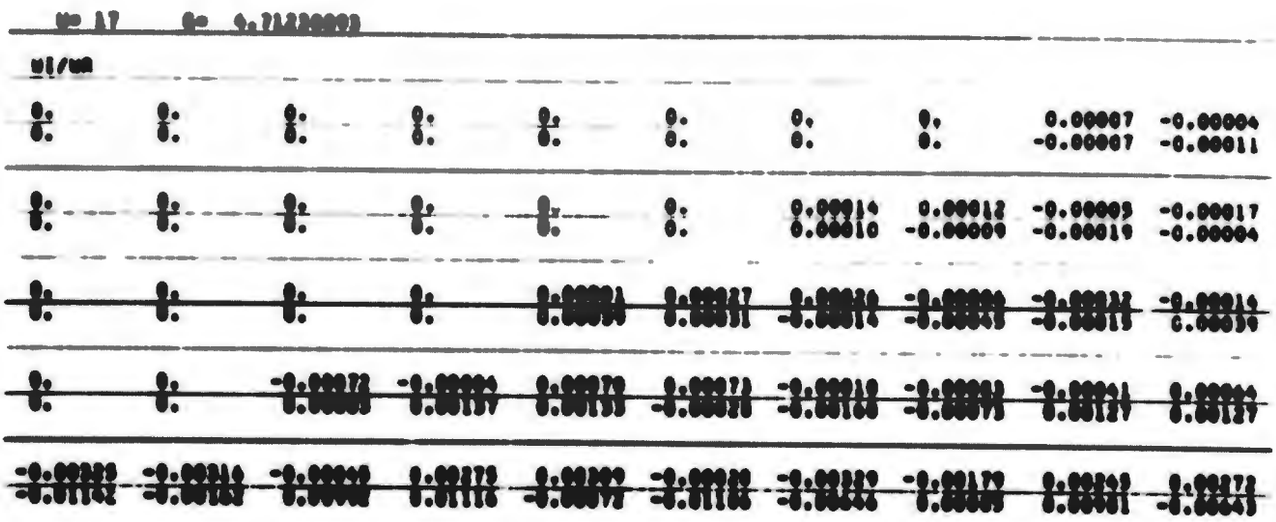

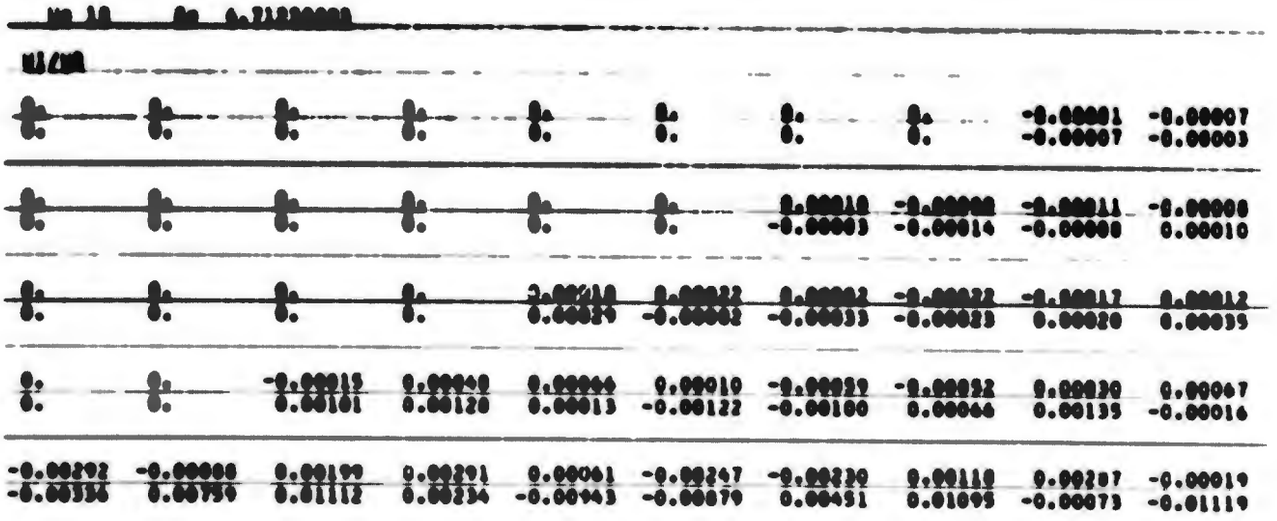

M= 19 G= 4.71238893

MI/MR

0.	0.	0.	0.	0.	0.	0.	0.	-0.00004	-0.00004
0.	0.	0.	0.	0.	0.	0.	0.	-0.00004	0.00003
0.	0.	0.	0.	0.	0.	0.00002	-0.00007	-0.00007	0.00002
0.	0.	0.	0.	0.	0.	-0.00009	-0.00008	0.00004	0.00011
0.	0.	0.	0.	0.00010	0.00006	-0.00014	-0.00017	0.00003	0.00019
0.	0.	0.	0.	0.00006	-0.00022	-0.00024	0.00007	0.00024	0.00007
0.	0.	0.00032	0.00036	0.00022	-0.00039	-0.00032	0.00006	0.00036	0.00019
0.	0.	0.00116	0.00048	-0.00005	-0.00107	0.00016	0.00119	0.00038	-0.00100
-0.00115	0.00136	0.00261	0.00113	-0.00168	-0.00240	0.00015	0.00251	0.00094	-0.00221
0.00548	0.01055	0.00435	-0.00676	-0.00969	0.00060	0.01010	0.00178	-0.00092	-0.00380

M= 20 G= 4.71238893

MI/MR

0.	0.	0.	0.	0.	0.	0.	0.	-0.00003	-0.00000
0.	0.	0.	0.	0.	0.	0.	0.	0.00001	0.00004
0.	0.	0.	0.	0.	0.	-0.00004	-0.00004	-0.00001	0.00004
0.	0.	0.	0.	0.	0.	-0.00007	0.00000	0.00008	0.00005
0.	0.	0.	0.	0.00009	-0.00008	-0.00015	-0.00003	0.00013	0.00010
0.	0.	0.	0.	-0.00014	-0.00022	-0.00002	0.00022	0.00014	-0.00016
0.	0.	0.00047	0.00027	-0.00023	-0.00047	-0.00011	0.00041	0.00032	-0.00028
0.	0.	0.00096	-0.00053	-0.00102	-0.00020	0.00092	0.00069	-0.00064	-0.00091
0.00086	0.00227	0.00143	-0.00100	-0.00225	-0.00059	0.00191	0.00157	-0.00127	-0.00190
0.00463	0.00605	-0.00423	-0.00955	-0.00252	0.00009	0.00667	-0.00539	-0.00039	0.00364

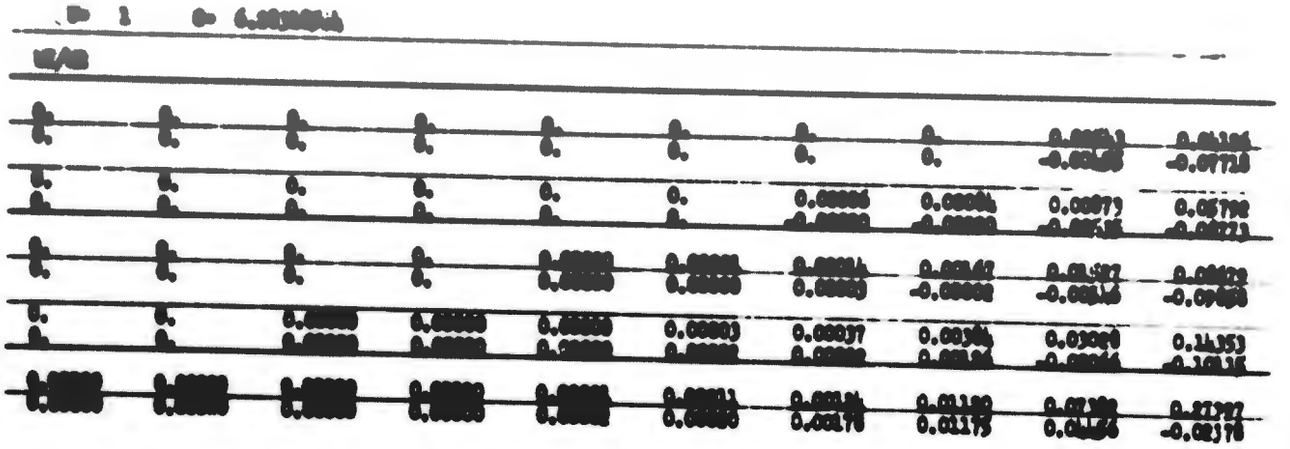

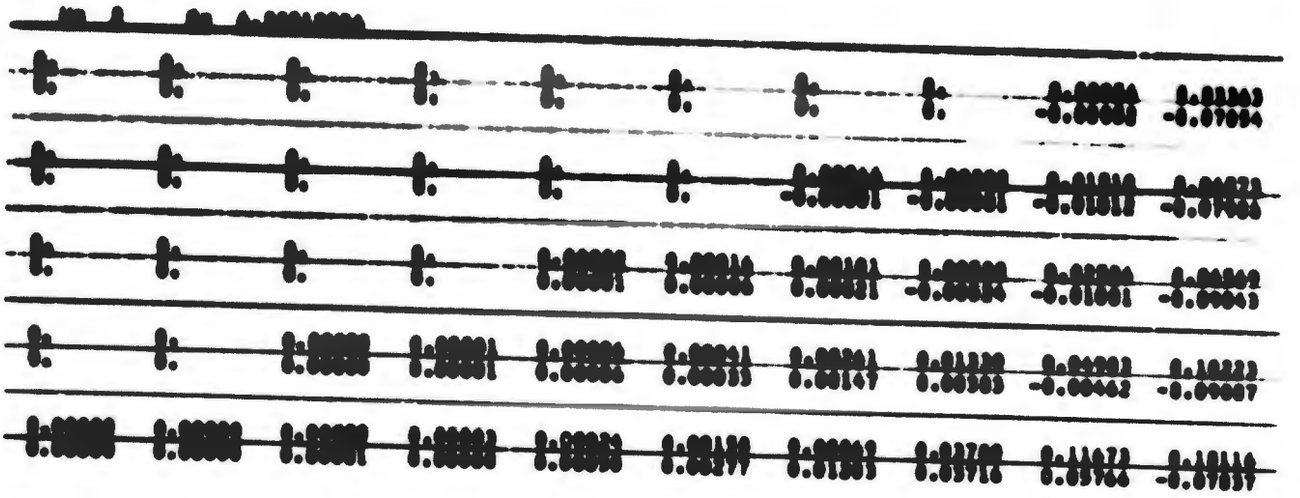

M= 3 G= 0.20110324

MI/MR

0.	0.	0.	0.	0.	0.	0.	0.	0.01145	0.02291
0.	0.	0.	0.	0.	0.	0.	0.	-0.01139	-0.06048
0.	0.	0.	0.	0.	0.	0.00131	0.00555	0.01754	0.0290
0.	0.	0.	0.	0.	0.	-0.00007	-0.00177	-0.01369	-0.04783
0.	0.	0.	0.	0.00011	0.00062	0.00285	0.01063	0.02986	0.03707
0.	0.	0.	0.	0.00006	0.00023	0.00049	-0.00103	-0.01993	-0.07716
0.	0.	0.00001	0.00007	0.00037	0.00177	0.00720	0.02326	0.05267	0.04952
0.	0.	0.00001	0.00008	0.00035	0.00134	0.00370	0.00503	-0.01294	-0.09095
0.00000	0.00001	0.00005	0.00031	0.00154	0.00660	0.02327	0.06321	0.11368	0.06210
0.00000	0.00003	0.00015	0.00074	0.00315	0.01111	0.03018	0.05428	0.02969	-0.12906

M= 4 G= 0.20110324

MI/MR

0.	0.	0.	0.	0.	0.	0.	0.	0.01009	0.01155
0.	0.	0.	0.	0.	0.	0.	0.	-0.01204	-0.04824
0.	0.	0.	0.	0.	0.	0.00247	0.00743	0.01984	0.01204
0.	0.	0.	0.	0.	0.	-0.00025	-0.00297	-0.01556	-0.05305
0.	0.	0.	0.	0.00040	0.00157	0.00521	0.01368	0.02933	0.01052
0.	0.	0.	0.	0.00021	0.00053	0.00061	-0.00299	-0.01876	-0.05904
0.	0.	0.00007	0.00030	0.00125	0.00438	0.01273	0.02840	0.03999	0.00212
0.	0.	0.00009	0.00035	0.00116	0.00307	0.00560	0.00273	-0.02163	-0.07330
0.00001	0.00007	0.00034	0.00141	0.00513	0.01500	0.03021	0.07140	0.07219	-0.03319
0.00005	0.00021	0.00090	0.00327	0.01006	0.02496	0.04546	0.04596	-0.02113	-0.12990

[redacted]

[redacted]

U= 7 G= 0.28318524

ml/mR

0.	0.	0.	0.	0.	0.	0.	0.	0.00142	-0.00798
0.	0.	0.	0.	0.	0.	0.	0.	-0.00892	-0.01299
0.	0.	0.	0.	0.	0.	0.00390	0.00438	0.00083	-0.01235
0.	0.	0.	0.	0.	0.	-0.00162	-0.00521	-0.01025	-0.01071
0.	0.	0.	0.	0.00250	0.00475	0.00683	0.00548	-0.00367	-0.01008
0.	0.	0.	0.	0.00087	0.00046	-0.00199	-0.00737	-0.01247	-0.00690
0.	0.	0.00144	0.00344	0.00695	0.01124	0.01273	0.00515	-0.01345	-0.02788
0.	0.	0.00168	0.00322	0.00472	0.00367	-0.00217	-0.01321	-0.01784	0.00121
0.00099	0.00276	0.00676	0.01419	0.02491	0.03207	0.02486	-0.00560	-0.04152	-0.03414
0.00308	0.00753	0.01580	0.02731	0.03572	0.02770	-0.00624	-0.04625	-0.03803	0.03660

U= 8 G= 0.28318524

ml/mR

0.	0.	0.	0.	0.	0.	0.	0.	-0.00113	-0.00002
0.	0.	0.	0.	0.	0.	0.	0.	-0.00609	-0.00548
0.	0.	0.	0.	0.	0.	0.00297	0.00171	-0.00325	-0.01055
0.	0.	0.	0.	0.	0.	-0.00206	-0.00467	-0.00636	-0.00239
0.	0.	0.	0.	0.00301	0.00447	0.00444	0.00257	-0.00740	-0.01296
0.	0.	0.	0.	0.00074	-0.00032	-0.00312	-0.00669	-0.00659	0.00269
0.	0.	0.00245	0.00482	0.00778	0.00938	0.00603	-0.00429	-0.01998	-0.01297
0.	0.	0.00269	0.00399	0.00408	0.00078	-0.00441	-0.01229	-0.00632	0.01336
0.00233	0.00542	0.01097	0.01859	0.02471	0.02167	0.00300	-0.02371	-0.03043	0.00353
0.00690	0.01396	0.02368	0.03146	0.02799	0.00382	-0.03019	-0.03875	0.00450	0.05323

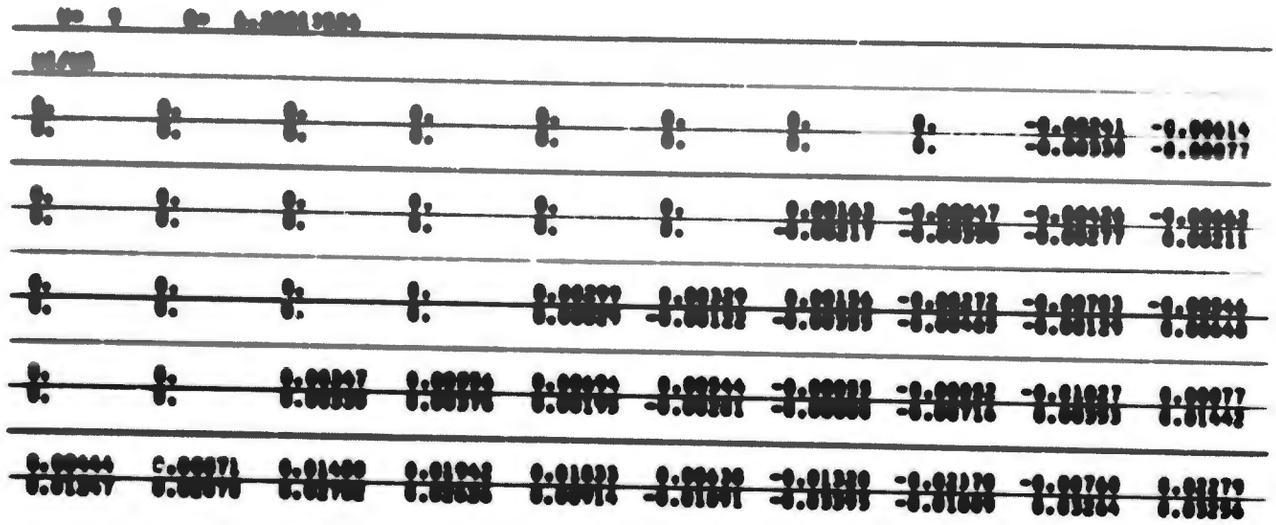

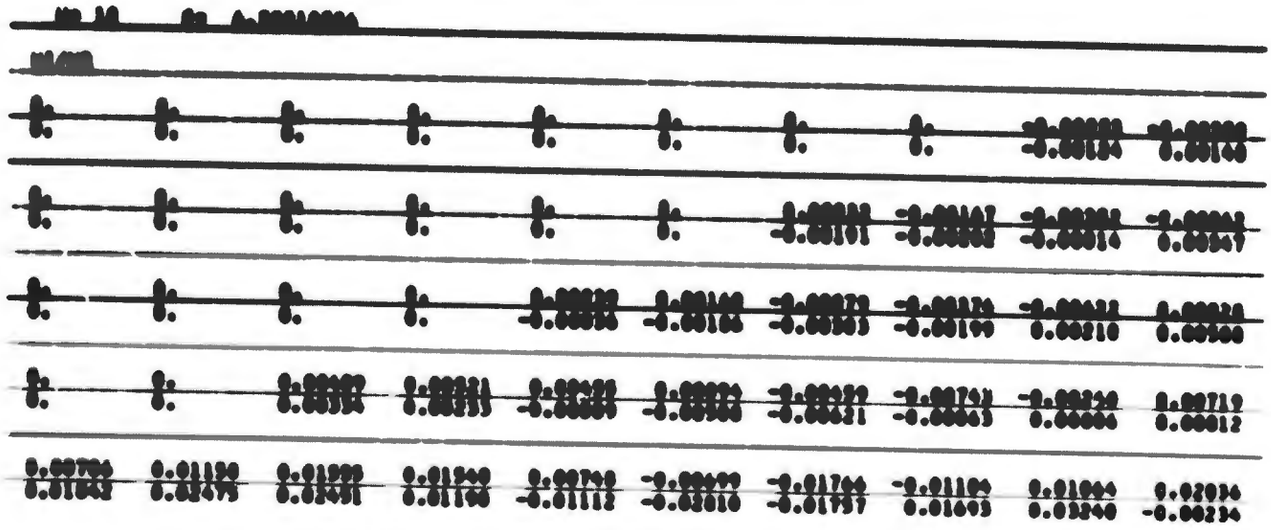

V= 11 G= 6.28318524

W1/WR

0.	0.	0.	0.	0.	0.	0.	0.	-0.00108	-0.00134
0.	0.	0.	0.	0.	0.	0.	0.	0.00013	0.00196
0.	0.	0.	0.	0.	0.	-0.00060	-0.00184	-0.00195	0.00014
0.	0.	0.	0.	0.	0.	-0.00133	-0.00064	0.00122	0.00282
0.	0.	0.	0.	0.00137	-0.00001	-0.00198	-0.00291	-0.00183	0.00284
0.	0.	0.	0.	-0.00064	-0.00145	-0.00179	0.00032	0.00313	0.00367
0.	0.	0.00397	0.00371	0.00145	-0.00240	-0.00918	-0.00333	0.00294	0.00672
0.	0.	0.00237	0.00014	-0.00316	-0.00495	-0.00223	0.00405	0.00683	0.00026
0.00942	0.01264	0.01297	0.00755	-0.00328	-0.01293	-0.01130	0.00344	0.01549	0.00610
0.02217	0.02270	0.01322	-0.00574	-0.02264	-0.01979	0.00002	0.02713	0.01068	-0.02492

V= 12 G= 6.28318529

W1/WR

0.	0.	0.	0.	0.	0.	0.	0.	-0.00097	0.00008
0.	0.	0.	0.	0.	0.	0.	0.	0.00072	0.00148
0.	0.	0.	0.	0.	0.	-0.00096	-0.00129	-0.00044	0.00130
0.	0.	0.	0.	0.	0.	-0.00063	0.00032	0.00146	0.00140
0.	0.	0.	0.	0.00029	-0.00103	-0.00193	-0.00123	0.00187	0.00271
0.	0.	0.	0.	-0.00122	-0.00142	-0.00035	0.00154	0.00234	0.00023
0.	0.	0.00301	0.00155	-0.00117	-0.00356	-0.00313	0.00077	0.00446	0.00269
0.	0.	0.00068	-0.00101	-0.00300	-0.00268	0.00166	0.00508	0.00236	-0.00446
0.01044	0.01098	0.00718	-0.00104	-0.00940	-0.01035	-0.00063	0.01000	0.00069	-0.00067
0.02066	0.01372	-0.00104	-0.01705	-0.01977	-0.00120	0.02063	0.01659	-0.01273	-0.02317

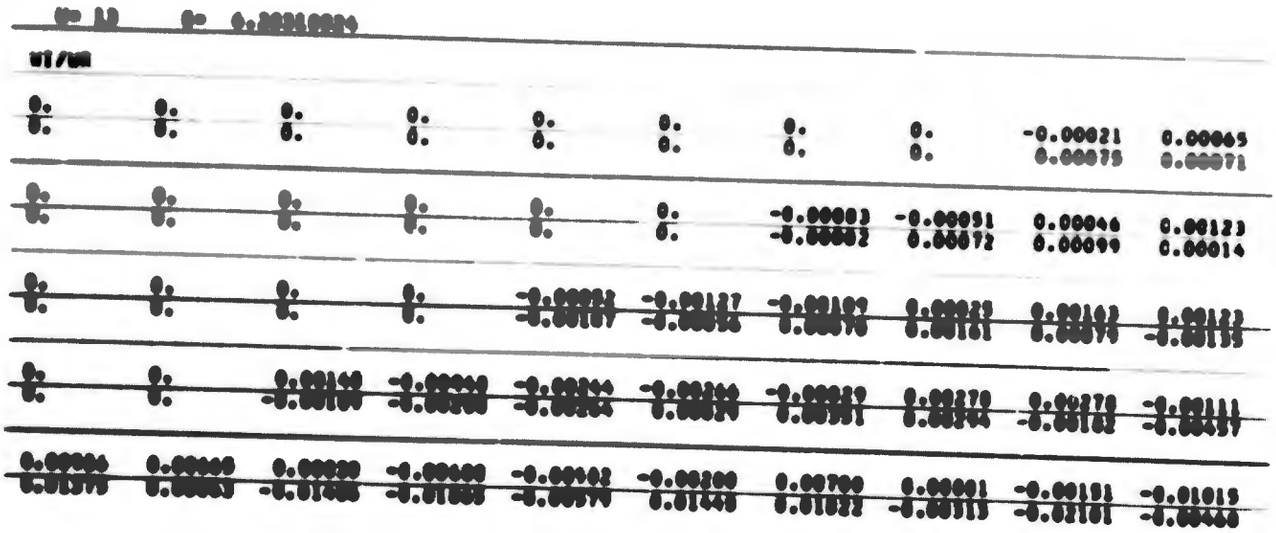

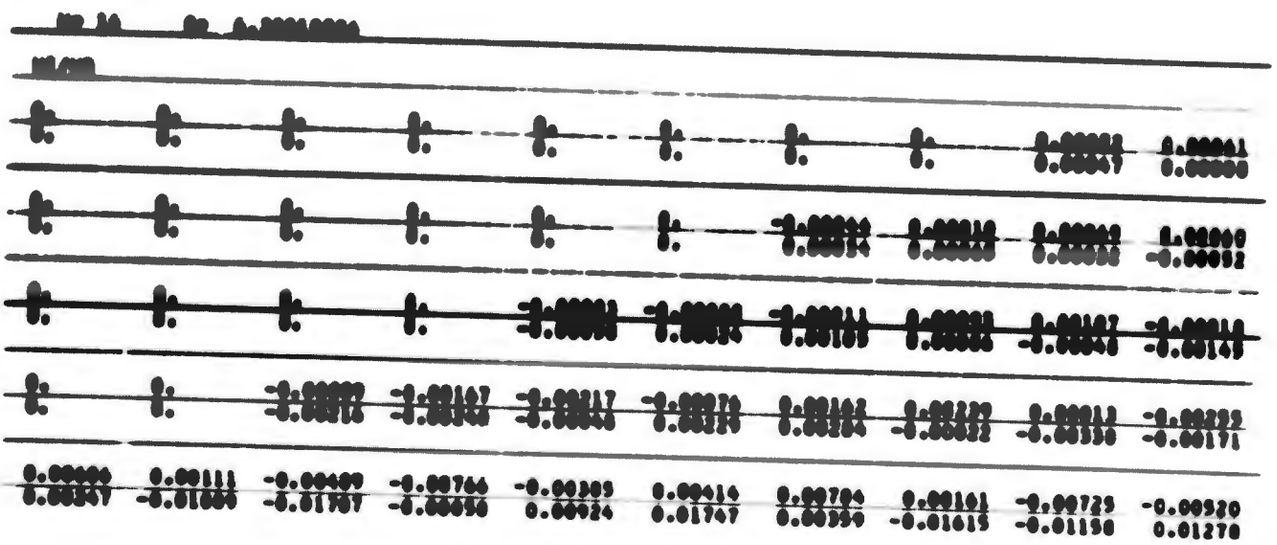

0. 0.	0. 0.	0. 0.	0. 0.	0. 0.	0. 0.	0. 0.	0. 0.	0.00032 0.00015	0.00031 -0.00022
0. 0.	0. 0.	0. 0.	0. 0.	0. 0.	0. 0.	-0.00004 0.00041	0.00037 0.00032	0.00047 -0.00017	0.00000 -0.00057
0. 0.	0. 0.	0. 0.	0. 0.	-0.00048 -0.00001	-0.00023 0.00066	0.00026 0.00076	0.00003 -0.00083	0.00018 -0.00054	-0.00008 -0.00046
0. 0.	0. 0.	-0.00114 -0.00218	-0.00174 -0.00008	-0.00093 0.00134	0.00006 0.00244	0.00100 0.00068	0.00072 -0.00222	-0.00152 -0.00221	-0.00172 0.00126
0.00157 -0.00031	-0.00368 -0.01333	-0.00042 -0.01814	-0.00423 0.00499	0.00209 0.01952	0.00650 0.00782	0.00328 -0.01067	-0.00447 -0.01431	-0.00999 0.00464	0.00195 0.01618

0. 0.	0. 0.	0. 0.	0. 0.	0. 0.	0. 0.	0. 0.	0. 0.	0.00022 -0.00007	0.00003 -0.00025
0. 0.	0. 0.	0. 0.	0. 0.	0. 0.	0. 0.	0.00019 0.00027	0.00033 -0.00001	0.00011 -0.00034	-0.00029 -0.00029
0. 0.	0. 0.	0. 0.	0. 0.	-0.00019 0.00030	0.00025 0.00061	0.00048 0.00018	0.00031 -0.00035	-0.00041 -0.00046	-0.00044 0.00010
0. 0.	0. 0.	-0.00137 -0.00186	-0.00072 0.00075	0.00037 0.00201	0.00143 0.00112	0.00094 -0.00126	-0.00077 -0.00215	-0.00154 0.00007	-0.00007 0.00233
-0.00244 -0.01360	-0.00334 -0.01089	-0.00428 0.00166	0.00065 0.01309	0.00314 0.01016	0.00299 -0.00561	-0.00220 -0.01423	-0.00259 -0.00180	-0.00074 0.01303	0.00343 0.00504

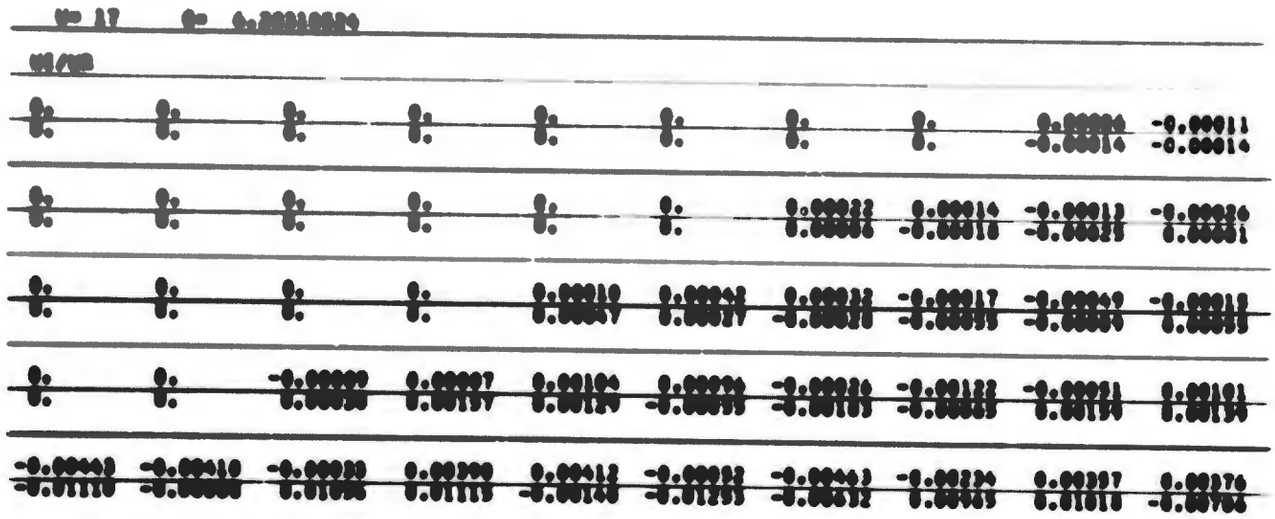

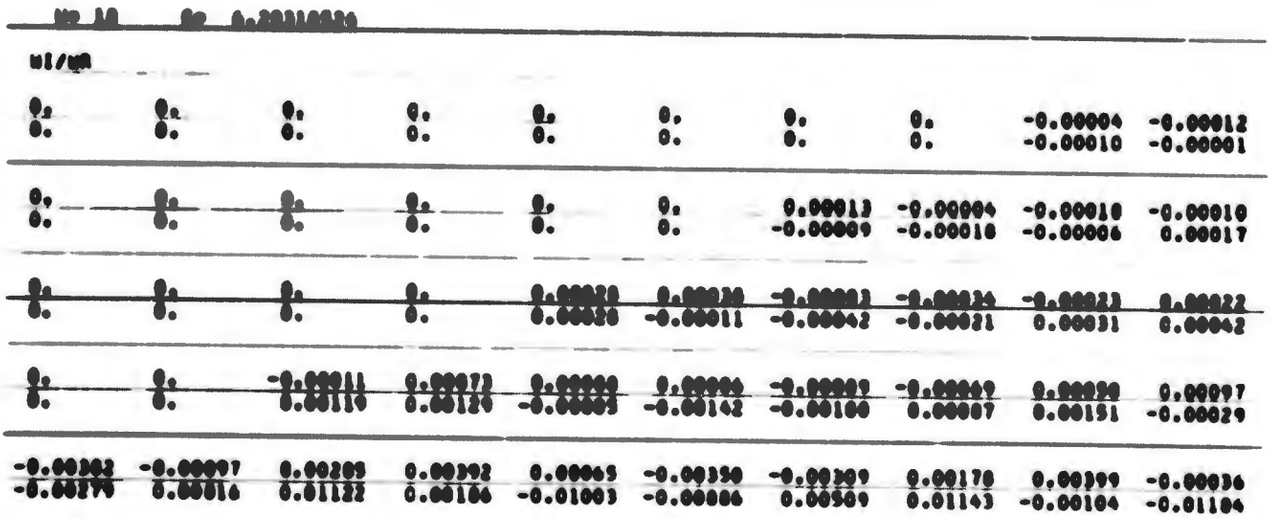

U= 19 G= 6.28318524

wl/wR

0.	0.	0.	0.	0.	0.	0.	0.	-0.00007	-0.00005
0.	0.	0.	0.	0.	0.	0.	0.	-0.00003	0.00006
0.	0.	0.	0.	0.	0.	0.00001	-0.00011	-0.00010	0.00005
0.	0.	0.	0.	0.	0.	-0.00013	-0.00008	0.00008	0.00015
0.	0.	0.	0.	0.00025	0.00005	-0.00022	-0.00023	0.00007	0.00029
0.	0.	0.	0.	-0.00050	-0.00038	-0.00029	0.00014	0.00036	0.00009
0.	0.	0.00049	0.00077	0.00024	-0.00059	-0.00071	0.00013	0.00002	0.00024
0.	0.	0.00120	0.00028	-0.00102	-0.00112	0.00030	0.00135	0.00035	-0.00127
-0.00138	0.00198	0.00354	0.00140	-0.00241	-0.00326	0.00033	0.00350	0.00123	-0.00313
0.00508	0.01071	0.00424	-0.00730	-0.00987	0.00099	0.01059	0.00371	-0.00946	-0.00597

U= 20 G= 6.28318524

wl/wR

0.	0.	0.	0.	0.	0.	0.	0.	-0.00005	0.00001
0.	0.	0.	0.	0.	0.	0.	0.	0.00002	0.00006
0.	0.	0.	0.	0.	0.	-0.00007	-0.00009	0.00000	0.00010
0.	0.	0.	0.	0.	0.	-0.00008	0.00003	0.00011	0.00004
0.	0.	0.	0.	0.00009	-0.00013	-0.00021	-0.00002	0.00021	0.00013
0.	0.	0.	0.	-0.00020	-0.00024	0.00002	0.00028	0.00015	-0.00022
0.	0.	0.00064	0.00034	-0.00036	-0.00065	-0.00011	0.00060	0.00044	-0.00042
0.	0.	0.00049	-0.00067	-0.00108	-0.00012	0.00106	0.00071	-0.00077	-0.00101
0.00128	0.00309	0.00184	-0.00147	-0.00308	-0.00072	0.00268	0.00212	-0.00182	-0.00273
0.00983	0.00586	-0.00466	-0.00979	-0.00229	0.00852	0.00676	-0.00579	-0.00868	0.00391

K= 1 Q= 9.42477787

MEAN

0.	0.	0.	0.	0.	0.	0.	0.	-0.00459	-0.05742
0.	0.	0.	0.	0.	0.	0.	0.	-0.00693	-0.05003
0.	0.	0.	0.	0.	0.	-0.00017	0.00074	-0.00116	-0.06108
0.	0.	0.	0.	0.	0.	-0.00015	-0.00047	-0.00066	-0.06488
0.	0.	0.	0.	0.00000	0.00003	0.00007	0.00113	0.00299	-0.05623
0.	0.	0.	0.	0.00000	0.00001	-0.00007	-0.00090	-0.00219	-0.09036
0.	0.	0.00000	0.00000	0.00000	0.00003	0.00031	0.00296	0.01452	-0.03015
0.	0.	0.00000	0.00000	0.00000	0.00001	0.00001	-0.00085	-0.01540	-0.12073
0.00000	0.00000	0.00000	0.00000	0.00001	0.00014	0.00142	0.01134	0.05846	0.07543
0.00000	0.00000	0.00000	0.00000	0.00001	0.00015	0.00120	0.00620	0.00800	-0.11091

K= 2 Q= 9.42477787

0.	0.	0.	0.	0.	0.	0.	0.	-.00363	-.05707
0.	0.	0.	0.	0.	0.	0.	0.	-.01041	-.04267
0.	0.	0.	0.	0.	0.	.00085	.00095	-.00198	-.06000
0.	0.	0.	0.	0.	0.	-.00086	-.00838	-.01491	-.05520
0.	0.	0.	0.	0.00002	0.00013	0.00075	0.00307	.00341	-.05966
0.	0.	0.	0.	0.00000	-0.00003	-0.00038	-0.00349	-.02151	-.07322
0.	0.	0.00000	0.00001	0.00008	0.00041	0.00243	0.00993	0.02086	-.04875
0.	0.	0.00000	0.00000	0.00003	0.00011	0.00003	-0.00352	-0.02058	-.09028
0.00000	0.00000	0.00000	0.00004	0.00031	0.00192	0.00981	0.03745	0.08593	-0.00027
0.00000	0.00000	0.00001	0.00006	0.00041	0.00208	0.00795	0.01823	-0.00006	-0.11657

U= 3 O= 9.42477787

0.	0.	0.	0.	0.	0.	0.	0.	-0.00567	-.05247
0.	0.	0.	0.	0.	0.	0.	0.	-0.01293	-.03080
0.	0.	0.	0.	0.	0.	0.00071	0.00145	-0.00444	-0.05688
0.	0.	0.	0.	0.	0.	-0.00084	-0.00460	-0.01822	-0.03835
0.	0.	0.	0.	0.00011	0.00054	0.00205	0.00500	0.00018	-0.06176
0.	0.	0.	0.	-0.00000	-0.00013	-0.00118	-0.00483	-0.00615	-0.04895
0.	0.	0.00001	0.00006	0.00041	0.00184	0.00653	0.01623	0.01529	-0.06780
0.	0.	0.00001	0.00005	0.00017	0.00039	-0.00030	-0.00783	-0.03628	-0.06531
0.00000	0.00001	0.00007	0.00040	0.00195	0.00795	0.02577	0.05983	0.06928	-0.08143
0.00000	0.00002	0.00013	0.00062	0.00253	0.00820	0.01904	0.00205	-0.02592	-0.10664

U= 4 O= 9.42477787

0.	0.	0.	0.	0.	0.	0.	0.	-0.00768	-0.04578
0.	0.	0.	0.	0.	0.	0.	0.	-0.01298	-0.01764
0.	0.	0.	0.	0.	0.	0.00123	0.00132	-0.00759	-0.05889
0.	0.	0.	0.	0.	0.	-0.00168	-0.00657	-0.01787	-0.02001
0.	0.	0.	0.	0.00039	0.00134	0.00352	0.00525	-0.00586	-0.05907
0.	0.	0.	0.	-0.00002	-0.00039	-0.00245	-0.00985	-0.02527	-0.02279
0.	0.	0.00008	0.00036	0.00139	0.00445	0.01102	0.01734	0.00046	-0.07618
0.	0.	0.00004	0.00020	0.00052	0.00070	-0.00156	-0.01289	-0.03660	-0.02820
0.00002	0.00010	0.00045	0.00184	0.00645	0.01872	0.04202	0.06165	0.02909	-0.12779
0.00004	0.00019	0.00078	0.00274	0.00795	0.01784	0.02617	0.00853	-0.05424	-0.06384

N= 5 G= 0.02077707

WI/WR

0. 0.	0. 0.	0. 0.	0. 0.	0. 0.	0. 0.	0. 0.	0. 0.	-0.00922 -0.01086	-0.03727 -0.00556
0. 0.	0. 0.	0. 0.	0. 0.	0. 0.	0. 0.	0.00153 -0.00262	0.00031 -0.00761	-0.01050 -0.01434	-0.04177 -0.00368
0. 0.	0. 0.	0. 0.	0. 0.	0.00090 [illegible]	0.00234 [illegible]	0.00437 -0.00305	0.00321 -0.01146	-0.01229 -0.01956	-0.04991 -0.00604
0. 0.	0. 0.	0.00031 0.00021	0.00106 0.00054	0.00314 0.00100	0.00756 0.00057	0.01332 -0.00404	0.01164 -0.01688	-0.01630 -0.02902	-0.06006 0.00522
0.00011 0.00025	0.00046 0.00089	0.00160 0.00201	0.00529 0.00752	0.01417 0.01623	0.03060 0.02552	0.04011 0.02057	0.03077 -0.01772	-0.03340 -0.06376	-0.12019 -0.00256

N= 6 G= 0.02077707

WI/WR

0. 0.	0. 0.	0. 0.	0. 0.	0. 0.	0. 0.	0. 0.	0. 0.	-0.00904 -0.00734	-0.02765 0.00361
0. 0.	0. 0.	0. 0.	0. 0.	0. 0.	0. 0.	0.00136 -0.00337	-0.00135 -0.00737	-0.01209 -0.00888	-0.03033 0.00802
0. 0.	0. 0.	0. 0.	0. 0.	0.00157 -0.00026	0.00312 -0.00161	0.00394 -0.00523	-0.00032 -0.01100	-0.01638 -0.01090	-0.03320 0.01536
0. 0.	0. 0.	0.00003 0.00035	0.00229 0.00105	0.00533 0.00129	0.00971 -0.00051	0.01136 -0.00720	0.00133 -0.01769	-0.02705 -0.01557	-0.04562 0.02706
[illegible] [illegible]	0.00151 0.00281	0.00441 0.00784	0.01106 0.01467	0.02305 0.02359	0.03706 0.02414	0.03792 0.00139	0.00219 -0.04043	-0.06351 -0.04392	-0.06098 0.05365

W= 7 G= 9.42477707

MI/MR

0.	0.	0.	0.	0.	0.	0.	0.	-0.00929	-0.01798
0.	0.	0.	0.	0.	0.	0.	0.	-0.00341	0.00098
0.	0.	0.	0.	0.	0.	0.00067	-0.00308	-0.01172	-0.01825
0.	0.	0.	0.	0.	0.	-0.00367	-0.00988	-0.00309	0.01397
0.	0.	0.	0.	0.00218	0.00322	0.00217	-0.00444	-0.01643	-0.01831
0.	0.	0.	0.	-0.00861	-0.00241	-0.00981	-0.00445	-0.00211	0.02182
0.	0.	0.00172	0.00387	0.00709	0.00948	0.00992	-0.00885	-0.02741	-0.01749
0.	0.	0.00099	0.00147	0.00091	-0.00257	-0.00467	-0.01416	-0.00054	0.03582
0.00136	0.00372	0.00886	0.01787	0.02887	0.03284	0.01459	-0.02919	-0.05867	-0.00307
0.00276	0.00658	0.01327	0.02144	0.02439	0.01083	-0.02168	-0.04358	-0.00376	0.07833

W= 8 G= 9.42477707

MI/MR

0.	0.	0.	0.	0.	0.	0.	0.	-0.00706	-0.00943
0.	0.	0.	0.	0.	0.	0.	0.	-0.00001	0.01061
0.	0.	0.	0.	0.	0.	-0.00036	-0.00424	-0.00942	-0.00794
0.	0.	0.	0.	0.	0.	-0.00338	-0.00358	0.00159	0.01458
0.	0.	0.	0.	0.00292	0.00244	-0.00014	-0.00494	-0.01255	-0.00374
0.	0.	0.	0.	-0.00186	-0.00303	-0.00333	-0.00455	0.00465	0.02030
0.	0.	0.00289	0.00526	0.00742	0.00646	-0.00131	-0.01438	-0.01843	0.00603
0.	0.	0.00145	0.00145	-0.00036	-0.00493	-0.00901	-0.00705	0.01103	0.03011
0.00318	0.00724	0.01419	0.02285	0.02751	0.01799	-0.01082	-0.04049	-0.02785	0.03955
0.00615	0.01285	0.01940	0.02339	0.01927	-0.00919	-0.03437	-0.02364	0.03357	0.06214

[illegible] 9 [illegible] 0.48877787

MI/MB

0. 0.	0. 0.	0. 0.	0. 0.	0. 0.	0. 0.	0. 0.	0. 0.	-0.00531 0.00229	-0.00291 0.00938
0. 0.	0. 0.	0. 0.	0. 0.	0. 0.	0. 0.	-0.00135 -0.00255	-0.00441 -0.00113	-0.00502 0.00429	0.00819 0.01146
0. 0.	0. 0.	0. 0.	0. 0.	0.00210 -0.00156	0.00095 -0.00319	-0.00204 -0.00582	-0.00710 -0.00644	-0.00046 0.00790	0.00505 0.01371
0. 0.	0. 0.	0.00397 0.00168	0.00576 0.00878	0.00501 -0.00273	0.00165 -0.00637	-0.00696 -0.00725	-0.01339 0.00104	-0.00545 0.01562	0.01003 0.01613
0.00682 0.01098	0.01156 0.01757	0.01646 0.02185	0.02266 0.01712	0.01792 -0.00126	-0.00132 -0.02489	-0.02606 -0.02612	-0.02944 0.00710	0.00753 0.04403	0.04914 0.01938

[illegible] 10 [illegible] 0.48877787

MI/MB

0. 0.	0. 0.	0. 0.	0. 0.	0. 0.	0. 0.	0. 0.	0. 0.	-0.00282 0.00316	0.00115 0.00657
0. 0.	0. 0.	0. 0.	0. 0.	0. 0.	0. 0.	-0.00150 -0.00150	-0.00287 0.00003	-0.00259 0.00400	0.00426 0.00671
0. 0.	0. 0.	0. 0.	0. 0.	-0.00139 -0.00197	-0.00271 -0.00375	-0.00374 -0.00170	-0.00414 0.00293	-0.00258 0.00790	0.00026 0.00570
0. 0.	0. 0.	0.00258 0.00117	-0.00298 -0.00672	-0.00564 -0.00568	-0.00838 -0.00501	-0.00879 -0.00393	-0.00741 0.00403	0.00025 0.01289	0.01772 0.00135
0.00948 0.01906	0.01584 0.00829	0.01906 0.01761	0.01652 0.00162	0.00247 -0.01765	-0.01618 -0.03266	-0.02514 -0.02678	-0.00029 0.02454	0.02784 0.03149	0.07968 -0.02109

W= 11 G= 9.42477787

WI/WA

0. 0.	0. 0.	0. 0.	0. 0.	0. 0.	0. 0.	0. 0.	0. 0.	-0.00074 0.00294	0.00287 0.00344
0. 0.	0. 0.	0. 0.	0. 0.	0. 0.	0. 0.	-0.00199 -0.00023	-0.00209 0.00190	0.00049 0.00386	0.00305 0.00224
0. 0.	0. 0.	0. 0.	0. 0.	0.00010 -0.00183	-0.00190 -0.00170	-0.00347 0.00036	-0.00209 0.00380	0.00320 0.00488	0.00772 -0.00067
0. 0.	0. 0.	0.00407 0.00013	0.00282 -0.00227	-0.00089 -0.00443	-0.00553 -0.00346	-0.00659 0.00228	-0.00015 0.00850	0.00973 0.00569	0.00964 -0.00814
0.01267 0.01878	0.01602 0.01739	0.01490 0.00673	0.00576 -0.01110	-0.00951 -0.02326	-0.01993 -0.01352	-0.01158 0.01571	0.01346 0.03059	0.02621 0.00111	0.00095 -0.03053

W= 12 G= 9.42477787

WI/WA

0. 0.	0. 0.	0. 0.	0. 0.	0. 0.	0. 0.	0. 0.	0. 0.	0.00061 0.00204	0.00287 0.00092
0. 0.	0. 0.	0. 0.	0. 0.	0. 0.	0. 0.	-0.00149 0.00062	-0.00095 0.00202	0.00191 0.00209	0.00374 -0.00076
0. 0.	0. 0.	0. 0.	0. 0.	-0.00089 -0.00154	-0.00222 -0.00043	-0.00287 0.00172	0.00043 0.00332	0.00419 0.00147	0.00300 -0.00383
0. 0.	0. 0.	0.00266 -0.00120	0.00017 -0.00319	-0.00337 -0.00338	-0.00520 -0.00005	-0.00217 0.00507	0.00475 0.00591	0.00794 -0.00162	0.00038 -0.01001
0.01355 0.01681	0.01321 0.00855	0.00672 -0.00661	-0.00519 -0.01946	-0.01529 -0.01623	-0.01275 0.00588	0.00462 0.02522	0.01981 0.01263	0.00992 -0.02263	-0.01778 -0.02641

ν= 13 G= 9.42677787

ml/mA

0. 0.	0. 0.	0. 0.	0. 0.	0. 0.	0. 0.	0. 0.	0. 0.	0.00114 0.00096	0.00193 -0.00058
0. 0.	0. 0.	0. 0.	0. 0.	0. 0.	0. 0.	-0.00070 0.00100	0.00056 0.00146	0.00201 0.00041	0.00168 -0.00197
0. 0.	0. 0.	0. 0.	0. 0.	-0.00138 -0.00063	-0.00168 -0.00059	-0.00034 0.00366	0.00297 0.00176	0.00301 -0.00111	0.00007 -0.00346
0. 0.	0. 0.	0.00069 -0.00224	-0.00199 -0.00295	-0.00391 -0.00114	-0.00269 0.00272	0.00189 0.00487	0.00564 0.00128	0.00285 -0.00558	-0.00513 -0.00604
0.01165 0.00968	0.00006 -0.00329	-0.00239 -0.01598	-0.01152 -0.01677	-0.01216 -0.00872	-0.00093 0.01894	0.01373 0.01725	0.01250 -0.00970	-0.00703 -0.02581	-0.01872 -0.00031

ν= 14 G= 9.42677787

ml/mA

0. 0.	0. 0.	0. 0.	0. 0.	0. 0.	0. 0.	0. 0.	0. 0.	0.00104 0.00009	0.00000 -0.00107
0. 0.	0. 0.	0. 0.	0. 0.	0. 0.	0. 0.	0.00092 0.00092	0.00101 0.00062	0.00130 -0.00065	-0.00007 -0.00178
0. 0.	0. 0.	0. 0.	0. 0.	-0.00126 0.00012	-0.00047 0.00138	0.00008 0.00149	0.00206 0.00004	0.00079 -0.00212	-0.00194 -0.00215
0. 0.	0. 0.	-0.00111 -0.00244	-0.00287 -0.00156	-0.00261 0.00122	0.00034 0.00363	0.00371 0.00234	0.00331 -0.00257	-0.00178 -0.00520	-0.00550 -0.00032
0.00603 -0.00084	-0.00057 -0.01276	-0.00059 -0.01610	-0.01090 -0.00444	-0.00336 0.01313	0.00884 0.01800	0.01212 -0.00851	-0.00034 -0.02079	-0.01399 -0.01043	-0.00716 0.01095

W= 15 G= 9.42477787

wi/wR

0. 0.	0. 0.	0. 0.	0. 0.	0. 0.	0. 0.	0. 0.	0. 0.	0.00061 -0.00038	-0.00003 -0.00089
0. 0.	0. 0.	0. 0.	0. 0.	0. 0.	0. 0.	0.00046 0.00055	0.00087 -0.00009	0.00038 -0.00095	-0.00085 -0.00092
0. 0.	0. 0.	0. 0.	0. 0.	-0.00069 0.00065	0.00029 0.00112	0.00131 0.00049	0.00110 -0.00101	-0.00063 -0.00171	-0.00204 -0.00014
0. 0.	0. 0.	-0.00208 -0.00166	-0.00230 0.00029	-0.00045 0.00254	0.00229 0.00252	0.00299 -0.00071	0.00001 -0.00302	-0.00362 -0.00202	-0.00293 0.00341
0.00061 -0.01010	-0.00034 -0.01905	-0.00946 -0.00761	-0.00478 0.00824	0.00918 0.01675	0.01052 0.00544	0.00242 -0.01456	-0.00915 -0.01508	-0.00948 0.00852	0.00535 0.01963

W= 16 G= 9.42477787

wi/wR

0. 0.	0. 0.	0. 0.	0. 0.	0. 0.	0. 0.	0. 0.	0. 0.	0.00016 -0.00047	-0.00041 -0.00044
0. 0.	0. 0.	0. 0.	0. 0.	0. 0.	0. 0.	0.00054 0.00011	0.00042 -0.00046	0.00027 -0.00078	-0.00087 -0.00007
0. 0.	0. 0.	0. 0.	0. 0.	-0.00002 0.00079	0.00079 0.00059	0.00095 -0.00038	-0.00081 -0.00119	-0.00123 -0.00061	-0.00162 0.00184
0. 0.	0. 0.	-0.00194 -0.00026	-0.00082 0.00168	0.00131 0.00231	0.00243 0.00034	0.00086 -0.00251	-0.00212 -0.00248	-0.00262 0.00128	0.00077 0.00348
-0.00403 -0.01348	-0.00804 -0.00912	-0.00537 0.00431	0.00294 0.01457	0.00858 0.00802	0.00526 -0.00865	-0.00509 -0.01576	-0.00928 0.00026	0.00015 0.01711	0.01008 0.00556

W= 17   G= 9.42477787

wI/wR

0. 0.	0. 0.	0. 0.	0. 0.	0. 0.	0. 0.	0. 0.	0. 0.	-0.00013 -0.00032	-0.00041 -0.00004
0. 0.	0. 0.	0. 0.	0. 0.	0. 0.	0. 0.	0.00036 -0.00019	-0.00002 -0.00047	-0.00049 -0.00024	-0.0005[illegible] 0.0004[illegible]
0. 0.	0. 0.	0. 0.	0. 0.	0.00049 0.00095	0.00079 -0.00004	0.00026 -0.00076	-0.00067 -0.00069	-0.00091 0.00036	0.00011 0.001[illegible]
0. 0.	0. 0.	-0.00096 0.00104	0.00066 0.00195	0.00187 0.00009	0.00119 -0.00147	-0.00105 -0.00234	-0.00223 -0.00005	-0.00038 0.00260	0.00229 0.00150
[illegible] -0.00987	-0.00567 0.00125	0.00069 0.01208	0.00669 0.01065	0.00590 -0.00367	-0.00203 -0.01428	-0.00791 -0.00539	-0.00299 0.01232	0.00683 0.01097	0.00608 -0.00953

W= 18   G= 9.42477787

wI/wR

0. 0.	0. 0.	0. 0.	0. 0.	0. 0.	0. 0.	0. 0.	0. 0.	-0.00022 -0.00010	-0.00022 0.00017
0. 0.	0. 0.	0. 0.	0. 0.	0. 0.	0. 0.	0.00009 -0.00029	-0.00025 -0.00025	-0.00036 0.00013	-0.00000 0.00044
0. 0.	0. 0.	0. 0.	0. 0.	0.00055 0.00013	0.00034 -0.00044	-0.00031 -0.00061	-0.00070 -0.00001	-0.00021 0.00074	0.00067 0.00053
0. 0.	0. 0.	0.00023 0.00197	0.00130 0.00112	0.00124 -0.00070	-0.00035 -0.00195	-0.00170 -0.00078	-0.00091 0.00168	0.00129 0.00189	0.00173 -0.00094
-0.00529 -0.00180	-0.00057 0.00459	0.00502 0.01118	0.00505 0.00023	0.00012 -0.01173	-0.00614 -0.00069	-0.00455 0.00708	0.00371 0.01273	0.00667 -0.00236	-0.00124 -0.01394

U= 19 G= 9.42477161

m1/m8

0.	0.	0.	0.	0	0.	0	0.	-0.00016	-0.00002
0.	0.	0.	0.	0.	0.	0.	0.	0.00005	0.00019
0.	0.	0.	0.	0.	0.	-0.00011	-0.00026	-0.00010	0.00023
0.	0.	0.	0.	0.	0.	-0.00021	-0.00000	0.00026	0.00022
0.	0.	0.	0.	0.00034	-0.00010	-0.00049	-0.00032	0.00032	0.00013
0.	0.	0.	0.	-0.00023	-0.00048	-0.00019	0.00042	0.00054	-0.00015
0.	0.	0.00099	0.00115	0.00008	-0.00120	-0.00108	0.00054	0.00152	0.00020
0.	0.	0.00117	-0.00016	-0.00150	-0.00111	0.00085	0.00180	0.00007	-0.00194
-0.00140	0.00361	0.00543	0.00154	-0.00438	-0.00505	0.00117	0.00596	0.00160	-0.00558
0.00729	0.01094	0.00310	-0.00882	-0.01017	0.00236	0.01201	0.00323	-0.01126	-0.00636

U= 20 G= 9.42477787

m1/m8

0.	0.	0.	0.	0.	0.	0.	0.	-0.00005	0.00009
0.	0.	0.	0.	0.	0.	0.	0.	0.00011	0.00010
0.	0.	0.	0.	0.	0.	0.00017	-0.00013	0.00010	0.00022
0.	0.	0.	0.	0.	0.	-0.00006	0.00014	0.00019	-0.00002
0.	0.	0.	0.	0.00002	-0.00033	-0.00033	0.00010	0.00044	0.00017
0.	0.	0.	0.	-0.00036	-0.00029	0.00020	0.00045	0.00009	-0.00046
0.	0.	0.00101	0.00033	-0.00079	-0.00105	0.00004	0.00116	0.00004	-0.00003
0.	0.	0.00019	-0.00107	-0.00119	0.00023	0.00148	0.00067	-0.00126	-0.00129
0.00246	0.00482	0.00240	-0.00281	-0.00487	-0.00067	0.00464	0.00323	-0.00336	-0.00449
0.01023	0.00510	-0.00597	-0.01034	-0.00143	0.00986	0.00685	-0.00713	-0.00954	0.00493

[illegible] = 1 [illegible] = 12.5643760

[illegible]	[illegible]	[illegible]	[illegible]	[illegible]	[illegible]	[illegible]	[illegible]	-0.000487	-0.05292
[illegible]	[illegible]	[illegible]	[illegible]	[illegible]	[illegible]	[illegible]	[illegible]	-0.000844	0.04321
[illegible]	[illegible]	[illegible]	[illegible]	[illegible]	[illegible]	0.00000	[illegible]	[illegible]	-0.06456
[illegible]	[illegible]	[illegible]	[illegible]	[illegible]	[illegible]	-0.00004	-0.00046	-0.00225	0.03918
[illegible]	[illegible]	[illegible]	[illegible]	0.00000	0.00001	0.00004	-0.00002	-0.00604	-0.07654
[illegible]	[illegible]	[illegible]	[illegible]	0.00000	0.00000	-0.00008	-0.00092	-0.00059	0.02838
[illegible]	[illegible]	[illegible]	[illegible]	[illegible]	[illegible]	[illegible]	[illegible]	[illegible]	[illegible]
[illegible]	[illegible]	[illegible]	[illegible]	[illegible]	[illegible]	[illegible]	[illegible]	[illegible]	[illegible]
[illegible]	[illegible]	[illegible]	[illegible]	[illegible]	[illegible]	[illegible]	[illegible]	[illegible]	[illegible]
[illegible]	[illegible]	[illegible]	[illegible]	[illegible]	[illegible]	[illegible]	[illegible]	[illegible]	[illegible]
0.00000	0.00000	0.00000	0.00000	0.00001	0.00014	0.00134	0.00926	0.03499	-0.01868
0.00000	0.00000	0.00000	0.00000	0.00001	0.00011	0.00074	0.00278	-0.00119	0.00038

[illegible] = 2 [illegible] = 12.5643760

[illegible]	[illegible]	[illegible]	[illegible]	[illegible]	[illegible]	[illegible]	[illegible]	-0.00898	-0.04590
[illegible]	[illegible]	[illegible]	[illegible]	[illegible]	[illegible]	[illegible]	[illegible]	-0.00027	0.04364
[illegible]	[illegible]	[illegible]	[illegible]	[illegible]	[illegible]	-0.00001	-0.00104	-0.01105	-0.05591
[illegible]	[illegible]	[illegible]	[illegible]	[illegible]	[illegible]	-0.00099	-0.00141	-0.00320	0.04205
[illegible]	[illegible]	[illegible]	[illegible]	0.00001	0.00007	0.00087	-0.00031	-0.01193	-0.06754
[illegible]	[illegible]	[illegible]	[illegible]	-0.00001	-0.00007	-0.00057	-0.00325	-0.00912	0.03617
[illegible]	[illegible]	[illegible]	[illegible]	[illegible]	[illegible]	[illegible]	[illegible]	[illegible]	[illegible]
[illegible]	[illegible]	[illegible]	[illegible]	[illegible]	[illegible]	[illegible]	[illegible]	[illegible]	[illegible]
[illegible]	[illegible]	[illegible]	[illegible]	[illegible]	[illegible]	[illegible]	[illegible]	[illegible]	[illegible]
[illegible]	[illegible]	[illegible]	[illegible]	[illegible]	[illegible]	[illegible]	[illegible]	[illegible]	[illegible]
0.00000	0.00000	0.00001	0.00005	0.00011	0.00125	0.00912	0.02963	0.04504	-0.06146
0.00000	0.00000	0.00001	0.00005	0.00011	0.00113	0.00472	0.00717	-0.00978	0.00535

L= 3 Q= 12.5663704

0. 0.	0. 0.	0. 0.	0. 0.	0. 0.	0. 0.	0. 0.	0. 0.	-0.01108 0.00091	-0.02[illegible] 0.04342
0. 0.	0. 0.	0. 0.	0. 0.	0. 0.	0. 0.	-0.00009 -0.00083	-0.00229 -0.00288	-0.01[illegible] -0.00210	-0.02[illegible] 0.04[illegible]
0. 0.	0. 0.	0. 0.	0. 0.	0.00006 -0.00005	0.00030 -0.00032	0.00063 -0.00163	-0.00133 -0.00542	-0.01704 -0.00823	-0.05294 0.04523
0. 0.	0. 0.	0.00001 0.00000	0.00006 0.00002	0.00037 0.00008	0.00126 -0.00028	0.00415 -0.00240	0.00951 -0.01034	-0.01[illegible] -0.01962	-0.03[illegible] 0.04249
0.00000 0.00000	0.00001 0.00002	0.00006 0.00011	0.00045 0.00050	0.00209 0.00191	0.00799 0.00558	0.02335 0.01056	0.04483 0.00520	0.02178 -0.02325	-0.09739 0.02179

L= 4 Q= 12.5637049

0. 0.	0. 0.	0. 0.	0. 0.	0. 0.	0. 0.	0. 0.	0. 0.	-0.01496 0.00291	-0.02078 0.04159
0. 0.	0. 0.	0. 0.	0. 0.	0. 0.	0. 0.	-0.00035 -0.00157	-0.00380 -0.00354	-0.01609 0.00094	-0.02734 0.04560
0. 0.	0. 0.	0. 0.	0. 0.	0.00027 -0.00017	0.00099 -0.00084	0.00077 -0.00308	-0.00311 -0.00732	-0.02019 -0.00330	-0.03410 0.05127
0. 0.	0. 0.	0.00000 0.00001	0.00005 0.00006	0.00022 -0.00000	0.00140 -0.00091	0.00635 -0.00490	0.00279 -0.01376	-0.02374 -0.01215	-0.04877 0.05095
0.00002 0.00004	0.00011 0.00016	0.00052 0.00065	0.00204 0.00217	0.00681 0.00587	0.01843 0.01158	0.03638 0.01239	0.03894 -0.00674	-0.02119 -0.03129	-0.09830 0.05006

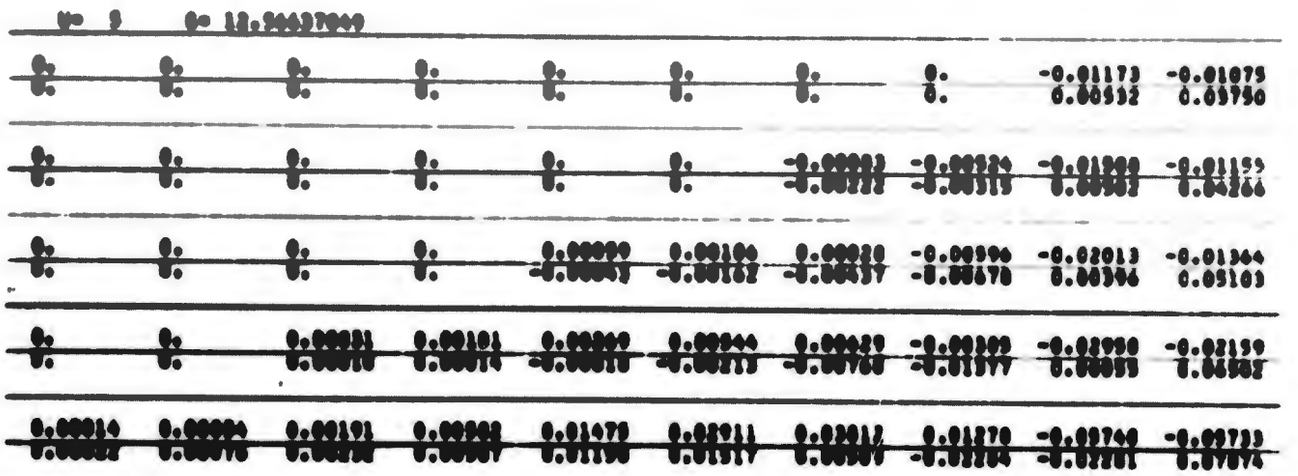

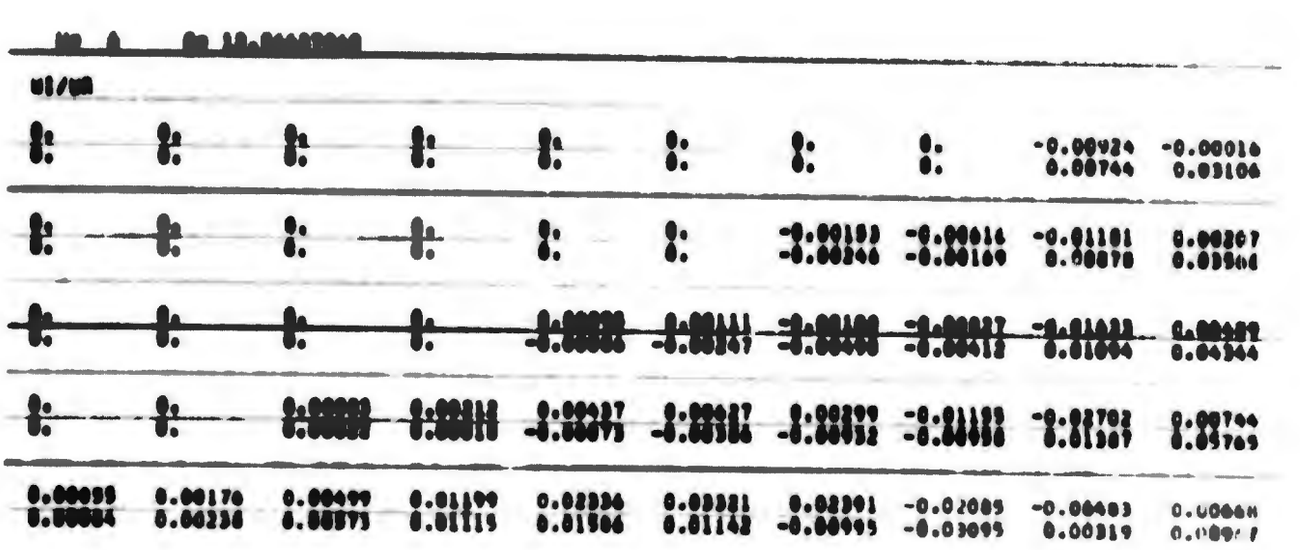

V= 7 G= 12.56637049

ml/mA

0.	0.	0.	0.	0.	0.	0.	0.	-0.00579	0.00740
0.	0.	0.	0.	0.	0.	0.	0.	0.00860	0.02293
0.	0.	0.	0.	0.	0.	-0.00228	-0.00618	-0.00703	0.01157
0.	0.	0.	0.	0.	0.	-0.00212	0.00049	0.01098	0.02563
0.	0.	0.	0.	0.00116	0.00060	-0.00276	-0.00914	-0.00950	0.01799
0.	0.	0.	0.	-0.00139	-0.00308	-0.00426	-0.00012	0.01517	0.03008
0.	0.	0.00169	0.00346	0.00540	0.00486	-0.00261	-0.01623	-0.01616	0.02961
0.	0.	0.00035	-0.00001	-0.00175	-0.00557	-0.00888	-0.00216	0.02281	0.03876
0.00162	0.00430	0.00990	0.01896	0.02800	0.02590	-0.00101	-0.04299	-0.03972	0.06125
0.00240	0.00551	0.01056	0.01560	0.01443	-0.00056	-0.02395	-0.02213	0.03412	0.07064

V= 8 G= 12.56637049

ml/mA

0.	0.	0.	0.	0.	0.	0.	0.	-0.00215	0.01135
0.	0.	0.	0.	0.	0.	0.	0.	0.00843	0.01430
0.	0.	0.	0.	0.	0.	-0.00202	-0.00513	-0.00189	0.01601
0.	0.	0.	0.	0.	0.	-0.00122	0.00256	0.01093	0.01448
0.	0.	0.	0.	0.00101	-0.00046	-0.00429	-0.00709	-0.00155	0.02351
0.	0.	0.	0.	-0.00187	-0.00313	-0.00249	0.00383	0.01533	0.01448
0.	0.	0.00274	0.00445	0.00495	0.00127	-0.00796	-0.01513	-0.00115	0.03835
0.	0.	0.00035	-0.00058	-0.00309	-0.00642	-0.00581	0.00589	0.02409	0.01462
0.00374	0.00829	0.01958	0.02343	0.02451	0.00848	-0.02399	-0.04160	0.00204	0.08047
0.00528	0.00992	0.01491	0.01560	0.00940	-0.01528	-0.02649	0.00130	0.05123	0.02613

M= 9 G= 12.56637049

ml/mA

0. 0.	0. 0.	0. 0.	0. 0.	0. 0.	0. 0.	0. 0.	0. 0.	0.00093 0.00700	0.01189 0.00650
0. 0.	0. 0.	0. 0.	0. 0.	0. 0.	0. 0.	-0.00289 -0.00001	-0.00324 0.00397	0.00238 0.00877	0.01565 0.00448
0. 0.	0. 0.	0. 0.	0. 0.	0.00042 -0.00211	-0.00172 -0.00247	-0.00484 -0.00010	-0.00474 0.00637	0.00511 0.01170	0.02153 0.00070
0. 0.	0. 0.	0.00362 0.00006	0.00446 -0.00155	0.00274 -0.00423	-0.00313 -0.00563	-0.01036 -0.00087	-0.00852 0.01142	0.01169 0.01764	0.03265 -0.00680
0.00702 0.00928	0.01296 0.01487	0.01965 0.01579	0.02205 0.00895	0.01250 -0.00809	-0.01130 -0.02357	-0.03291 -0.01372	-0.01916 0.02584	0.03608 0.04285	0.05983 -0.02312

M= 10 G= 12.56637049

ml/mA

0. 0.	0. 0.	0. 0.	0. 0.	0. 0.	0. 0.	0. 0.	0. 0.	0.00291 0.00473	0.00986 0.00059
0. 0.	0. 0.	0. 0.	0. 0.	0. 0.	0. 0.	-0.00239 0.00114	-0.00100 0.00427	0.00490 0.00930	0.01184 -0.00262
0. 0.	0. 0.	0. 0.	0. 0.	-0.00047 -0.00194	-0.00245 -0.00121	-0.00405 0.00211	-0.00078 0.00674	0.00843 0.00589	0.01435 -0.00818
0. 0.	0. 0.	0.00383 -0.00061	0.00313 -0.00265	-0.00055 -0.00448	-0.00632 -0.00306	-0.00856 0.00414	0.00041 0.01229	0.01736 0.00667	0.01741 -0.01914
0.01091 0.01519	0.01650 0.01547	0.01944 0.01696	0.01377 -0.00276	-0.00367 -0.01875	-0.02356 -0.01905	-0.02394 0.00764	0.00960 0.03592	0.04514 0.01340	0.01683 -0.05238

U= 11 G= 12.56637049

ml/mA

0.	0.	0.	0.	0.	0.	0.	0.	0.00361	0.00650
0.	0.	0.	0.	0.	0.	0.	0.	0.00226	-0.00290
0.	0.	0.	0.	0.	0.	-0.00144	0.00094	0.00538	0.00694
0.	0.	0.	0.	0.	0.	0.00185	0.00348	0.00168	-0.00608
0.	0.	0.	0.	-0.00132	-0.00281	-0.00215	0.00257	0.00847	0.00551
0.	0.	0.	0.	-0.00155	0.00028	0.00358	0.00505	0.00014	-0.01110
0.	0.	0.00305	0.00075	-0.00355	-0.00679	-0.00354	0.00743	0.01471	0.00075
0.	0.	-0.00152	-0.00329	-0.00340	0.00048	0.00713	0.00846	-0.00392	-0.02028
0.01409	0.01700	0.01369	0.00117	-0.01596	-0.02247	-0.00392	0.02776	0.02873	-0.02179
0.01488	0.01198	0.00183	-0.01307	-0.01967	-0.00343	0.02430	0.02515	-0.01407	-0.04889

U= 12 G= 12.56637049

ml/mA

0.	0.	0.	0.	0.	0.	0.	0.	0.00320	0.00307
0.	0.	0.	0.	0.	0.	0.	0.	0.00020	-0.00408
0.	0.	0.	0.	0.	0.	-0.00032	0.00209	0.00422	0.00163
0.	0.	0.	0.	0.	0.	0.00196	0.00201	-0.00108	-0.00627
0.	0.	0.	0.	-0.00179	-0.00208	0.00009	0.00422	0.00353	-0.00106
0.	0.	0.	0.	-0.00042	0.00148	0.00337	0.00221	-0.00371	-0.00910
0.	0.	0.00135	-0.00178	-0.00492	-0.00440	0.00207	0.00965	0.00668	-0.01020
0.	0.	-0.00231	-0.00306	-0.00117	0.00396	0.00691	0.00210	-0.00992	-0.01286
0.01489	0.01299	0.00382	-0.01031	-0.01905	-0.00996	0.01446	0.02685	0.00115	-0.03686
0.01240	0.00365	-0.00984	-0.01819	-0.00952	0.01383	0.02564	0.00110	-0.03520	-0.01983

W= 12 G= 12.56637049

wl/wB

0. 0.	0. 0.	0. 0.	0. 0.	0. 0.	0. 0.	0. 0.	0. 0.	0.00213 -0.00108	0.00032 -0.00397
0. 0.	0. 0.	0. 0.	0. 0.	0. 0.	0. 0.	0.00062 0.00150	0.00227 0.00044	0.00221 -0.00245	-0.00161 -0.00498
0. 0.	0. 0.	0. 0.	0. 0.	-0.00105 0.00098	-0.00070 0.00201	0.00178 0.00224	0.00308 -0.00054	0.00163 -0.00486	-0.00524 -0.00459
0. 0.	0. 0.	-0.00069 -0.00252	-0.00346 -0.00178	-0.00409 0.00137	-0.00053 0.00485	0.00555 0.00386	0.00697 -0.00360	-0.00178 -0.00982	-0.01248 -0.00250
0.01203 0.00943	0.00525 -0.00648	-0.00626 -0.01582	-0.01539 -0.01245	-0.01204 0.00500	0.00561 0.02176	0.02103 0.01145	0.01107 -0.02008	-0.01941 -0.02745	-0.02693 0.01335

W= 10 G= 12.56637049

wl/wB

0. 0.	0. 0.	0. 0.	0. 0.	0. 0.	0. 0.	0. 0.	0. 0.	0.00096 -0.00190	-0.00119 -0.00221
0. 0.	0. 0.	0. 0.	0. 0.	0. 0.	0. 0.	0.00110 0.00074	0.00187 -0.00072	0.00028 -0.00245	-0.00202 -0.00184
0. 0.	0. 0.	0. 0.	0. 0.	-0.00097 0.00111	0.00033 0.00179	0.00227 0.00063	0.00216 -0.00220	-0.00147 -0.00370	-0.00219 -0.00017
0. 0.	0. 0.	-0.00227 -0.00186	-0.00343 0.00011	-0.00164 0.00369	0.00279 0.00305	0.00229 -0.00026	0.00177 -0.00416	-0.00436 -0.00528	-0.00790 0.00529
0.00094 -0.00581	-0.00342 -0.01349	-0.01211 -0.01590	-0.01212 0.00018	0.00009 0.01647	0.01497 0.01566	0.01406 -0.04799	-0.00717 -0.02525	-0.02266 -0.00442	-0.00367 0.02987

U= 15 G= 12.56637049

wl/wR

0.	0.	0.	0.	0.	0.	0.	0.	-0.00007	-0.00157
0.	0.	0.	0.	0.	0.	0.	0.	-0.00127	-0.00078
0.	0.	0.	0.	0.	0.	0.00107	0.00072	-0.00095	-0.00242
0.	0.	0.	0.	0.	0.	-0.00082	-0.00120	-0.00157	0.00021
0.	0.	0.	0.	-0.00007	0.00131	0.00184	0.00014	-0.00275	-0.00292
0.	0.	0.	0.	0.00123	0.00092	-0.00076	-0.00242	-0.00145	0.00244
0.	0.	-0.00273	-0.00198	0.00108	0.00402	0.00290	-0.00272	-0.00438	-0.00105
0.	0.	-0.00057	0.00179	0.00323	0.00128	-0.00330	-0.00562	0.00051	0.00753
-0.00144	-0.00936	-0.01128	-0.00314	0.00984	0.01372	0.00038	-0.01629	-0.01110	0.01375
-0.01118	-0.01346	-0.00375	0.01175	0.01638	0.00045	-0.01944	-0.01325	0.01642	0.02298

U= 16 G= 12.56637049

wl/wR

0.	0.	0.	0.	0.	0.	0.	0.	-0.00058	-0.00120
0.	0.	0.	0.	0.	0.	0.	0.	-0.00071	0.00073
0.	0.	0.	0.	0.	0.	0.00067	-0.00014	-0.00129	-0.00122
0.	0.	0.	0.	0.	0.	-0.00051	-0.00106	-0.00046	0.00122
0.	0.	0.	0.	0.00043	0.00135	0.00070	-0.00123	-0.00229	-0.00028
0.	0.	0.	0.	0.00087	-0.00049	-0.00141	-0.00153	0.00036	0.00282
0.	0.	-0.00197	0.00008	0.00268	0.00294	-0.00051	-0.00437	-0.00287	0.00373
0.	0.	0.00088	0.00248	0.00184	-0.00138	-0.00394	-0.00163	0.00409	0.00497
-0.00714	-0.01007	-0.00490	0.00587	0.01198	0.00456	-0.01021	-0.01276	0.00415	0.01701
-0.01283	-0.00624	0.00747	0.01525	0.00581	-0.01300	-0.01625	0.00328	0.02166	0.00234

0. 0.	0. 0.	0. 0.	0. 0.	0. 0.	0. 0.	0. 0.	0. 0.	-0.00065 -0.00015	-0.00056 0.00065
0. 0.	0. 0.	0. 0.	0. 0.	0. 0.	0. 0.	0.00016 -0.00063	-0.00061 -0.00055	-0.00095 0.00036	-0.00006 0.00124
0. 0.	0. 0.	0. 0.	0. 0.	0.00092 0.00025	0.00079 -0.00072	-0.00039 -0.00123	-0.00153 -0.00026	-0.00092 0.00152	0.00134 0.00168
0. 0.	0. 0.	-0.00046 0.00179	0.00167 0.00198	0.00256 -0.00019	0.00063 -0.00274	-0.00265 -0.00733	-0.00318 0.00164	0.00100 0.00424	0.00458 0.00052
-0.00079 -0.00774	-0.00572 0.00307	0.00294 0.01327	0.00081 0.00885	0.00655 -0.00721	-0.00533 -0.01564	-0.01171 -0.00257	-0.00190 0.01659	0.01227 0.01072	0.00793 -0.01481

0. 0.	0. 0.	0. 0.	0. 0.	0. 0.	0. 0.	0. 0.	0. 0.	-0.00043 0.00021	-0.00000 0.00099
0. 0.	0. 0.	0. 0.	0. 0.	0. 0.	0. 0.	-0.00023 -0.00046	-0.00003 -0.00002	-0.00034 0.00044	0.00059 0.00049
0. 0.	0. 0.	0. 0.	0. 0.	0.00071 -0.00050	0.00004 -0.00008	-0.00024 -0.00054	-0.00027 0.00060	0.00017 0.00135	0.00168 0.00016
0. 0.	0. 0.	0.00075 0.00174	0.00206 0.00040	0.00113 -0.00172	-0.00179 -0.00231	-0.00108 0.00015	-0.00047 0.00304	0.00294 0.00188	0.00240 -0.00267
-0.00007 0.00121	0.00004 0.01099	0.00707 0.01050	0.00715 -0.00256	-0.00179 -0.01148	-0.00095 -0.00741	-0.00117 0.01094	0.00724 0.01346	0.00975 -0.00595	-0.00308 -0.01725

U= 19 G= 12.56637049

MI/MR

0. 0.	0. 0.	0. 0.	0. 0.	0. 0.	0. 0.	0. 0.	0. 0.	-0.00013 0.00031	0.00028 0.00031
0. 0.	0. 0.	0. 0.	0. 0.	0. 0.	0. 0.	-0.00037 -0.00015	-0.00036 0.00031	0.00016 0.00053	0.00065 0.00006
0. 0.	0. 0.	0. 0.	0. 0.	0.00023 -0.00057	-0.00049 -0.00057	-0.00081 0.00010	-0.00012 0.00093	0.00095 0.00054	0.00007 -0.00001
0. 0.	0. 0.	0.00158 0.00082	0.00129 -0.00093	-0.00054 -0.00199	-0.00206 -0.00068	-0.00114 0.00188	0.00159 0.00221	0.00242 -0.00087	-0.00046 -0.00111
-0.00001 0.00871	0.00576 0.01065	0.00705 0.00108	0.00071 -0.01079	-0.00714 -0.00988	-0.00654 0.00441	0.00325 0.01383	0.00915 0.00167	0.00110 -0.01435	-0.00949 -0.00629

W= 20 G= 12.56637049

MI/MR

0. 0.	0. 0.	0. 0.	0. 0.	0. 0.	0. 0.	0. 0.	0. 0.	0.00008 0.00023	0.00029 0.00003
0. 0.	0. 0.	0. 0.	0. 0.	0. 0.	0. 0.	-0.00029 0.00011	-0.00003 0.00035	0.00037 0.00020	0.00036 -0.00031
0. 0.	0. 0.	0. 0.	0. 0.	-0.00022 -0.00050	-0.00041 -0.00008	-0.00021 0.00057	0.00048 0.00040	0.00078 -0.00025	-0.00005 -0.00093
0. 0.	0. 0.	0.00125 -0.00037	-0.00000 -0.00156	-0.00147 -0.00106	-0.00134 0.00095	0.00062 0.00202	0.00201 0.00025	0.00056 -0.00222	-0.00200 -0.00141
0.00414 0.01032	0.00449 0.00365	0.00230 -0.00777	-0.00488 -0.01065	-0.00469 0.00031	0.00020 0.01176	0.00729 0.00041	0.00402 -0.00059	-0.00403 -0.01055	-0.00443 0.00713

APPENDIX II

ZERNIKE POLYNOMIALS

TABLE 2. ZERNIKE POLYNOMIALS

$$R_\nu^m(\zeta) = \sum_{\nu=0}^{(n-m)/2} \frac{(-1)^\nu (n-\nu)!\, \zeta^{n-2\nu}}{\nu!\left(\frac{n-m}{2}-\nu\right)!\left(\frac{n+m}{2}-\nu\right)!}, \quad (n-m) \text{ even}$$

m	n	$R_n^m(\zeta)$
0	0	1
	2	$-1 + 2\zeta^2$
	4	$1 - 6\zeta^2 + 6\zeta^4$
	6	$-1 + 12\zeta^2 - 30\zeta^4 + 20\zeta^6$
	8	$1 - 20\zeta^2 + 90\zeta^4 - 140\zeta^6 + 70\zeta^8$
	10	$-1 + 30\zeta^2 - 210\zeta^4 + 560\zeta^6 - 630\zeta^8 + 252\zeta^{10}$
	12	$1 - 42\zeta^2 + 420\zeta^4 - 1680\zeta^6 + 3150\zeta^8 - 2772\zeta^{10} + 924\zeta^{12}$
	14	$-1 + 56\zeta^2 - 750\zeta^4 + 4200\zeta^6 - 11550\zeta^8 + 16632\zeta^{10} - 12012\zeta^{12} + 3432\zeta^{14}$
1	1	ζ
	3	$-2\zeta + 3\zeta^3$
	5	$3\zeta - 12\zeta^3 + 10\zeta^5$
	7	$-4\zeta + 30\zeta^3 - 60\zeta^5 + 35\zeta^5$
	9	$5\zeta - 60\zeta^3 + 210\zeta^5 - 280\zeta^7 + 126\zeta^9$
	11	$-6\zeta + 105\zeta^3 - 560\zeta^5 + 1260\zeta^7 - 1260\zeta^9 + 462\zeta^{11}$
	13	$7\zeta - 168\zeta^3 + 1260\zeta^5 - 4200\zeta^7 + 6930\zeta^9 - 5544\zeta^{11} + 1716\zeta^{13}$
m	n	
2	2	ζ^2
	4	$-3\zeta^2 + 4\zeta^4$
	6	$6\zeta^2 - 20\zeta^4 + 15\zeta^6$
	8	$-10\zeta^2 + 60\zeta^4 - 105\zeta^6 + 56\zeta^8$

3	3	ζ^3
	5	$-4\zeta^3 + 5\zeta^5$
	7	$10\zeta^3 - 30\zeta^5 + 21\zeta^7$
	9	$-20\zeta^3 + 105\zeta^5 - 168\zeta^7 + 84\zeta^9$
	11	$35\zeta^3 - 280\zeta^5 + 756\zeta^7 - 840\zeta^9 + 330\zeta^{11}$
	13	$-56\zeta^3 + 630\zeta^5 - 2520\zeta^7 + 4620\zeta^9 - 3960\zeta^{11} + 1287\zeta^{13}$
4	4	ζ^4
	6	$-5\zeta^4 + 6\zeta^6$
	8	$15\zeta^4 - 42\zeta^6 + 28\zeta^8$
	10	$-35\zeta^4 + 168\zeta^6 - 252\zeta^8 + 120\zeta^{10}$
	12	$70\zeta^4 - 504\zeta^6 + 1260\zeta^8 - 1320\zeta^{10} + 495\zeta^{12}$
	14	$-126\zeta^4 + 1260\zeta^6 - 4620\zeta^8 + 7920\zeta^{10} - 6435\zeta^{12} + 2002\zeta^{14}$
5	5	ζ^5
	7	$-6\zeta^5 + 7\zeta^7$
	9	$21\zeta^5 - 56\zeta^7 + 36\zeta^9$
	11	$-56\zeta^5 + 252\zeta^7 - 360\zeta^9 + 165\zeta^{11}$
	13	$126\zeta^5 - 840\zeta^7 + 1980\zeta^9 - 1980\zeta^{11} + 715\zeta^{13}$
6	6	ζ^6
	8	$-7\zeta^6 + 8\zeta^8$

7	7	ζ^7
	9	$-8\zeta^7 + 9\zeta^9$
	11	$36\zeta^7 - 90\zeta^9 + 55\zeta^{11}$
	13	$-120\zeta^7 + 495\zeta^9 - 660\zeta^{11} + 286\zeta^{13}$
8	8	ζ^8
	10	$-9\zeta^8 + 10\zeta^{10}$
	12	$45\zeta^8 - 110\zeta^{10} + 66\zeta^{12}$
	14	$-165\zeta^8 + 660\zeta^{10} - 858\zeta^{12} + 364\zeta^{14}$
9	9	ζ^9
	11	$-10\zeta^9 + 11\zeta^{11}$
	13	$55\zeta^9 - 132\zeta^{11} + 78\zeta^{13}$

MODIFIED ZERNIKE POLYNOMIALS OF LOMMEL FUNCTIONS

$$Z_n^m(W_m) = \sum_{\nu=0}^{\frac{(n-m)}{2}} \frac{(-1)^\nu (\frac{n-m}{2})!\ (\frac{m+n}{2}+\nu)!}{(\frac{n-m}{2}-\nu)!\ (\frac{n+m}{2})!(\nu!)^2} W_m^\nu\ (v,u) = \sum_{\nu=0}^{\frac{(n-m)}{2}} C_{mn}^\nu\ W_m^\nu$$

(I) Polynomials of odd degree (m - odd)

$$Z_1^1\ (W_1) = W_1^o$$

$$Z_3^1\ (W_1) = W_1^o - 3\ W_1^1$$

$$Z_5^1\ (W_1) = W_1^o - 8\ W_1^1 + 10\ W_1^2$$

$$Z_7^1\ (W_1) = W_1^o - 15\ W_1^1 + 45\ W_1^2 - 35\ W_1^3$$

$$Z_9^1\ (W_1) = W_1^o - 24\ W_1^1 + 126\ W_1^2 - 224\ W_1^3 + 126\ W_1^4$$

$$Z_{11}^1\ (W_1) = W_1^o - 35\ W_1^1 + 280\ W_1^2 - 840\ W_1^3 + 1050\ W_1^4 - 462\ W_1^5$$

$$Z_{13}^1\ (W_1) = W_1^o - 48\ W_1^1 + 540\ W_1^2 - 2400\ W_1^3 + 4950\ W_1^4 - 4752\ W_1^5 + 1716\ W_1^6$$

$$Z_3^3\ (W_3) = W_3^o$$

$$Z_5^3\ (W_3) = W_3^o - 5\ W_3^1$$

$$Z_7^3\ (W_3) = W_3^o - 12\ W_3^1 + 21\ W_3^2$$

$$Z_9^3\ (W_3) = W_3^o - 21\ W_3^1 + 84\ W_3^2 - 84\ W_3^3$$

$$Z_{11}^3(W_3) = W_3^o - 32\ W_3^1 + 216\ W_3^2 - 480\ W_3^3 + 330\ W_3^4$$

$$Z_{13}^3(W_3) = W_3^o - 45\ W_3^1 + 450\ W_3^2 - 1650\ W_3^3 + 2470\ W_3^4 - 1287\ W_3^5$$

$$z_5^5(W_5) = W_5^0$$

$$z_7^5(W_5) = W_5^0 - 7\,W_5^1$$

$$z_9^5(W_5) = W_5^0 - 16\,W_5^1 + 36\,W_5^2$$

$$z_{11}^5(W_5) = W_5^0 - 27\,W_5^1 + 135\,W_5^2 - 165\,W_5^3$$

$$z_{13}^5(W_5) = W_5^0 - 40\,W_5^1 + 330\,W_5^2 - 880\,W_5^3 + 715\,W_5^4$$

$$z_7^7(W_7) = W_7^0$$

$$z_9^7(W_7) = W_7^0 - 9\,W_7^1$$

$$z_{11}^7(W_7) = W_7^0 - 20\,W_7^1 + 55\,W_7^2$$

$$z_{13}^7(W_7) = W_7^0 - 33\,W_7^1 + 198\,W_7^2 - 286\,W_7^3$$

$$z_9^9(W_9) = W_9^0$$

$$z_{11}^9(W_9) = W_9^0 - 11\,W_9^1$$

$$z_{13}^9(W_9) = W_9^0 - 24\,W_9^1 + 78\,W_9^2$$

$$z_{11}^{11}(W_{11}) = W_{11}^0$$

$$z_{13}^{11}(W_{11}) = W_{11}^0 - 13\,W_{11}^1$$

(II) Polynomials of Even Degree

$$z_0^0(W_0) = W_0^0$$

$$z_2^0(W_0) = W_0^0 - 2W_0^1$$

$$z_4^0(W_0) = W_0^0 - 6W_0^1 + 6W_0^2$$

$$z_6^0(W_0) = W_0^0 - 12W_0^1 + 30W_0^2 - 20W_0^3$$

$$z_8^0(W_0) = W_0^0 - 20W_0^1 + 90W_0^2 - 140W_0^3 + 70W_0^4$$

$$z_{10}^0(W_0) = W_0^0 - 30W_0^1 + 210W_0^2 - 560W_0^3 + 630W_0^4 - 252W_0^5$$

$$z_2^2(W_2) = W_2^0$$

$$z_4^2(W_2) = W_2^0 - 4W_2^1$$

$$z_6^2(W_2) = W_2^0 - 10W_2^1 + 15W_2^2$$

$$z_8^2(W_2) = W_2^0 - 18W_2^1 + 63W_2^2 - 56W_2^3$$

$$z_{10}^2(W_2^2) = W_2^0 - 28W_2^1 + 168W_2^2 - 336W_2^3 + 210W_2^4$$

$$z_4^4(W_4) = W_4^0$$

$$z_6^4(W_4) = W_4^0 - 6W_4^1$$

$$z_8^4(W_4) = W_4^0 - 14W_4^1 + 28W_4^2$$

$$z_{10}^4(W_4) = W_4^0 - 24W_4^1 + 108W_4^2 - 120W_4^3$$

$$z_6^6(W_6) = w_6^0$$

$$z_8^6(W_6) = w_6^0 - 8\,w_6^1$$

$$z_{10}^6(W_6) = w_6^0 - 18\,w_6^1 + 45\,w_6^2$$

$$z_8^8(W_8) = w_8^0$$

$$z_{10}^8(W_8) = w_8^0 - 10\,w_8^1$$

$$z_{10}^{10}(W_{10}) = w_{10}^0$$

APPENDIX III

TABLES OF THE STRIP APPROXIMATION PATTERN FACTOR AND AN/TPS-1D SAMPLE PATTERN CALCULATIONS

TABLE 3

TABLES OF THE STRIP APPROXIMATION PATTERN FACTOR $F_n(\gamma, u)$

$$F_n(\gamma, u) = e^{-j\frac{(2n+1)^2}{128}\gamma}\left\{e^{j\left(\frac{2n-1}{8}\right)u}\left(\frac{\sin \xi_n}{\xi_n}\right) + e^{j\left(\frac{2n-1}{8}\right)u}\left(\frac{\sin \xi_{-n}}{\xi_{-n}}\right)\right\}$$

The following is a list of computer notations used in the tables for the variables in the above equation

R = Real part of $F_n(\gamma, u)$

I = Imaginary part of $F_n(\gamma, u)$

U = u

GAMMA = γ

N = n

PI = π

The tables were calculated for N (=n) = 1, 2, 3, 4 for the values of $\gamma = \pi/4, \pi/2, \pi, \frac{3\pi}{2}, 2\pi, 3\pi, 4\pi$ and u = 0, 0.5, 1.0, 1.5,...., 20. The tables are arranged with a fixed value of n on a given page, γ as a column variable and us as a row variable, i.e. the tables are arranged as shown in the following diagram.

TABLE 3

TABLES OF THE STRIP APPROXIMATION FACTOR

	N(=n) = 1			
	GAMMA (= γ) =	PI/4 (= $\pi/4$)	PI/2 = ($\pi/2$)	...
U (=u)=0.	R (= Re $F_n(\gamma,u)$)	Re F_1 ($\pi/4$,0)	Re F_1 ($\pi/2$, 0)	...
	I (= Im $F_n(\gamma,u)$)	Im F_1 ($\pi/4$,0)	Im F_1 ($\pi/2$, 0)	...
U (=u)=0.5	R (=(Re $F_n(\gamma,u)$)	Re F_1 ($\pi/4$,0.5)	Re F_1 ($\pi/2$, 0.5)	
	I (= Im $F_n(\gamma,u)$)	Im F_1 ($\pi/4$,0.5)	Im F_1 ($\pi/2$, C.5)	...

N= 1   DATE 040364 TIME 2.89 CASE 1 PAGE 1

GAMMA=		PI/4	PI/2	PI	3PI/2	2PI	3PI	4PI
U= 0.	R	1.9999	1.9996	1.9986	1.9968	1.9944	1.9874	1.9776
	I	-0.0123	-0.0245	-0.0491	-0.0735	-0.0980	-0.1466	-0.1948
U= 0.5	R	1.9947	1.9944	1.9934	1.9917	1.9892	1.9822	1.9725
	I	-0.0122	-0.0244	-0.0488	-0.0732	-0.0975	-0.1458	-0.1938
U= 1.0	R	1.9791	1.9789	1.9779	1.9761	1.9737	1.9669	1.9573
	I	-0.0120	-0.0240	-0.0480	-0.0720	-0.0959	-0.1436	-0.1907
U= 1.5	R	1.9534	1.9531	1.9521	1.9504	1.9481	1.9414	1.9321
	I	-0.0117	-0.0234	-0.0468	-0.0701	-0.0934	-0.1398	-0.1857
U= 2.0	R	1.9176	1.9174	1.9164	1.9148	1.9125	1.9061	1.8971
	I	-0.0113	-0.0225	-0.0450	-0.0675	-0.0899	-0.1346	-0.1788
U= 2.5	R	1.8722	1.8720	1.8711	1.8695	1.8674	1.8613	1.8527
	I	-0.0107	-0.0214	-0.0429	-0.0642	-0.0855	-0.1280	-0.1700
U= 3.0	R	1.8176	1.8174	1.8165	1.8151	1.8131	1.8073	1.7993
	I	-0.0100	-0.0201	-0.0402	-0.0602	-0.0802	-0.1200	-0.1595
U= 3.5	R	1.7543	1.7541	1.7533	1.7520	1.7501	1.7448	1.7374
	I	-0.0093	-0.0186	-0.0371	-0.0556	-0.0741	-0.1108	-0.1473
U= 4.0	R	1.6829	1.6827	1.6820	1.6808	1.6791	1.6742	1.6675
	I	-0.0084	-0.0168	-0.0335	-0.0504	-0.0672	-0.1005	-0.1336
U= 4.5	R	1.6040	1.6038	1.6032	1.6021	1.6006	1.5963	1.5902
	I	-0.0075	-0.0149	-0.0298	-0.0447	-0.0596	-0.0892	-0.1185
U= 5.0	R	1.5183	1.5182	1.5176	1.5167	1.5154	1.5116	1.5064
	I	-0.0064	-0.0129	-0.0257	-0.0386	-0.0514	-0.0770	-0.1023
U= 5.5	R	1.4267	1.4266	1.4261	1.4253	1.4242	1.4211	1.4167
	I	-0.0053	-0.0107	-0.0214	-0.0321	-0.0427	-0.0640	-0.0850
U= 6.0	R	1.3300	1.3299	1.3295	1.3289	1.3280	1.3255	1.3220
	I	-0.0042	-0.0084	-0.0168	-0.0252	-0.0336	-0.0503	-0.0669
U= 6.5	R	1.2290	1.2289	1.2286	1.2281	1.2275	1.2256	1.2230
	I	-0.0030	-0.0060	-0.0121	-0.0181	-0.0242	-0.0362	-0.0481
U= 7.0	R	1.1246	1.1245	1.1244	1.1240	1.1236	1.1224	1.1207
	I	-0.0018	-0.0036	-0.0072	-0.0108	-0.0145	-0.0217	-0.0289
U= 7.5	R	1.0178	1.0177	1.0176	1.0175	1.0173	1.0168	1.0160
	I	-0.0005	-0.0011	-0.0023	-0.0035	-0.0047	-0.0071	-0.0095
U= 8.0	R	0.9094	0.9094	0.9094	0.9094	0.9095	0.9096	0.9097
	I	0.0008	0.0014	0.0027	0.0039	0.0052	0.0077	0.0101
U= 8.5	R	0.8004	0.8005	0.8006	0.8007	0.8010	0.8018	0.8028
	I	0.0021	0.0039	0.0076	0.0113	0.0150	0.0222	0.0294
U= 9.0	R	0.6918	0.6918	0.6920	0.6924	0.6929	0.6942	0.6962
	I	0.0034	0.0064	0.0125	0.0185	0.0246	0.0366	0.0485

DATE [illegible] TIME 2.09 CASE 1 PAGE 2

[illegible]	PI/4	PI/2	PI	3PI/2	2PI	3PI	4PI
U= 9.5 R	0.5844	0.5846	0.5847	0.5852	0.5859	0.5879	0.5907
I	0.0047	0.0089	0.0172	0.0256	0.0340	0.0505	0.0670
U=10.0 R	0.4790	0.4791	0.4795	0.4801	0.4810	0.4836	0.4872
I	0.0060	0.0113	0.0219	0.0324	0.0430	0.0640	0.0847
U=10.5 R	0.3766	0.3767	0.3772	0.3779	0.3790	0.3821	0.3865
I	0.0073	0.0136	0.0263	0.0390	0.0516	0.0767	0.1017
U=11.0 R	0.2779	0.2780	0.2785	0.2794	0.2807	0.2843	0.2894
I	0.0085	0.0159	0.0305	0.0451	0.0597	0.0888	0.1175
U=11.5 R	0.1835	0.1837	0.1843	0.1853	0.1867	0.1908	0.1965
I	0.0099	0.0181	0.0345	0.0509	0.0673	0.0999	0.1322
U=12.0 R	0.0943	0.0945	0.0952	0.0963	0.0979	0.1023	0.1086
I	0.0112	0.0202	0.0383	0.0563	0.0743	0.1104	0.1456
U=12.5 R	0.0107	0.0109	0.0117	0.0129	0.0145	0.0194	0.0262
I	0.0125	0.0223	0.0417	0.0612	0.0806	0.1193	0.1576
U=13.0 R	-0.0667	-0.0665	-0.0656	-0.0643	-0.0625	-0.0574	-0.0502
I	0.0139	0.0242	0.0449	0.0656	0.0862	0.1273	0.1684
U=13.5 R	-0.1375	-0.1372	-0.1363	-0.1349	-0.1330	-0.1276	-0.1200
I	0.0152	0.0261	0.0478	0.0694	0.0911	0.1343	0.1771
U=14.0 R	-0.2013	-0.2010	-0.2001	-0.1986	-0.1966	-0.1909	-0.1832
I	0.0165	0.0279	0.0503	0.0728	0.0953	0.1400	0.1846
U=14.5 R	-0.2579	-0.2576	-0.2566	-0.2550	-0.2529	-0.2471	-0.2390
I	0.0180	0.0296	0.0526	0.0757	0.0987	0.1446	0.1901
U=15.0 R	-0.3071	-0.3067	-0.3057	-0.3040	-0.3019	-0.2960	-0.2879
I	0.0195	0.0312	0.0546	0.0780	0.1013	0.1479	0.1942
U=15.5 R	-0.3488	-0.3484	-0.3473	-0.3456	-0.3434	-0.3373	-0.3290
I	0.0210	0.0328	0.0563	0.0798	0.1032	0.1501	0.1966
U=16.0 R	-0.3831	-0.3827	-0.3816	-0.3798	-0.3776	-0.3713	-0.3628
I	0.0226	0.0343	0.0577	0.0811	0.1044	0.1511	0.1976
U=16.5 R	-0.4100	-0.4095	-0.4083	-0.4065	-0.4040	-0.3976	-0.3890
I	0.0242	0.0357	0.0588	0.0819	0.1049	0.1509	0.1967
U=17.0 R	-0.4290	-0.4286	-0.4277	-0.4258	-0.4234	-0.4173	-0.4090
I	0.0258	0.0371	0.0596	0.0822	0.1047	0.1496	0.1943
U=17.5 R	-0.4426	-0.4420	-0.4404	-0.4384	-0.4358	-0.4290	-0.4220
I	0.0275	0.0384	0.0602	0.0820	0.1038	0.1473	0.1907
U=18.0 R	-0.4489	-0.4482	-0.4466	-0.4443	-0.4418	-0.4357	-0.4281
I	0.0291	0.0396	0.0605	0.0814	0.1023	0.1440	0.1856
U=18.5 R	-0.4491	-0.4482	-0.4463	-0.4441	-0.4415	-0.4354	-0.4288
I	0.0307	0.0406	0.0604	0.0803	0.1001	0.1397	0.1792

GAMMA=		PI/4	PI/2	PI	3PI/2	2PI	3PI	4PI
U=19.0	R	-0.4436	-0.4426	-0.4405	[illegible]	-0.4385	-0.4296	-0.4221
	I	0.0322	0.0415	[illegible]	[illegible]	[illegible]	0.1344	0.1717
U=19.5	R	-0.4330	[illegible]	[illegible]	[illegible]	[illegible]	[illegible]	-0.4111
	I	0.0335	[illegible]	[illegible]	[illegible]	[illegible]	[illegible]	0.1631
U=20.0	R	-0.4180	-0.4160	-0.4142	-0.4114	[illegible]	-0.4023	-0.3954
	I	0.0345	0.0425	[illegible]	[illegible]	[illegible]	0.1210	0.1535

N= 2 [illegible] CASE 2 PAGE 4

GAMMA=		PI/4	PI/2	PI	3PI/2	2PI	3PI	4PI
U= 0.	R	1.9965	1.9860	1.9444	1.8759	1.7830	1.5259	1.1967
	I	-0.1106	-0.2202	[illegible]	[illegible]	[illegible]	[illegible]	[illegible]
U= 0.5	R	[illegible]	[illegible]	[illegible]	[illegible]	[illegible]	[illegible]	[illegible]
	I	-0.1001	-0.2157	-0.4276	-0.6320	-0.8254	-1.1666	-1.4209
U= 1.0	R	1.8530	1.8434	1.8095	1.7432	1.6577	1.4244	1.1242
	I	-0.1013	-0.2022	[illegible]	-0.5926	-0.7742	[illegible]	-1.3525
U= 1.5	R	1.6791	[illegible]	1.6373	[illegible]	[illegible]	[illegible]	[illegible]
	I	-0.0904	-0.1804	-0.3577	-0.5209	[illegible]	-0.9709	-1.2026
U= 2.0	R	1.4459	1.4390	1.4116	1.3665	1.3065	1.1353	0.9166
	I	[illegible]	-0.1512	[illegible]	[illegible]	[illegible]	[illegible]	[illegible]
U= 2.5	R	1.1627	1.1577	1.1375	[illegible]	[illegible]	[illegible]	[illegible]
	I	-0.0501	-0.1101	-0.2304	-0.3412	-0.4409	-0.6300	-0.7896
U= 3.0	R	0.8413	0.8387	0.8261	0.8060	0.7704	0.7023	0.6024
	I	[illegible]	[illegible]	[illegible]	[illegible]	[illegible]	[illegible]	-0.5345
U= 3.5	R	[illegible]	[illegible]	[illegible]	[illegible]	[illegible]	[illegible]	[illegible]
	I	-0.0171	-0.0342	-0.0684	-0.1022	-0.1359	-0.2003	-0.2614
U= 4.0	R	0.1361	0.1373	0.1423	0.1509	0.1614	0.1900	0.2230
	I	[illegible]	[illegible]	[illegible]	[illegible]	[illegible]	[illegible]	[illegible]
U= 4.5	R	-0.2107	-0.2103	-0.2031	-0.1914	-0.1518	-0.0725	[illegible]
	I	0.0234	0.0507	0.0999	0.1463	0.1883	0.2340	0.2916
U= 5.0	R	-0.5591	-0.5530	-0.5338	-0.4909	-0.4524	-0.3200	-0.1605
	I	[illegible]	[illegible]	[illegible]	[illegible]	[illegible]	[illegible]	[illegible]
U= 5.5	R	[illegible]	[illegible]	[illegible]	[illegible]	[illegible]	[illegible]	[illegible]
	I	0.0623	0.1242	0.2456	0.3615	0.4693	0.6517	0.7771
U= 6.0	R	-1.1391	-1.1310	[illegible]	[illegible]	-0.9726	-0.7739	-0.5267
	I	[illegible]	[illegible]	[illegible]	[illegible]	[illegible]	[illegible]	[illegible]
U= 6.5	R	[illegible]	[illegible]	[illegible]	[illegible]	[illegible]	[illegible]	[illegible]
	I	0.0873	0.1740	0.3445	0.5081	0.6614	0.9236	1.1171
U= 7.0	R	-1.5223	-1.5120	-1.4730	[illegible]	[illegible]	[illegible]	[illegible]
	I	[illegible]	[illegible]	[illegible]	[illegible]	[illegible]	[illegible]	[illegible]
U= 7.5	R	-1.6263	-1.6167	[illegible]	[illegible]	[illegible]	[illegible]	[illegible]
	I	0.0966	0.1920	[illegible]	[illegible]	0.7320	1.0262	1.2023
U= 8.0	R	[illegible]	[illegible]	[illegible]	[illegible]	[illegible]	[illegible]	[illegible]
	I	[illegible]	[illegible]	[illegible]	[illegible]	[illegible]	[illegible]	[illegible]
U= 8.5	R	-1.6481	-1.6318	[illegible]	[illegible]	[illegible]	[illegible]	[illegible]
	I	0.0996	0.1700	0.3547	[illegible]	[illegible]	0.9736	1.1900
U= 9.0	R	[illegible]	[illegible]	[illegible]	[illegible]	[illegible]	[illegible]	[illegible]
	I	[illegible]	[illegible]	[illegible]	[illegible]	[illegible]	[illegible]	[illegible]

WAVE GAMMA TIME 2.00 CASE 2 PAGE 5

GAMMA=		PI/4	PI/2	PI	3PI/2	2PI	3PI	4PI
U= 9.5	R	-1.4262	-1.4166	-1.3866	-1.3807	-1.3003	-1.1703	-0.9074
	I	0.0002	0.1304	0.2713	[illegible]	0.5207	0.7593	0.9510
U=10.0	R	-1.2452	-1.2412	-1.2237	[illegible]	-1.1669	-1.0666	-0.9351
	I	0.0535	0.1075	0.2130	[illegible]	0.4197	0.6091	0.7750
U=10.5	R	-1.0307	-1.0266	-1.0203	-1.0067	-0.9877	-0.9334	-0.8576
	I	0.0371	0.0740	0.1499	0.2243	0.2977	0.4403	0.5746
U=11.0	R	-0.7013	-0.7011	-0.7003	-0.7000	-0.7064	-0.7771	-0.7505
	I	0.0197	[illegible]	0.0823	0.1269	0.1607	0.2686	0.3801
U=11.5	R	-0.5380	-0.5397	-0.5461	-0.5564	-0.5701	-0.6047	-0.6420
	I	0.0021	0.0059	0.0143	0.0230	0.0307	0.0794	0.1416
U=12.0	R	-0.2020	-0.2053	-0.2086	-0.3196	-0.3403	-0.4235	-0.5129
	I	-0.0148	-0.0277	[illegible]	-0.0710	-0.0862	-0.0959	-0.0710
U=12.5	R	-0.0336	-0.0365	-0.0574	[illegible]	-0.1299	-0.2406	-0.3750
	I	-0.0364	-0.0577	-0.1106	-0.1900	-0.2007	-0.2574	-0.2605
U=13.0	R	0.1973	0.1912	0.1675	0.1290	0.0760	-0.0620	-0.2356
	I	-0.0439	[illegible]	-0.1620	-0.2300	-0.2900	-0.3905	-0.4630
U=13.5	R	0.4026	0.3956	0.3603	0.3342	0.2643	0.1037	-0.0969
	I	-0.0540	-0.1052	-0.2034	-0.2959	-0.3001	-0.5137	-0.5870
U=14.0	R	0.5757	0.5600	0.5306	0.4012	0.4260	0.2537	0.0390
	I	-0.0620	-0.1205	-0.2333	-0.3403	-0.4305	-0.5900	-0.6970
U=14.5	R	0.7118	0.7036	0.6738	0.6254	0.5597	0.3029	0.1592
	I	-0.0676	-0.1294	-0.2500	-0.3604	-0.4735	-0.6523	-0.7702
U=15.0	R	0.8003	0.8006	0.7710	0.7230	0.6402	0.4904	0.2697
	I	-0.0606	-0.1316	-0.2557	-0.3562	-0.4646	-0.6727	-0.8037
U=15.5	R	0.8644	0.8569	0.8295	0.7866	0.7271	0.5603	0.3648
	I	-0.0663	-0.1270	-0.2404	-0.3642	-0.4730	-0.6613	-0.7992
U=16.0	R	0.8814	0.8746	0.8503	0.8122	0.7609	0.6220	0.4429
	I	-0.0607	-0.1177	-0.2290	-0.3376	-0.4400	-0.6204	-0.7503
U=16.5	R	0.8622	0.8564	0.8363	0.8052	0.7634	0.6503	0.5030
	I	-0.0520	-0.1025	-0.2013	-0.2971	-0.3886	-0.5538	-0.6802
U=17.0	R	0.8114	0.8067	0.7915	0.7605	0.7379	0.6547	0.5466
	I	-0.0405	-0.0823	-0.1646	-0.2449	-0.3224	-0.4664	-0.5913
U=17.5	R	0.7343	0.7311	0.7213	0.7071	0.6885	0.6378	0.5683
	I	-0.0267	-0.0507	-0.1220	-0.1843	-0.2455	-0.3630	-0.4751
U=18.0	R	0.6375	0.6357	0.6315	0.6265	0.6202	0.6027	0.5749
	I	-0.0111	-0.0327	-0.0757	-0.1107	-0.1621	-0.2519	-0.3460
U=18.5	R	0.5275	0.5273	0.5268	0.5327	0.5305	0.5532	0.5640
	I	0.0050	-0.0054	-0.0279	-0.0514	-0.0769	-0.1371	-0.2136

OMEGA=	PI/4	PI/2	PI	3PI/2	2PI	3PI	4PI
U=19.0 R	0.4111	0.4125	0.4195	0.4317	0.4487	[illegible]	0.5435
I	0.0232	0.0219	0.0189	0.0141	0.0090	-0.0251	-0.0020
U=19.5 R	0.2946	0.2976	0.3097	0.3293	0.3961	0.4264	0.5093
I	[illegible]	[illegible]	[illegible]	[illegible]	[illegible]	[illegible]	[illegible]
U=20.0 R	0.1036	0.1082	0.2067	0.2387	0.2656	[illegible]	0.4443
I	0.0569	0.0722	0.1016	0.1200	0.1402	0.1604	0.1497

N= 3 [illegible] [illegible] [illegible] 2.00 CASE 3 PAGE 7

GAMMA=		PI/4	PI/2	PI	3PI/2	2PI	3PI	4PI
U= 0.	R	1.9753	[illegible]	[illegible]	[illegible]	[illegible]	-0.4065	-1.3094
	I	-0.3054	[illegible]	-1.1[illegible]	-1.[illegible]	-1.[illegible]	-1.7500	-1.0746
U= 0.5	R	1.0785	1.[illegible]	1.5612	1.1205	0.6211	-0.4541	-1.2[illegible]
	I	-0.2096	-0.5714	-1.[illegible]	-1.4[illegible]	-1.7176	-1.6743	-1.0[illegible]
U= 1.0	R	1.5902	1.5401	1.[illegible]	0.9717	0.[illegible]	-0.3609	-1.0320
	I	-0.2441	-0.4[illegible]	-0.[illegible]	-1.[illegible]	-1.[illegible]	-1.4313	-0.9030
U= 1.5	R	1.1631	1.1227	[illegible]	0.[illegible]	0.4261	-0.2109	-0.7143
	I	-0.1736	-0.3420	-0.[illegible]	-0.[illegible]	-1.0479	-1.0535	-0.7019
U= 2.0	R	0.6179	0.5993	0.5273	0.4149	0.2729	-0.0463	-0.3204
	I	-0.0050	-0.1[illegible]	-0.3[illegible]	-0.4511	-0.5391	-0.5783	-0.4440
U= 2.5	R	0.0181	0.[illegible]	0.[illegible]	0.[illegible]	0.[illegible]	0.1347	0.1050
	I	0.0100	0.0192	0.0310	0.0327	0.0185	-0.0527	-0.1500
U= 3.0	R	-0.5757	-0.5477	-0.4407	-0.2705	-0.0033	0.3006	0.5172
	I	0.1036	0.2037	0.[illegible]	0.5071	0.5674	0.4715	0.1535
U= 3.5	R	-1.1041	-1.0[illegible]	-0.[illegible]	-0.[illegible]	-0.2575	0.4[illegible]	0.[illegible]
	I	0.1052	0.3047	0.6053	0.9233	1.0516	0.9437	0.4439
U= 4.0	R	-1.5156	-1.4539	-1.2[illegible]	-0.[illegible]	-0.4100	0.5057	1.1210
	I	0.2464	0.[illegible]	0.[illegible]	1.2[illegible]	1.4225	1.3107	0.6965
U= 4.5	R	-1.7712	-1.[illegible]	-1.[illegible]	-1.[illegible]	-0.[illegible]	0.5172	1.2[illegible]
	I	0.2011	0.5563	1.[illegible]	1.4232	1.6444	1.5620	0.[illegible]
U= 5.0	R	-1.0409	-1.7[illegible]	-1.5151	-1.1076	-0.6[illegible]	0.4622	1.2411
	I	0.2863	0.[illegible]	1.[illegible]	1.4[illegible]	1.6975	1.6528	1.0[illegible]
U= 5.5	R	-1.7453	-1.[illegible]	-1.[illegible]	-1.[illegible]	-0.[illegible]	0.[illegible]	1.[illegible]
	I	0.2619	0.5172	0.[illegible]	1.3479	1.5004	1.5057	1.0477
U= 6.0	R	-1.4757	-1.4206	-1.2[illegible]	-0.9625	-0.6[illegible]	0.1040	0.0375
	I	0.2114	0.[illegible]	0.[illegible]	1.1031	1.[illegible]	1.3712	0.9987
U= 6.5	R	-1.0719	-1.[illegible]	-0.[illegible]	-0.[illegible]	-0.5333	-0.[illegible]	0.[illegible]
	I	0.1407	0.2[illegible]	0.[illegible]	0.[illegible]	0.9164	1.0341	0.8687
U= 7.0	R	-0.5704	-0.57[illegible]	-0.5422	-0.4919	-0.4106	-0.1990	0.0994
	I	0.0578	0.1195	0.[illegible]	0.[illegible]	0.4432	0.6197	0.6693
U= 7.5	R	-0.0476	-0.[illegible]	-0.[illegible]	-0.[illegible]	-0.2719	-0.3739	-0.2[illegible]
	I	-0.0202	-0.0539	-0.[illegible]	-0.0923	-0.0534	0.1445	0.4176
U= 8.0	R	0.4461	0.4327	0.3[illegible]	0.1165	-0.1053	-0.5063	-0.6476
	I	-0.1080	-0.2114	-0.3[illegible]	-0.4[illegible]	-0.5275	-0.3180	0.1351
U= 8.5	R	0.9125	0.[illegible]	0.[illegible]	0.4011	0.0[illegible]	-0.5002	-0.9212
	I	-0.1736	-0.3409	-0.6343	-0.[illegible]	-0.9297	-0.7324	-0.1543
U= 9.0	R	1.2490	1.1924	0.9725	0.6370	0.2317	-0.5857	-1.0074
	I	-0.2184	-0.4297	-0.[illegible]	-1.[illegible]	-1.2216	-1.0608	-0.4267

U= 9.5	R	1.4008	1.3899	1.1595	0.8871	0.5968	-0.3812	-1.1987
	I	-0.2387	-0.4785	-0.8840	-1.2882	-1.5782	-1.6759	-0.6897
U=10.0	R	1.4993	1.4484	1.2282	0.9965	0.4883	-0.3936	-1.0200
	I	-0.2333	-0.4883	-0.8720	-1.1925	-1.3898	-1.3897	-0.8585
U=10.5	R	1.4815	1.3926	1.1781	0.9021	0.5867	-0.2176	-0.8877
	I	-0.2039	-0.4033	-0.7693	-1.0643	-1.2824	-1.3192	-0.9376
U=11.0	R	1.1745	1.1432	1.0210	0.8278	0.5781	-0.0139	-0.5788
	I	-0.1549	-0.3076	-0.5931	-0.8551	-1.0852	-1.1089	-0.9818
U=11.5	R	0.8488	0.8367	0.7785	0.6869	0.5367	0.1788	-0.2988
	I	-0.0924	-0.1884	-0.3661	-0.5345	-0.6894	-0.8874	-0.9867
U=12.0	R	0.4632	0.4671	0.4797	0.4984	0.4874	0.3848	0.0995
	I	-0.0239	-0.0512	-0.1151	-0.1981	-0.3033	-0.4086	-0.7788
U=12.5	R	0.0884	0.0818	0.1573	0.2859	0.3827	0.5388	0.4213
	I	0.0430	0.0880	0.1316	0.1364	0.0818	-0.1992	-0.5898
U=13.0	R	-0.3179	-0.2838	-0.1557	0.0338	0.2588	0.4182	0.4897
	I	0.1011	0.1981	0.3879	0.4339	0.4317	0.1943	-0.3373
U=13.5	R	-0.6357	-0.5985	-0.4297	-0.1854	0.1011	0.4389	0.6888
	I	0.1446	0.2798	0.5125	0.6651	0.7122	0.4488	-0.1843
U=14.0	R	-0.8656	-0.8186	-0.6412	-0.3737	-0.0517	0.3822	0.9947
	I	0.1696	0.3298	0.6111	0.8099	0.8991	0.7188	0.1968
U=14.5	R	-0.9918	-0.9385	-0.7751	-0.5145	-0.1957	0.4538	0.9838
	I	0.1741	0.3405	0.6376	0.8593	0.9788	0.8783	0.3884
U=15.0	R	-1.0185	-0.9718	-0.8254	-0.6083	-0.3185	0.3738	0.7729
	I	0.1592	0.3137	0.5943	0.8140	0.9542	0.8888	0.5853
U=15.5	R	-0.9298	-0.8817	-0.7951	-0.6282	-0.4137	0.0913	0.5838
	I	0.1276	0.2549	0.4913	0.6892	0.8237	0.9221	0.7283
U=16.0	R	-0.7675	-0.7326	-0.6921	-0.6011	-0.4717	-0.1191	0.2868
	I	0.0858	0.1728	0.3444	0.5023	0.6344	0.8138	0.8027
U=16.5	R	-0.5485	-0.5477	-0.5426	-0.5268	-0.4882	-0.3144	0.0279
	I	0.0333	0.0784	0.1737	0.2882	0.3988	0.4895	0.8183
U=17.0	R	-0.3013	-0.3148	-0.3583	-0.4164	-0.4487	-0.4727	-0.3888
	I	-0.0175	-0.0168	0.0882	0.0985	0.1422	0.4358	0.7815
U=17.5	R	-0.0545	-0.0786	-0.1630	-0.2834	-0.4119	-0.5771	-0.4622
	I	-0.0629	-0.1019	-0.1562	-0.1695	-0.1088	0.2929	0.6333
U=18.0	R	0.1663	0.1342	0.0207	-0.1416	-0.3244	-0.4138	-0.4289
	I	-0.0977	-0.1678	-0.2792	-0.3388	-0.3849	-0.0156	0.4687
U=18.5	R	0.3414	0.3053	0.1787	-0.0039	-0.2158	-0.5098	-0.7887
	I	-0.1184	-0.2081	-0.3576	-0.4528	-0.4217	-0.2894	0.2734

DATE [illegible] TIME 2.09 CASE 3 PAGE 9

GAMMA=		PI/4	PI/2	PI	3PI/2	2PI	3PI	4PI
U=19.0	R	0.4586	0.4227	0.2966	0.1187	-0.0933	-0.4983	-0.6957
	I	-0.1229	-0.2200	-0.3042	-0.4956	-0.5311	-0.3595	0.0654
U=19.5	R	0.5135	0.4819	0.3745	[illegible]	[illegible]	-0.3561	-0.6132
	I	-0.1111	-0.2038	-0.3663	[illegible]	[illegible]	-0.4500	-0.1375
U=20.0	R	0.5095	0.4056	0.4063	0.2985	0.1467	-0.1796	-0.4670
	I	-0.0048	-0.1632	-0.3046	-0.4169	-0.4914	-0.5021	-0.3184

N= 4 DATE 040364 TIME 2.09 CASE 4 PAGE 10

GAMMA=		PI/4	PI/2	PI	3PI/2	2PI	3PI	4PI
U= 0.	R	1.9079	1.6411	0.7057	-0.4419	-1.3683	-1.4865	0.1399
	I	-0.9916	-1.1299	-1.8295	-1.8609	-1.2599	0.7482	1.6203
U= 0.5	R	1.7276	1.4879	0.6444	-0.3914	-1.2396	-1.3531	0.1060
	I	-0.5341	-1.0167	-1.6540	-1.6866	-1.1310	0.6620	1.2079
U= 1.0	R	1.2214	1.0994	0.4714	-0.2514	-0.0466	-0.9773	0.0176
	I	-0.3738	-0.7108	-1.1619	-1.1972	-0.8238	0.4258	0.9159
U= 1.5	R	0.4876	0.4204	0.2176	-0.0534	-0.2965	-0.4279	-0.1001
	I	-0.1404	-0.2609	-0.4499	-0.4066	-0.3734	0.0906	0.3747
U= 2.0	R	-0.3324	-0.2737	-0.0729	0.1576	0.3132	0.1948	-0.2004
	I	0.1177	0.2216	0.3627	0.3095	0.1397	-0.2669	-0.2333
U= 2.5	R	-1.0013	-0.9175	-0.3483	0.3338	0.0533	0.7779	-0.2696
	I	0.3704	0.6644	1.0618	1.0399	0.6245	-0.5660	-0.7935
U= 3.0	R	-1.6173	-1.3021	-0.5610	0.4351	1.2172	1.2165	-0.2569
	I	0.5124	0.9795	1.5092	1.5876	0.9955	-0.7385	-1.2015
U= 3.5	R	-1.8614	-1.5823	-0.6765	0.4382	1.3336	1.4329	-0.1619
	I	0.5730	1.0983	1.7690	1.7959	1.1005	-0.7447	-1.3823
U= 4.0	R	-1.7161	-1.4049	-0.6702	0.3417	1.1016	1.3912	0.0013
	I	0.5219	0.9928	1.6299	1.6867	1.1718	-0.5821	-1.3047
U= 4.5	R	-1.2722	-1.1139	-0.5588	0.1670	0.7964	1.1025	0.1906
	I	0.3711	0.7109	1.1029	1.2669	0.9514	-0.2059	-0.9067
U= 5.0	R	-0.6009	-0.5053	-0.3307	-0.0473	0.2594	0.6230	0.3022
	I	0.1523	0.2996	0.5213	0.6219	0.5896	0.0784	-0.4913
U= 5.5	R	0.1690	0.1095	-0.0726	-0.2533	-0.3183	0.0422	0.5099
	I	-0.0902	-0.1053	-0.2221	-0.1218	0.0962	0.4297	0.0060
U= 6.0	R	0.0777	0.7267	0.2004	-0.4046	-0.0195	-0.5336	0.5252
	I	-0.3008	-0.5085	-0.9024	-0.8221	-0.3837	0.6895	0.6361
U= 6.5	R	1.4042	1.1088	0.4329	-0.4571	-1.1449	-1.0014	0.4283
	I	-0.4609	-0.0733	-1.3985	-1.3493	-0.7060	0.7990	1.0969
U= 7.0	R	1.6900	1.4144	0.5057	-0.4263	-1.2332	-1.2002	0.2224
	I	-0.5195	-0.9879	-1.5985	-1.6102	-1.0425	0.7326	1.2730
U= 7.5	R	1.5012	1.3725	0.6347	-0.2904	-1.0731	-1.3253	-0.0569
	I	-0.4701	-0.9009	-1.4967	-1.5052	-1.1122	0.5035	1.2492
U= 8.0	R	1.2200	1.0803	0.5744	-0.0009	-0.7041	-1.1354	-0.3937
	I	-0.3429	-0.6509	-1.1156	-1.2343	-0.9884	0.1636	0.9963
U= 8.5	R	0.6495	0.6025	0.4185	0.1361	-0.2089	-0.7518	-0.6040
	I	-0.1693	-0.2932	-0.9400	-0.6907	-0.6909	-0.2214	0.5675
U= 9.0	R	-0.0153	0.0363	0.1970	0.3296	0.3130	-0.2490	-0.7498
	I	0.0643	0.1122	0.1115	-0.0440	-0.2992	-0.5595	[illegible]

WAVE GAMMA TIME 2.00 CASE 4 PAGE II

GAMMA=		PI/4	PI/2	PI	3PI/2	2PI	3PI	4PI
U= 9.5	R	-0.6442	-0.5003	-0.0501	0.4567	0.7523	0.2793	-0.7400
	I	0.2553	0.4767	0.7104	0.5703	0.1376	-0.7795	-0.4635
U=10.0	R	-1.1204	-0.9311	-0.2797	0.4017	1.0020	0.7305	-0.5937
	I	0.3076	0.7312	1.1442	1.0639	0.5541	-0.0330	-0.8719
U=10.5	R	-1.3627	-1.1602	-0.4534	0.4066	1.0777	1.0501	-0.3063
	I	0.4382	0.0319	1.3303	1.3291	0.0248	-0.7070	-1.1055
U=11.0	R	-1.3391	-1.1642	-0.5441	0.2399	0.9545	1.1651	0.0610
	I	0.4015	0.7674	1.2607	1.3367	0.4519	-0.4303	-1.1277
U=11.5	R	-1.0702	-0.9561	-0.5460	0.0232	0.5760	1.0721	0.4361
	I	0.2097	0.5996	0.9642	1.1006	0.9307	-0.0597	-0.9427
U=12.0	R	-0.6225	-0.5006	-0.4463	-0.1907	0.1300	0.7971	0.7420
	I	0.1289	0.2578	0.4078	0.6798	0.7637	0.3267	-0.5935
U=12.5	R	-0.0921	-0.1482	-0.2829	-0.3782	-0.3036	0.3977	0.9129
	I	-0.0461	-0.0732	-0.0304	0.1643	0.4407	0.6410	-0.1519
U=13.0	R	0.4153	0.2999	-0.0009	-0.4769	-0.6609	-0.0490	0.9007
	I	-0.1999	-0.3666	-0.5144	-0.3439	0.0791	0.8221	0.2964
U=13.5	R	0.8063	0.6511	0.1242	-0.4743	-0.6650	-0.4642	0.7246
	I	-0.3037	-0.5674	-0.8642	-0.7513	-0.2765	0.8303	0.6683
U=14.0	R	1.0169	0.8557	0.2981	-0.3715	-0.8025	-0.7750	0.3922
	I	-0.3403	-0.6429	-1.0226	-0.9906	-0.5221	0.6649	0.8993
U=14.5	R	1.0230	0.8888	0.4137	-0.1914	-0.7206	-0.9341	-0.0253
	I	-0.3073	-0.5077	-0.9744	-1.0314	-0.7449	0.3623	0.9542
U=15.0	R	0.8416	0.7595	0.4557	0.0272	-0.4232	-0.9234	-0.4463
	I	-0.2164	-0.4232	-0.7462	-0.8832	-0.7897	-0.0129	0.8327
U=15.5	R	0.5245	0.5074	0.4217	0.2376	-0.0507	-0.7558	-0.7069
	I	-0.0905	-0.1909	-0.3902	-0.9906	-0.7016	-0.3012	0.5673
U=16.0	R	0.1446	0.1900	0.3221	0.3956	0.2907	-0.4711	-0.9706
	I	0.0423	0.0568	-0.0093	-0.2213	-0.5042	-0.6660	0.2156
U=16.5	R	-0.2203	-0.1252	0.1772	0.4609	0.5564	-0.1267	-0.9822
	I	0.1544	0.2690	0.3400	0.1409	-0.2379	-0.8094	-0.1525
U=17.0	R	-0.5035	-0.3030	0.0134	0.4436	0.6000	0.2137	-0.7962
	I	0.2246	0.4502	0.5074	0.4520	0.0603	-0.7063	-0.4682
U=17.5	R	-0.6614	-0.5425	-0.1422	0.3269	0.6677	0.4918	-0.4569
	I	0.2417	0.4477	0.6931	0.6397	0.3060	-0.5994	-0.6773
U=18.0	R	-0.6797	-0.5070	-0.2655	0.1451	0.5107	0.6654	-0.0313
	I	0.2066	0.3944	0.6528	0.6914	0.4954	-0.2967	-0.7609
U=18.5	R	-0.5730	-0.5239	-0.3397	-0.0625	0.2603	0.7134	0.3960
	I	0.1311	0.2670	0.4916	0.6146	0.5913	0.0585	-0.5502

[illegible]		PI/4	PI/2	PI	3PI/2	2PI	3PI	4PI
[illegible]	R	-0.3705	-0.3797	[illegible]	-0.2521	[illegible]	[illegible]	[illegible]
	I	0.0345	0.0994	0.2568	0.4407	[illegible]	0.3916	-0.4045
U=19.5	R	-0.1453	-0.1925	-0.3107	[illegible]	-0.2777	0.4463	0.9430
	I	[illegible]	[illegible]	[illegible]	0.2153	[illegible]	[illegible]	-0.2351
[illegible]	R	0.0770	[illegible]	-0.2567	-0.4383	[illegible]	[illegible]	[illegible]
	I	-0.1339	-0.2018	-0.2101	-0.0127	0.3046	0.7418	0.0443

AN/TPS-1D SAMPLE PATTERN CALCULATIONS

The calculation of the Fresnel zone radiation patterns of the AN/TPS-1D is simplified by the fact that the reflector is approximately a rectangular portion of a paraboloid. Thus a plane wave is obtained across the aperture of the reflector and the phase of the field in the aperture may be neglected. Using the two principal plane patterns of the hog-horn primary antenna which are shown in figure III-1 and the drawing of the reflector shown in figure III-2 the aperture distribution may be calculated. The phase center of the horn is assumed to be located at the center of the horn aperture and the origin of the coordinate system shown in figure III-1 is located at this phase center. The X and Y coordinates of a point on the reflector may be obtained from the dimensions given in this figure and the Z coordinate may be determined from the equation of the paraboloid:

$$X^2 + Y^2 = 162.4\ (40.6 - Z)$$

The field of the rectangular horn aperture is assumed to be the product of the fields in each of the two principal planes.

First the aperture is broken into eight strips each of width 21 inches, and each of height 46.4 inches. The field along the center line of each strip must be calculated to determine $I(\gamma)$, $n = 1,2,3,4$. To do this it is necessary to calculate the angles θ and φ subtended by these centerlines. The angle φ is approximately constant along a given centerline and may be calculated by applying the law of cosines to the triangle OO'B. The angles θ_C and θ_A may be calculated approximately from the triangle OCB and OAB respectively, for example

$$\cos \theta_A = \frac{\overline{OA}^2 + \overline{OB}^2 - \overline{BA}^2}{2(OA)(OB)} = \frac{4.05 + 4.08 - .04}{2(2.01)(2.02)} = .996$$

$$\theta_A = 5.1^\circ$$

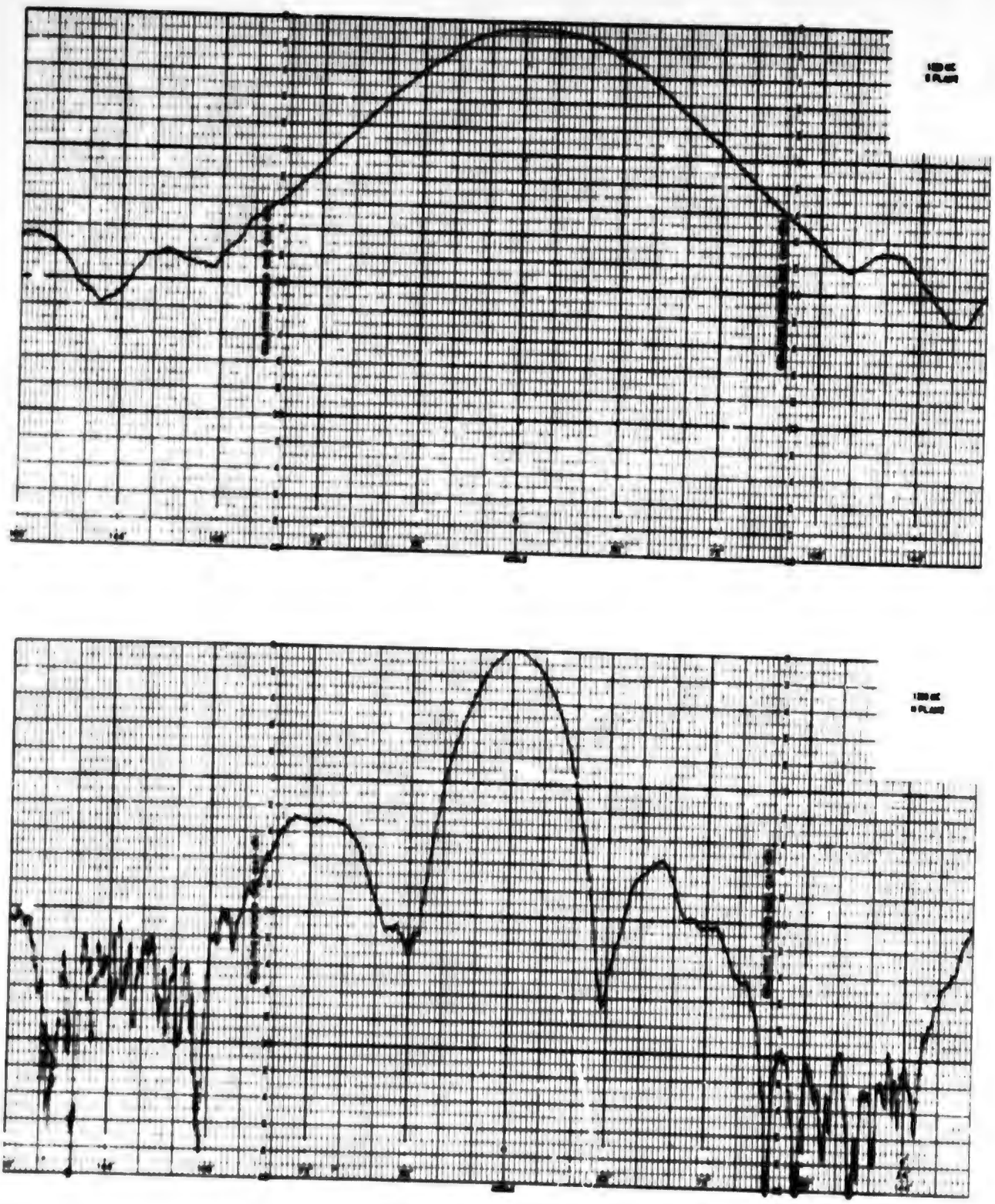

Figure III-1. AN/TPS-1D Primary Feed Horn Patterns

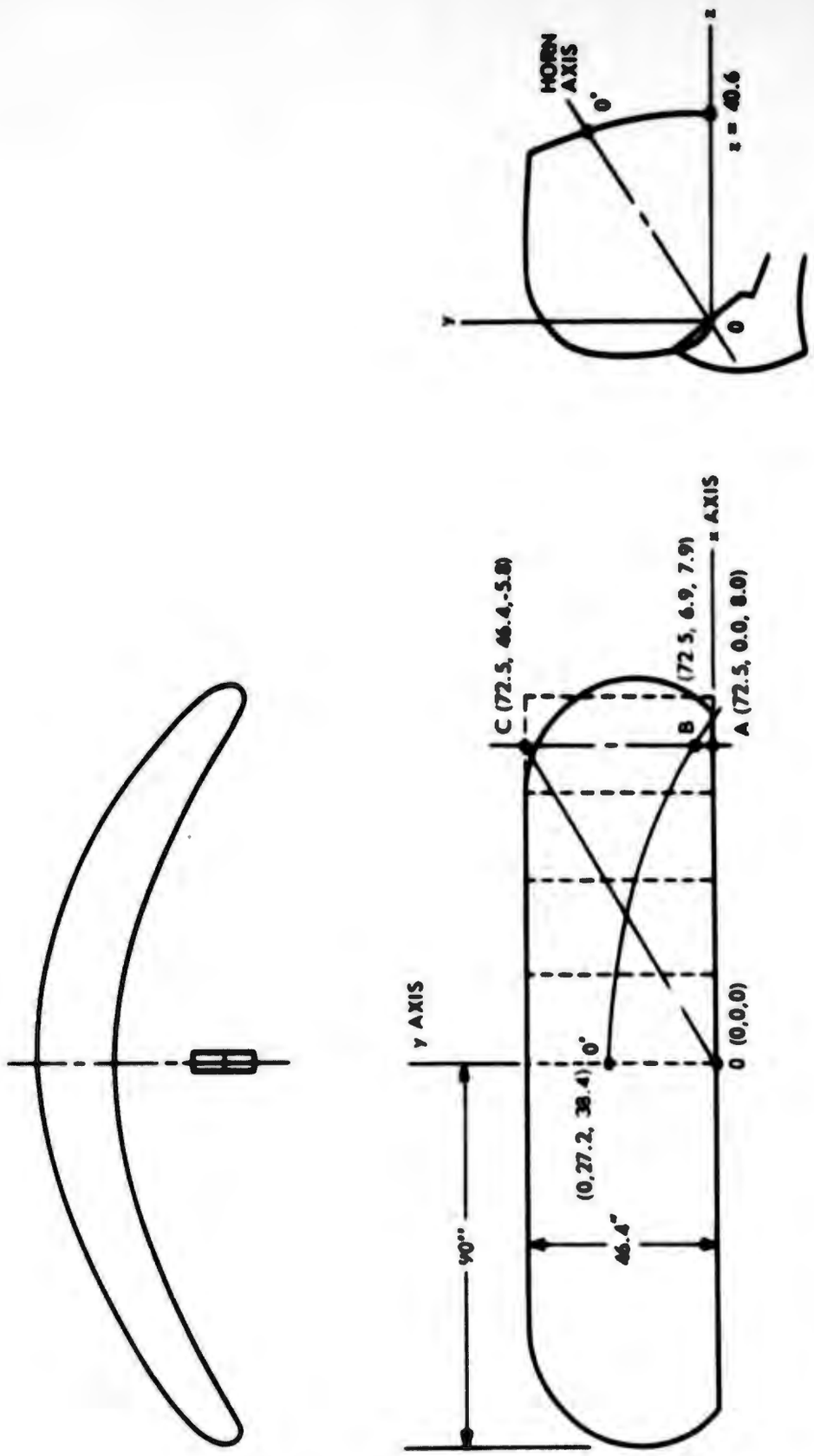

Figure III-2. Outline of the AN/TPS-1D Showing the Coordinate System and Principal Dimensions

likewise $\theta_B = 27.6$ and $\varphi_A \cong \varphi_B \cong \varphi_C \cong 82^\circ$

Then the field at the point A may be determined from the principal plane patterns in figure 77, from the E plane pattern $F_e(82^\circ) = .270$ and $F_h(5.1^\circ) = .944$. Thus $F(\theta, \phi) = F_h(\theta)\, F_e(\phi) = (.285)(.944) = .256$.

It was assumed that θ varied linearly with the aperture coordinate $y_s = Y$ and the calculated field along the center-line of the fourth strip is shown in figure III-3. Since we are in the far field of each strip $I_4(\gamma)$ may be determined by integrating this illumination function. The same procedure is carried through for each of the strips, performing the integration with a planimeter for each of the four strips, with the following results:

$I_1 = .870$, $I_2 = .610$, $I_3 = .353$, $I_4 = .179$

I_1 was normalized to simplify the calculations,

$I_1 = 1.000$, $I_2 = .701$, $I_3 = .406$, $I_4 = .206$

From these constants the field may be calculated from table 3, Volume II and equation (61) of Volume I

$$E(\gamma, u) = \sum_{n=1}^{4} I_n(\gamma)\, F_n(\gamma, u)$$

this calculation is shown in table 4 in detail for $\gamma = 4\pi$, (R = 33 feet) for $u = 0, 0.5, 1.0, \cdots, 16.0$ ($\theta = 0, \cdots, 16^\circ$) note that θ is calculated from $u = ka/2 \sin\theta$, $a/2 = 84"$ and that $u \cong \theta$ by coincidence over this range of u. This computed data is shown plotted along with the experimental AN/TPS-ID pattern in figure 31 of Volume I of this report.

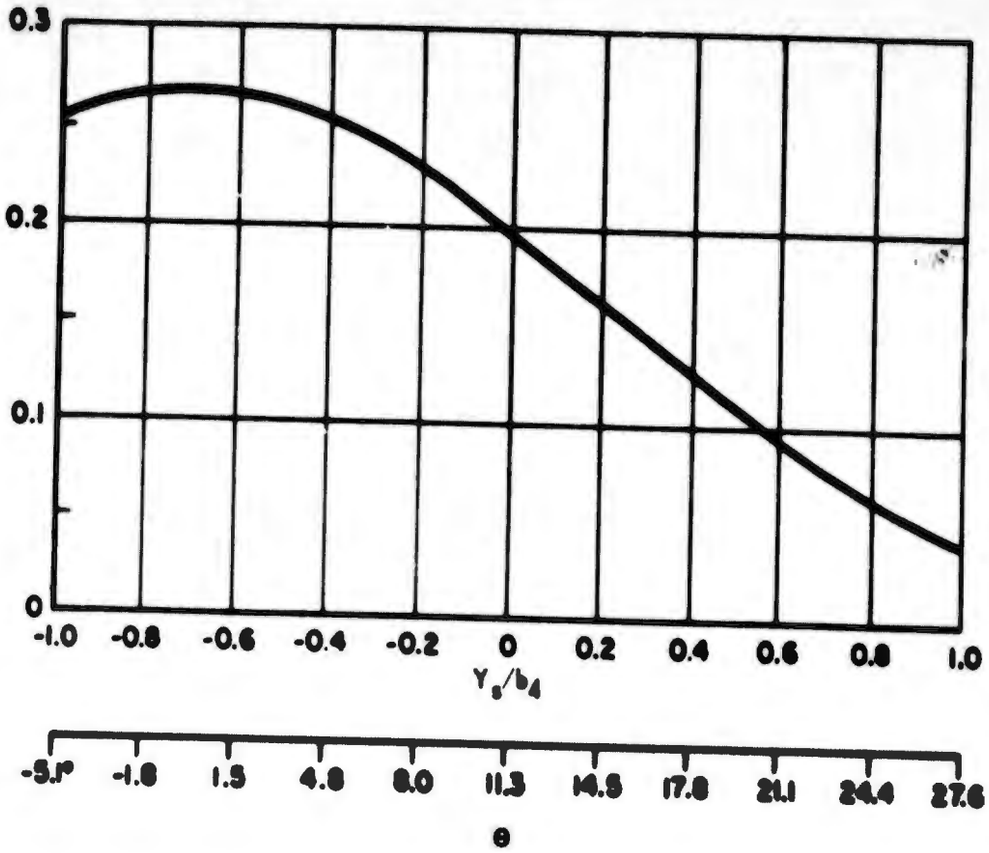

Figure III-3. Plot of $F_4(y_s)$, the Illumination Function of the Fourth Strip, vs. Angle θ and Aperture Coordinate y_s

TABLE 4

Evaluation of the Series $E(4w, u) = \sum_{1}^{4} I_n(4) F_n(4w, u)$ for the AN/TPS-1D Antenna

u	1.000 Re F_1	1.000 Im F_1	.701 Re F_2	.701 Im F_2	.406 Re F_3	.406 Im F_3	.206 Re F_4	.206 Im F_4
0.0	1.977	-.195	.839	-1.022	-.532	-.436	.029	.293
0.5	1.973	-.194	.826	-1.002	-.503	-.419	.022	.265
1.0	1.956	-.191	.788	-.941	-.419	-.367	.004	.189
1.5	1.932	-.186	.726	-.843	-.290	-.285	-.021	.076
2.0	1.898	-.179	.642	-.712	-.130	-.180	-.043	-.048
2.5	1.852	-.170	.540	-.554	.043	-.061	-.056	-.163
3.0	1.800	-.159	.422	-.375	.210	.062	-.053	-.248
3.5	1.738	-.147	.293	-.183	.353	.180	-.033	-.285
4.0	1.668	-.134	.157	.013	.455	.283	.000	-.269
4.5	1.590	-.118	.018	.204	.508	.362	.041	-.203
5.0	1.506	-.102	-.119	.383	.504	.410	.079	-.101
5.5	1.417	-.085	-.247	.543	.446	.425	.104	.018
6.0	1.321	-.067	-.368	.684	.340	.405	.108	.131
6.5	1.223	-.048	-.473	.783	.240	.353	.088	.218
7.0	1.121	-.029	-.562	.852	.040	.272	.046	.262
7.5	1.016	-.010	-.631	.885	-.120	.170	-.012	.257
8.0	.910	.010	-.679	.880	-.263	.055	-.073	.205
8.5	.803	.030	-.705	.841	-.374	-.063	-.124	.117
9.0	.696	.048	-.709	.768	-.441	-.173	-.154	.010
9.5	.591	.067	-.692	.667	-.459	-.268	-.154	-.095
10.0	.487	.085	-.655	.543	-.426	-.339	-.122	-.180
10.5	.386	.101	-.596	.403	-.348	-.381	-.063	-.228
11.0	.289	.117	-.532	.252	-.235	-.390	014	-.232
11.5	.196	.132	-.450	.100	-.100	-.368	.090	-.194
12.0	.108	.145	-.359	-.050	.040	-.316	.153	-.122
12.5	.026	.156	-.263	-.188	.171	-.239	.188	-.031
13.0	-.050	.166	-.165	-.310	.277	-.145	.187	.061
13.5	-.120	.175	-.068	-.412	.349	-.041	.149	.138
14.0	-.183	.182	.025	-.489	.379	.062	.082	.198
14.5	-.239	.187	.111	-.539	.367	.158	-.005	.197
15.0	-.287	.190	.189	-.563	.314	.238	-.092	.172
15.5	-.328	.190	.256	-.559	.230	.295	-.162	.117
16.0	-.361	.190	.310	-.531	.116	.319	-.202	.044

TABLE 4 (Cont.)

u	$\sum_{1}^{4} I_n \text{ Re } F_n$	$\sum_{1}^{4} I_n \text{ Im } F_n$	$\lvert E(4\pi, u)\rvert^2$	$\lvert E\rvert^2_{\text{normalized}}$	$\lvert E\rvert^2_{\text{dt.}}$	ϕ (degrees)
0.0	2.313	-1.360	7.20	1.000	0.0	0.0
0.5	2.318	-1.350	7.20	1.000	0.0	0.5
1.0	2.329	-1.310	7.14	.993	0.0	1.0
1.5	2.347	-1.238	7.04	.978	0.1	1.5
2.0	2.367	-1.119	6.85	.951	0.2	2.0
2.5	2.379	- .948	6.56	.911	0.4	2.5
3.0	2.379	- .720	6.18	.858	0.7	3.0
3.5	2.351	- .435	5.72	.795	1.0	3.5
4.0	2.280	- .107	5.21	.724	1.4	4.0
4.5	2.157	.245	4.71	.654	1.8	4.5
5.0	1.970	.590	4.23	.588	2.3	5.0
5.5	1.720	.901	3.77	.524	2.8	5.5
6.0	1.401	1.153	3.29	.459	3.4	6.0
6.5	1.088	1.306	2.89	.401	4.0	6.5
7.0	.645	1.359	2.26	.314	5.0	7.0
7.5	.253	1.302	1.76	.244	6.1	7.5
8.0	-.105	1.150	1.33	.185	7.3	8.0
8.5	-.400	.925	1.02	.142	8.5	8.5
9.0	-.608	.653	.796	.111	9.5	9.0
9.5	-.714	.371	.647	.0898	10.5	9.5
10.0	-.716	.109	.525	.0729	11.4	10.0
10.5	-.621	-.105	.397	.0551	12.6	10.5
11.0	-.464	-.253	.279	.0413	13.8	11.0
11.5	-.264	-.330	.179	.0249	16.0	11.5
12.0	-.058	-.343	.121	.0168	17.8	12.0
12.5	.122	-.302	.106	.0147	16.3	12.5
13.0	.249	-.228	.114	.0158	18.0	13.0
13.5	.310	-.140	.116	.0161	17.9	13.5
14.0	.303	-.047	.0940	.0130	18.9	14.0
14.5	.234	.003	.0548	.00761	21.2	14.5
15.0	.124	.037	.0167	.00232	26.3	15.0
15.5	-.004	.043	.00186	.000258	35.9	15.5
16.0	-.137	.022	.0193	.00268	25.7	16.0